I. The effects of Variations in Certain Parameters Upon the Efficiency of *In Vivo* Hemodialysis with a Kiil Dialyzer

II. Interfacial Structure of Concurrent Air - Water Flow in a Two-Inch Diameter Horizontal Tube

Thesis by

Malcolm Cameron Morrison

In Partial Fulfillment of the Requirements

For the Degree of

Doctor of Philosophy

California Institute of Technology

Pasadena, California

1969

ACKNOWLEDGMENT

Where would I be without the Institute, noble CIT, which has held me in its loving womb for the past 8+ years. Perennial general budget research funds bought for me what I couldn't steal, and GRA's and GTA's did the same for me in the outside world. The Stauffer Chemical Company and the National Science Foundation also contributed to my support. I owe a lot to my first advisor, Dr. Richard Seagrave, now at Iowa State, who interested me in two-phase flow. I owe more, however, to Dr. Giles R. Cokelet, now at Montana State, who very kindly took me after my second graduate year and worked with me on both two-phase flow and artificial kidneys. May I repay them both someday for their time and effort spent nurturing me. Dr. Corcoran has influenced me favorably since he accomplished my conversion in my first chemical engineering course during my sophomore year. If I had not been able to finagle Dr. Shair out of some of his desperately needed laboratory space, my 30-foot long experimental apparatus would have been 15 feet. Milton E. Rubini, M.D., and Joseph H. Miller, M.D., of Wadsworth Veteran's Hospital made the work on artificial kidneys possible.

My eternal gratitude to my parents, who have already provided me with the best possible inheritance--fond memories of childhood and an excellent education.

And last but not least to the Gertrude, who did her share and more, and to the Malcolm-fink, who really isn't, and to the Rat, bless his little ratly heart.

Dun Eistein!

PART I

ABSTRACT

Regression analyses are performed on in vivo hemodialysis data for the transfer of creatinine, urea, uric acid and inorganic phosphate to determine the effects of variations in certain parameters on the efficiency of dialysis with a Kiil dialyzer. In calculating the mass transfer rates across the membrane, the effects of cell-plasma mass transfer kinetics are considered. The concept of the effective permeability coefficient for the red cell membrane is introduced to account for these effects. A discussion of the consequences of neglecting cell-plasma kinetics, as has been done to date in the literature, is presented.

A physical model for the Kiil dialyzer is presented in order to calculate the available membrane area for mass transfer, the linear blood and dialysate velocities, and other variables. The equations used to determine the independent variables of the regression analyses are presented. The potential dependent variables in the analyses are discussed.

Regression analyses were carried out considering overall mass-transfer coefficients, dialysances, relative dialysances, and relative permeabilities for each substance as the dependent variables. The independent variables were linear blood velocity, linear dialysate velocity, the pressure difference across the membrane, the elapsed time of dialysis, the blood hematocrit, and the arterial plasma concentrations of each substance transferred. The resulting correlations are tabulated, presented graphically, and discussed. The implications of these correlations are discussed from the viewpoint of a research investigator and from the viewpoint of patient treatment.

Recommendations for further experimental work are presented.

PART II

ABSTRACT

The interfacial structure of concurrent air-water flow in a two-inch diameter horizontal tube in the wavy flow regime has been measured using resistance wave gages. The median water depth, r.m.s. wave height, wave frequency, extrema frequency, and wave velocity have been measured as functions of air and water flow rates. Reynolds numbers, Froude numbers, Weber numbers, and bulk velocities for each phase may be calculated from these measurements. No theory for wave formation and propagation available in the literature was sufficient to describe these results.

The water surface level distribution generally is not adequately represented as a stationary Gaussian process. Five types of deviation from the Gaussian distribution function were noted in this work. The presence of the tube walls and the relatively large interfacial shear stresses precludes the use of simple statistical analyses to describe the interfacial structure. A detailed study of the behavior of individual fluid elements near the interface may be necessary to describe adequately wavy two-phase flow in systems similar to the one used in this work.

TABLE OF CONTENTS

LIST OF FIGURES

PART I

PART II

LIST OF TABLES

PART II

Appendix B

PROPOSITIONS

Proposition II.

Proposition III.

PART I

THE EFFECTS OF VARIATIONS IN CERTAIN PARAMETERS UPON THE EFFICIENCY OF *IN VIVO* HEMODIALYSIS WITH A KIIL DIALYZER.

INTRODUCTION

Over one hundred thousand Americans die each year as a result of kidney diseases or from effects related to kidney diseases (42). Although hemodialysis has been clinically feasible for twenty-five years, virtually nothing can be done for these over one hundred thousand people; nor will anything appreciable be done until the extremely high costs of dialysis, which result from the relative technical inefficiency of the process, are substantially reduced. The effect of deaths due to kidney disease upon society is increased by the predilection of the disease for young adults. Kidney disease is the major cause of death from chronic illnesses in young adults. The loss of these young adults who are parents of young children and who are just beginning to contribute to the nation's economy has a greater sociologic and economic effect than the loss of older individuals whose children are grown and whose careers are largely completed. In addition, kidney disease results in the greatest loss of time from work among women and among the entire population under 25 (42).

The need for an efficient and inexpensive method of hemodialysis is obvious, and significant progress towards this goal has been achieved. The first artificial kidney was developed over forty years ago. Acutely ill patients have been treated for twenty-five years with artificial kidneys, but chronically ill patients have been successfully treated for less than a decade. Significant engineering interest in hemodialysis has also existed for less than a decade. Sometimes the engineering research has had little practical effect on the application of hemodialysis to the benefit of the patient. This

work attempts to elucidate points which will not only be of engineering significance in the design and analysis of artificial kidneys but which will also have an immediate effect on the application of hemodialysis to benefit patients.

The effects of variations of volumetric blood flow rate upon the efficiency of *in vivo* and *in vitro* hemodialysis have been investigated frequently during the past twenty years (18, 27, 49, 52). In a classic paper (52), Wolf investigated the effects of blood flow and bath volume on the *in vitro* rate of material exchange in a Brigham-Kolff type drum kidney. The effect of blood flow on the transfer rate was not the same for all compounds tested by Wolf. Wolf defined the dialysance of a substance as being the quantity of a substance transferred between blood and dialysate per unit time divided by the maximum concentration gradient of that substance between the blood and the dialysate, or

$$D = \frac{\dot{m}}{c_{b_i} - c_{d_i}} \qquad [1]$$

Different materials have different characteristic dialysances; so the concept of relative dialysance, or the ratio of the dialysance of a given substance to that of a standard substance, such as urea or chloride, measured at the same conditions, was introduced. The relative dialysances of all substances were found to be differing functions of volumetric blood flow rate, all other conditions being identical. M. J. Sweeney (46) proposed a modification of Wolf's relative dialysance concept to remove this dependency of the relative

dialysance upon volumetric blood flow rate.

Sweeney proposed a relative permeability coefficient based upon the permeability coefficient for a substance. The permeability coefficient for a substance x is defined by

$$P = \frac{D\ max}{A} \ln \left[\frac{1}{1 - \frac{D}{D\ max}} \right] \qquad [2]$$

The maximum dialysance for a countercurrent flow dialyzer, such as the Kiil dialyzer, is equal to the lesser of the blood and dialysate flow rates. The lesser quantity is almost invariably the blood flow rate. This permeability coefficient is a simplification of a permeability presented by Galletti (21). His permeability for a countercurrent flow dialyzer is

$$P = \frac{Q_b\ Q_d}{A\ (Q_d - Q_b)} \ln \left[\frac{1 - \frac{D}{Q_d}}{1 - \frac{D}{Q_b}} \right] \qquad [2a]$$

This permeability can be shown to be identical to the overall mass-transfer coefficient used later in this work. If Q_d is much greater than Q_b, then [2a] simplifies to [2].

The relative permeability coefficient for a substance is then

$$P_r = \frac{P}{P_s} \qquad [3]$$

Sweeney reported the <u>In Vitro</u> relative permeability coefficients for a number of solutes and for several membranes using the Klung and Twin-Coil dialyzers. Over the range of artificial blood flow

rates studied, the relative permeability coefficient was found to be independent of artificial blood flow rate. Sweeney noted that the need for *in vivo* testing was obvious before this concept could become clinically relevant.

The effects of various other operating parameters have been studied. R. B. Freeman (18) and H. W. Brown (9) pointed out the influence of temperature on the rate of material transfer. H. W. Brown also studied the influence of membrane thickness on the *in vitro* transfer rate through the membrane. This work was carried further by C. Wilcox (51), who compared the *in vitro* permeabilities of six cellulose membranes with the values of each of six physical properties for the membranes. The physical properties of the membrane may, of course, be modified to alter the transfer rate of compounds through the membrane. Craig (13, 38) has shown how mechanical stretching of the membrane may have a very strong effect on the transfer rate of materials through the membrane. One-dimensional stretching reportedly elongates the pores in the membrane and therefore decreases the rate of transfer of materials through the pores. Two-dimensional stretching apparently increases the size of the pores and thus increases the transfer rate. There is some evidence that this two-dimensional stretching effect causes the transfer of large macromolecules in a Klung dialyzer (1). Bluemle (8) presented some evidence that dialyzer membrane supports which cause the membrane to be stretched in a two-dimensional fashion result in higher transfer rates across a dialyser membrane than supports which cause the membrane to be stretched in a one-dimensional fashion when a pressure gradient is applied across the membrane. This evidence, however, is

not conclusive since the supports cause changes in the blood flow patterns in the dialyzer which also effects the transfer rate.

A number of mathematical models of hemodialysis have been proposed in the literature (23, 24, 28, 31, 53). Since these models involve a number of simplifying assumptions, their ultimate usefulness is not yet clear. All mathematical approaches assume that the overall mass-transfer coefficient is independent of the volumetric flow rates of blood and of pressure differences across the membrane. The effects of changes in the blood and dialysate compositions on the mass-transfer coefficients of materials are neglected. Changes in contained blood volume in dialyzers, which results in changes in available membrane area, blood and dialysate film thicknesses, and membrane stretch are assumed in these approaches to have no effects on transfer rates.

The purpose of this work is to investigate how the changes in certain parameters of in vivo hemodialysis affect the rates of transfer across the dialysis membrane. Using in vivo hemodialysis data supplied by Wadsworth Veterans Hospital in Los Angeles, California, and dialyzer dimensions for the Western Gear Kiil dialyzer supplied by the Western Gear Corporation in Lynwood, California, the effects of variations of dialysis parameters on the overall mass-transfer coefficients can be determined. The results will enable more accurate mathematical approaches to hemodialysis to be formulated. The results also point out an error in the method of determination of mass-transfer rates for in vivo hemodialysis. This error has significant implications for prior data reported in the literature and for the definitions

of certain concepts basic to hemodialysis. The results also point out certain deficiencies in the manner in which in vivo hemodialysis data are collected. These deficiencies were present when the data analyzed in this work were collected. For this reason, certain indicated results of this work must be viewed with caution. Further experimental data are necessary, and the results of this work elucidate considerably the considerations which must be borne in mind when taking further in vivo experimental data.

HEMODIALYSIS WITH A KIIL DIALYZER

Kiil Dialyzer Characteristics

The Kiil dialyzer, as manufactured by Western Gear, Sweden Freezer, and other firms, consists of a clamping apparatus, three machined polypropylene boards, and four cellophane-derivative membranes. The Kiil dialyzer manufactured by Western Gear has the boards machined as shown in Figures 1 and 2. The overall dimensions and board characteristics are presented in Figure 1 and the details of the groove machining are presented in Figure 2. There are 150 groves per board, 75 on each side of the central flattened area. The two end boards are machined this way on one side only; the central board is machined this way on both sides.

The assembled dialyzer consists of the bottom board, then two membranes with a blood port between them at each end of the boards, then the central board, then two more membranes with blood ports between them at the ends, then the top board. The clamping assembly surrounds the boards and clamps everything together. Blood flows through the blood ports into the space between the membranes in each

of the two layers. The dialysate flows through dialysate ports in the polypropylene boards and through the grooves of the boards both above and below each of the blood layers between the membranes. The dialysate flows countercurrent to the blood flow.

Assembly and Preparation of Dialyzers for Dialysis

The assembly and preparation of dialyzers for dialysis undoubtedly has an appreciable effect on the efficiency of the dialysis. This is largely because the procedure cannot be done identically each time and because certain steps in the procedure influence the mass-transfer rate during dialysis. For this reason, the assembly and preparation procedure used at Wadsworth Hospital is outlined here.

Before assembly, the boards are scrubbed with a soap and water solution and rinsed while the membranes are being thoroughly soaked in distilled water. The membranes are standard PT 150 Cuprophane. When the membranes are completely wetted, assembly is begun. The bottom half of the clamping assembly is placed on a cart, and then the bottom board is placed on the assembly with the machined side up. A membrane is placed over the grooved, machined side of the board. All membranes are placed on the boards by the following procedure. Two people grasp the wet membrane between thumb and forefinger at each of the four corners of the membrane. The membrane is held over the board and slightly stretched longitudinally until it is slightly longer than the 38" length of the boards. The membrane will not stretch much longitudinally. Then one side of the membrane is placed on the board and the membrane is rolled down on the board starting at this side and proceeding to the other side. This

procedure prevents the entrapment of large air bubbles between the board and the membrane. Some lateral stretching is applied to the membrane as it is being laid down. The membrane stretches laterally much easier than it stretches longitudinally. Any wrinkles in the membrane are then removed by hand. Next two blood ports are laid on top of the membrane in the proper position and another membrane is laid down. The first layer is completed by placing the central board down on the second membrane.

The second layer is then assembled exactly as the first layer was. After the top board is laid down, the top half of the clamping assembly is positioned and the clamps tightened. The clamps around the center of the dialyzer are tightened first. All clamps are tightened with a torque wrench to the same tightness, 15 ft.-lb. of torque.

Next the assembled dialyzer is pressure tested with air to make sure there are no leaks. First the dialysate sides of both layers are pressured to 240 mm. Hg pressure difference across the membrane and held for a specified length of time. Then each blood layer is successively pressurized to 240 mm. Hg and held for a specified length of time.

The two blood layers are then filled with a formalin solution to sterilize the surfaces which are to come in contact with blood. The liquid level in the formalin storage tank is about 42" above the dialyzer so the dialyzer is pressurized by this procedure to about 80 mm. Hg. This pressure is soon relieved by ultrafiltration. The dialyzer must have the formalin solution in it for at least two hours

but may contain it for up to two weeks.

When the dialyzer is ready to be used, tap water is run through the dialysate sides to remove the formalin by dialysis through the membrane. Finally the blood layers are flushed briefly with sterile saline solution and the dialyzer is taken into the ward with the saline solution in the blood layers. The flush with saline solution again pressurizes the dialyzer to about 100 mm. Hg pressure across the membrane.

Experimental Data

Dr. Joseph H. Miller of the chronic dialysis unit at Wadsworth Veterans Hospital supervised the obtainment of a great deal of experimental data at that hospital in the past five years. Data were taken for a large number of patients on several types of dialyzers under varying conditions. Most of the data were for dialysis on Kiil dialyzers. Only about half of this available data for Kiil dialyses was used in this work.

There were many reasons why the remainder of the Kiil dialysis data were not used, but in essence all of these reasons are equivalent to saying that their reliability was doubted for the purposes for which their use was intended. Some data were for dialyses in which the dialysate was partially recirculated. All data used were for dialyses using no recirculation of dialysate. Some patients had a transfusion or took in a significant quantity of food and drink during dialysis. This strongly affects the patient's blood hematocrit, which was assumed constant during dialysis, so these data were not used. Often, some flow rate or pressure value was not

recorded and these points were not used. Occasionally some concentration value was not recorded and the data at this point in time were not used for the component involved, although other components were not affected. A very few, less than five, data points were not used bacause some value was patently absurd. Data which appeared very suspicious but which were not obviously absurd were not thrown out.

Table I identifies each of the nine dialyses for which data were used. The first three columns give the information used at Wadsworth Hospital to identify the data. The patient number is used throughout this work to identify the dialysis. The negative balance is the total amount of weight the patient lost during the entire twelve-hour dialysis. It is not significant except that it points out the two dialyses during which the patient had appreciable ultrafiltration.

The hematocrit of the patient's blood is listed in Table I. Hematocrit is the volume per cent or volume fraction of the blood occupied by the cells of the blood. All values were taken on blood obtained at the start of dialysis. The blood sample was placed in a standard, constant cross-sectional area cylindrical cell for the micro-determination of hematocrit. The samples were spun 15 minutes in a centrifuge to separate the cells and the cell-plasma interface was noted relative to the height of material in the tube. The ratio of the depth of cells to the depth of material in the tube is the blood hematocrit fraction. Some blood samples were spun down immediately after they were taken and some were not spun down for hours. When two values of hematocrit are presented in Table I, these two

values are from micro-samples taken from the same large blood sample. The two numbers should, of course, be the same. The procedure is reputedly able to report hematocrit to within ± 0.5 hematocrit per cent, and the data indicate this is the case. Since hematocrit was taken only at the start of dialysis, the hematocrit was assumed to be constant throughout the dialysis for each patient. As was mentioned, data for patients for which there was reason to believe this might not be true were not used in this work.

Table II presents the elapsed times of dialysis and the measured flow rates at each time point. The elapsed time is measured from the start of dialysis and is accurate to within two minutes. Note that measurements have been obtained for elapsed times in the range of 30 - 360 minutes. The range of blood flow rate is from 110 to 280 ml per minute. Blood flow rate was measured with a Kiron electromagnetic sine wave flowmeter, model EC 7000. Tests carried out by Dr. Miller indicate that the proper use of this flowmeter gives the blood flow rate to within 3% of the actual value. Dialysate flow rates do not vary over a very large range. The range is from 430 to 760 ml per minute, and the great majority of the flow rates are within 50 ml/min. of 500 ml/min. Dialysate flow rate was measured by collecting the dialysate outflow in a 500 ml graduate cylinder and measuring the time taken to fill the cylinder. This procedure is estimated to be accurate to within 3%, assuming the flow rate does not change during the time the cylinder is filling.

Table III presents the measured pressures on the blood and dialysate sides of the dialyzer at each point in time. All pressures

were measured in the inlet and outlet tubings connected to the dialyzer at distances of 1 - 2 feet from the dialyzer. The pressures were measured by inserting into the lines a needle connected to a calibrated aneroid pressure gauge. For each dialysis, all pressures were recorded relative to a particular reference elevation. These reference elevations were not the same for each dialysis nor were they all recorded. Although the absolute magnitudes of pressure therefore cannot be used for any purpose, the pressure differences across the membrane can be used because they are independent of the reference pressure points. The pressures should be accurate to within 5%.

Table IV indicates the average blood-side pressure, the average dialysate-side pressure, and the average pressure difference across the membrane in the dialyzer. These figures follow directly from the figures presented in Table III. Pressure differences across the dialyzer membrane range from 29 to 154 mm. Hg. These pressure difference figures are estimated to be accurate to within ± 5% for the larger values.

Tables V and VI present the measured concentrations of each component in the inlet and outlet plasma streams. These concentration determinations were carried out on plasma samples by the renal laboratory of the Wadsworth Hospital chronic dialysis unit under the direction of Miss Cybil Gordon. All values were obtained using the Technicon Auto Analyzer made by the Technicon Instruments Corporation. All values are estimated by Miss Gordon to be within 5% of the true value. References for the methods used to determine

creatinine (25, 48), urea nitrogen (29, 44, 48), uric acid (48), and inorganic phosphate (17, 48) are available in the literature. The inorganic phosphate value is the total concentration of both bound and unbound inorganic phosphate in the plasma.

The concentration of each component in the outlet dialysate stream was also measured, but these concentrations were so low that they could not be accurately measured. The values, good to ± 20%, are presented in Table VII.

Figure 3 shows the experimentally obtained curve for the capacitance (blood hold-up volume) of a Western Gear Kiil dialyzer. Details of the original work by Dr. Joseph H. Miller are available (11). The test was static. The blood side of the dialyzer was filled with saline solution at a measured pressure. The dialysate side was at atmospheric pressure. The curves are not corrected for the solution which was ultrafiltrated during the experiment. About 20 ml of solution was estimated to be ultrafiltrated during the entire time period of the test. Correcting for the ultrafiltration would move the deflation curve so that it would be much closer to the inflation curve. The correction would also steepen somewhat the slopes of the curves at higher pressure differences across the membrane because most of the ultrafiltration would occur at these higher pressure differences. The pressure differences in the data analyzed in this work range from 29 - 154 mm. Hg. In this range the inflation curve, obtained when the dialyzer was being inflated by the addition of saline solution, is judged to represent best the capacitance of a Kiil dialyzer. The effects of assuming that a different curve

represents the capacity of a Kiil dialyzer are discussed further on.

This curve is assumed to be representative of all of the nine dialyzers used when the analyzed data were taken. In fact, the capacitance of each of the nine dialyzers would be expected to vary because of differences in membrane characteristics and differences in assembly techniques for the dialyzers. Also, before a dialyzer is connected to a patient it is inflated and deflated three times. This capacitance data does not indicate what effect repeated inflations have on the subsequent capacitance of the dialyzer. The application of this capacitance curve to represent each of the nine dialyzers involved incorporates a certain amount of error into the analysis.

EMPIRICAL MODEL FOR HEMODIALYSIS

Transfer Equation

The instantaneous rate of material transfer from blood to dialysate when there is no accumulation in the blood side is

$$\dot{m} = Q_{bi}\, c_{bi} - Q_{bo}\, c_{bo} \qquad [4]$$

Throughout the literature, this equation always appears simplified to the following form

$$\dot{m} = Q_b\, (c_{bi} - c_{bo}) \qquad [4a]$$

Equation [4a] is strictly true only when the volumetric blood flow rates into and out of the dialyzer are the same. It has been realized that this equation neglects the results of ultrafiltration (5). Ultrafiltration, the removal of water from the blood in the dialyzer,

results in the blood flow rate into the dialyzer being greater than the blood flow rate leaving the dialyzer. Since volumetric blood flow rate for our data is measured prior to the dialyzer, the use of this quantity in equation [4a] results in a calculated mass-transfer rate less than the rate which would be calculated by the use of equation [4].

Equation [4], however, calculates the total mass-transfer rate from the blood at steady state. When ultrafiltration occurs, this total mass transfer rate is higher than the mass transfer rate caused by chemical potential gradients because bulk flow of water through the membrane results in material being transferred by the "solvent drag" process (5). For this reason, the use of volumetric blood flow rates measured prior to the dialyzer in equation [4a] makes the transfer rate calculated from equation [4a] a more accurate representation of the mass-transfer rate caused by chemical potential gradients provided the rate of ultrafiltration is less than about 10% of the blood flow rate. Barenberg (5) has shown that under most circumstances the neglect of ultrafiltration when calculating mass-transfer rates is not serious during hemodialysis. Randall Cook (12) showed, using data from Wadsworth Hospital in Los Angeles, that the rate of ultrafiltration is at most 3 - 4% of the common blood flow rates. This maximum figure is identical to the experimental error in measuring blood flow rates.

It is not generally realized that equation [4] may be used incorrectly because it neglects the effects of bound-free transfer kinetics and of cell-plasma transfer kinetics, although an oblique

reference to this has appeared in the literature (47).

In calculating in vivo mass transfer, however, equation [4] is not used in the literature. Rather the in vivo mass transfer is calculated by the equation

$$\dot{m} = Q_b (c_{p_i} - c_{p_o}) \qquad [5]$$

This equation also neglects the effects of ultrafiltration and the effects of cell-plasma transfer kinetics. The use of equation [5] to calculate in vivo mass transfer is apparently due to the indiscriminate and interchangable use of the words "blood" and "plasma" in the literature. This unfortunate turn of events probably could be traced back to the early history of artificial kidneys when the new artificial kidneys were naturally described in terms of the familiar expressions applied to the functioning of the human kidney. The human kidney ultrafiltrates the blood and separates the cells and proteins before removing the desired products from the ultrafiltrate. Then it recombines the plasma with the blood stream. It apparently became accepted practice to refer to the "blood concentration" when one was actually referring to the concentration in the ultrafiltrate of the plasma, which is approximately equal to the concentratration in the plasma. This practice carried over into the description of artificial kidneys which removed materials from the whole blood, not the ultrafiltrate of plasma. Experimentally one measures blood flow rates and plasma concentrations, so in view of the historical use of the word "blood" when "plasma" was more nearly intended, the appearance and assumed equivalence of equations

[4] and [5] would not be unexpected.

As mentioned, however, both equations [4] and [5] neglect the effect of cell-plasma transfer kinetics on the transfer of materials. This is a serious error. The total material removed from the blood is the sum of the material removed from the plasma and the material removed from the cells. In other words, still neglecting ultrafiltration and the effects of binding kinetics,

$$\dot{m} = [Q_b\ (1 - H)]\ [c_{p_i} - c_{p_o}] + (Q_b)\ (H)\ (c_{c_i} - c_{c_o}) \qquad [6]$$

The volume of white cells and platelets is usually about 1% of a given volume of blood. In individuals with chronic kidney disease, the volume fraction of blood which is red cells is usually in the range from 18 to 35%. Data on component concentrations in white cells and platelets are not available, so one of two assumptions must be made. One can assume that no material is transferred out of the white cells and platelets and that the hematocrit is the volume fraction of red cells in the blood, (This makes the use of 1 - H in the first term of [6] slightly in error.) or one can assume that white cells and platelets behave as red cells and the hematocrit is the total volume fraction of all blood cells. This work assumes the latter since the hematocrit data reported is the total volume fraction of cells. Inasmuch as white cells and platelets comprise such a small fraction of the cellular volume, both assumptions will give essentially equivalent results.

The available data from Wadsworth Hospital do not record concentrations of solutes in patients' red cells, so the material

transferred from the red cells must be related to the material transferred from the plasma. Arbritton (2) reports the standard values of equilibrium concentrations of many components in plasma and red cells. These standard values are average values determined from many measurements on the blood of healthy individuals. Individuals undergoing hemodialysis are not healthy, and their average cell and plasma concentrations are quite different. This work assumes, however, that for every patient the data covers, the ratio of the equilibrium concentration of a particular component in the red cells to the equilibrium concentration of that component in the plasma is equal to the ratio of the standard red cell concentration reported by Arbritton to the standard plasma concentration. This ratio is called the equilibrium partition coefficient, K_p. Obviously this assumption should be verified by experimental measurements, and until then it should be regarded with great caution. The assumption is necessary, however, if the available data are to be analyzed. Table VIIIa presents the pertinent red cell and plasma concentrations and their ratios.

The equilibrium blood concentration of a component is then related to the experimentally measured plasma concentration by the equation

$$c_{b_e} = c_p (1 - H) + H [K_p (c_p)] \qquad [7]$$

or

$$c_{p_e} = c_p [1 + (K_p - 1) H] \qquad [8]$$

The equilibrium blood concentration is not necessarily of interest in calculating material transfers. The blood concentration of

interest is the "effective blood concentration." The effective blood concentration differs from the equilibrium blood concentration in that it considers the rate of transfer of the material across the red cell membrane relative to the residence time distribution of the blood in the dialyzer. The effective blood concentration of a substance is the amount of that substance per unit volume in the blood which theoretically could be transferred out of the blood during the time that the blood passes through the dialyzer. The effective blood concentration of a substance depends upon the concentrations of the component in the plasma and in the cells, the hematocrit, the rate of transfer of the substance out of the cells into the plasma, and the residence time distribution function of the blood in the dialyzer. Not much work has been done to obtain the residence time distribution function in dialyzers. The work that has been done with twin coil dialyzers (32) indicates that the deviations of the residence time distribution function from the ideal function are appreciable but are not of unusual interest.

The effective blood concentration of a substance takes into account the fact that if mass transfer occurs under the conditions which presently exist in artificial kidneys the substance will always be removed from the plasma but may or may not be removed from the cells. If the maximum residence time of the blood in the dialyzer is significantly less than the length of time that is necessary under the circumstances involved for an appreciable amount of the material within the cells of the blood to exit through the cellular membranes, then the material in the cells cannot participate in the transfer

process in the dialyzer. The substance in the cells is "frozen" into the cells so far as the processes occurring in the dialyzer are concerned, and the effective blood concentration is independent of the cellular concentration. On the other hand, if the substance involved is transferred out of the red cells so rapidly that some or virtually all of the material in the cells can leave the cells in a time much shorter than the minimum residence time of the blood in the dialyzer, the effective blood concentration depends on both the plasma and cellular concentration.

Let us assume again that the cell concentrations may be adequately represented by considering them all as only red cells. Then, analogous to the development of equation [8], the effective blood concentration is related to the experimentally measured plasma concentration by

$$c_b = c_p \, [1 + (J_b - 1) \, H] \qquad [9]$$

in which J_b is the effective partition coefficient for blood for the substance in the dialyzer under the conditions involved. In hemodialysis, two conditions which are important in the determination of the limits of J_b are the facts that material is removed from the blood and the residence time of the blood in the body is about thirty minutes while the residence time of the blood in the dialyzer is less than two minutes. For the conditions existing in hemodialysis, the effective partition coefficient's lower limit is zero. It has this value when the substance involved is "frozen" into the cells so far as the processes occurring in the dialyzer are concerned. The

effective partition coefficient's upper limit is the value of the equilibrium partition coefficient. It has this value when virtually all of the material in the cells can be transferred out of the cells in a time much shorter than the minimum residence time of the blood in the dialyzer. This means, essentially, that the blood at the dialyzer outlet is at equilibrium so far as the concentration distribution of this component is concerned. Under most conceivable conditions, it also means that the transfer of the material across the red cell membrane is not a limiting step in the transfer process anywhere in the dialyzer, and equilibrium between cells and plasma can be maintained throughout the dialyzer.

The numerical value of the effective partition coefficient is affected by many variables. The parameters which affect the equilibrium partition coefficient also affect the effective partition coefficient. These parameters include the chemical potentials of each substance in the cell-plasma system. These are in turn dependent upon individual concentrations, the temperature, and the pressure of the blood. Red cell membrane characteristics will also affect the effective partition coefficient. In addition, because the effective partition coefficient is defined relative to the time that the blood is in the dialyzer, the value of the coefficient will depend on this time and therefore on characteristics of the dialyzer and the dialysis system.

Data are available for the rates of transfer between red cell and plasma for three of the components analyzed in this work. Since the rate of transfer between red cell and plasma is very strongly

affected by the composition of the cell and plasma fluid (45), data taken from normal blood and from saline solutions cannot be directly applied to determine rates in the blood environment of patients undergoing hemodialysis. Nonetheless, the data are useful to point out the orders of magnitude involved.

Urea enters and leaves the red cell very rapidly (50). In response to a concentration gradient between plasma and cell, the cell becomes 90% saturated in 0.5 second. Therefore the effective partition coefficient for urea is assumed equal to the equilibrium partition coefficient.

Uric acid penetrates the red cell relatively rapidly (35). Measured half-times of penetration range from 10 - 40 minutes depending upon the conditions. However, since the residence time of blood in the Kiil dialyzer is 1 to 2 minutes, uric acid is probably best treated as not being transferred out of the cells during the time the blood is in the dialyzer. Kiil dialyzers can have quite uneven blood velocity distribution patterns, however, and blood elements which move slowly through the dialyzer would lose some of the uric acid in the cells. Nonetheless, the effective partition coefficient is assumed as zero. Results obtained from the regression analysis tend to confirm that this is the proper choice.

Inorganic phosphorus, in the form of phosphate, enters and leaves the cell quite slowly relative to the time required for the blood to pass through the dialyzer (37, 50). The half-time of penetration is about 2 1/2 hours. Thus the effective partition coefficient for inorganic phosphate is assumed to be zero.

Data on the transfer rate of creatinine across the human erythrocyte membrane in a plasma solution are not available. The half-time of transfer for creatinine into red cells in a salt water medium was measured at 10 minutes (22). Other measurements on various organic bases not including creatinine imply that the half-time of transfer of creatinine in plasma would be in the order of one minute or less (43). Results from the regression analyses, which will be discussed further on, indicate that this last estimate is true. Therefore, the effective partition coefficient of creatinine is taken as equal to the equilibrium partition coefficient.

The effective partition coefficient and the effective blood concentration are the quantities used to calculate correctly the mass-transfer rate between the blood and the dialysate in any dialyzer. The mass-transfer rate, still neglecting ultrafiltration and binding kinetics, is

$$\dot{m} = Q_b \, [c_{pi} - c_{po}] \, [1 + (J - 1) \, H)] \qquad [10]$$

Equation [10] follows from equations [6] and [9] only if the value of J_b at the dialyzer inlet equals the value of J_b at the outlet. This is not always true, and for this reason the J factor for use in hemodialysis is best defined not by [9] but by

$$J \equiv \frac{c_{ci} - c_{co}}{c_{pi} - c_{po}} \qquad [9a]$$

The J factor appearing in [10] is defined by equation [9a]. For hemodialysis the residence time of the blood in the body is greater than the residence time of the blood in the dialyzer and substances

are removed from blood. Under these conditions the value of J, like J_b, must lie between zero and the value of the equilibrium partition coefficient.

Equation [10] is only equal to equation [5] when the effective partition coefficient is unity, a very special case. The difference between using equation [10] and equation [5] for urea, which has an effective partition coefficient of 0.88, is slight.

The effective partition coefficient of a substance may be calculated from experimental outlet dialysate concentrations. The amount of the substance removed from the blood in the dialyzer equals the amount of the substance added to the dialysate; or, neglecting ultrafiltration,

$$Q_b \left[c_{p_i} - c_{p_o}\right] \left[1 + (J - 1)\, H\right] = Q_d \left[c_{d_o} - c_{d_i}\right] \qquad [11]$$

This may be rearranged to give

$$J = \left[\frac{Q_d \left(c_{d_o} - c_{d_i}\right)}{Q_b \left(c_{p_i} - c_{p_o}\right)} - 1\right] \frac{1}{H} + 1 \qquad [12]$$

Effective partition coefficients for our four substance range in value from zero to two, and the hematocrit fraction is the order of 1/4. The quantity in brackets in equation [12] is, therefore, the difference of two nearly equal numbers and exceedingly accurate measurements must be made to get an accurate value for the effective partition coefficient.

Although the experimental measurements available did not possess the desired accuracy, effective partition coefficients were

calculated from the data using equation [12]. An analysis of error propagation from the estimated errors in the measurements resulted in the average values for the effective partition coefficients which are presented in Table VIIIb.

The values of the effective partition coefficient for urea and phosphate agree well with the values assumed for this work on the basis of the reported rates of transfer across the red cell membrane. The predicted value of the creatinine coefficient is lower than the assumed value which is equal to the value of the equilibrium partition coefficient. Because there is no direct data available for the rate of transfer of creatinine across the red cell membrane, it is possible that the effective partition coefficient value is less than the equilibrium partition coefficient value. Because the effective partition coefficient value for creatinine can be between 0.6 to 1.4, the equilibrium value of 2.0 was used for this work. The reliability of the average predicted effective partition coefficient was not sufficient to warrant its use.

The average predicted effective partition coefficient value for uric acid disagrees with the value assumed (zero) for this work. No explanation for this disagreement is apparent. Because the experimental dialysate concentrations are so low, there is a possibility that an error in the zeroing of the measuring device would result in a systematic error in the measured outlet dialysate concentrations which could result in the disagreement shown.

Certain concepts of hemodialysis need to be re-examined in the light of the use of effective blood concentrations to determine

mass transfer. Clearance, defined as the hypothetical volume of plasma completely cleared of a substance in a unit time, is represented by

$$C = \frac{Q_b[C_{p_i} - C_{p_o}]\ [1 + (J - 1)\ H]}{C_{p_i}} \qquad [13]$$

neglecting ultrafiltration and transfers of bound material. Dialysance is commonly defined as the quantity of a substance transferred between blood and dialysate per unit of time per unit concentration difference of that substance between the inlet blood and the inlet dialysate (46, 52). It is also commonly stated that the dialysance is equal to the clearance when the entering dialysate is devoid of the substance. Hence the concentration gradient spoken of in the definition of dialysance is meant to be the gradient between the plasma and the dialysate entering the dialyzer. Dialysance then is

$$D = \frac{Q_b\ [C_{p_i} - C_{p_o}]\ [1 + (J - 1)\ H]}{C_{p_i} - C_{d_i}} \qquad [14]$$

Accordingly, dialysance should be more carefully defined as "the quantity of a substance transferred between blood and dialysate per unit of time in response to the concentration gradient of that substance between the plasma and the dialysate entering the dialyzer."

Dialysance may, of course, be defined in any fashion desired; but it is worth noting that the concentration gradient between plasma and dialysate may not be the best representation of the driving force for the mass transfer. Equation [10] suggests that the gradient

should be expressed as the difference between the effective blood concentration and the dialysate concentration. The flow pattern in the dialyzer has a strong influence on the "best" choice for the gradient to represent the driving force. If only plasma were in direct contact with the membrane, the obvious gradient to represent the transfer across the membrane would be the plasma-dialysate gradient. If only cells were in contact with the membrane, the choice for the gradient would be the cell-dialysate gradient. This latter case could be brought about in at least two ways. First, many dialyzers with very poor flow patterns have an accumulation of red cell "sludge" in those regions of the dialyzers where the blood flow is particularly slow. In addition, after six hours of dialysis a noticeable coating of foreign material, probably largely lymphocytes, forms on the membrane surface (3). Interestingly, this coating results in a very substantial drop in efficiency of the dialyzer (3).

Even if there is no cell coating on the membrane, the best choice for the blood-side concentration to use in calculating the gradient is influenced by the flow pattern. Experimental evidence indicates that at low hematocrits cells tend to accumulate in the center of the blood channel and away from the membrane walls (6, 40, 41). If this is true, then for cases in which there is no red cell "sludge" or lymphocyte membrane coating the concentration gradient is probably best represented by the plasma-dialysate gradient. In any case, work should be carried out to elucidate further this subject. Until such work is done, the plasma-dialysate gradient will

probably be used to represent the driving force because the plasma concentration of a substance is so easily obtained relative to the cell concentrations and effective blood concentrations.

Another hemodialysis concept which needs re-examining is the concept of maximum dialysance introduced by Sweeney (47). Using the usual dialysance equation, which follows from equation [4a],

$$D = \frac{Q_b (c_{b_i} - c_{b_o})}{c_{b_i} - c_{d_i}} = \frac{Q_d (c_{d_o} - c_{d_i})}{c_{b_i} - c_{d_i}} \qquad [15]$$

Sweeney determined the maximum possible dialysance for any substance. For a countercurrent-flow dialyzer, such as the Kiil, the maximum dialysance is the lower of the volumetric flow rates of the blood and the dialysate. The lower flow rate is invariably the blood flow rate. For a concurrent or random flow pattern, the maximum dialysance according to Sweeney is

$$D_{max} = \frac{Q_b \cdot Q_d}{Q_b + Q_d} = \left[\frac{1}{Q_b} + \frac{1}{Q_d}\right]^{-1} \qquad [16]$$

This maximum dialysance concept is useful because it expresses maximum achievable dialysance only as a function of blood and dialysate flow rates and independent of other variables, such as concentrations. Thus maximum dialysance provides a goal for the design of artificial kidneys, and it is used as such in the literature.

For <u>in vivo</u> measurements, however, dialysance is correctly described by equation [14], not by equation [15]. Equation [15] is correct for <u>in vitro</u> measurements in which the "blood" is a homogeneous saline solution. Maximum dialysance <u>in vivo</u> is not

equivalent to maximum dialysance *in vitro* in which artificial blood solutions are used. From Sweeney's arguments, the maximum *in vivo* dialysance for a countercurrent-flow dialyzer with blood flow substantially lower than dialysate flow is

$$D_{max} = Q_b\,[1 + (J - 1)\,H] \qquad [17]$$

and the maximum dialysance for concurrent and random-flow dialyzers is

$$D_{max} = \frac{Q_b \cdot Q_d \cdot [1 + (J - 1)\,H]}{Q_b\,[1 + (J - 1)\,H] + Q_d} = \left[\frac{1}{Q_b\,[1 + (J - 1)\,H]} + \frac{1}{Q_d}\right]^{-1} \qquad [18]$$

The maximum dialysance *in vivo* is therefore dependent on certain characteristics of the patient-dialyzer system and is not identical even for the same patient for all substances being removed from the blood.

Parameters of Dialysis

The total resistance to mass transfer through the membrane in hemodialysis is the result of three resistances acting in series. The first is the resistance to transfer within the blood boundary layer. The second is the resistance to transfer through the membrane itself. The third, and the least important under conditions of actual dialysis, is the resistance to transfer through the dialysate boundary layer. The parameters which affect each of these three resistances will in turn affect the overall resistance, although the effect on the overall resistance will be diminished somewhat. The variables which would be expected to influence the resistances

are well known from the voluminous mass-transfer work on other systems.

The variables which affect mass transfer in hemodialysis may be divided, albeit somewhat arbitrarily, into two groups. One group would consist of those variables which are, as a rule, fixed during the course of a particular dialysis; but which may vary substantially from one dialysis to another. One such variable, and probably the most important one, is the inherent membrane resistance to transfer, or the "tightness" of the membrane used, for a particular dialysis. Naturally this resistance is a function of the chemical composition of the membrane. More importantly, it is also a function of the method of manufacture used for the membrane and even of the exact conditions existing when that particular piece of membrane was manufactured and formed. The resistance of the membrane may be modified before and during the course of a dialysis by stretching and other means, but experience has shown that even under substantially different methods of handling at dialysis centers, each membrane of a particular lot behaves quite similarly to membranes of the same lot and usually quite different from membranes of the same type but of a different lot. Other variables in this group would include certain characteristics of blood, such as hematocrit, protein concentrations, etc., which are relatively constant for a particular patient during a dialysis but which vary from one patient to another.

The second group of variables would consist of those variables which vary substantially not only from one dialysis to another but also during the course of a particular dialysis. A great number of more readily measured variables appear in this group. Blood and

dialysate velocities and volumetric flow rates, available membrane areas, blood layer thicknesses, the stretch imposed on the membrane by the difference in pressure across the membrane, and the elapsed time of dialysis are some such variables. This work deals primarily with the effects of variables in this second group on mass-transfer rates during dialysis.

Four parameters upon which blood film resistance to mass transfer might be expected to depend can be determined from the available data. Blood velocities, both linear and volumetric, are available. The effect of volumetric blood flow rate changes on the mass transfer in a Kiil dialyzer has been investigated. This volumetric blood flow rate has not, however, been converted to linear blood velocities by using dialyzer dimensions. Dialyzer dimensions may also be used to calculate the blood layer thickness. Should the diffusivity of the substance vary with the plasma concentration of the substance, the blood film resistance would also depend on this concentration. In addition, hematocrit should exert a significant influence on the mass transfer of materials which transfer relatively slowly out of the red cells. Because the blood composition is changing with time, it is conceivable that the blood film resistance to mass transfer through the membrane would vary with the elapsed time of dialysis.

Resistance to transfer in the membrane is known to be affected by the stretching of the membrane in a two-dimensional or one-dimensional fashion. One-dimensional stretch of the membrane during dialysis can be calculated from the dialyzer liquid capacitance and the dialyzer dimensions. It is also conceivable that the membrane

characteristics might change during dialysis and thus the membrane resistance may show some dependence on the elapsed time of dialysis. The deposition of a coating during dialysis would be one such possibility. The resistance of each of the membranes cannot be known at the start of dialysis since the necessary information was not available.

Dialysate flow rate is set at a relatively high value in order to make the dialysate film resistance relatively small. Still, it is possible that variations in the conditions of dialysis would vary the dialysate film resistance enough to cause a noticable variation in the total resistance. The parameter which would most likely bring about the largest variation would be the dialysate flow rate. It is possible to calculate linear dialysate velocities from the information available.

Equations For Linear Velocities and Available Area

The membrane area available for transfer and the linear blood and dialysate velocities may be calculated using Figures 1, 2, and 3. On each polypropylene board are machined 150 grooves such as the one shown in Figure 2. For the model, let us approximate the dialyzer board shown in Figure 1 with a hypothetical dialyzer board in which the region coming in contact with fluids is simply a rectangular surface with 150 grooves all 35 inches long.

A dialyzer built with these hypothetical boards will then have a total of 600 of the sections shown in Figure 2, 300 in each layer. Each section is 35 inches long. In each section, the cross-sectional area of blood in cm^2 is related to the total volume of blood in the

dialyzer in cm^3 by the equation

$$(600)(L)(S_b) = V_b \quad [19]$$

or

$$S_b = 1.875 \times 10^{-5} V_b \quad [20]$$

The total cross-sectional area not blocked by the membrane support of the section shown in Figure 2 is found graphically to be 0.01458 cm^2 so the cross sectional area in cm^2 per section of dialysate is

$$S_d = 0.01458 - S_b \quad [21]$$

neglecting the area taken up by the thin membrane. Cuprophane is about 0.035 mm thick when wet [51] and the cross-sectional area of the groove space occupied by membrane is about 5% of the total open cross sectional area. The neglect of membrane thickness causes the calculated linear dialysate velocity to be consistantly about 6% low. Since linear dialysate velocity does not enter importantly henceforth, the neglect of the membrane thickness is acceptable.

As the blood volume in the dialyzer increases, the membrane is stretched in a one-dimensional fashion to accomodate the increase. An increase in dialyzer blood volume pushes the membrane farther down the walls of the membrane support in each groove. Assuming that each groove is identical to every other and that the membrane does not sag between supports but goes directly and horizontally across from one support to the next, it is possible to calculate the total membrane width per section and the available membrane

width per section as a function of the blood cross-sectional area per section by graphically integrating over the section shown in Figure 2. The results of the graphical integrations are plotted in Figures 4 and 5. Figure 4 presents the total membrane width per section, i.e., the length of membrane necessary to stretch across the width of the section and to enclose the specified blood cross-sectional area. Figure 5 presents the available membrane width per section as a function of blood cross-sectional area per section. The available membrane width per section is simply the length of membrane per section which is not resting against the walls of the membrane support. Thus dialysate and blood are both in contact with the membrane over this length and mass transfer between fluids may occur over this length of membrane.

The average blood layer thickness is calculated by dividing the blood cross-sectional area per section by the 0.2032 cm or 0.080 inch width of the section and multiplying the result by 2, the number of boards forming one layer. There is a close relationship between membrane stretch and blood layer thickness. The thicker the blood layer, the more the membrane must stretch one-dimensionally to enclose the blood. The nature of the relationship is shown in Figure 6. The relationship is almost linear.

All of the results thus far have been obtained from only graphical treatment of the hypothetical dialyzer board dimensions. All of these variables may be expressed as functions of the pressure difference across the membrane if the dialyzer capacitance curve is known. As previously mentioned, we assume the dialyzer capa-

citance curve for all of the dialyzers is represented by the inflation curve marked on Figure 3. Using this relationship for blood volume in the dialyzer and pressure difference across the membrane and equation [20] the curve in Figure 7 relating blood cross-sectional area per section to pressure difference across the membrane is obtained. The curve is fitted by the following equations

[22]

$$S_b = 3.65 \times 10^{-3} + 1.40 \times 10^{-5} \Delta p_m \qquad 25 < \Delta p_m < 50$$

$$S_b = 3.82 \times 10^{-3} + 1.06 \times 10^{-5} \Delta p_m \qquad 50 < \Delta p_m < 170$$

The linear blood velocity in cm/min in the dialyzer is calculated by dividing the volumetric flow rate of blood in ml/min by 600 S_b since there are 600 sections in the two-layer Kiil.

The curve in Figure 4 is represented analytically in the range of interest to us by

[23]

$$W_m = 0.19230 + 6.80\ S_b$$

where the total width is in cm and the area in cm^2. The curve in Figure 5 is represented analytically in the range of interest by

[24]

$$W_{a_m} = 0.19098 - 8.04\ S_b$$

where the width is in cm and the area in cm^2. The total membrane width (and hence the one-dimensional stretch of the membrane) and the available membrane width are only a function of the pressure difference across the membrane once the dialyzer dimensions have been specified.

There are 600 sections in the two-layer Kiil, and our hypothetical board places the length of these grooves at 35 inches or 88.9 cm. The total available membrane area in cm^2 is then

$$A_{a_m} = (600.)88.9\ W_{a_m} = 53{,}340\ W_{a_m} \qquad [25]$$

The nominal area for transfer is the area of the actual Kiil dialyzer boards which is in contact with the fluids. This nominal area, often used in the literature as an approximation to the transfer area of the membrane, is the sum of the area of the rectangular space occupied by the grooves and the two triangular spaces connecting the groove space to the blood ports (see Figure 1). The nominal area for transfer for each membrane is 402.75 in^2 or 2598.40 cm^2. Figure 8 shows the per cent of this nominal membrane area that is available for transfer according to equation [25]. The magnitude of the dependence of the available membrane area upon pressure difference across the membrane is also shown in Figure 8.

Regression Equations and Techniques for Overall Mass-Transfer Coefficient

The overall mass-transfer coefficient, sometimes called the **permeability**, for a dialyzer is defined for this work by the following equation

$$\dot{m} = PA_{a_m} \frac{(c_{p_i} - c_{d_o}) - (c_{p_o} - c_{d_i})}{\ln \frac{c_{p_i} - c_{d_o}}{c_{p_o} - c_{d_i}}} \qquad [26]$$

Rearranging the above equation to isolate the overall mass-transfer coefficient gives

$$P = \frac{\dot{m} \ln \dfrac{C_{p_i} - C_{d_o}}{C_{p_o} - C_{d_i}}}{A_{a_m}[(C_{p_i} - C_{d_o}) - (C_{p_o} - C_{d_i})]} \qquad [26a]$$

The overall mass-transfer coefficient defined by equation [26] is the coefficient historically used to describe the process of mass transfer in hemodialyzers. By considering momentum and concentration boundary layer lengths and thicknesses in hemodialyzers, one can raise legitimate questions as to the desirability of using such an overall coefficient. Nonetheless, no better alternatives are available, and the coefficient defined by equation [26] continues to be used.

This coefficient is a function of many parameters. It may arbitrarily be represented as a function of certain unknown variables X_1, X_2, ... X_n by the relation

$$P = K \cdot X_1^{a_1} \cdot X_2^{a_2} \cdot \ldots \cdot X_n^{a_n} \qquad [27]$$

in which K is a constant and a_1, a_2, ..., a_n are the powers to which the variables are raised. This expression allows non-linear dependencies of P on each of the n variables. It does not, however, allow one to determine whether the variables cause P to change because of variations in the blood film resistance, the membrane resistance, or the dialysate film resistance. Intuitive physical reasoning must be used to determine which of the three resistances the variations of each of the n variables affects. Equation [27] may be linearized by

taking logarithms of both sides to obtain

$$\log P = a_o + a_1 \log X_1 + a_2 \log X_2 + \ldots + a_n \log X_n \qquad [28]$$

where $a_o = \log K$

Equation [28] presents the logarithm of the overall mass-transfer coefficient as a linear function of the logarithms of the individual variables. It is therefore possible to use equation [28] to perform a linear regression analysis to determine the dependence of P for in vivo dialyses upon various parameters of dialysis.

The overall mass-transfer coefficient value is determined from equation [26]. The mass-transfer rate is calculated using equation [10] and the available membrane area using equation [25]. The log-mean gradient used in equation [26] is the gradient between plasma and dialysate. As noted previously, there is some question as to whether or not this is the proper choice for the gradient when the red cells are effectively permeable during dialysis, as is the case for creatinine and urea. Mass-transfer coefficients based upon the log-mean gradient between effective blood concentration and dialysate concentration were calculated for these components. Although the magnitudes of the P values were affected, the results of the regression analyses were not. In this work, therefore, all reported results are based upon the log-mean gradient between plasma and dialysate.

For these dialyses, dialysate was not recirculated so all four components are not present in the inlet dialysate and all $c_{d_i} = 0$. The outlet dialysate concentration c_{d_o} is calculated from

$$C_{d_o} = \frac{Q_b}{Q_d} [C_{p_i} - C_{p_o}] [1 + (J - 1) H] \quad [29]$$

Many models using many variables were fitted to equation [28] and regressed. Some of these will be discussed later. The final analyses were carried out to regress the logarithm of P with respect to six variables: linear blood velocity, the linear dialysate velocity, the pressure difference across the membrane, the elapsed time of dialysis, the blood hematocrit fraction, and the plasma concentration at the dialyzer inlet. Linear dialysate velocity failed to correlate for any of the four substances and so is not included in the resulting discussions. This failure to correlate is logical because previous work (20, 23) has shown that dialysate flow rates of the magnitude encountered here are so high that changes in the dialysate flow rate do not affect transfer. The pressure difference across the membrane was used as a variable instead of the membrane stretch or the blood layer thickness. Membrane stretch and blood layer thickness cannot both be used as dependent variables in the regression analysis because, as Figure 6 shows, they are closely related to one another. A regression analysis cannot differentiate between a dependency of the dependent variable on membrane stretch from a dependency on blood layer thickness. Since both membrane stretch and blood layer thickness are functions only of the pressure difference across the membrane, it is more reasonable to use the pressure difference as the variable in the regression analysis than either one of the two derived variables.

The regression analysis program used was the REGRES subroutine

kept on file at the Caltech computing center. A copy of this subroutine in Fortran IV language is presented in Appendix A. A detailed discussion of the subroutine is available (39). The technique of application of the multiple regression analysis is discussed in many texts (15). The definition and significance of the statistical terms involved in the program similarly appear in many references (7, 15, 32). The multiple regression solution gives the least squares "best" value of the coefficients a_o, a_1, a_2, $\cdots a_n$ for the particular sample of observations. The input data was assumed homogeneous, each point therefore having equal weight.

REGRESSION ANALYSES RESULTS

Overall Mass-Transfer Coefficient Regression Results

The results of the analysis of the overall mass-transfer coefficient for each of the four substances are presented in Tables IX and X and Figures 11 through 15. The mass-transfer coefficient for each substance is represented by the expression

$$P_{eqn} = K\ (v_b)^{a_1}\ (\Delta p_m)^{a_2}\ (1 + t)^{a_3}\ (H)^{a_4}\ (c_{p_i})^{a_5} \qquad [30]$$

The values for the constant and the exponents are given in Table IX. For instance, creatinine's mass-transfer coefficient is given by

$$P_{eqn} = 4.601 \times 10^{-3}\ (v_b)^{0.245}\ (1 + t)^{0.077} \qquad [31]$$

Table IX also presents the standard deviation of the exponential value and the confidence limit of that exponential value according to the regression analysis. When the variable did not have a

confidence limit exceeding 80% the confidence limit was not given except in a few special cases.

Table X presents the average value of the mass-transfer coefficient for all the experimental points for each substance. It also presents the standard error of this average mass-transfer coefficient value for all the experimental points. Because not all the experimental points were common to each of the four substances, the average value for each substance cannot be compared to one another because different average conditions were present for each substance.

The standard error of the difference at each experimental point between the predicted P value according to [30] and the actual P value calculated from the experimental data is also given in Table X for each component. The standard error of the mass-transfer differences expressed as a percentage of the average P value is the value of the following expression

$$\frac{100}{P_{avg}} \sqrt{\frac{\sum_{i=1}^{M} \left[P(i) - P_{eqn}(i) \right]^2}{M}} \qquad [32]$$

where there are M experimental points available to determine P. This standard error of differences was one of two criteria used to determine the desirability of each model. The first and most important criterion was the consideration of how accurately the variables of the model and their calculated exponents represented the actual physical processes occurring in the dialyzer. This largely involved intuitive reasoning because of the lack of extensive, mean-

ingful experimental data. The second criterion was the consideration of the magnitude of the standard error of the differences. The minimization of this quantity implies that the predicted equation from the model best fits the data. The final results of the regression analysis did minimize this standard error of differences.

One can compare the mass-transfer coefficient magnitudes for different substances by calculating the predicted mass-transfer coefficient according to equation [30] at certain specified reference conditions. Reference, or standard, values for mass-transfer coefficients, dialysances, relative dialysances, and relative permeabilities in this work are those values of the quantity which exist under the following conditions in the Kiil:

a. volumetric blood flow rate of 200 ml/min
b. volumetric dialysate flow rate of 500 ml/min
c. pressure difference across the membrane of 50 mm Hg
d. elapsed time of dialysis of 30 minutes
e. blood hematocrit fraction of 0.26
f. for phosphate, an arterial plasma concentration of 7.0 mg% inorganic phosphate

Conditions (a) and (c) coupled with the dimensions of the Kiil dialyzer result in a reference blood velocity of 76.62835 cm/min and a reference available membrane area of 8321.57 cm^2. Reference values of the mass-transfer coefficient are presented in Table X.

The reference values reported may be used to calculate the value of the mass-transfer coefficient at any conditions of dialysis. Reference values of the mass-transfer coefficients also enable one

to compare the magnitudes of the coefficients for different substances at the reference conditions. Of course, as the reference conditions change, so will the reference values, and the reference values will not all change in the same fashion.

Figure 9 and Figure 10 are two typical scatter diagrams for the results obtained. Figure 9 is the scatter diagram for the creatinine dialysance dependency on the linear blood velocity. This was the dependency with the highest confidence limits so the scatter diagram shows the least scatter of points. Figure 10 is the diagram for the pressure difference dependence of the dialysance of phosphate. This was the dependency with the lowest confidence limits and the scatter diagram shows the greatest amount of scatter of the experimental points. The lines drawn through Figures 9 and 10 represent the changes in the dialysance as the variable involved changes from the standard value when all other variables are at their standard values. The change in the dialysance is calculated by using the exponents presented in Table X. The points on the plots are derived from the experimental data. The dialysance is calculated from the experimental data according to equation [14]. Then the dialysance value for each point was corrected to that dialysance value which would exist if all variables but the one plotted on the abscissa were at the standard values for the variables. For example, for the creatinine points plotted in Figure 9 the corrected dialysance at each point is calculated from

$$D_{corr} = D \left(\frac{1.5}{1 + t}\right)^{0.077} \qquad [33]$$

This corrected dialysance is compared to the reference dialysance value and the percentage difference from the reference value is plotted on the ordinate.

Figure 11 shows the dependence of each of the four mass-transfer coefficients on linear blood velocity. The exponents for creatinine and urea are close enough that both values fall well within the range of the standard deviations of both exponents, as may be seen from Table IX. The uric acid and phosphate dependency curves are each substantially removed from all the other curves and so indicate a clearly different dependence upon blood velocity. The mass-transfer coefficient increases as blood velocity increases, which is expected since it has long been known that an increase in volumetric blood flow rate through a dialyzer increases the efficiency of transfer.

By the use of a Wilson plot, values for the membrane resistance and the blood film resistance may be calculated from the results of the regression analysis. The total resistance to mass-transfer across the membrane, which is the reciprocal of the permeability, is the sum of the individual resistances for the membrane and the blood film (30)

$$R_t = \frac{1}{p} = R_m + R_b \qquad [34]$$

The membrane resistance is unaffected by alterations in the blood flow rate, so equation [34] may be written

$$R_t = R_m + B_v^a \qquad [35]$$

If the resistance of the blood film is a power function of one

velocity, then a plot of the total resistance versus the velocity to the pertinent power a yields a straight line whose slope is the value of the constant B and whose intercept is the value of the membrane resistance R_m (30). The total resistance was calculated by using the results of the regression analysis and considering all variables except the linear blood velocity to be at reference values. The results of the Wilson plot are presented in Table XVII. Figure 24 presents a typical Wilson plot as was constructed in this work. The reference membrane resistance and reference blood film resistance are those values of the resistances which exist at the reference conditions.

These results may be compared to theoretical predictions. The blood film resistance is proportional to the linear velocity to the -0.8 power for turbulent flow (30), to the -0.33 power for laminar flow between two infinite parallel plates when the momentum and mass-transfer boundary layers are developing, and to the θ zero power in laminar flow when all boundary layers are fully developed (26, 34). The blood film resistances in this work are proportional to the velocity to the -0.2 to -0.5 power. Since the Reynolds number of blood in the dialyzer is about 2, this presumably implies that the irregularities in the dialyzer dimensions prevent the boundary layers from ever truly fully developing in the dialyzer. Thus, these results suggest that mass transfer in Kiil dialyzers occurs by molecular diffusion across developing boundary layers.

Figure 12 shows the dependence of the transfer coefficients upon the imposed pressure difference across the membrane. Creatinine

shows no dependence provided the available membrane area for transfer is calculated as a function of pressure difference according to equation [25]. If the available transfer area is assumed a constant, then the mass-transfer coefficient for creatinine decreases as the pressure difference increases. The mass-transfer coefficient of phosphate also shows no definite dependence on pressure difference. As Table IX indicates, however, the confidence limit is not too low, and it is possible that more experimental data could show a dependence.

The transmembrane pressure difference dependency is not, however, considered accurately determined, although the differences in the dependency from one component to another are genuine. To verify the applicability of the regression analysis results to individual dialyses, the mass-transfer coefficient data for a given component and independent variable were corrected as discussed earlier for the scatter diagrams in Figures 9 and 10. The corrected mass-transfer coefficients for each individual dialysis were plotted as a function of the independent variable to ascertain that the best line drawn through the data for each dialysis had the same directional slope as the line from the regression analysis using all the data. For all components and all independent variables except the transmembrane pressure difference, the slope of the regression analysis line was of the same sign as the slopes of the lines drawn through all points for individual dialyses. For the transmembrane pressure difference dependency of both urea and uric acid, however, only three of the nine dialyses had negative slopes like the regression

analysis line. Four dialyses had lines with positive slopes (P increasing as Δp_m increases) and two dialyses had lines of approximately zero slope.

For every dialysis, the slope of the pressure difference dependency line was the same for both urea and uric acid. This fact, coupled with regression analyses results using various dialyzer capacitance curves, suggests that the disagreement between the slope of the regression analysis line and the slopes of many of the individual dialysis lines for transmembrane pressure difference dependence is due to differences in the dialyzer capacitance curve from dialyzer to dialyzer, and hence from dialysis to dialysis. An alteration in the dialyzer capacitance curve pictured in Figure 3 does not affect the results of the regression analysis for any of the independent variables except the pressure difference across the membrane. It does slightly alter the magnitude of the mass-transfer coefficients because of the change in available membrane area for mass transfer, and it does alter the pressure difference dependence of the mass-transfer coefficients because of the change in the dependence of the available membrane area upon the transmembrane pressure difference. Although the differences of the transmembrane pressure difference dependence from one component to another remain unaffected by the apparent variations in dialyzer capacitance from one dialysis to another, the accurate determination of the pressure difference dependence of the mass-transfer coefficients must be done using dialyzers with known capacitance curves.

The dependency of the total permeability upon the pressure

difference across the membrane may be examined further using a modification of the Wilson technique. An alteration in the pressure difference across the membrane stretches the membrane. The stretching of the membrane changes the thickness of the blood layer, which in turn alters the resistance of the blood layer to transfer. In addition, evidence in in vitro systems has shown that one-dimensional stretching of the membrane hinders the transfer of sugar molecules through the membrane (13). It is not clear whether the transfer of smaller molecules would be similarly affected. Presumably, then, the variation of the total permeability may result from variations in both the blood film resistance and the membrane resistance. If both resistances are affected by changes in the pressure difference across the membrane, a Wilson plot of resistance versus pressure difference cannot be constructed with the information available. In order to construct a Wilson plot for the variations in total resistance caused by changes in the pressure difference across the membrane, one must first assume that changes in pressure difference affect only one of the resistances in series.

If this assumption is made and a Wilson plot prepared from the data, then the results of the Wilson plot may be analyzed to check at least partially the validity of the original assumption. If an extrapolation of the resultant straight line of the Wilson plot gives a negative value for the total resistance for any pressure difference greater than or equal to zero, then the assumption must be false since this situation is not physically possible.

Also, the resistance at zero pressure difference as determined by extrapolation is presumably the value of the resistance unaffected by changes in pressure difference. If the value of this resistance does not agree with physical intuition or with the values obtained from other Wilson plots for the same data in which another variable was considered, then presumably the original assumption was false. On the other hand, if the results from the Wilson plot pass the two tests mentioned, there is a reasonable basis, but not a conclusive basis, for believing that the assumption and the results based on it are correct.

For urea, the assumption that only one resistance is affected by the changes in pressure difference yielded excellent results from the Wilson plot. Table XVII shows that membrane resistance is unaffected by variations in the pressure difference across the membrane. For uric acid, the assumption that only one resistance is affected by pressure difference changes did not yield completely satisfactory results. The membrane resistance in Table XVII for uric acid for the pressure difference Wilson plot results is almost twice that calculated from the velocity Wilson plot. Nonetheless, the scatter in the original data could result in this difference.

The average thickness of the blood film is a function of the pressure difference to the 0.146 power, so the Wilson plot results for pressure difference may be expressed in terms of the average blood film thickness. When this is done, the blood film resistance of urea is proportional to the blood layer thickness to the +1.4 power and R_b of uric acid is proportional to the blood layer

thickness to the +0.7 power. For turbulent flow, the predicted power is +0.2; for undeveloped laminar flow, the +0.33 power; and for fully developed laminar flow, the +1.0 power (26, 34) The Wilson plot results for urea and uric acid suggest fully developed laminar flow, but the lack of dependencies for creatinine and phosphate cast doubt on this. As mentioned previously, the regression analysis results for pressure difference dependence are not so good as desired, so the Wilson plot results are also indefinite.

Figure 13 illustrates the dependence of each mass-transfer coefficient upon time. Urea has no dependency. Phosphate, uric acid, and creatinine all show an increase in mass-transfer coefficient with increasing time of dialysis within the time span of 30 - 360 minutes of dialysis. Extrapolation of any of the curves presented in Figures 9 - 23 outside of the range or presentation is risky, but in the case of the time dependency curves it is almost guaranteed to be wrong. Experimental evidence has been presented (3) to show that after six hours of dialysis a coating of foreign material begins to form on the membrane which severely decreases the efficiency of dialysis. Thus curves in Figure 13, which show an increase in efficiency with time, should certainly not be extended beyond the first six hours of dialysis.

As was the case with the results of the regression analysis for the dependency of P upon the transmembrane pressure difference, a Wilson plot may be prepared for each component using the elapsed

time as a variable. Again, to obtain results one must first assume, and later check, that only one of the two resistances is affected by the change in time. When this assumption is made for creatinine, uric acid, and phosphate, each Wilson plot of R_t versus $(1 + t)^{\alpha}$ indicated that the change with time was due to some variation in the membrane resistance. For each of the three substances, the membrane resistance decreased with time inversely to $(1 + t)$. This result is somewhat anomalous since no prior investigation has shown a membrane resistance which decreases during the course of dialysis. One investigation previously mentioned, noted qualitatively the formation of a coating on the membranes of dialyzers after six hours of dialysis (3). In addition, Spaeth (45) has shown that in oxygenators with silicone-rubber membranes fresh blood induces no increase in membrane resistance but traumatized blood does cause membrane fouling after a short period of use in an oxygenator and hence an increase in membrane resistance. The apparent decrease in membrane resistance noted in this work should be investigated further and confirmed by other work.

Figure 14 shows the dependencies of the uric acid and phosphate mass-transfer coefficients upon the level of the patient's blood hematocrit. Urea and creatinine, which were assumed to maintain equilibrium between cells and plasma in the blood, show no dependence upon hematocrit. This is to be expected and tends to confirm our choice of setting the effective partition coefficient of creatinine equal to the equilibrium partition coefficient. Uric acid and phosphate, which were assumed to be frozen into the cells

during passage through the dialyzer, show a very strong decrease in mass-transfer coefficient with increasing blood hematocrit. The direction of the effect, increasing P values with decreasing hematocrit, is what one would expect, although the magnitude of the changes in P is quite large for the relatively small changes in hematocrit. At least two processes probably contribute to the effect of hematocrit on the mass-transfer coefficient. The presence of impermeable particles in the flowing blood increases the effective path length that the substance molecule must travel to reach the membrane, thus slowing down the transfer rate because of an increase in the blood film resistance. Also, the greater the fraction of cells in the blood, the greater the area of the membrane which will be in contact with the cells at a given time. When the material involved cannot be transferred across the cell membrane, the membrane area in contact with the cells is effectively shielded from the plasma and transfer cannot take place across this shielded membrane area.

Wilson plots to explain the dependency of the total permeability in terms of the membrane and blood film resistances could not be prepared. If one assumes that the hematocrit affects only one of the resistances, then one can only construct a straight-line Wilson plot by allowing negative resistances. This indicates the assumption that the hematocrit variations only affect one resistance is not valid, and indeed one would expect this to be the case.

A quantitative hypothesis describing the effect of hematocrit upon the total permeability results when an analytical model of a

dialyzer developed by Grimsrud and Babb (4, 24) is combined with certain assumptions regarding the behavior of red cells in the dialyzer. Grimsrud and Babb approximated the blood layer in the dialyzer as being confined between two semi-infinite parallel plates. Assuming fully-developed laminar flow, constant diffusivity, and negligible axial diffusion, the governing equation for mass transfer in the system is

$$\frac{\partial^2 c}{\partial y^2} = \frac{3}{2}\frac{v_{avg}}{\mathcal{D}}\left(1 - \frac{y^2}{h^2}\right)\frac{\partial c}{\partial x} \qquad [36]$$

where the x-coordinate is in the direction of flow and the y-coordinate is perpendicular to the membrane surfaces. The necessary boundary conditions for the problem are the following:

$$\frac{\partial c}{\partial y} = 0 \quad \text{at dialyzer centerline}$$

$$c = c_i \quad \text{at dialyzer inlet} \qquad [37]$$

$$-\mathcal{D}\frac{\partial c}{\partial y} = \mathcal{P}c \quad \text{at membrane}$$

The solution of this set of equations expresses the Sherwood number in terms of eigenvalues which are functions of the parameters of the system. The Sherwood number for the two-layer Kiil is about 1.0. For Sherwood numbers around 1.0, one can determine from Babb and Grimrud's solution that the total permeability is related to the membrane permeability and the diffusivity by the following equation:

$$P = K\,\mathcal{P}^{0.76}\,\mathcal{D}^{0.24} \qquad [38]$$

Equation [38] is valid for an inhomogeneous media, such as blood, when the diffusivity and membrane permeabilities are the

effective values which exist at the particular concentration of suspended particles. One can determine the dependence upon hematocrit of the total permeability of a dialyzer for a substance impermeable in red cells by estimating the dependence of ρ and Ω upon variations in blood hematocrit.

The effective diffusivity in blood for any substance is estimated in this work from a theory developed by Fricke (19). This theory has been confirmed experimentally by measuring the rate of diffusion of dissolved gases through blood (45). Related experimental data exist in the literature (14), but the use of the theory of Fricke is probably better for this work (45). For hematocrits around 0.25, Fricke's theory states that Ω is proportional to the hematocrit to the -0.52 power, so that

$$P = K \rho^{0.76} H^{-0.13} \qquad [39]$$

The total permeability is strongly dependent upon the variations of the effective membrane permeability. The effective membrane permeability is reduced by the presence of impermeable, inert particles in the blood because the contact of these particles with the membrane effectively masks off the contacted membrane and reduces the available area for transfer. Part of the contact between these impermeable particles (which can be red cells, white cells, lymphocytes, proteins, and platelets) and the membranes is between particles which have adhered to the membrane either as individual particles or as a sludge. Platelets, lymphocytes, and proteins are known to adhere to the membrane throughout dialyzers, and cells are known to settle out of blood when the blood is flowing

slowly in "dead spaces" and to form sludges. Part of the contact between membrane and particles occurs when particles which are in motion are momentarily in sliding contact with the membrane.

The membrane area in contact with flowing red cells may be estimated by assuming a particular orientation of the cells with respect to the membrane. A red cell has the approximate shape of a filled-in doughnut with opposing concave surfaces enclosing the "top" and "bottom" of the cell. The maximum radius of the cell is 8.5 microns and the maximum thickness is 2 microns. The volume of an individual cell is 87 cubic microns, or just 77% of the volume of a cylindrical disk of identical radius and thickness. To determine the membrane area in contact with red cells, assume that the blood next to the membrane is of the same hematocrit as the bulk blood and that the cells are in contact with the membrane at their concave surfaces. Experimental evidence is available which suggests that this orientation of the cells with respect to the membrane surface in a flowing stream is the most probable orientation (36).

Under these assumptions, the fraction of the membrane area masked by the flowing cells can be determined by considering a small rectangular prism of blood 2 microns thick with a square cross-section impinging upon the membrane surface. The prism contains one cell and the length of the side of the square surface of the prism is adjustable. The length of the side of the square surface is uniquely determined by the hematocrit of the blood in the prism, since the hematocrit is equal to the ratio of the volume

of the red cell to the volume of the prism. The fraction of the membrane area covered by the prism which is masked off at a particular blood hematocrit is determined by calculating the length of the square side of the prism necessary to produce that hematocrit in the prism and then noting what fraction of the area of the square surface of membrane is masked off by the red cell. For example, at 25% hematocrit 32.5% of the membrane area is masked by the cell in the rectangular prism and this fraction is the fraction of the area masked in the entire dialyzer under the assumptions used in this work. By calculating results for hematocrits in the range covered by the data used in this work, one can determine that the available membrane area, and hence the effective membrane permeability, is proportional to the hematocrit to the -0.48 power for hematocrits around 25%. From equation [39], one can see that the variations in effective diffusivity and the variations in effective membrane permeability caused by cells in sliding contact with the membrane account for the total permeability being proportional only to the hematocrit to the -0.5 power.

The remainder of the total permeability's dependency upon hematocrit is presumably caused by the presence of particles in a stationary state upon the membrane. If the fraction of the membrane area which is masked by inert particles is equal to 2.3 times the hematocrit fraction, then the final predicted dependency of the total permeability upon hematocrit is that the permeability is proportional to the hematocrit to the -1.53 power. This value is in accord with the experimental results.

Although the model discussed above can offer a quantitative explanation for the observed dependence of the total permeabilities of uric acid and phosphate upon hematocrit, some objections can be raised to it. The results are quite sensitive to the effects of inert particle masking of the membrane surface, and the lack of quantitative experimental results in this regard necessitates the use of untried assumptions to estimate this effect. Under the assumptions used for the above model, slightly less than 60% of the membrane surface is apparently covered by some rather permanent adhesion of particles. This seems a high percentage, and the masking of this portion of the membrane should result in a higher membrane resistance than was calculated in this work from Wilson plots. Nonetheless, this model based upon the work of Grimsrud and Babb may offer some clues towards the eventual determination of the mechanism by which hematocrit affects transfer in hemodialyzers.

Figure 13 provides an indication that for the nine dialyses examined the hematocrit of each patient did not change appreciably during the course of the dialyses analyzed. For uric acid and phosphate, a change in hematocrit with time would result in a change in the mass-transfer coefficient with time. The curves in Figure 14 imply that the change in P with time for both substances would be nearly the same. Although the mass-transfer coefficients of both uric acid and phosphate show a change with time, the change of each is materially different. The change in the uric acid P with time is much less than the change in the phosphate P with time, although Figure 14 shows that the dependency of the uric acid P on hematocrit is slightly stronger than

the dependency of the phosphate P. This evidence indicates that the hematocrit of the individual patient remained fairly constant with time during the first six hours of dialysis for the dialyses being examined. Of course, any dialysis for which prior inspection showed this might not be true was not analyzed in this work.

Only inorganic phosphate, of the four components considered, showed any dependency of the overall mass-transfer coefficient upon the experimentally measured total arterial plasma concentration. This dependency is shown in Figure 15. This effect is only an apparent effect caused by the fact that the measured plasma concentrations are total concentrations, that is, the sum of both bound and unbound (free) forms of the component in the plasma. A significant portion of the phosphate in the plasma is not free but is bound to the proteins. Only the free inorganic phosphate is available for transfer.

One may show that the dependency of the overall mass-transfer coefficient upon the total arterial plasma concentration is caused by the use of total plasma concentrations in equation [26] rather than the proper free plasma concentrations for inorganic phosphate by assuming the bound inorganic phosphate remains at constant concentration throughout a single blood pass and calculating values for the overall mass-transfer coefficient using free plasma concentrations in equation [26]. Although the free plasma concentrations of inorganic phosphate were not measured, one can determine them using the regression analysis results above and the assumption just mentioned. The bound plasma inorganic phosphate is calculated to

be 1.40 mg%, and the overall mass-transfer coefficient calculated using free concentrations is not affected by changes in concentrations. At reference Q_b, Q_d, Δ_{Pm}, and H values, the P based on free concentrations has the value 0.00925 cm/min. Other regression analysis analysis results are not affected.

To develop the model for the regression analysis a number of simplifying assumptions were made. To ascertain that the effect of these assumptions is not serious, certain alterations were made in the model to determine what effects would result from errors in the simplifying assumptions. One such assumption was that the capacitance of every dialyzer is described by the inflation curve of Figure 3. To determine the significance of this assumption, the capacitance of every dialyzer was assumed to be described by the deflation curve of Figure 3. Using this curve new expressions were developed for the available membrane area and the linear blood velocity in the dialyzer and the regression analysis was repeated. The new mass-transfer coefficient values were slightly higher because the available membrane area was decreased. The magnitudes of the blood velocities involved were somewhat decreased, but the dependencies of each mass-transfer coefficient upon the blood velocities were unaffected. Time, hematocrit, and arterial concentration dependencies were unaffected. The pressure difference dependencies were increased somewhat, but not by a significant factor. This increase was because the use of the deflation curve to determine available membrane area made that area less sensitive to changes in pressure.

By using the inflation curve of Figure 3 and the values of the pressure difference across the membrane at each point in time, one is in effect assuming that the membrane stretches reversibly during dialysis. Partial irreversibility can be assumed by using for the pressure difference at each point in time of a dialysis the largest pressure difference across the membrane recorded during the dialysis up to that time. This was done, and the results were not substantially different from those assuming reversible membrane stretching. Mass-transfer coefficients which had no dependence upon certain variables when the membrane was assumed to behave reversibly showed no dependence when the membrane was assumed to behave irreversibly. Mass-transfer coefficients which had a dependence upon certain variables under the assumption of a reversible membrane generally had increased values of the exponent (hence stronger dependencies) when the membrane was assumed irreversible. The increases, however, were always less than the standard deviation of the original exponent. The assumption of the irreversibility of the membrane stretch was not used because the magnitudes of the stretches involved were quite small (less than 5% of the width) and the experimental evidence available tended to point to reversible stretching under these conditions.

Different values for the effective partition coefficient were employed in the model to determine the effects of a change in J from the value assumed for the final results. For each component, the only alteration in the final results was that the magnitudes of the average and reference mass-transfer coefficients were

altered.

The manner in which the blood samples were handled results in some probable error in the values of the measured outlet plasma concentrations of uric acid and phosphate. When the blood leaves the dialyzer and is taken out of the venous line to be sampled, the red cells and the plasma are not in equilibrium with respect to uric acid and phosphate concentrations. The red cells, because of their relatively impermeable membranes, have a chemical composition which is still that which existed in equilibrium with the plasma at some time before the blood flowed through the dialyzer. When the blood flowed through the dialyzer, uric acid and phosphate were removed from the plasma but not from the cells, and a disequilibrium was established. The moment the blood leaves the dialyzer, the blood begins to proceed towards the equilibrium state for cell-plasma concentrations in uric acid and phosphate. Material is transferred out of the cells into the plasma, so the plasma concentration of uric acid and phosphate rises. Unless equilibrium is reached, this process will continue to occur until the red cells are separated from the plasma. This separation occurs after the samples have been spun down in the centrifuge for fifteen minutes during the hematocrit determination proceedure. Most blood samples were apparently not spun down immediately after being taken. Some samples were spun down immediately; some were not spun down for several hours. This has an obvious resultant effect on the measured plasma concentration of those substances whose effective partition coefficients are less than the equilibrium

partition coefficients.

Whether or not the blood entering the dialyzer has cell-plasma equilibrium depends primarily upon the rate of transfer across the cell membrane and the blood flow rate through the dialyzer. The volume of blood in the human body passes through the Kiil dialyzer in about 30 minutes. The half-time of transfer of uric acid across the red cell membrane is apparently about 10 - 20 minutes. Thus it is fair to conclude that the blood entering the Kiil dialyzer is close to equilibrium with respect to the cell-plasma concentration of uric acid. The half-time of transfer of phosphate across the red cell membrane is the order of magnitude of 2 - 3 hours. Thus the blood entering the Kiil dialyzer is probably not quite in equilibrium with respect to cell-plasma concentrations of phosphate.

For uric acid and phosphate, the regression analysis was performed using a corrected value for the outlet plasma concentration of each of the substances. The inlet blood was still assumed to be in cell-plasma equilibrium, but the assumption that the reported plasma concentration for the outlet blood stream was in fact that which existed at the dialyzer outlet was abandoned and the assumption was made that the samples were allowed to sit around before the separation of the cells until there was cell-plasma equilibrium. Under this assumption the reported plasma concentration for the outlet blood stream is too high. Assuming that the cells in the outlet blood stream were at the concentration which exists in equilibrium with the plasma at the dialyzer inlet,

one can calculate the corrected outlet plasma concentration using a material balance.

When the regression analysis was completed using this new, corrected outlet plasma concentration for uric acid and phosphate, the magnitudes of the average and reference values of the mass-transfer coefficients were 23% higher for uric acid and 36% higher for phosphate. The dependencies of the mass-transfer coefficients on all variables except blood hematocrit were unaffected. The dependencies of both mass-transfer coefficients upon blood hematocrit were somewhat lessened, but the exponent for the hematocrit was decreased by only about half of the standard deviation of the exponent value for the original model for both compounds.

Finally, the material transferred in the dialyzer has been calculated by equation [10] for this model. This equation neglects the effects of ultrafiltration upon the transfer. Randall Cook (12) determined that the ultrafiltration rate in ml/min is related to the pressure difference across the membrane in mm Hg by the equation

$$\text{ultrafiltration rate} = \frac{1.35\ \Delta p_m + 23.4}{60} \qquad [40]$$

This equation is only a first approximation to the rate of ultrafiltration, but it is as good as is available. When water is ultrafiltrated through the membrane, a certain amount of solutes will be transferred across the membrane by "solvent drag" (5). Just how much solute will be transferred per unit of water transferred is unknown. It would at the least be zero. It would at

the most be equal to that amount of substance which exists in a unit volume of the bulk plasma.

To determine the maximum possible effects of neglecting ultrafiltration, the mass transfer across the membrane was corrected by subtracting out that material and water which was transferred by ultrafiltration. The difference between the rates of fluid flow into and out of the dialyzer was equal to the ultrafiltration rate of water. Two corrections were made to account for the solute removed by the solvent drag. The first correction was to assume no material besides water passed through the membrane. The second correction was to assume that the water passed through the membrane as plasma with the average concentrations of each component equal to those measured at the dialyzer inlet. These assumptions represent the two possible extreme occurrences.

The changes in the regression analysis results were not important. The magnitudes of the mass-transfer coefficients were changed slightly. The only dependencies which were affected were the dependencies of the mass-transfer coefficients upon the pressure difference across the membrane. The magnitudes of the pressure difference exponents were changed to greater numbers when the maximum possible amount of solute material was assumed to be transferred by solvent drag, and to lesser numbers when no solute material was assumed to be transferred by solvent drag. But in all cases, the exponents remained negative when the confidence limits were significant. From a physical standpoint, the

neglect of ultrafiltration is believed quite reasonable; and these results indicate that under no circumstances could the neglect of ultrafiltration for these analyzed dialyses significantly alter the final results other than to change slightly the magnitudes of the mass-transfer coefficients.

The original regression analyses were performed by representing the total permeability as a function of the product of each independent variable raised to a certain power. Using the results of the Wilson plots, a modified regression analysis was made to check the validity of constructing Wilson plots from the results of the regression analysis. The calculated total permeability was corrected, as discussed earlier, to the reference values of t, H, and c_{p_i}. Then the value of the reference membrane resistance for each component as presented in Table XVII was subtracted from the reciprocal of the corrected total permeability and this quantity, equivalent to a hematocrit-independent blood-film resistance, was entered as the dependent variable in a regression analysis. The independent variables were $v_b^{\alpha 1}$ and $\Delta p_m^{\alpha 2}$, again expressed as a product. In each case the values from the regression analysis for α_1 and α_2 were identical to the results from the Wilson plot, indicating that constructing Wilson plots using the results of the original analysis gives accurate values for the blood-film and membrane resistance values.

Dialysance Regression Analysis Results

For the regression analysis of the dialysance of each substance,

the dialysance at each experimental point was calculated by

$$D = \frac{Q_b \, [c_{p_i} - c_{p_o}] \, [1 + (J - 1) \, H]}{c_{p_i} - c_{d_i}} \qquad [41]$$

Equation [41] calculates the in vivo dialysance for each substance. Using the results of the regression analysis for the mass-transfer coefficient of each substance, dialysance could also be calculated at any specified Q_b, Q_d, Δ_{p_m}, t, H, c_{p_i}, and c_{d_i} values by first solving the following two equations simultaneously for c_{p_o} and c_{d_o}.

$$P_{eqn} \, A_{a_m} \frac{(c_{p_i} - c_{d_o}) - (c_{p_o} - c_{d_i})}{\ln \dfrac{c_{p_i} - c_{d_o}}{c_{p_o} - c_{d_i}}} = Q_b \, [c_{p_i} - c_{p_o}] \, [1 + (J - 1) \, H] \qquad [42]$$

$$c_{d_o} = \frac{Q_b}{Q_d} \, [c_{p_i} - c_{p_o}] \, [1 + (J - 1) \, H] \qquad [43]$$

and then calculating the dialysance from the equation

$$D_{eqn} = \frac{P_{eqn} \, A_{a_m} \, [(c_{p_i} - c_{d_o}) - (c_{p_o} - c_{d_i})]}{\ln \dfrac{c_{p_i} - c_{d_o}}{c_{p_o} - c_{d_i}} \, (c_{p_i} - c_{d_i})} \qquad [44]$$

after having solved for A_{e_m} and v_b from equations [22] and [25] and for P_{eqn} from the previous regression analysis results. The regression analysis of the dialysances calculated from [41] resulted in an expression of the form

$$D = \text{Const } (v_b)^{a_1} (\Delta p_m)^{a_2} (1 + t)^{a_3} (H)^{a_4} (c_{p_i})^{a_5} \quad [45]$$

Dialysances calculated by [45] were compared with dialysances calculated from [44]. In every case the agreement was satisfactory.

The results of the regression analysis of dialysances are presented in Tables XI and XII and Figures 15 through 19 in the same fashion that the mass-transfer coefficients results were presented. Table XI presents the constant and exponents necessary to calculate the predicted dialysances at any conditions according to equation [45]. Table XII presents the calculated average dialysance for each component, its standard error, the standard error of the dialysance differences (calculated according to equation [32] in the same fashion as was the standard error of the P differences), and the reference value of the dialysance for each substance.

Figure 16 shows the dependence of each dialysance as calculated by equation [45] on the linear blood velocity through the dialyzer. Figure 9 shows the scatter diagram for this dependence for creatinine. Dialysance has a stronger dependence upon blood velocity than the mass-transfer coefficient. This is the only variable for which this is true; for pressure difference, elapsed

time of dialysis, hematocrit, and arterial plasma phosphate concentration the dialysance of a given substance is a weaker function of the variable concerned than the mass-transfer coefficient. When a variable does not strongly influence the calculation of c_{p_o} and c_{d_o} according to equations [42] and [43]. equation [44] predicts that dialysance will have a lesser, or weaker, dependence on this variable than the overall mass-transfer coefficient. When calculating the mass-transfer rate in the numerator of [44], any increase, or decrease, in the mass-transfer coefficient because of changes in these variables will result in a decrease, or increase, respectively, in the log-mean concentration gradient which partially compensates for the change in mass-transfer coefficient. Thus the dialysance has a weaker dependence on variables which don't strongly affect the calculation of c_{p_o} and c_{d_o} according to [42] and [43]. The linear blood velocity, however, is closely related to the volumetric blood flow rate; and the volumetric blood flow rate strongly influences the calculation of c_{p_o} and c_{d_o} according to equations [42] and [43]. The net result of this influence is that dialysance of a substance depends more strongly on linear blood velocity than does the overall mass-transfer coefficient of the same substance.

The dialysance dependence upon the pressure difference across the membrane is shown in Figure 16. The scatter diagram for the dependence of the phosphate dialysance upon pressure difference is shown in Figure 10. Phosphate dialysance shows a dependency upon the pressure difference across the membrane although according

to the results of the mass-transfer coefficient regression analysis, the mass-transfer coefficient of phosphate does not show such a dependency. This results not from any particular physical phenomenum, but rather from the arbitrary analytical procedure of correlating only those variables whose confidence limits exceed 80%. For the phosphate overall mass-transfer coefficient, the pressure difference across the membrane failed to correlate by only a small margin. For phosphate dialysance, the pressure difference barely met the 80% confidence limit required to correlate. The relatively small change in the confidence limit was sufficient in this case to cause the variable to correlate for dialysance but not for the overall mass-transfer coefficient.

Figure 18 presents graphically the dependencies of the dialysances upon the elapsed time of dialysis. Once again, phosphate has the strongest dependence and creatinine and uric acid have weaker dependencies. Figure 19 presents the dialysance dependence upon the blood hematocrit, and Figure 15 presents the dependence of the phosphate dialysance on the arterial plasma concentration of phosphate. The results are expected in view of the results for mass-transfer coefficients.

Regression Analysis Results for Relative Dialysance and Relative Permeability

Because the values of both the dialysance and the overall mass-transfer coefficient have been known historically to vary with the volumetric blood flow rate in different fashions for different substances, efforts have been made to find some constant

parameter which can describe the dialysances of all substances at all blood flow rates. Two parameters have been examined for this purpose. The relative dialysance of a substance x, defined by

$$D_r = \frac{D}{D_s} \qquad [46]$$

and first examined by Wolf (47), was found to vary with the blood flow rate differently for each substance and thus not be satisfactory. The relative permeability, first proposed and examined by Sweeney (46) was defined by him as

$$P_r = \frac{P}{P_s} \qquad [47]$$

where the permeability of a substance x is given by equation [2]. Sweeney (46) found for in vitro tests that the relative permeability of a substance does not vary from a constant value. These results suggest that the relative permeability may be a useful concept for hemodialysis, even though the derivation of permeabilities from a simple mass-transfer expression gives no indication that the relative permeability of a substance should be any less a function of a parameter than dialysance, relative dialysance, or the overall mass-transfer coefficient.

Sweeney (46) and Wolf (52) based their relative dialysance and relative permeability measurements upon the dialysance of chloride as a standard reference substance. They tested only to see if the relative dialysance and the relative permeability coefficients for certain substances varied with changes in the

volumetric blood flow rates through the dialyzers. Wolf used a rotating-drum dialyzer and Sweeney used a Twin-Coil dialyzer and a Klung dialyzer.

Since chloride dialysances were not available for this work, the standard reference substance for the calculation of *in vivo* relative dialysances and relative permeabilities using the data available to us from the Kiil dialyzers was chosen to be urea. The dialysance at each experimental point was calculated from equation [41]. Relative dialysances for each substance at each experimental point were then calculated from equation [46]. Permeabilities and relative permeabilities for each experimental point were calculated by equations [2] and [47] respectively. The maximum dialysance for a counterflow dialyzer such as a Kiil is the volumetric blood flow rate. The regression analysis results for relative dialysances and relative permeabilities are tabulated in Tables XIII through XVI and are plotted in Figures 15 and 20 through 23.

Tables XIII through XVI present the data in the same form as was used for the mass-transfer coefficient and dialysance results. Similarly, the figures show the changes in both of the relative coefficients from the standard values when a particular variable is altered. The results as a whole are not surprising. They clearly indicate that for *in vivo* dialyses using Kiil dialyzers, neither the concept of relative dialysance nor the concept of relative permeability has much use, if any, in the generalization of mass-transfer results.

Implications of Results

The reliability of the magnitudes of the reported overall mass-transfer coefficients, dialysances, relative dialysances, and relative permeabilities is not as good as is desired. To a large extent this results from the lack of appreciation of cell-plasma mass-transfer kinetics when the data were taken. The reliability of further investigations into hemodialysis should be materially enhanced by an appreciation of cell-plasma mass-transfer kinetics and its effect upon experimental data.

Any substance whose effective partition coefficient is less than the equilibrium partition coefficient will not be in cell-plasma equilibrium in the blood outlet stream from the dialyzer. When a sample of blood is removed from the dialyzer outlet stream, the concentrations of these substances in both the cells and in the plasma will continuously change until equilibrium is established. The rate of change of these concentrations can vary markedly, since equilibrium may take only a few seconds to establish or may take days to establish. In order to obtain an accurate measurement of the plasma and, if needed, the cell concentrations of the substances in a blood sample not at equilibrium, the cells and plasma must be separated before the disequilibrium state of the blood is significantly altered or the blood should be allowed to reach an equilibrium state and the cell and plasma concentrations measured at this equilibrium state corrected in some manner back to the conditions existing in the stream leaving the dialyzer. One particular problem to be borne in mind

is that the usual method of separating cells and plasma, centrifugal spinning, takes 15 minutes to complete.

If the half-time of transfer out of the red cell into the plasma for a particular substance is of the order of magnitude of several hours or more, then one can separate the cells and plasma of any blood sample by the conventional centrifugal spinning technique before any disequilibrium state existing in the sample is materially altered. The samples should not be allowed to sit around long before being separated, however. For these substances, the usual methods produce accurate plasma concentrations in a blood sample not at equilibrium.

If the half-time of transfer out of the red cell into the plasma for a particular substance is of the order of magnitude of an hour or less, then one cannot separate the cells and plasma of blood samples not in equilibrium by the usual centrifugal spinning technique before the state of disequilibrium is altered somewhat. If the disequilibrium state is only slightly removed from the equilibrium state, the alteration may be unimportant. The use of a different, more rapid method to separate the cells and plasma would allow accurate determinations of cell and plasma concentrations. One possible such method would be the use of a small cell to ultrafiltrate sufficient protein-free plasma out of the blood sample in a short time. Such a method may be feasible for substances with half-times of transfer greater than about five minutes.

It is also possible to obtain accurate values for the cell

and plasma concentrations at the dialyzer outlet by allowing the outlet blood sample to reach equilibrium. If the equilibrium partition coefficient is used to determine cell concentrations from experimentally measured plasma concentrations, the equilibrium partition coefficient must be known at the temperature of the sample at equilibrium. This approach is best for substances with short half-times of transfer. Provided that the cell concentration of the substance concerned is known at the dialyzer inlet and that one can assume that none of the material was transferred out of the cells during the passage of the blood through the dialyzer or that a known amount was transferred, then one can use a material balance to determine the concentration of the substance in the plasma at the dialyzer outlet. If the inlet blood stream is at cell-plasma equilibrium, the concentration of the substance in the cells may be determined from knowledge of the plasma concentration and the equilibrium partition coefficient. Substances with half-times greater than 15 to 20 minutes may not be at cell-plasma equilibrium at the dialyzer inlet because a volume of blood approximately equal to the body volume of blood passes through the Kiil dialyzer every 30 minutes.

The dependence of the transfer rates of uric acid and phosphate upon the blood hematocrit is quite strong. Because the range of hematocrit fraction examined extended only from 0.249 to 0.275, the extension of the curves illustrating the effects of hematocrit dependence to hematocrit fractions below 0.24 and above 0.28 is not justifiable. The curves do suggest, however,

that allowing the blood hematocrit of hemodialysis patients to be as low as is feasible could result in a very significant increase in the efficiency of removal from the body of those substances whose effective partition coefficients are less than the equilibrium partition coefficients. This group of substances probably includes most of the materials, and all of the cations, which can be removed from the body by dialysis techniques today.

Insofar as the treatment of patients is concerned, not too much significance can be attached to the dependencies of mass-transfer rates upon the pressure difference across the membrane and the elapsed time of dialysis. Not only are the fundamental processes causing these dependencies not clear, but the values of these two parameters are not quantities which can be varied at will during dialysis over significant ranges. The choice of a particular pressure difference across the membrane is governed by the desired rate of ultrafiltration of fluid from the patient, although this work indicates that the minimum feasible pressure difference across the membrane is best for mass transfer of urea, uric acid, and possibly phosphate.

CONCLUSIONS

This work examined for the first time the effects of hematocrit upon the macroscopic mass-transport equations in hemodialyzers and upon the data-taking techniques necessary to obtain accurate clinical measurements of hemodialysis parameters. Clinical data and the modified macroscopic mass-transport equations were used to calculate in vivo total permeabilities as has been done before.

New results were obtained from these total permeability values by analyzing the data with regression analyses and Wilson plots.

The regression analysis confirmed previously-known dependencies of in vivo permeabilities upon volumetric blood flow rates. New insights were obtained, however, by considering linear velocities in the regression analyses and using the results to form Wilson plots. Such plots showed that about 75% of the resistance to transfer is in the blood layer, as was previously inferred from in vitro studies, and that the blood layer resistances had dependencies upon the blood velocity approximately equal to what would be expected from theory for undeveloped laminar flow. Considering the blood layer in the dialyzer as being contained between two infinite flat plates results in a theoretical length for the development of the concentration boundary layer of about 1 inch (24). The results of this work therefore indicate that the concentration boundary layer in the blood in Kiil dialyzers is being constantly broken and reformed throughout the dialyzer. Such an effect would be caused by irregularities in the dialyzer dimensions--such as could result from the manufacturing process, from the warping of the dialyzer with age, and from the clamping of the dialyzer during assembly--and by alterations in the blood layer thickness caused by uneven deposition of inert particles such as cells.

A dependence of some in vivo permeabilities upon the pressure difference across the membrane, which had not been noticed before, was found and the dependency related to the changing thickness of the blood layer by means of Wilson plots. No apparent effect

of one-dimensional membrane stretching was noticed. Such an effect has been noticed in in vitro systems.

The permeability of some substances was found to increase as the time of dialysis increased up to 6 hours, and Wilson plots suggested that this effect was due to changes in the membrane resistance. This effect has not been noticed in prior work. Indeed, prior work has indicated an increase in total resistance with time after an initial six hour period. Further work needs to be done to explain this apparent initial rise in permeability.

The regression analysis revealed for the first time a strong dependence of the total permeability of some substances upon the hematocrit of the patient. Those substances whose rate of transfer out of red cells is relatively slow will show a total permeability in the Kiil dialyzer strongly dependent upon the patient's hematocrit. A quantitative model to predict this effect was formulated using theoretical results of Grimsrud and Babb and of Fricke and certain assumptions concerning contact between the dialyzer membrane and cellular material.

Relative dialysances and relative permeabilities were examined for the first time using extensive in vivo data to determine their value as parameters to describe hemodialysis. No apparent advantage to their use was found.

RECOMMENDATIONS FOR FURTHER WORK

Although this work does not definitively answer very many questions, it makes up for this shortcoming, or perhaps compounds it, by raising a vertible host of new questions. Some of the more

important assumptions necessary to reduce the data to a form suitable for the regression analysis are questionable in nature. The weaknesses of these assumptions then reduce the reliability of the results of the regression analysis, particularly the reliability of the magnitudes of the independent variables in the regression analyses.

The value for the effective partition coefficient for each substance was assumed from the results of data taken under conditions substantially dissimilar to the conditions which exist in hemodialysis. A great deal of experimental work needs to be done to determine properly effective partition coefficients for substances transferred during hemodialysis. Are the values a strong function of temperature? For any given substance, is the value of the effective partition coefficient identical for all individuals? Results from experiments of this type would have broad implications for all mass-transfer research involving blood, not only for mass transfer in a hemodialyzer. After the determination of reliable effective partition coefficients, one can determine procedures to determine accurately the plasma and cell concentrations of substances in blood in a state of disequilibrium. The concept of effective partition coefficients is a general one, in that it will be involved in all hemodialysis considerations regardless of the type of dialyzer used. Indeed, it will be involved in all mass-transfer processes involving blood.

Potentially the most significant effect on the mass-transfer rate of some materials is exerted by the blood hematocrit. Data

over a much wider range of hematocrit should be taken to verify the dependencies of the mass-transfer rates of uric acid and phosphate on hematocrit. Work should be done to determine what other compounds show this effect of hematocrit upon mass-transfer rate. Inasmuch as the presence of red cells hinders the dialysance of certain substances, the possibility of ultrafiltrating the blood prior to dialysis should be examined. Membranes are now available to ultrafiltrate blood. For dialyzing poisons, when it is particularly desirable to remove the substance quickly, the ultrafiltration of blood prior to dialysis may result in increasing the dialysis rate several fold if the poison is impermeable red cells. Also, the fundamental processes resulting in the effect should be clarified.

Neither relative dialysance nor relative permeability appear to offer hope of being a single, relatively constant parameter which can be used to determine mass-transfer rates of all compounds under widely varying conditions. The search for such a parameter, assuming it exists, must continue along new lines.

Finally, one potentially important aspect of mass transfer in hemodialyzers has of necessity been largely neglected in this work. This is the possible effect of the binding of components in the blood to plasma proteins and to the cells on the mass-transfer rate from the blood. The errors which may result if total, rather than free, concentrations are used to calculate the mass-transfer coefficient according to equation [26] were mentioned in regard to phosphate. Phosphate, unlike creatinine, urea, and uric acid, has

an appreciable fraction of its plasma concentration bound to the proteins. Since only free plasma molecules or ions can be transferred across the membrane, if total concentration is used in equation [26] to calculate the log-mean gradient, the P value will depend on the particular value of the total concentration, even though the mass-transfer rate will not. This apparent dependency of P on the arterial inorganic phosphate concentration is undesirable.

This work has not, however, considered the effects of the binding kinetics upon the mass transfer of a substance from the blood. Although no bound substance may be transferred across the membrane, the transfer of the free form of the substance out of the plasma will upset the equilibrium between the bound and unbound forms of the substance. In reaction to this disequilibrium, some of the bound form of the substance will become free, and then may be transferred out of the blood. Whether or not any of the substance initially bound as the blood enters the dialyzer will be removed before the blood leaves the dialyzer will depend entirely on the rate of the "unbinding" reactions (16).

Obviously, the situation is entirely analogous to the situation when material may or may not be removed from the cell water. This situation has already been considered in detail. If equation [10] is rewritten to include the effects of binding to both cells and proteins, there results, still neglecting ultrafiltration.

$$\dot{m} = Q_b\,(1 - H)\,(c^f_{p_i} - c^f_{p_o}) + Q_b\,H\,(c^f_{c_i} - c^f_{c_o}) \qquad [48]$$

$$+ Q_b\,H\,(c^b_{c_i} - c^b_{c_o}) + Q_b\,(1 - H)\,(c^b_{c_i} - c^b_{c_o})$$

This equation may be rewritten in terms of J factors in the following form

$$\dot{m} = Q_b \, (c^f_{p_i} - c^f_{p_o}) \, [(1 + J^b_p) + (J^f_c + J^b_c - 1 - J^b_p) \, H] \qquad [48a]$$

where $J^b_p \equiv \dfrac{c^b_{p_i} - c^b_{p_o}}{c^f_{p_i} - c^f_{p_o}}$ and $J^f_c \equiv \dfrac{c^f_{c_i} - c^f_{c_o}}{c^f_{p_i} - c^f_{p_o}}$ and $J^b_c \equiv \dfrac{c^b_{c_i} - c^b_{c_o}}{c^f_{p_i} - c^f_{p_o}}$

The last two terms on the right side of equation [48] have been assumed equal to zero in this work for two reasons: first, there were no data available on the patients' protein concentrations; and second, there were no data in the literature concerning the rates of the "unbinding" reactions for the substances involved. For most dialyzable substances, some poisons probably excepted, the magnitudes of the last two terms are probably easily neglectable. Research should be done on this question, of course.

Again, any disequilibrium between bound and free forms of a substance will hinder the attainment of accurate experimental measurements of plasma concentrations of the free form.

NOMENCLATURE

A area ($cm.^2$)

C clearance, or amount of substance removed per minute divided by the blood or plasma concentration (ml./min.)

c concentration (mg.%)

$\mathcal{D}$ diffusivity ($cm.^2$/min.)

D dialysance, or amount of substance removed per minute divided by the maximum blood or plasma-bath concentration gradient (ml./min.)

h distance from center of blood layer to membrane surface

K a constant

L flow path length (cm.)

$\dot{m}$ mass-transfer rate (mg./100 min.)

P overall mass-transfer coefficient, or permeability (cm./min.)

$\mathcal{P}$ membrane permeability (cm./min.)

p pressure (mm. Hg)

Q volumetric flow rate (ml./min.)

R resistance to mass-transfer (min./cm.)

S cross-sectional area of flow path in one section perpendicular to direction of flow ($cm.^2$)

t elapsed time of dialysis (hours)

v velocity (cm./min.)

V volume ($cm.^3$)

w width of flow path in one section (cm.)

Δ difference or change in

Subscripts

a available for mass transfer

b blood

c cell

d dialysate

e equilibrium

i inlet

m membrane

o outlet

P partition

p plasma

r relative

s standard

t total

avg average

corr corrected

eqn predicted by the equation

Superscripts

b bound

f free

BIBLIOGRAPHY

1. Alexander, R. W. Trans. Am. Soc. Art. Int. Organs, 11, 95 (1965).

2. Arbritton, E. C. (Editor). "Standard Values in Blood," W. B. Saunders Company, Philadelphia, 1952.

3. Babb, Albert L., et al. "Engineering Aspects of Artificial Kidney Systems," pp. 289 - 331 of "Chemical Engineering in Medicine and Biology," edited by Daniel Hershey. Plenum Press, New York, 1967.

4. Babb, A. L., et al. Chem. Eng. Prog. Symp. Series, No. 84, 64, 110 (1968).

5. Barenberg, Robert L. and Kiley, John E. Trans. Am. Soc. Art. Int. Organs, 7, 9 (1961).

6. Bennett, Leon. Science, 155, 1554 (1967).

7. Beyer, William H. (Editor). "Handbook of Tables for Probability and Statistics," Chemical Rubber Co., Cleveland, 1966.

8. Bluemle, L. W. et al. Trans. Am. Soc. Art. Int. Organs, 6, 38 (1960).

9. Brown, H. W. and Schreiner, G. E. Trans. Am. Soc. Art. Int. Organs, 8, 187 (1962).

10. Buckles, R. G. et al. A. I. Ch. E. J., 14, 703 (1968).

11. Connolly, E. G. and Miller, Joseph H. "In Vitro and In Vivo Evaluation of a Kiil-Western Dialyzer Light-Weight Membrane Support Board." Research Report No. 679 - 262, Western Gear Corporation, Lynwood, California, September, 1967.

12. Cook, Randall. "Predetermining the Weight Loss in Artificial Kidney Dialysis by Knowing Various Parameters, and the Determination of the Linear Dependence of the Rate of Weight

12. "Loss on the Pressure Gradient Across the Artificial Kidney," Student Report for Ch. E. 50 (Prof. Corcoran Instructor), March 13, 1967.

13. Craig, L. C. and Konigsberg, William. J. Phys. Chem., 65, 166 (1961).

14. Currie, J. A. Brit. J. Appl. Phys., 11, 318 (1960).

15. Davies, Owen L. (Editor). "Statistical Methods in Research and Production," Third Edition. Hafner Publishing Company, New York, 1961.

16. Desgrez, P. and De Traverse, P. M. (Editors). "Transport Function of Plasma Proteins," Elserier Publishing Company, New York, 1966.

17. Fiske, C. H. and Subbarow, Yellapragada. Jour. Biol. Chem., 66, 375 (1925).

18. Freeman, R. B., et al. Trans. Am. Soc. Art. Int. Organs, 10, 174 (1964).

19. Friske, Hugo. Phys. Rev. 24, 575, 1924.

20. Fry, D. L. and Hoover, P. L. Trans. Am. Soc. Art. Int. Organs, 10, 98 (1964).

21. Galletti, P. M. Proc. Third Int. Congr. Nephrol., 3, 237 (1966).

22. Gary - Bobo, C. and Lindenberg, A. B. J. Physiol. (Paris), 52, 106 (1960).

23. Grimsrud, Lars and Babb, Albert L. Trans. Am. Soc. Art. Int. Organs, 10, 101 (1964).

24. Grimsrud, Lars and Babb, Albert L. Chem. Eng. Prog. Symp. Series, 62, No. 66, 19 (1966).

25. Hawk, P. B., Oser, B. L., and Summerson, W. H. "Practical Physiological Chemistry," 12th Edition, 506, The Blakiston Company, Philadelphia, 1947.

26. Knudsen, James G. and Katz, Donald L. "Fluid Dynamics and Heat Transfer," 384, McGraw-Hill, New York, 1958.

27. Leonard, E. F. Trans. Am. Soc. Art. Int. Organs, 6, 33 (1960).

28. Leonard, E. F. and Bluemle, L. W. Trans. N. Y. Acad. Sci., Series II, 21, 585 (1959).

29. Marsh, Walton H. et al. Am. Jour. Clin. Path., 28, 681 (1957).

30. McAdams, William H. "Heat Transmission," Third Edition, 345, McGraw-Hill, New York, 1954.

31. Michaels, Alan S. Trans. Am. Soc. Art. Int. Organs, 12, 387 (1966).

32. Mickley, H. S., Sherwood, T. K., and Reed, C. E. "Applied Mathematics in Chemical Engineering,: McGraw-Hill, New York, 1957.

33. Miron, Y. and Leonard, E. F. Trans. Am. Soc. Art. Int. Organs, 10, 26 (1964).

34. Norris, R. H. and Streid, D. D. Trans. A. S. M. E., 62, 525 (1940).

35. Overgaard-Hansen, K. and Lassen, U. V. Nature, (London), 184, 553 (1959).

36. Phiobs, R. H. and Burton, A. C. Federation Proceedings, 24, 156 (1965).

37. Prankerd, T. A. J. and Altman, K. I. Biochemical Journal, 58, 622 (1954).

38. "Proceedings of the Conference of Hemodialysis, November 9 - 10, 1964," 20 - 30, National Institutes of Health, Bethesda, Maryland.

39. Ralston, Anthony and Wilf, Herbert S. "Mathematical Methods for Digital Computers," John Wiley and Sons, New York, 1960.

40. Rapetti, Ronald V. and Leonard, E. F. Trans. Am. Soc. Art. Int. Organs, 10, 311 (1964).

41. Rapetti, R. V. and Leonard, E. F. Chem. Eng. Prog. Symp. Series, No. 66, 62, 80 (1966).

42. Rubini, Milton E., "Feasibility of Chronic Hemodialysis in California," Volume I (1966), and Volume II (1967), State of California Department of Public Health, Berkeley, California.

43. Schanker, et al. Jour. Phar. and Exp. Ther., 133 325 (1961).

44. Skeggs, Leonard T. Am. Jour. Clin. Path., 28, 311 (1957).

45. Spaeth, E. E. and Friedlander, S. K. Biophysical Journal, 7, 827 (1967).

46. Sweeney, M. J. Trans. Am. Soc. Art. Int. Organs, 12, 39 (1966).

47. Sweeney, M. J. and Galetti, P. M. Trans. Am. Soc. Art. Int. Organs, 10, 3 (1964).

48. "Technicon Auto Analyzer Manual," Technicon Instruments Corporation, Chauncey, New York, 1963. Method file N - 11a for creatinine; N - 10 for urea nitrogen; N - 13a for uric acid; and N - 4a for inorganic phosphate.

49. Versaci, A. A. et al. Trans. Am. Soc. Art. Int. Organs, 10, 186 (1964).

50. Whittam, R. "Transport and Diffusion in Red Blood Cells," The Williams and Wilkins Company, Baltimore, 1964.

51. Wilcox, C., et al. Trans. Am. Soc. Art. Int. Organs, 12, 44 (1966).

52. Wolf, A. V. et al. J. Clin. Invest., 30, 1062 (1951).

53. Yoder, Richard D. J. Appl. Physiol., 18, 141 (1963).

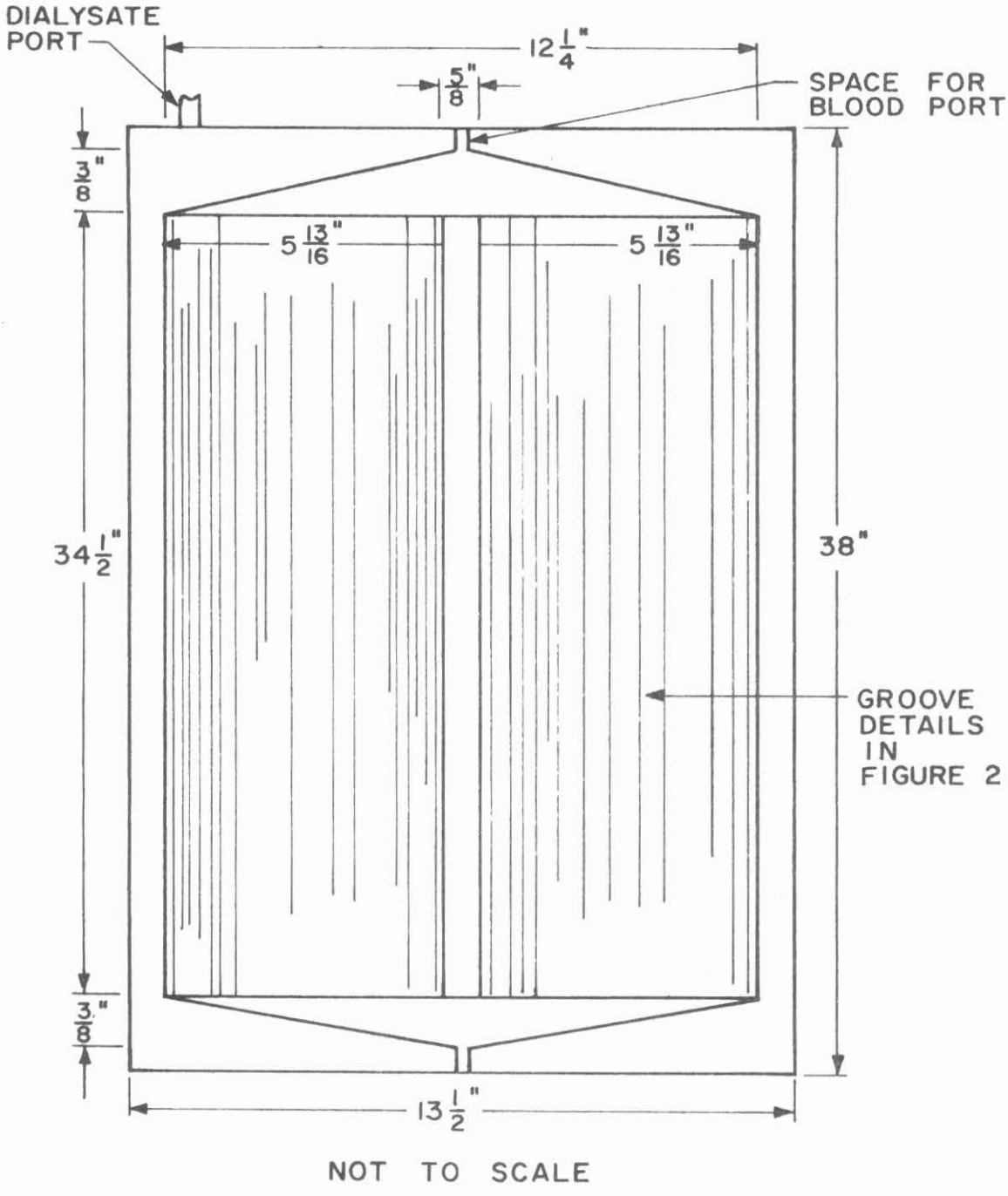

FIGURE 1. Dialyzer Dimensions

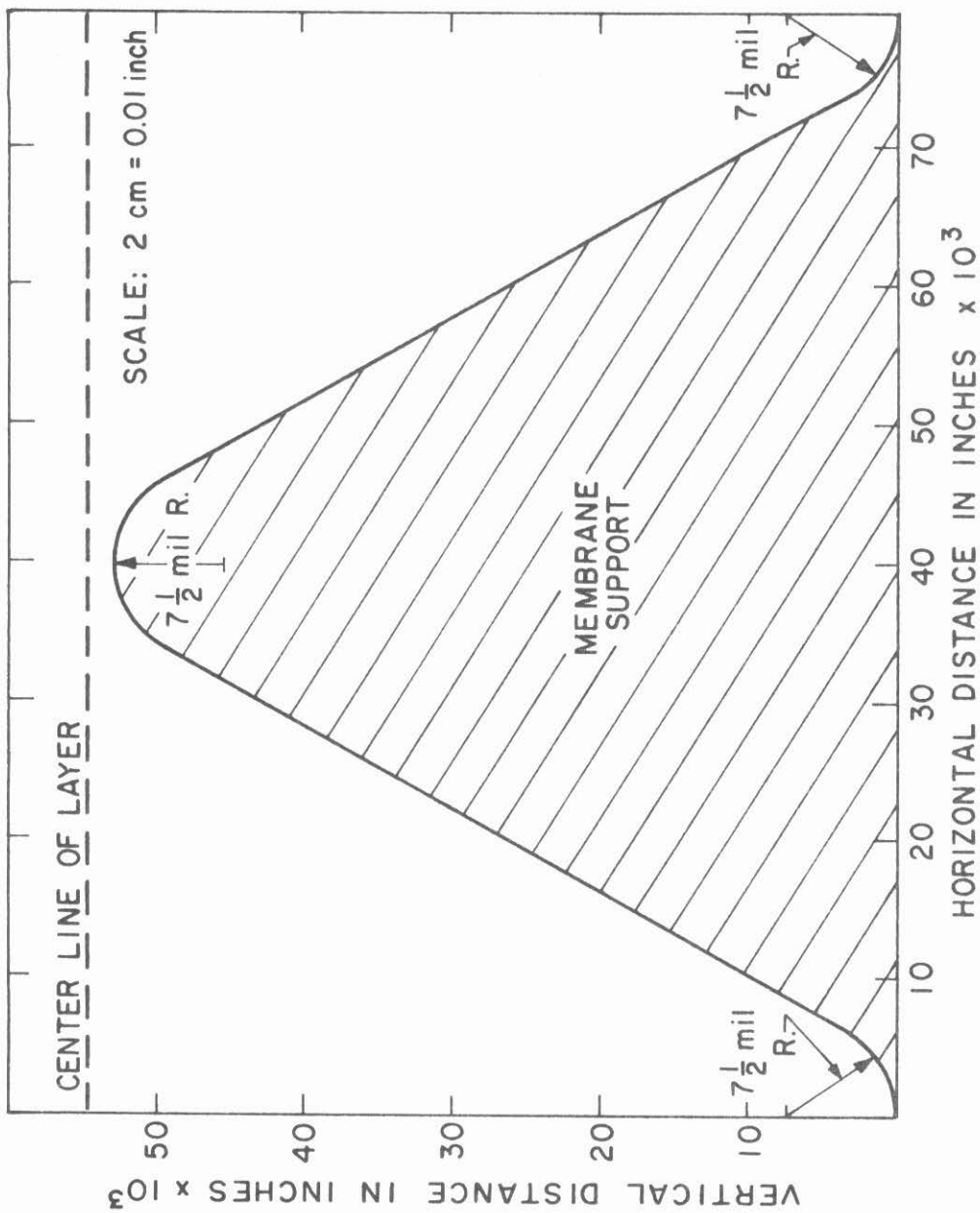

FIGURE 2. Dialyzer Groove Dimensions

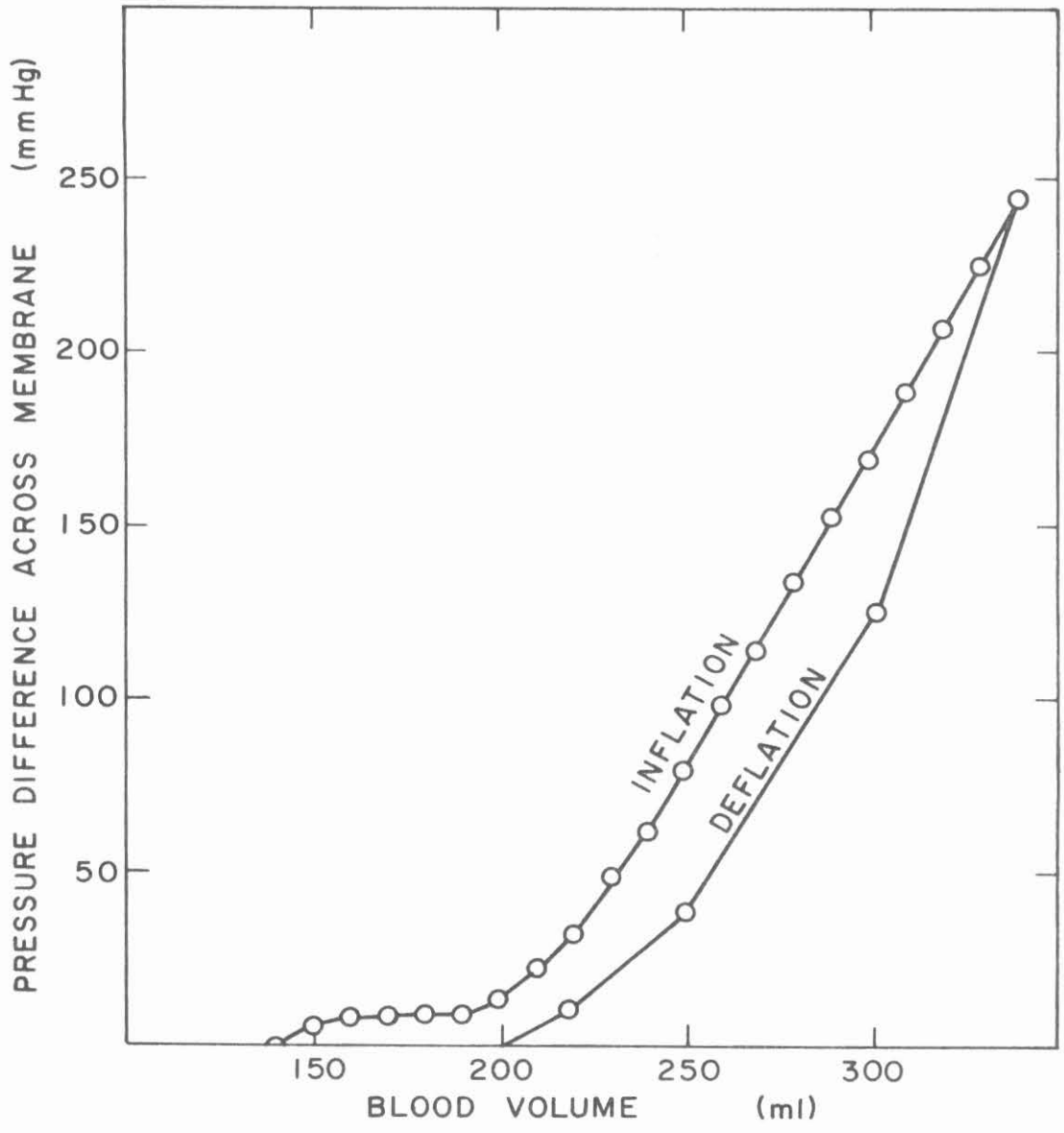

FIGURE 3. Dialyzer Capacitance

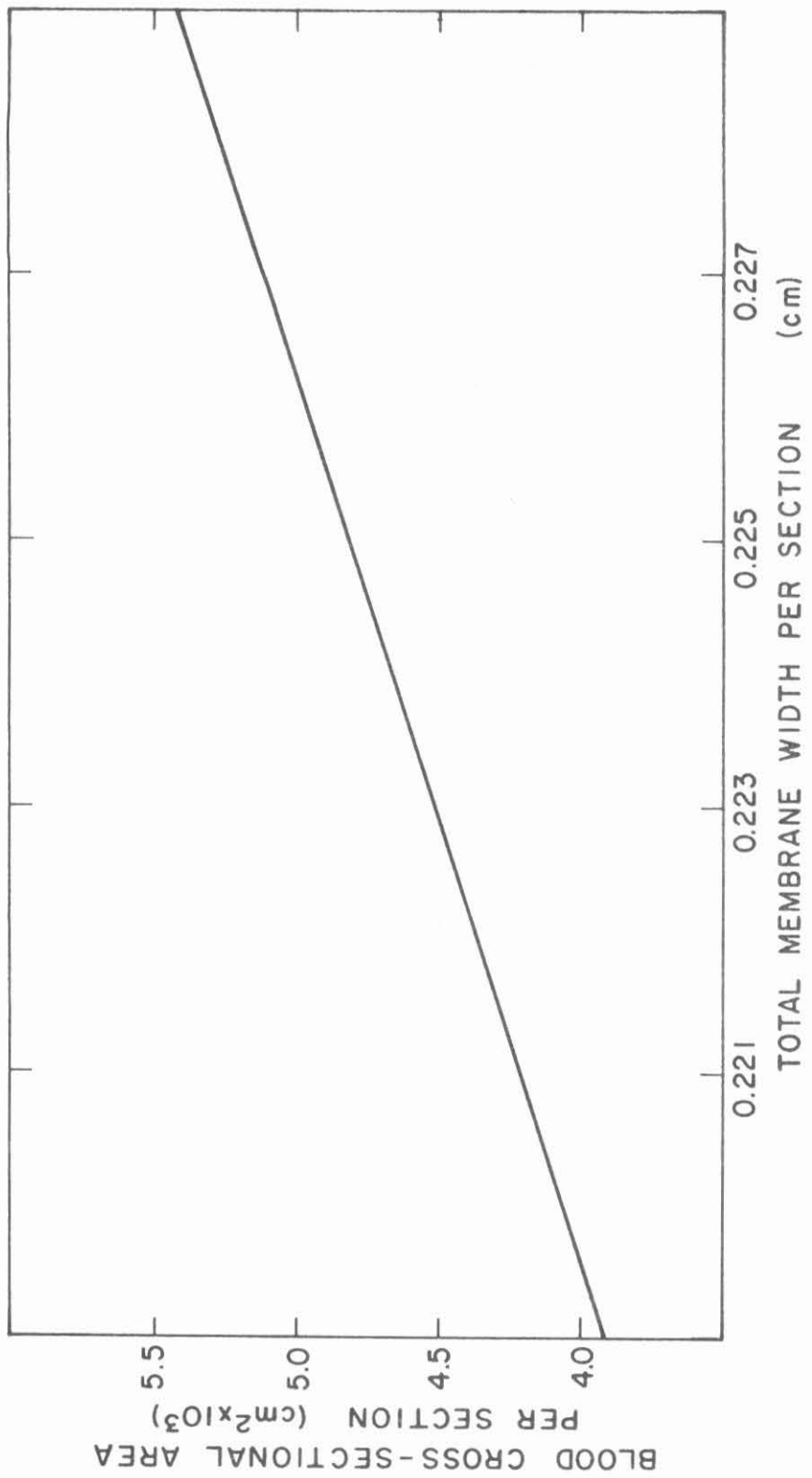

FIGURE 4. Total Membrane Width per Section

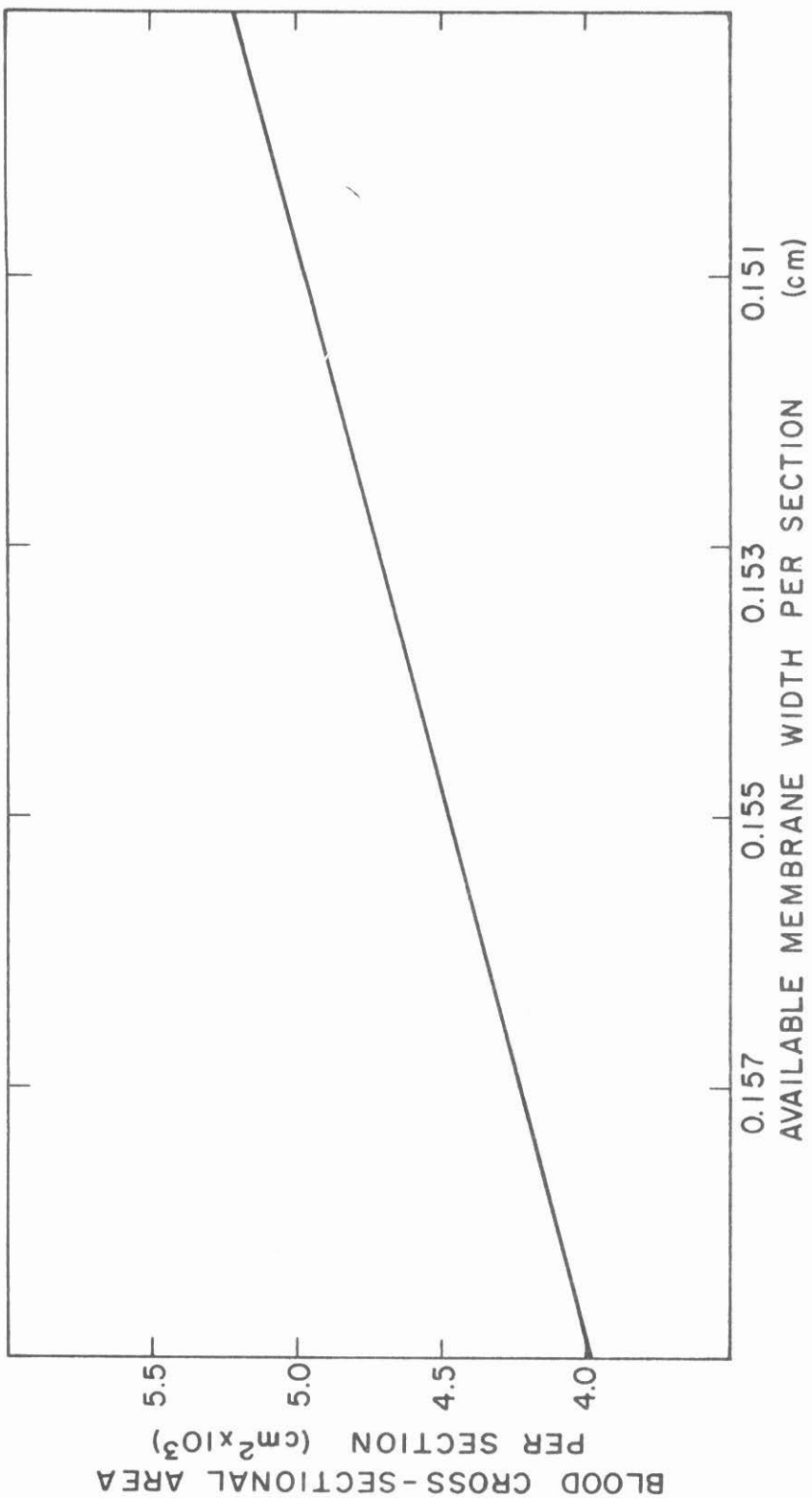

FIGURE 5. Available Membrane Width per Section

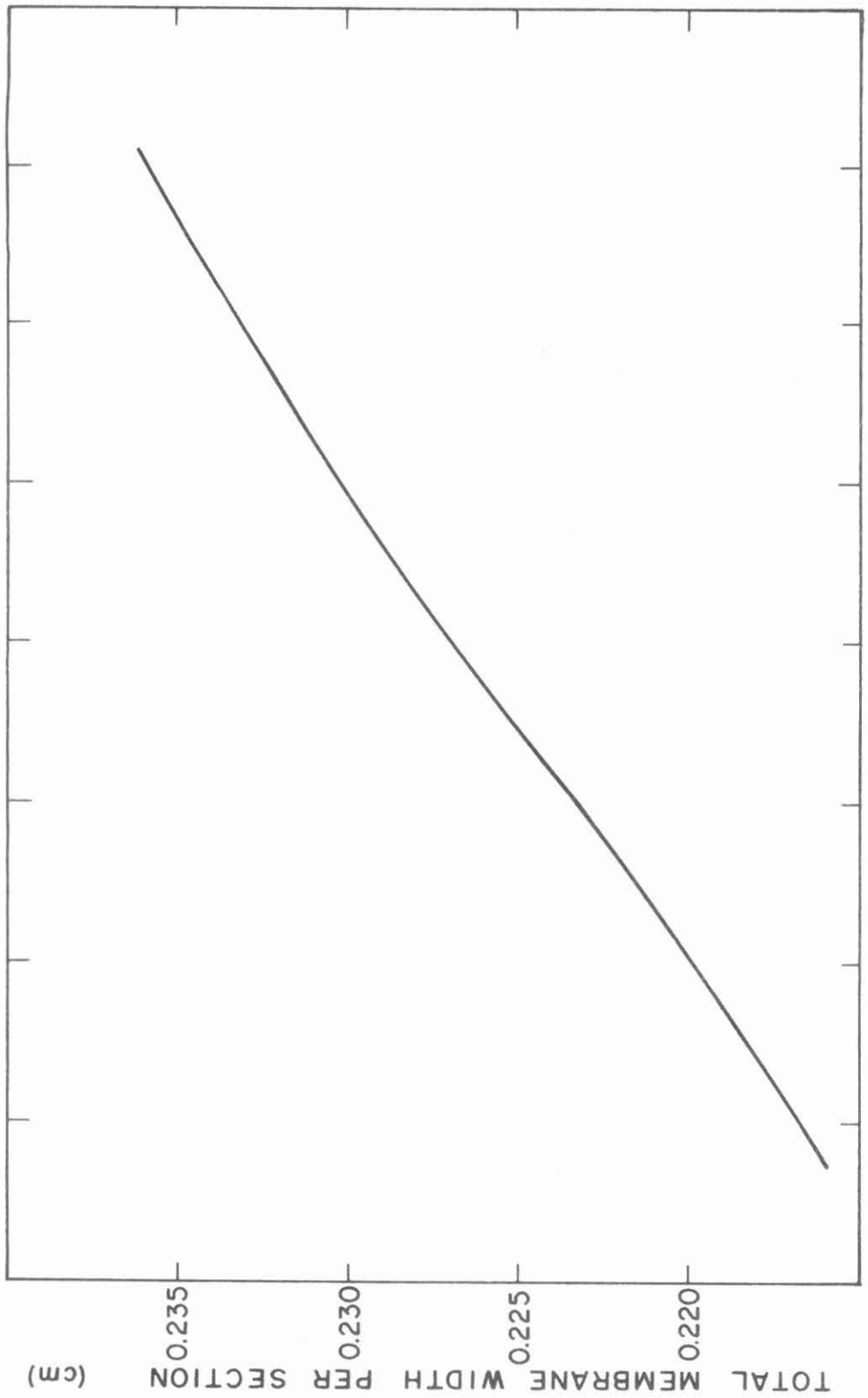

FIGURE 6. Relationship between Membrane Stretch and Blood Layer Thickness

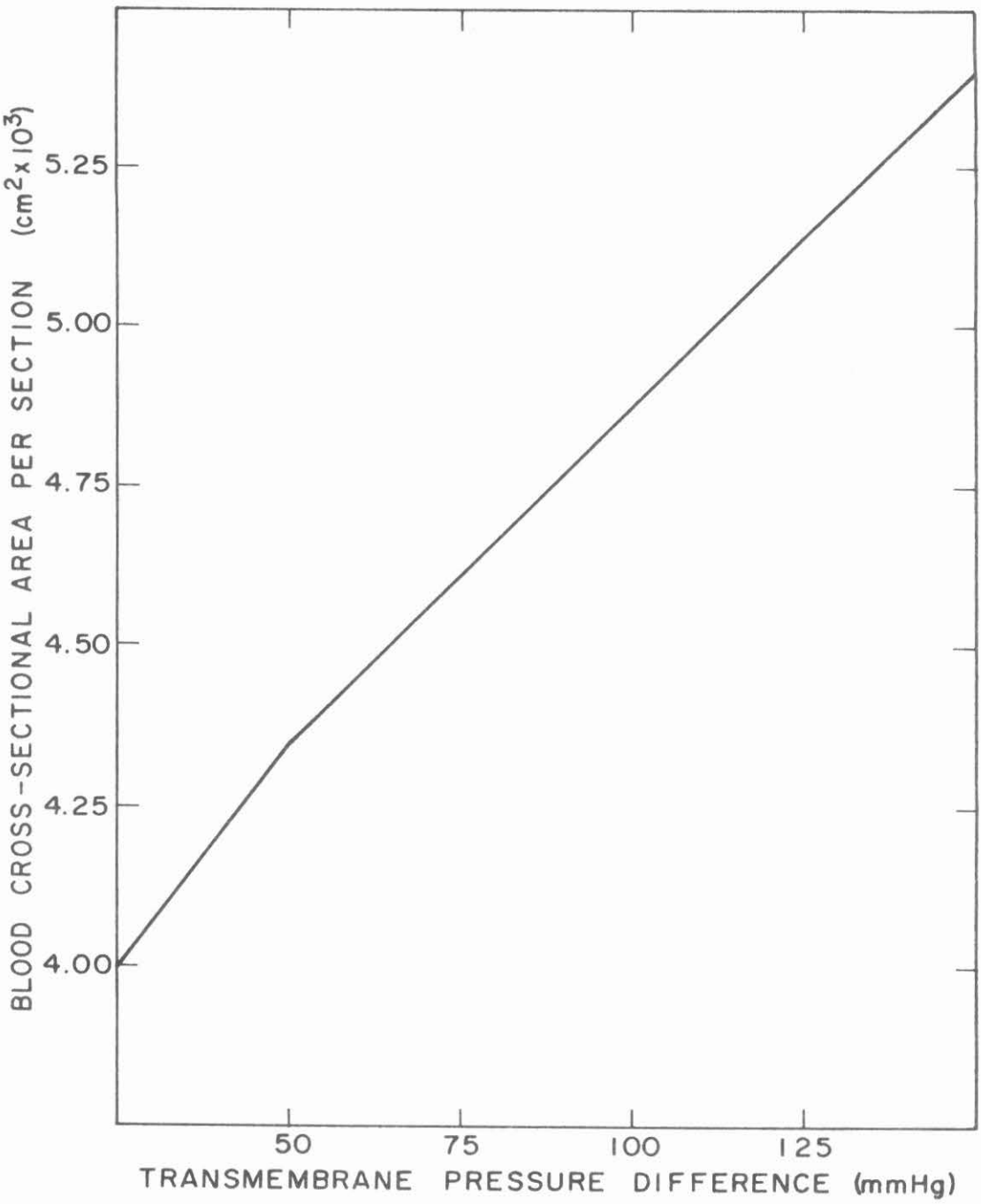

FIGURE 7. Blood Cross-Sectional Area per Section

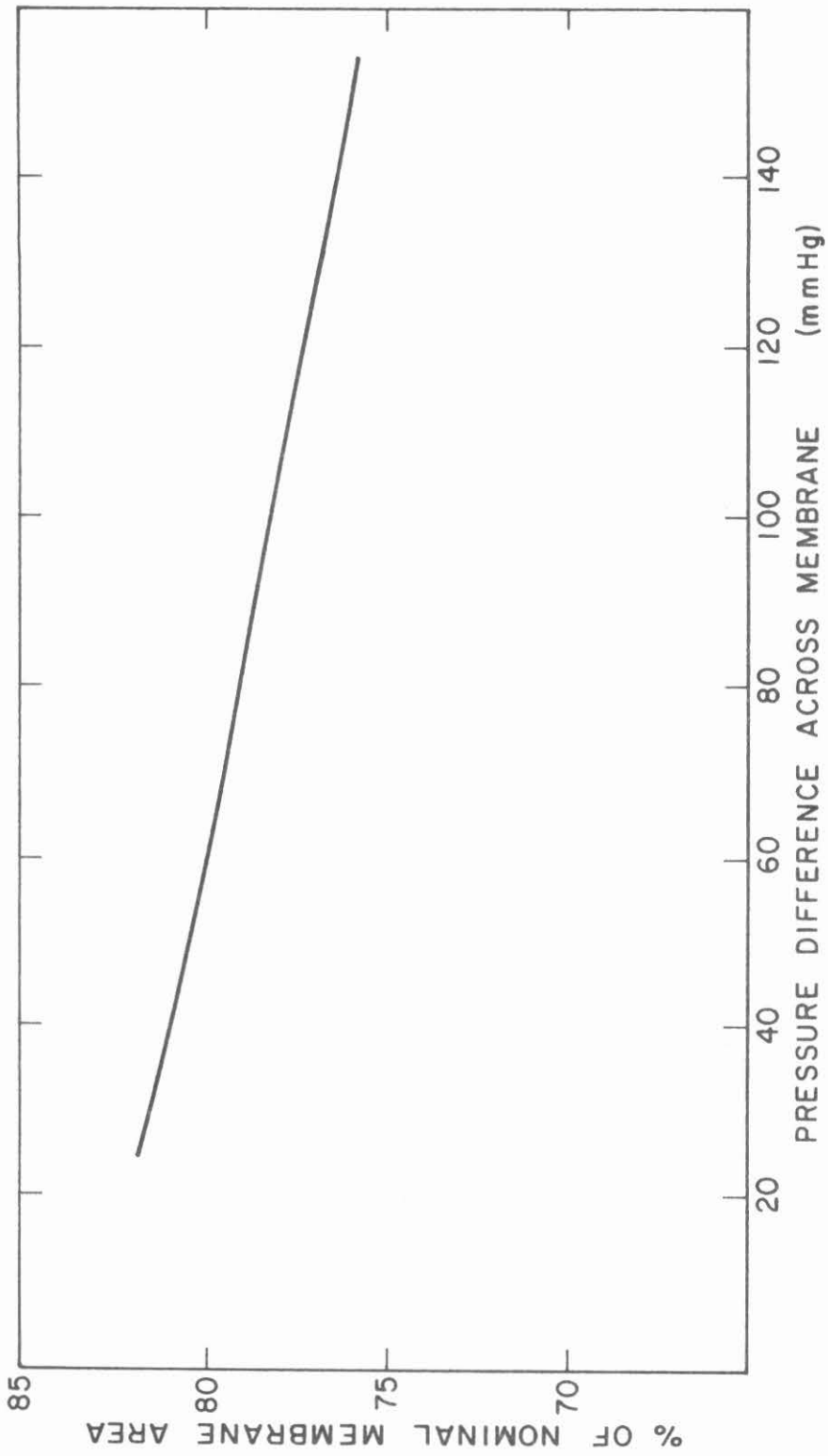

FIGURE 8. Available Membrane Area

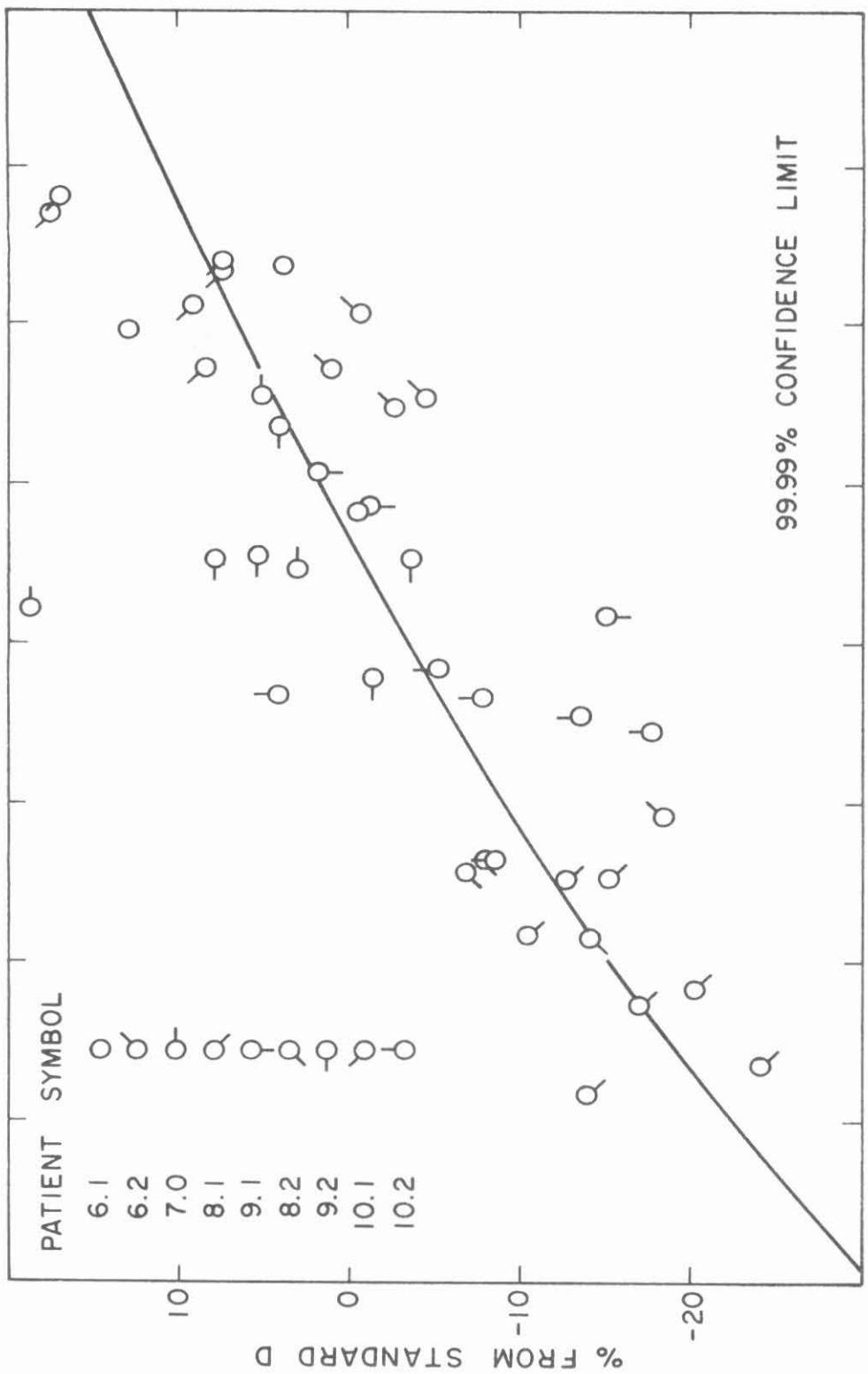

FIGURE 9. Creatinine Dialysance Linear Blood Velocity Dependence

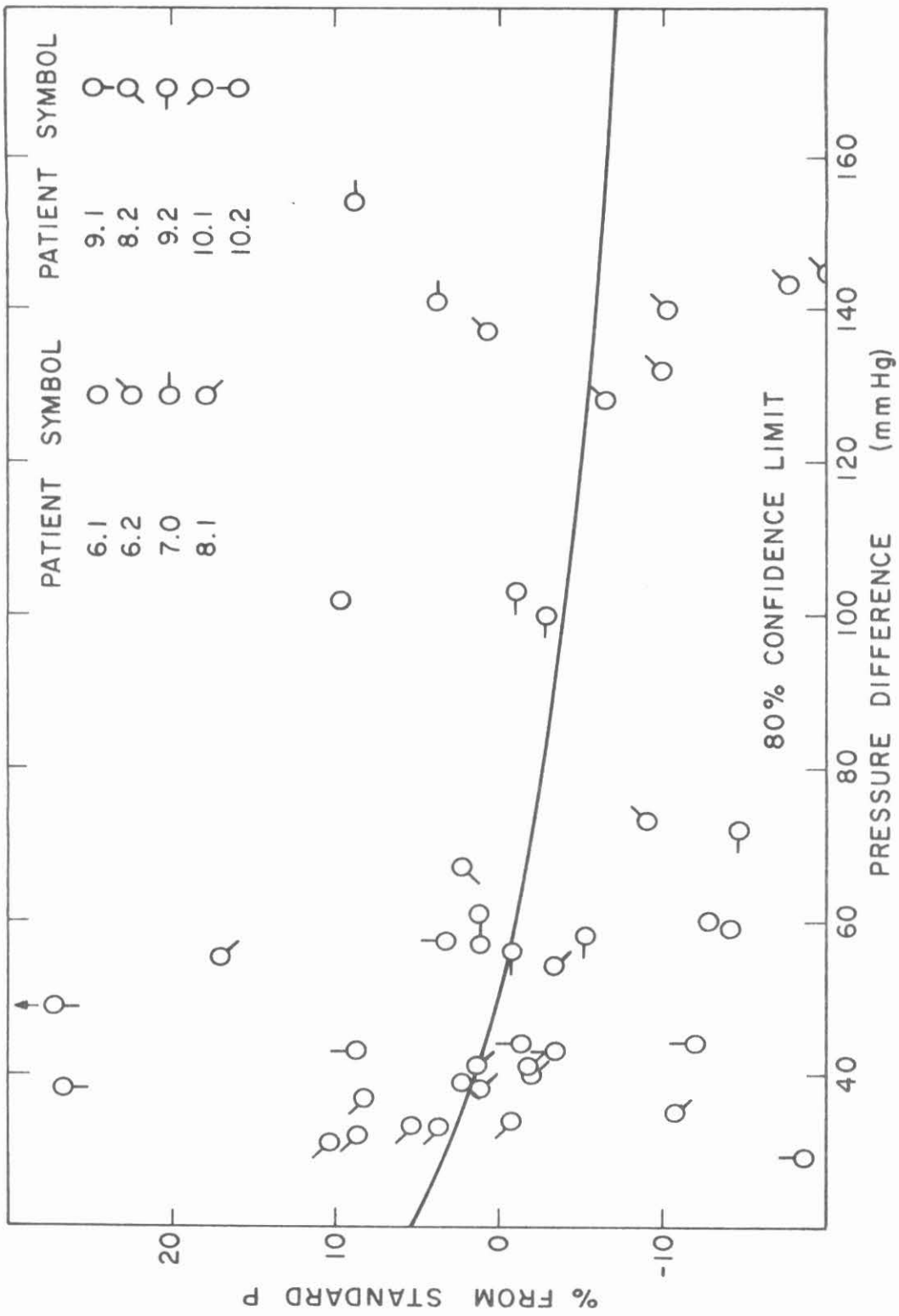

FIGURE 10. Phosphate Dialysance Pressure Difference Dependence

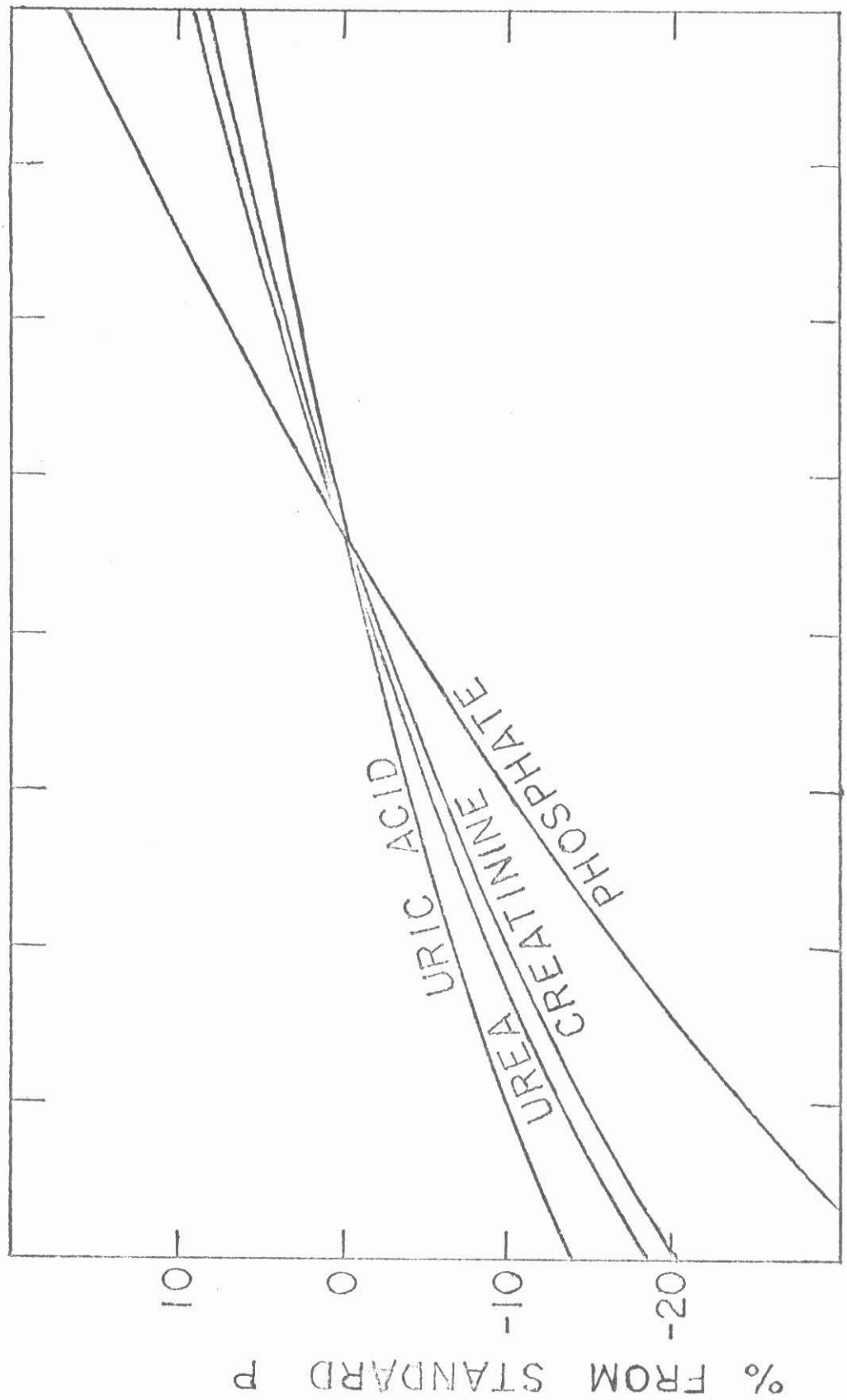

Figure 11. Overall Mass-Transfer Coefficient Dependence upon Blood Velocity

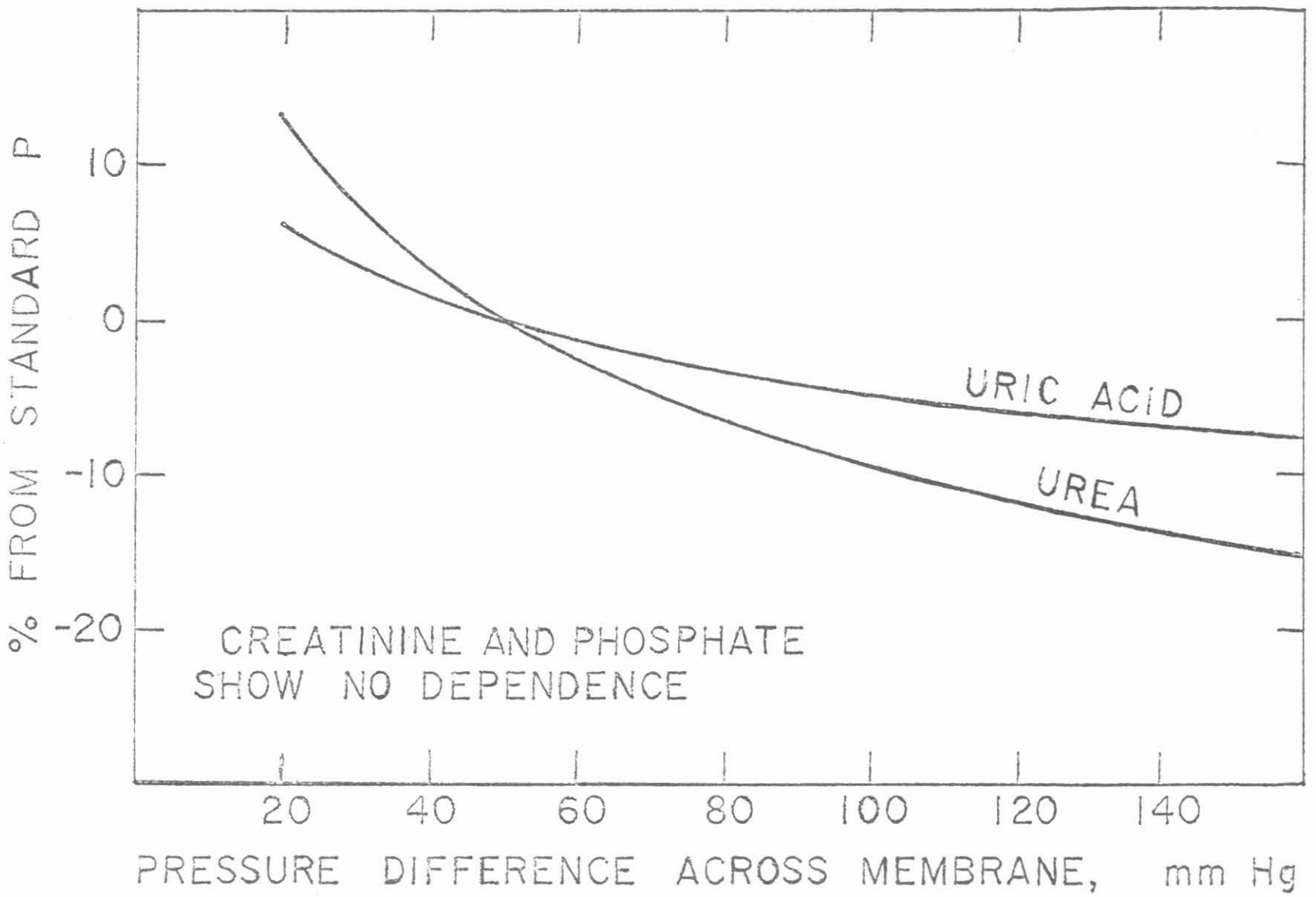

Figure 12. Overall Mass-Transfer Coefficient Dependence on Pressure Difference

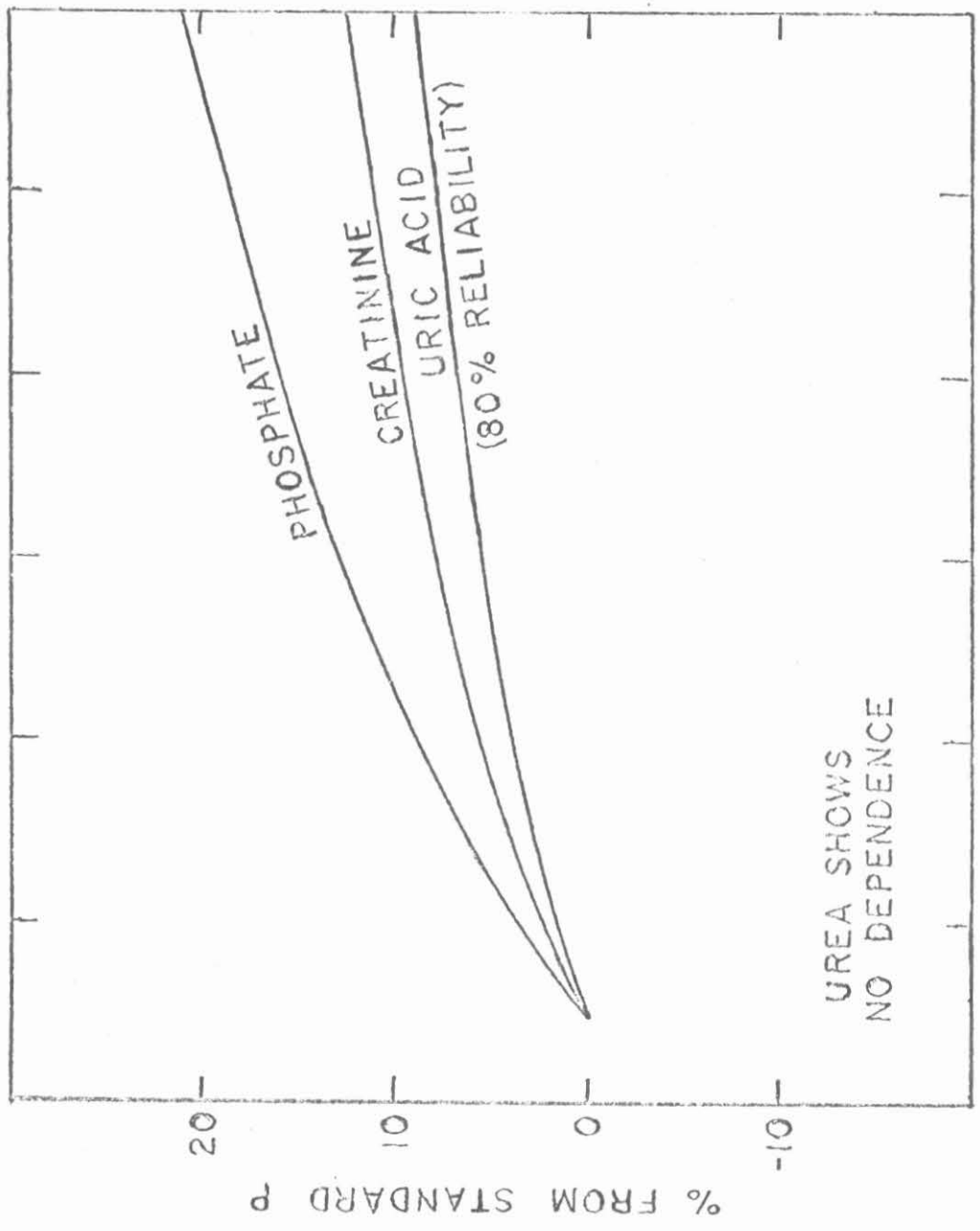

Figure 13. Overall Mass-Transfer Coefficient Dependence upon Time

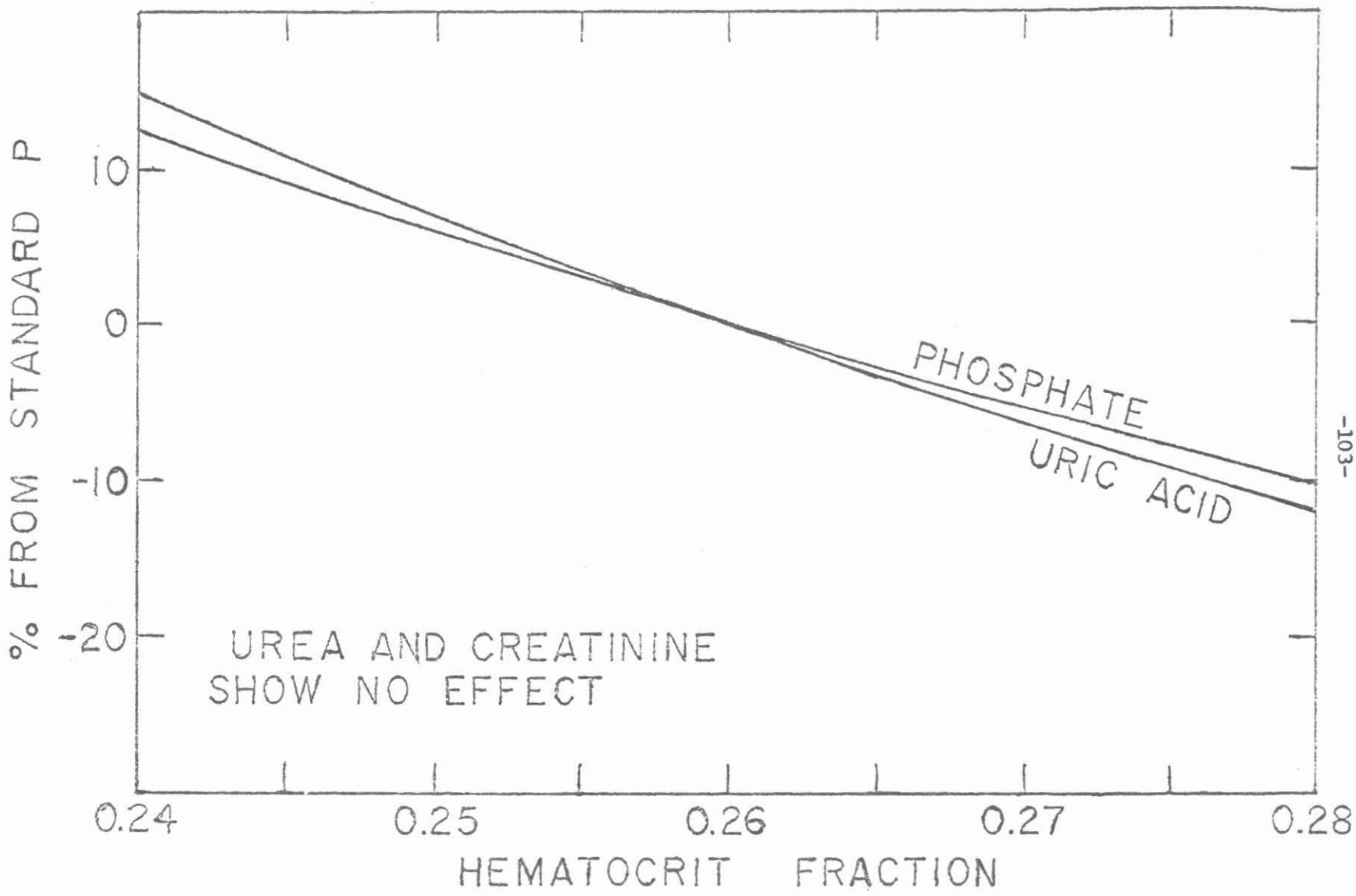

Figure 14. Overall Mass-Transfer Coefficient Dependence upon Hematocrit

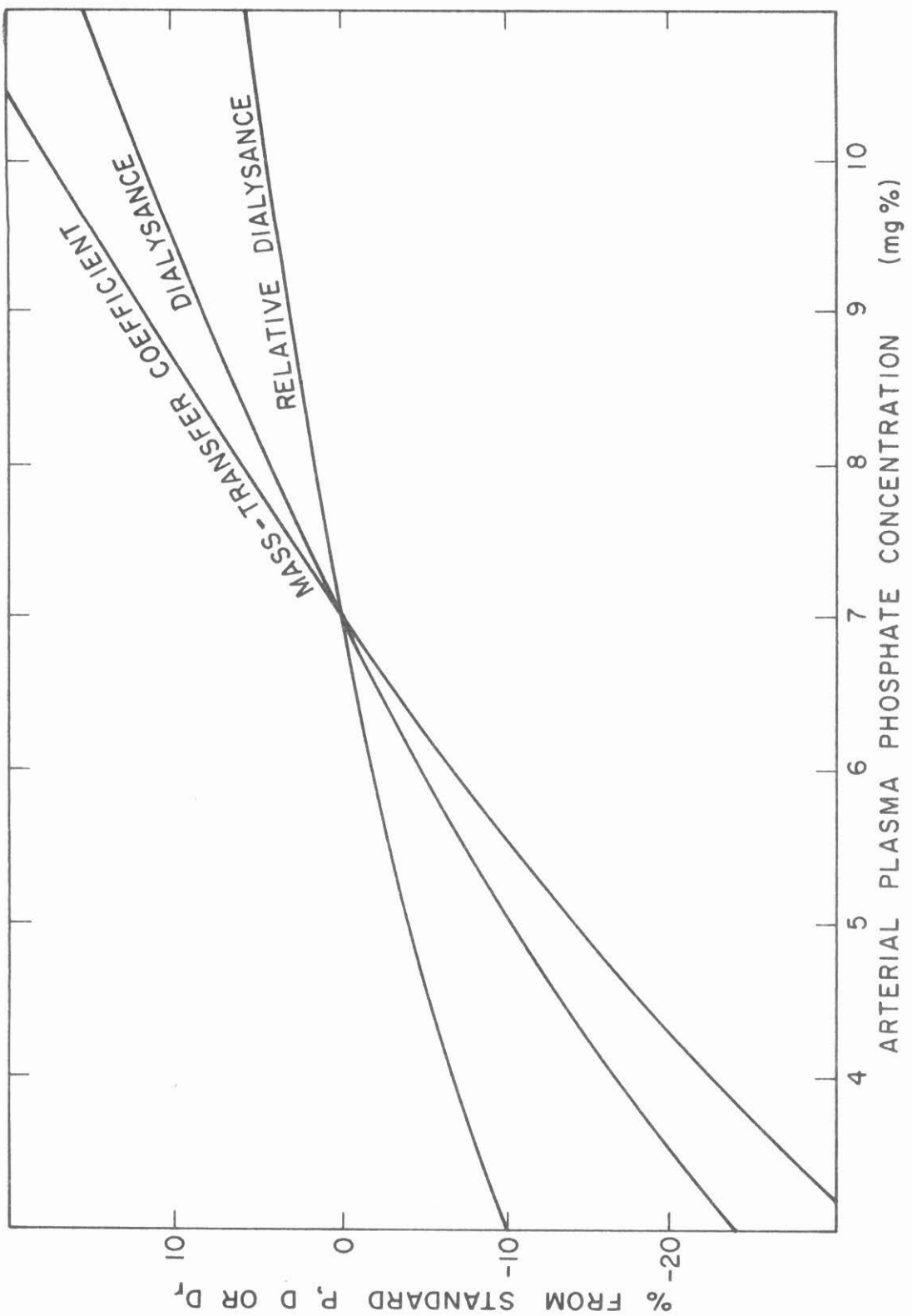

FIGURE 15. Phosphate Coefficient Dependencies on Arterial Plasma Concentration

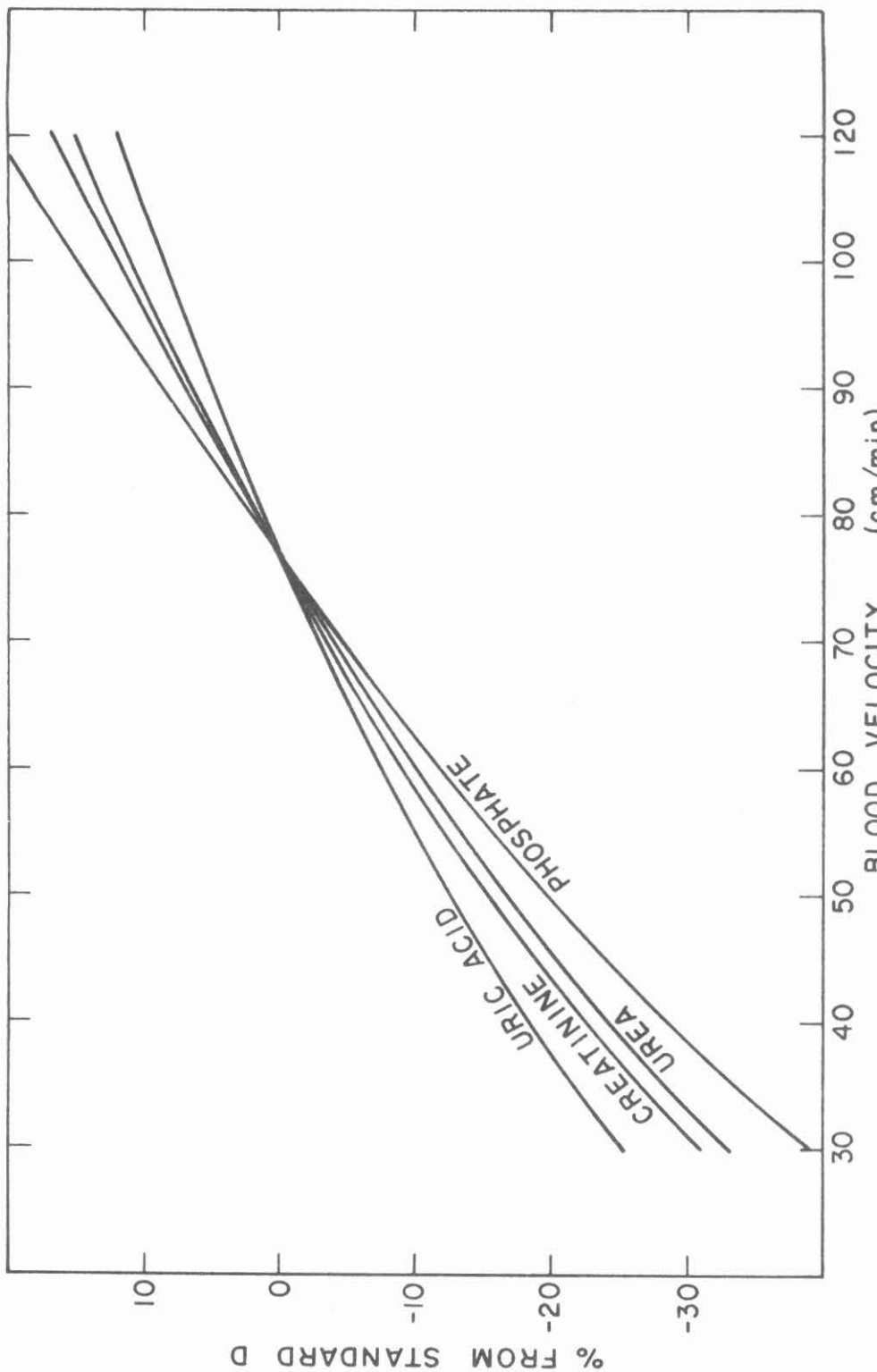

FIGURE 16. Dialysance Dependence upon Blood Velocity

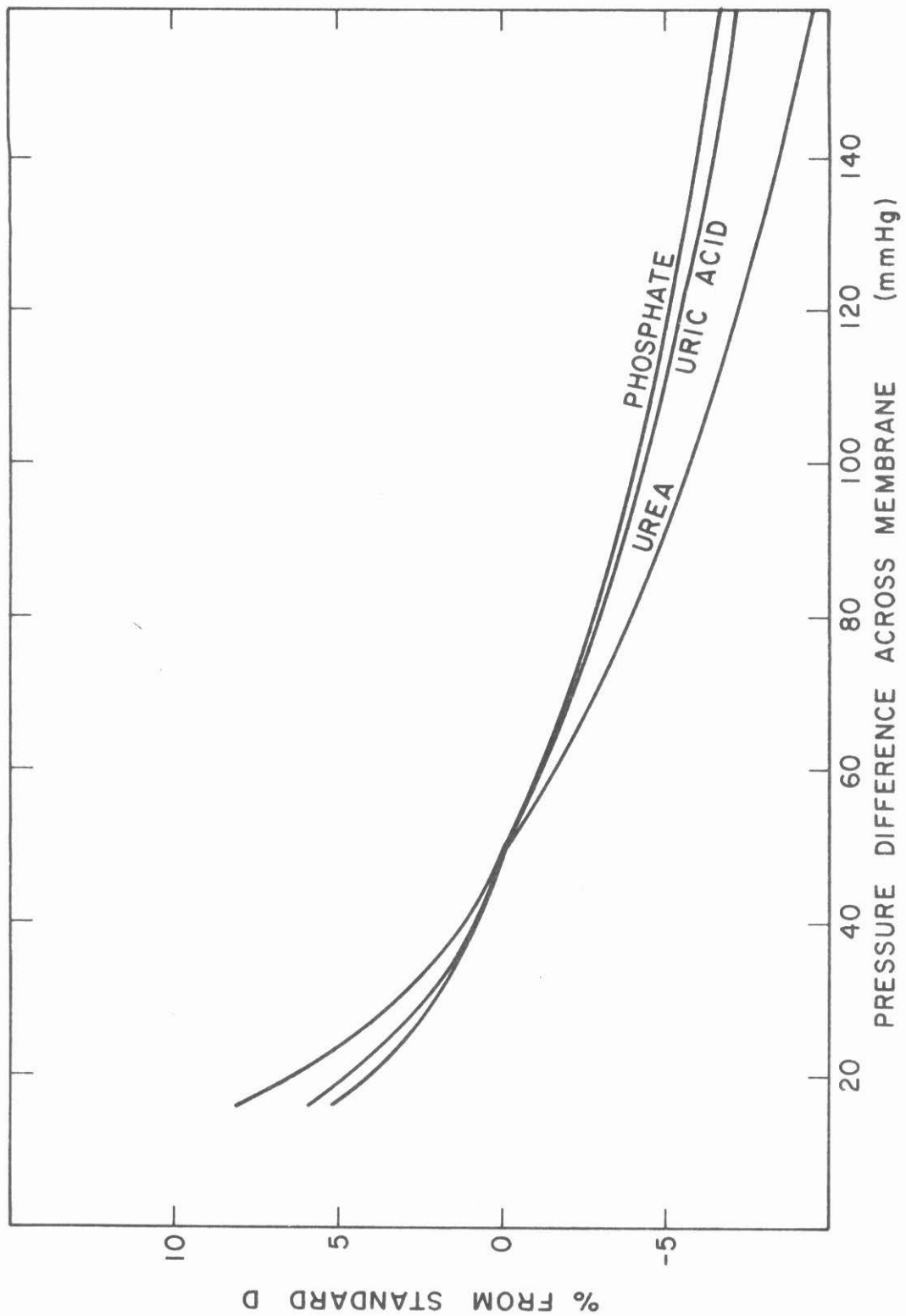

FIGURE 17. Dialysance Dependence upon Pressure Difference

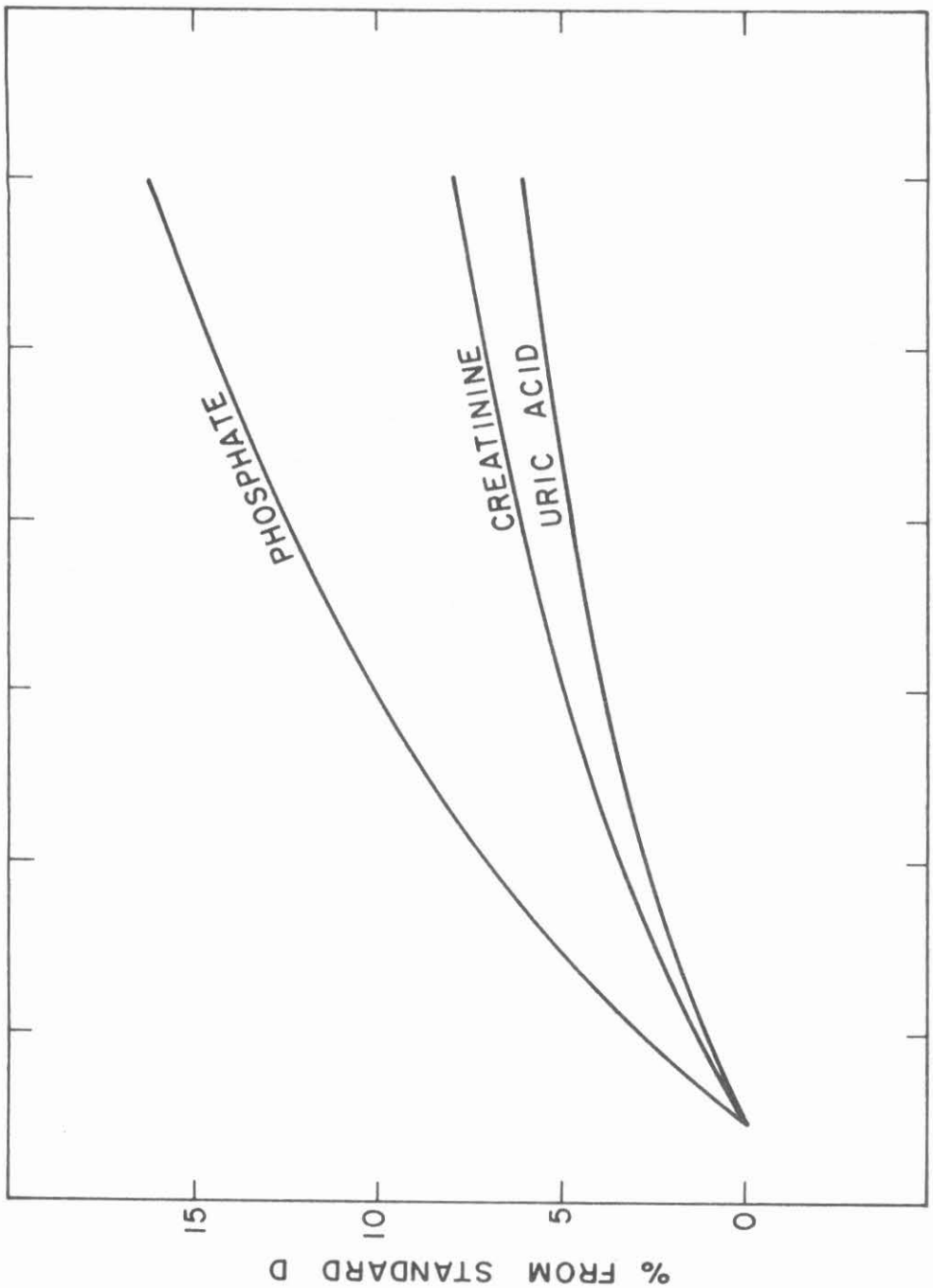

FIGURE 18. Dialysance Dependence upon Elapsed Time of Dialysis

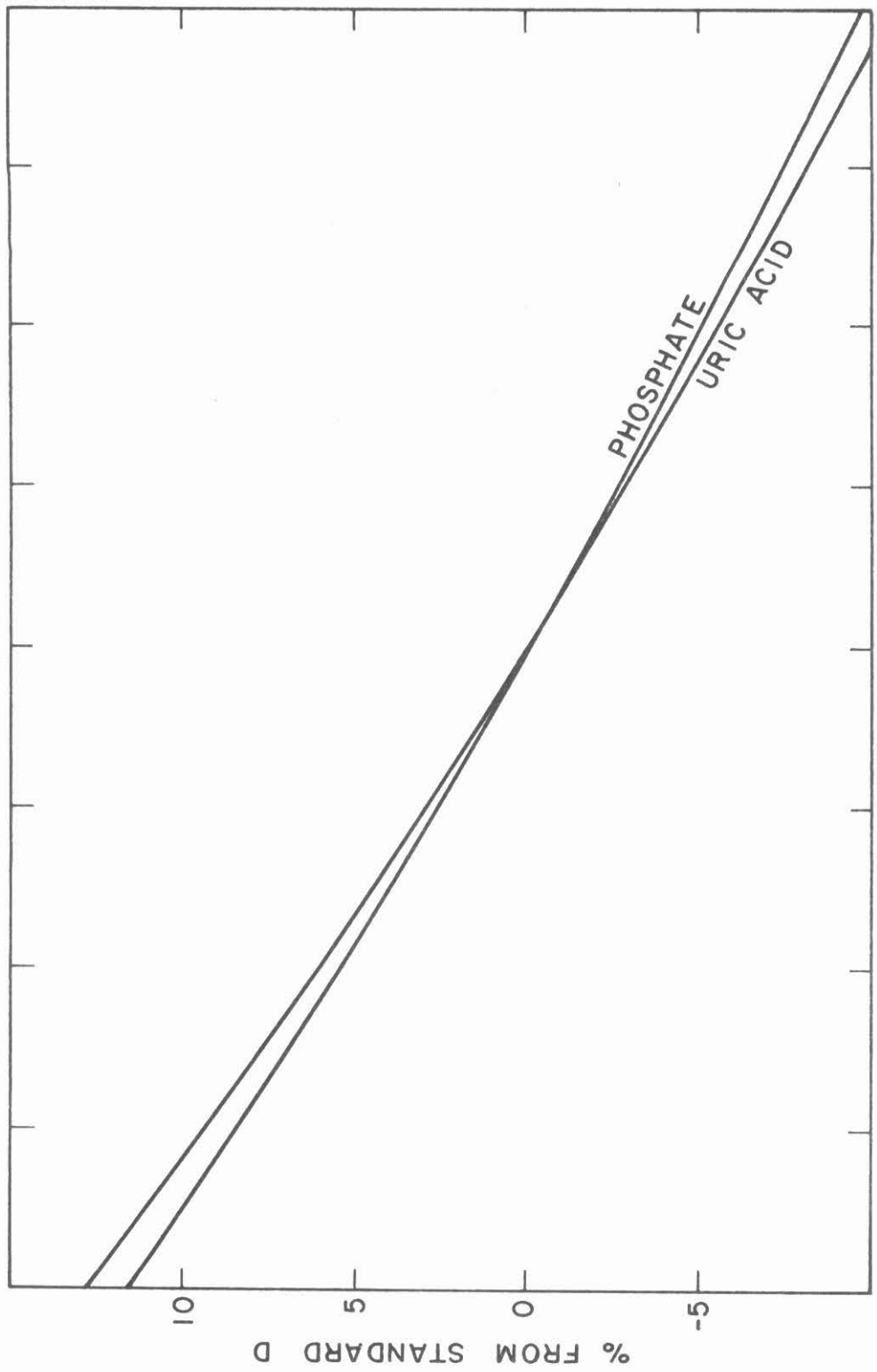

FIGURE 19. Dialysance Dependence upon Hematocrit

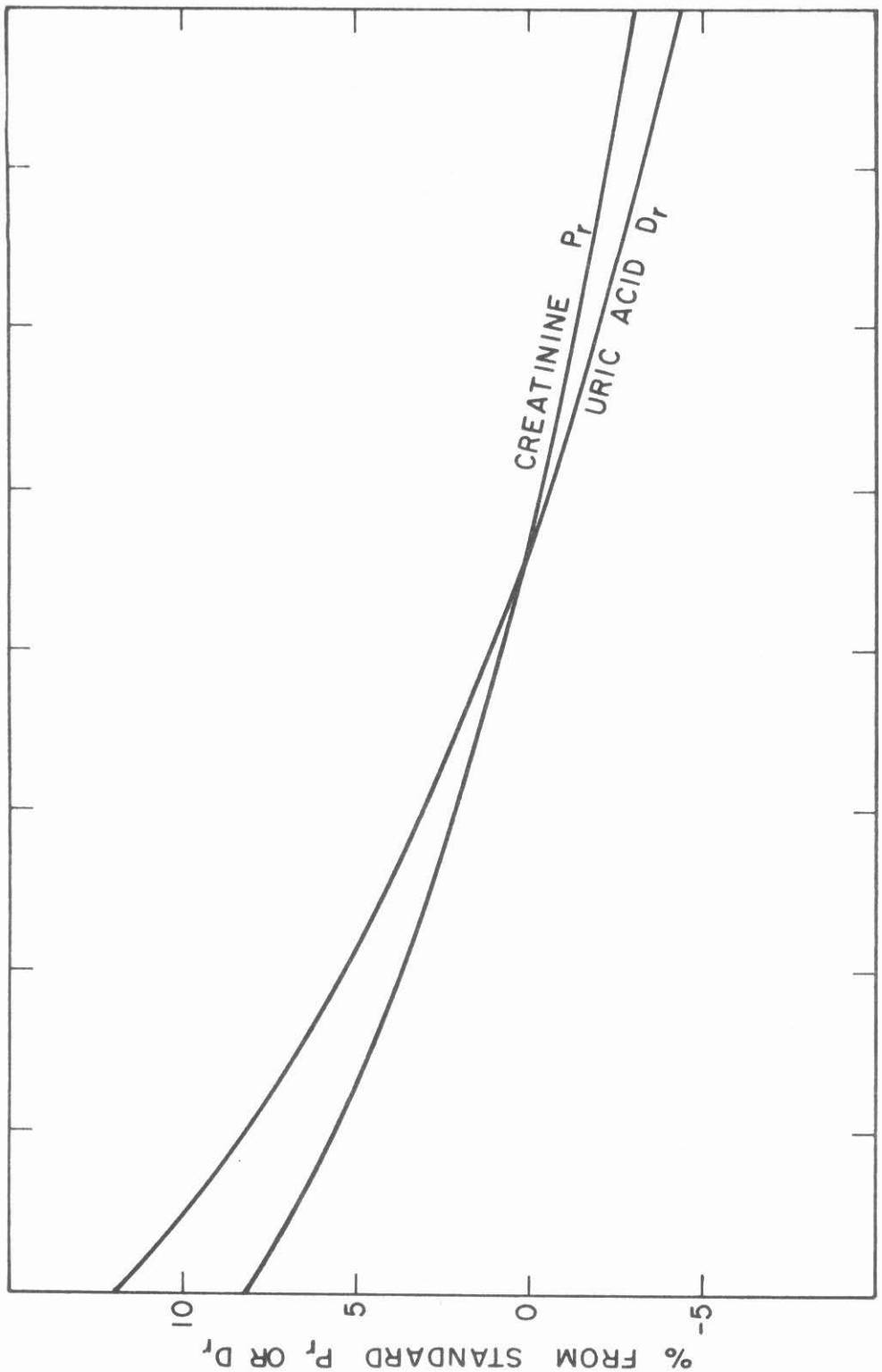

FIGURE 20. Relative Coefficient Dependencies upon Blood Velocity

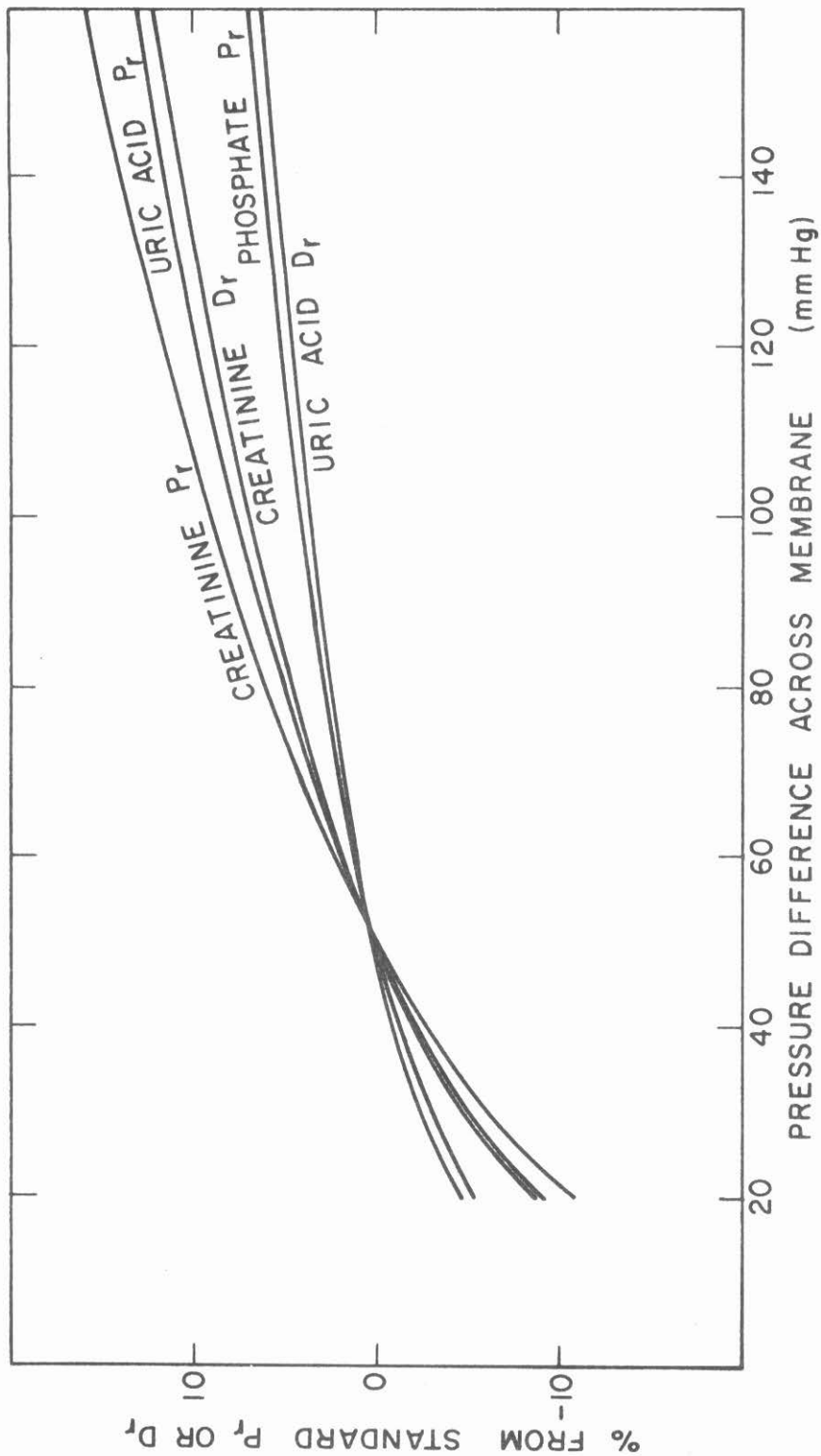

FIGURE 21. Relative Coefficient Dependencies upon Pressure Difference

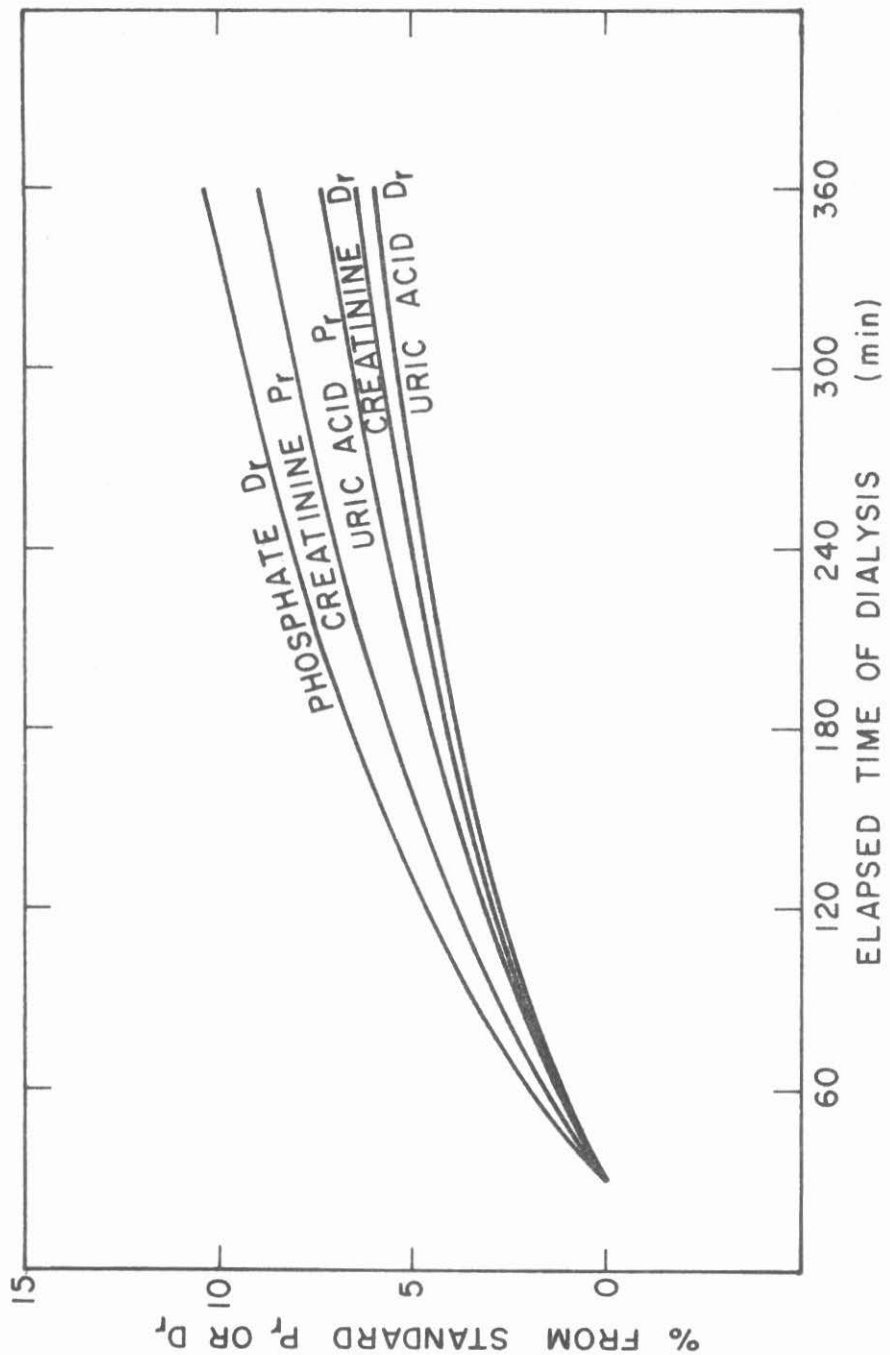

FIGURE 22. Relative Coefficient Dependencies upon Time

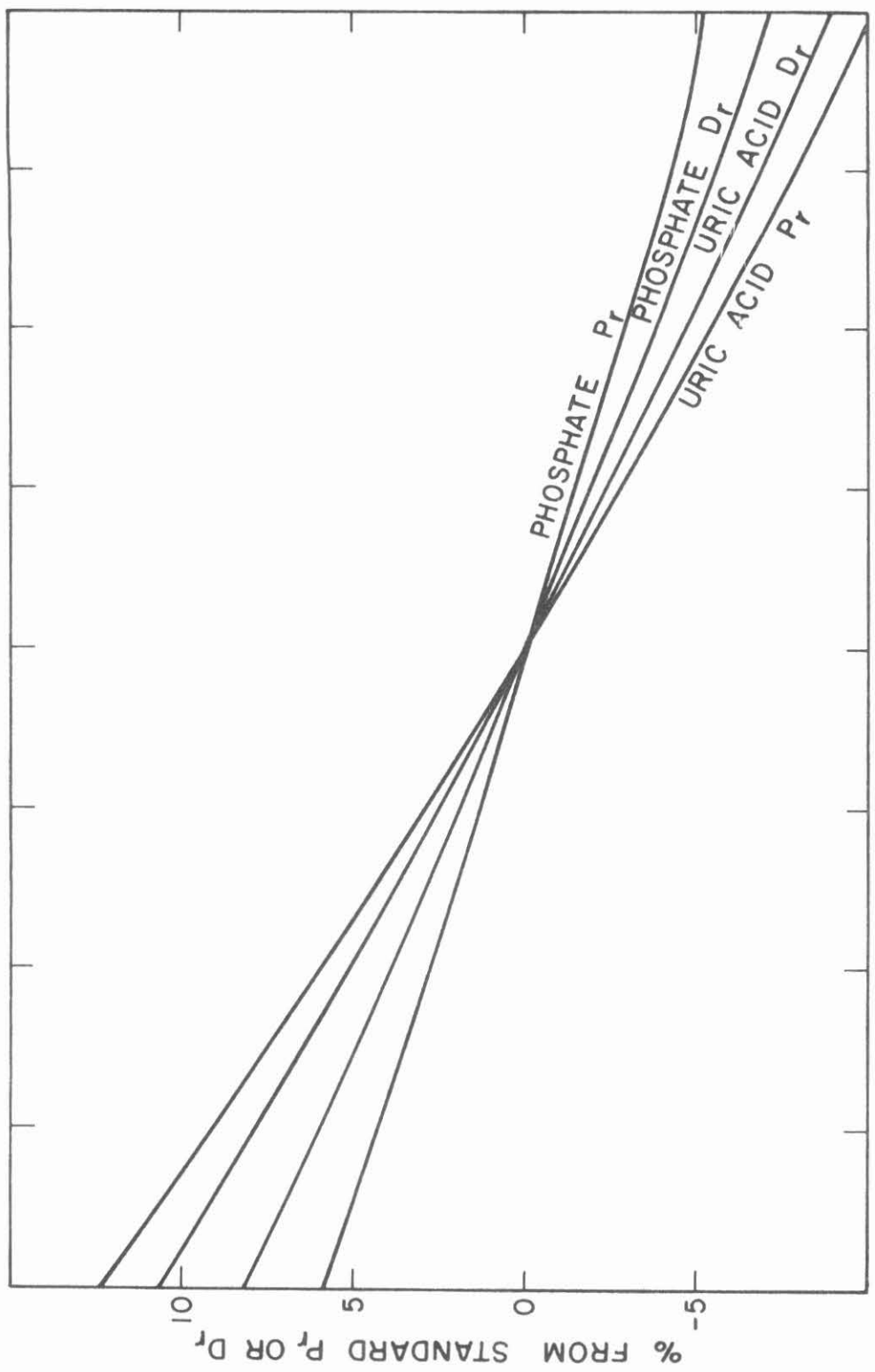

FIGURE 23. Relative Coefficient Dependence upon Hematocrit

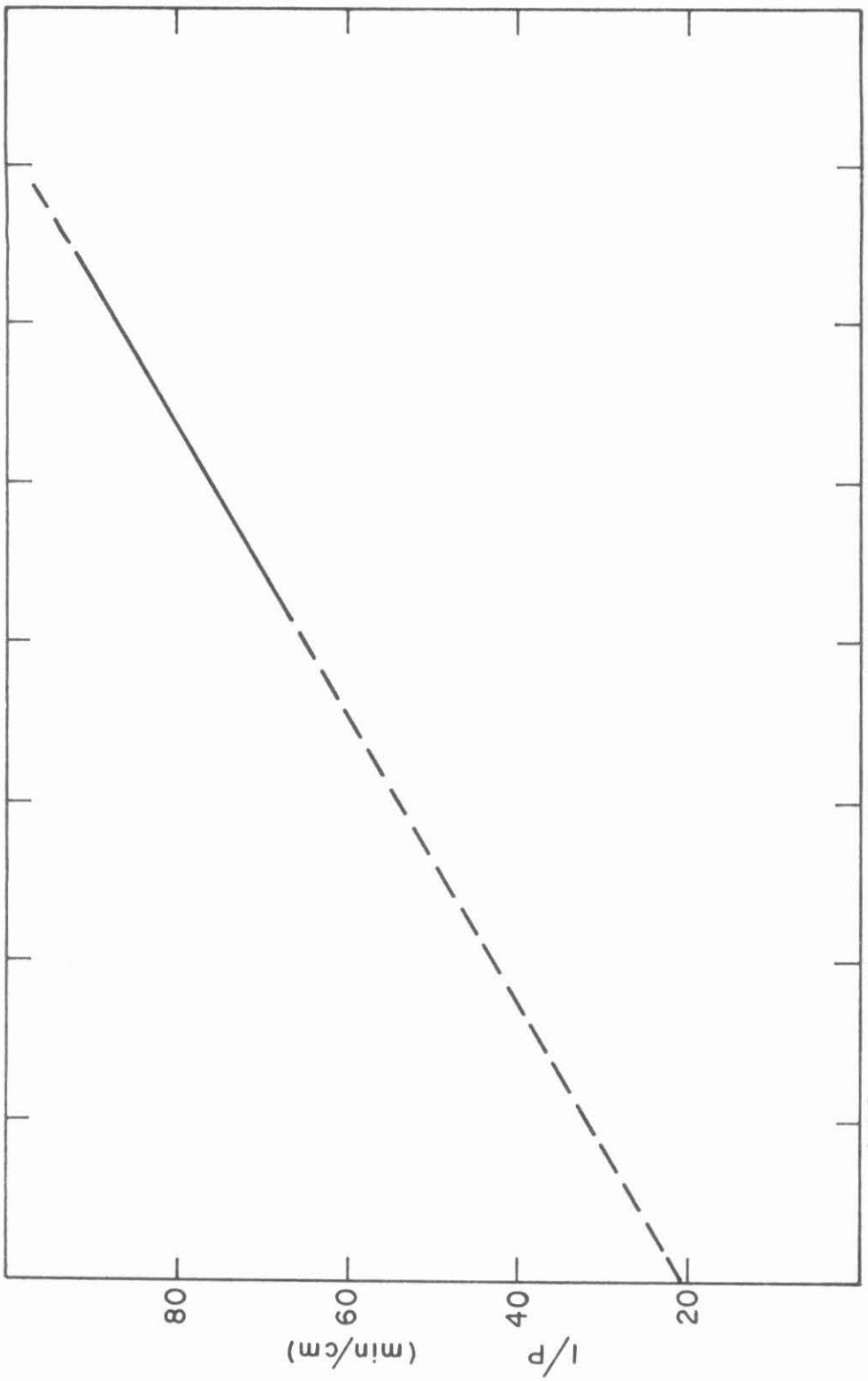

Figure 24. Wilson Plot for Creatinine Blood Velocity

TABLE I. DIALYSIS DATA IDENTIFICATION

Name of Patient	Dialysis Series Number	Dialysis Date	Patient Number	Hematocrit Percent	Total Negative Balance(kg)
Saito	9	1/18/66	6.1	26.8	1.3
Saito	9	2/1/66	6.2	26.5	2.8
Shaeffer	8a	1/14/66	7.0	25.0	2.6
Vollmer	11	4/26/66	8.1	25.5	-0.6
Folley	11	5/3/66	9.1	25.0/25.8	1.0
Vollmer	11	5/10/66	8.2	27.2/27.8	-0.2
Folley	11	5/17/66	9.2	24.8/25.0	0.7
Cooper	13a	10/20/66	10.1	27.5	0.1
Cooper	13a	11/1/66	10.2	25.0/25.0	0.8

TABLE II. BLOOD AND DIALYSATE FLOW RATES

Patient Number	Elapsed Time (min.)	Blood Flow Rate (mℓ/min.)	Dialysate Flow Rate (mℓ/min.)
6.1	30	240	620
	60	250	480
	120	200	440
	300	230	480
	360	220	500
6.2	30	250	580
	60	270	600
	120	280	520
	180	185	520
	240	270	500
	300	270	520
	360	260	520
7.0	60	227	760
	300	238	560
	360	236	560
8.1	30	140	580
	60	140	580
	120	130	555
	180	110	515
	240	120	510
	300	125	465
	360	110	490
9.1	75	210	515
	105	200	510
	135	180	530
8.2	60	140	650
	120	145	495
	300	140	510

Patient Number	Elapsed Time (min.)	Blood Flow Rate (mℓ/min.)	Dialysate Flow Rate (mℓ/min.)
9.2	60	200	495
	90	220	550
	120	200	470
	150	230	460
	180	200	525
10.1	60	245	510
	120	225	430
	180	230	500
	240	240	495
	300	215	500
	360	230	470
10.2	30	150	500
	60	170	515
	120	170	515
	240	175	500
	300	165	525
	360	160	450

TABLE III. EXPERIMENTAL DIALYZER PRESSURE MEASUREMENTS

Patient Number	Elapsed Time (min.)	Blood Inlet Pressure (mm Hg)	Blood Outlet Pressure (mm Hg)	Dialysate Inlet Pressure(mm Hg)	Dialysate Outlet Pressure(mm Hg)
6.1	30	114	40	18	14
	60	110	40	18.5	14
	120	108	44	17.8	14
	300	88	40	-35.5	-41
	360	96	42	-30	-34
6.2	30	120	50	15.5	8
	60	110	52	-54.5	-64
	120	112	54	-57.5	-66.5
	180	109	36	-55	-63
	240	118	48	-50	-58
	300	106	48	-52.5	-60
	360	110	46	-52	-61
7.0	60	98	46	-	-
	300	80	40	-79	-84
	360	96	52	-78	-82
8.1	30	77	33	17	11.5
	60	76	34	17	11
	120	70	33	16	11
	180	66	38	15	9
	240	64	30	16	9
	300	64	30	- 4-1/2	-9
	360	60	36	- 3	-10-1/2
9.1	75	96	36	20	14
	105	95	38	25	19
	135	80	40	25	19
8.2	60	68	34	16	10
	120	75	34	13	9
	300	72	28	-14	-20

Patient Number	Elapsed Time (min.)	Blood Inlet Pressure (mm Hg)	Blood Outlet Pressure (mm Hg)	Dialysate Inlet Pressure(mm Hg)	Dialysate Outlet Pressure(mm Hg)
9.2	60	93	34	8.5	3
	90	90	38	-32	-40
	120	90	37	-35	-43
	150	110	45	8	2
	180	87	35	9	2
10.1	60	82	32	23	17
	120	80	26	23	17-1/2
	180	66	31	21	15
	240	81	28	24	18
	300	79	28	23	18
	360	80	28	24	19
10.2	30	88	38	8	4
	60	80	32	16	10
	120	80	34	18	10
	240	83	36	18	12
	300	86	37	20	16
	360	81	32	31	25

TABLE IV. DIALYZER PRESSURES

Patient Number	Elapsed Time (min.)	Average Blood Side Pressure (mm Hg)	Average Dialysate Side Pressure (mm Hg)	Pressure Difference (mm Hg)
6.1	30	77	16	61
	60	75	16.3	59
	120	76	16	60
	300	64	-38	102
	360	69	-32	101
6.2	30	85	12	73
	60	81	-59	140
	120	83	-62	145
	180	72.5	-59	132
	240	83	-54	137
	300	77	-56	143
	360	78	-56	134
7.0	60	72	-	57
	300	60	-81	141
	360	74	-80	154
8.1	30	55	14	41
	60	55	14	41
	120	52	14	38
	180	52	12	40
	240	47	12	35
	300	47	-7	54
	360	48	-7	55
9.1	75	66	17	49
	105	66	22	44
	135	60	22	38
8.2	60	52	13	39
	120	55	11	44
	300	50	-17	67

Patient Number	Elapsed Time (min.)	Average Blood Side Pressure (mm Hg)	Average Dialysate Side Pressure (mm Hg)	Pressure Difference (mm Hg)
9.2	60	64	6	58
	90	64	-36	100
	120	64	-39	103
	150	77	5	72
	180	61	5	56
10.1	60	57	20	37
	120	53	20	33
	180	49	18	31
	240	55	21	34
	300	53	20	33
	360	54	22	32
10.2	30	63	6	57
	60	56	13	43
	120	57	14	43
	240	60	16	44
	300	62	18	44
	360	57	28	29

TABLE V. INLET PLASMA CONCENTRATION

Patient Number	Elapsed Time (min)	Inlet Plasma Concentration of Creatinine (mg %)	Inlet Plasma Concentration of Plasma Urea Nitrogen(mg %)	Inlet Plasma Concentration of Uric Acid (mg %)	Inlet Plasma Concentration of Inorganic Phosphate(mg %)
6.1	30	10.00	41.80	6.00	5.55
	60	9.38	39.00	5.70	4.96
	120	-	35.60	5.40	4.70
	300	7.31	27.00	4.45	4.25
	360	-	24.50	-	-
6.2	30	10.96	50.50	8.75	5.40
	60	10.40	47.50	8.15	5.00
	120	9.64	43.50	7.45	4.70
	180	9.06	39.00	7.00	4.45
	240	8.41	36.00	6.65	4.45
	300	-	-	6.10	4.30
	360	-	31.00	5.70	4.51
7.0	60	12.26	80.40	8.60	7.75
	300	9.50	54.00	6.30	6.10
	360	8.87	51.00	5.55	6.00
8.1	30	15.80	109.00	8.40	10.10
	60	14.70	104.00	7.70	8.90
	120	13.30	94.00	6.85	7.10
	180	12.70	87.00	6.35	6.90
	240	11.90	79.00	5.80	6.43
	300	11.40	70.00	5.40	6.05
	360	10.90	64.00	5.00	5.62
9.1	75	9.65	35.20	5.50	4.00
	105	9.40	-	5.20	-
	135	8.70	31.80	4.70	3.95

Patient Number	Elapsed Time (min)	Inlet Plasma Concentration of Creatinine (mg %)	Inlet Plasma Concentration of Plasma Urea Nitrogen(mg %)	Inlet Plasma Concentration of Uric Acid (mg %)	Inlet Plasma Concentration of Inorganic Phosphate(mg %)
8.2	60	17.50	93.50	7.62	7.80
	120	14.40	82.00	6.91	-
	300	12.30	62.10	5.39	6.15
9.2	60	10.50	55.00	6.55	4.60
	90	10.20	53.00	6.22	4.45
	120	9.60	52.00	5.72	4.35
	150	9.15	45.00	5.25	4.40
	180	9.00	46.50	5.08	4.35
10.1	60	7.25	54.00	6.90	7.15
	120	6.70	49.10	6.30	6.65
	180	6.25	44.20	5.85	6.50
	240	5.90	39.20	5.55	6.10
	300	5.55	36.00	5.20	5.90
	360	5.05	32.50	4.80	5.70
10.2	30	8.40	83.50	8.50	8.30
	60	8.25	84.00	8.30	8.05
	120	7.05	72.30	7.45	6.80
	240	6.00	57.00	6.00	5.95
	300	5.50	50.60	5.50	5.55
	360	4.90	44.40	4.95	5.00

TABLE VI. OUTLET PLASMA CONCENTRATIONS

Patient Number	Elapsed Time (min)	Outlet Plasma Concentration of Creatinine (mg %)	Outlet Plasma Concentration of Plasma Urea Nitrogen(mg %)	Outlet Plasma Concentration of Uric Acid (mg %)	Outlet Plasma Concentration of Inorganic Phosphate (mg %)
6.1	30	6.83	24.50	4.65	4.25
	60	6.72	24.50	4.45	4.00
	120	-	21.70	4.10	3.65
	300	5.03	15.80	3.30	3.15
	360	-	13.10	-	-
6.2	30	8.02	34.00	6.70	4.30
	60	7.83	34.00	6.55	4.10
	120	7.21	32.00	6.00	3.95
	180	6.23	26.00	5.35	3.45
	240	6.28	25.70	5.35	3.50
	300	-	-	5.05	3.55
	360	-	21.50	4.60	3.30
7.0	60	8.33	46.20	6.20	5.45
	300	6.49	33.80	4.70	4.40
	360	5.58	30.70	4.00	4.25
8.1	30	9.10	47.50	5.45	6.20
	60	8.55	46.50	5.05	5.40
	120	6.85	37.50	4.00	4.30
	180	6.45	33.00	3.65	4.00
	240	6.20	33.50	3.45	4.05
	300	5.90	29.50	3.20	3.75
	360	4.65	21.00	2.45	2.90
9.1	75	6.40	19.00	3.80	2.65
	105	6.15	-	3.60	-
	135	5.80	16.70	3.30	2.55

Patient Number	Elapsed Time (min)	Outlet Plasma Concentration of Creatinine (mg %)	Outlet Plasma Concentration of Plasma Urea Nitrogen(mg %)	Outlet Plasma Concentration of Uric Acid (mg %)	Outlet Plasma Concentration of Inorganic Phosphate (mg %)
8.2	60	9.60	37.50	4.85	5.05
	120	8.05	37.70	4.26	-
	300	6.90	27.90	3.42	4.00
9.2	60	7.00	32.50	4.79	3.45
	90	6.70	32.00	4.45	3.40
	120	6.25	29.50	4.05	3.25
	150	6.20	29.30	3.92	3.45
	180	5.60	24.50	3.50	3.15
10.1	60	4.90	30.00	5.15	5.15
	120	4.45	26.80	4.60	4.75
	180	4.20	23.80	4.35	4.50
	240	3.85	22.00	4.20	4.45
	300	3.55	19.20	3.75	4.10
	360	3.35	18.40	3.50	3.95
10.2	30	4.90	40.20	5.63	5.25
	60	4.75	39.00	5.35	5.00
	120	4.35	34.40	4.90	4.55
	240	3.65	28.40	3.90	3.95
	300	3.50	27.50	3.60	3.85
	360	2.95	23.80	3.20	3.55

TABLE VII. OUTLET DIALYSATE CONCENTRATIONS

Patient Number	Elapsed Time	Creatinine (mg %)	Urea (mg %)	Uric Acid (mg %)	Inorganic Phosphate (mg %)
6.1	30	1.23	6.2	0.55	-
	60	1.38	7.7	0.65	-
	120	-	5.8	0.60	-
	300	1.00	4.5	0.50	-
	360	-	-	-	-
6.2	30	-	9.0	0.85	-
	60	-	8.5	0.75	-
	120	-	8.0	0.80	-
	180	-	7.0	0.75	-
	240	-	6.5	0.70	-
	300	-	-	0.65	-
	360	-	5.5	0.60	-
7.0	60	1.23	8.2	0.50	-
	300	1.35	7.6	0.60	-
	360	1.19	7.1	0.50	-
8.1	30	1.80	15.5	0.80	0.65
	60	1.95	16.0	0.85	0.65
	120	1.60	13.0	0.65	0.40
	180	1.50	11.5	0.60	0.35
	240	1.50	10.5	0.55	0.32
	300	1.50	10.5	0.50	0.32
	360	1.40	10.0	0.50	0.32
9.1	75	1.55	6.5	0.55	0.20
	105	0.60	-	0.55	-
	135	1.30	5.5	0.45	0.11
8.2	60	1.70	12.7	0.40	0.55
	120	1.95	14.8	0.50	-
	300	1.40	9.8	0.20	0.50

Patient Number	Elapsed Time	Creatinine (mg %)	Urea (mg %)	Uric Acid (mg %)	Inorganic Phosphate (mg %)
9.2	60	1.55	10.0	0.65	0.35
	90	1.40	9.0	0.62	0.30
	120	1.45	8.5	0.65	0.35
	150	1.40	8.2	0.60	0.35
	180	1.30	7.0	0.52	0.30
10.1	60	1.15	9.2	0.70	0.65
	120	1.15	9.3	0.75	0.70
	180	1.00	7.0	0.60	0.55
	240	0.95	6.0	0.60	0.50
	300	0.90	5.5	0.50	0.45
	360	0.85	5.1	0.50	0.55
10.2	30	1.10	16.1	1.00	0.75
	60	1.05	16.0	0.95	0.80
	120	0.95	13.5	0.85	0.65
	240	0.80	11.0	0.70	0.65
	300	0.75	11.0	0.70	0.70
	360	0.70	9.2	0.60	0.60

TABLE VIIIa

Component	Standard Red Blood Cell Concentration (mg %)	Standard Plasma Concentration (mg %)	Equilibrium Partition Coefficient
Creatinine	1.8	0.91	2.0
Urea	30	34	0.88
Uric Acid	1.9	3.8	0.50
Inorganic Phosphate	2.4	3.2	0.75

From Arbitton, E.C. (Editor),"Standard Values in Blood", W. B. Saunders Company, Philadelphia, 1952.

TABLE VIIIb

Component	Average Predicted Effective Partition Coefficient	Assumed Effective Partition Coefficient
Creatinine	1.0 ± 0.4	2.0
Urea	1.0 ± 0.3	0.88
Uric Acid	0.7 ± 0.5	0.0
Inorganic Phosphate	-0.1 ± 0.5	0.0

TABLE IX. REGRESSION ANALYSIS RESULTS FOR OVERALL TRANSFER COEFFICIENTS

Substance	Constant	Variable	Exponent	Standard Deviation of Exponent	Confidence Limits (%)
Creatinine	4.601×10^{-3}	v_b $(\frac{cm}{min})$	0.245	0.062	99.6
		Δp_m (mm Hg)	0	-	-
		(1+ t)(hours)	0.077	0.029	97.8
		H	0	-	-
		c_{p_i} (mg %)	0	-	-
Urea	1.0272×10^{-2}	v_b	0.220	0.085	97.7
		Δp_m	-0.141	0.039	99.6
		1 + t	0	-	-
		H	0	-	-
		c_{p_i}	0	-	-
Uric Acid	3.779×10^{-4}	v_b	0.164	0.070	96.5
		Δp_m	-0.068	0.029	96.1
		1 + t	0.056	0.030	91.7
		H	-1.71	0.42	99.7
		c_{p_i}	0	-	-
Inorganic Phosphate	5.377×10^{-5}	v_b	0.428	0.118	99.6
		Δp_m	0	-	∿50
		1 + t	0.123	0.048	97.6
		H	-1.46	0.66	95.4
		c_{p_i}	0.456	0.110	99.7

TABLE X. OVER-ALL MASS-TRANSFER COEFFICIENTS

Substance	Average Value of P (cm/min.)	Standard Error of P (%)	Standard Error of $P - P_{eqn}$ Differences (%)	Reference Value of $P(\frac{cm}{min})$
Creatinine	0.01441	11.1	9.0	0.01374
Urea	0.01491	14.2	11.7	0.01536
Uric Acid	0.00624	10.9	8.9	0.00606
Phosphate	0.00620	16.5	13.0	0.00626

TABLE XI. REGRESSION ANALYSIS RESULTS FOR DIALYSANCES

Substance	Constant	Variable	Exponent	Standard Deviation of Exponent	Confidence Limits(%)
Creatinine	15.23	v_b (cm/min)	0.393	0.046	99.99
		Δp_m (mm Hg)	0	-	-
		1 + t (hours)	0.049	0.022	95.8
		H	0	-	-
		c_{p_i} (mg %)	0	-	-
Urea	18.92	v_b	0.427	0.060	99.99
		Δp_m	-0.086	0.028	99.1
		1 + t	0	-	-
		H	0	-	-
		c_{p_i}	0	-	-
Uric Acid	1.781	v_b	0.311	0.057	99.9
		Δp_m	-0.064	0.024	98.0
		1 + t	0.038	0.024	85.0
		H	-1.50	0.34	99.8
		c_{p_i}	0	-	-
Inorganic Phosphate	0.4318	v_b	0.526	0.096	99.9
		Δp_m	-0.059	0.039	80.0
		1 + t	0.098	0.039	97.3
		H	-1.38	0.53	97.5
		c_{p_i}	0.324	0.099	99.3

TABLE XII. DIALYSANCES

Substance	Average Value of D (m_ℓ/min)	Standard Error of D (%)	Standard Error of $D - D_{eqn}$ Differences (%)	Reference Value of D (m_ℓ/min)
Creatinine	86.4	11.2	6.6	85.4
Urea	83.1	13.3	8.5	86.4
Uric Acid	41.4	10.0	7.2	41.2
Phosphate	41.1	15.0	10.5	42.1

TABLE XIII. REGRESSION ANALYSIS RESULTS FOR RELATIVE DIALYSANCES

Substance	Constant	Variable	Exponent	Standard Deviation of Exponent	Confidence Limits (%)
Creatinine	0.6688	v_b $(\frac{cm}{min})$	0	-	~50
		Δp_m (mm Hg)	0.098	0.017	99.9
		1 + t (hrs)	0.041	0.017	96.7
		H	0	-	-
		c_{p_i} (mg %)	0	-	-
Uric Acid	0.1200	v_b	-0.123	0.046	98.0
		Δp_m	0.052	0.020	97.7
		1 + t	0.038	0.019	92.7
		H	-1.26	0.27	99.8
		c_{p_i}	0	-	-
Inorganic Phosphate	0.09828	v_b	0	-	-
		Δp_m	0	-	-
		1 + t	0.065	0.025	97.8
		H	-0.98	0.32	99.0
		c_{p_i}	0.125	0.053	96.4

TABLE XIV. RELATIVE DIALYSANCES

Substance	Average Value of D_r	Standard Error of D_r (%)	Standard Error of $D_r - D_{r_{eqn}}$ Differences	Reference D_r Value
Creatinine	1.047	7.5	5.2	0.998
Uric Acid	0.505	9.2	5.8	0.479
Phosphate	0.499	8.8	7.3	0.483

TABLE XV. REGRESSION ANALYSIS RESULTS FOR RELATIVE PERMEABILITIES

Substance	Constant	Variable	Exponent	Standard Deviation of Exponent	Confidence Limits (%)
Creatinine	0.8583	v_b $(\frac{cm}{min})$	-0.085	0.048	89.7
		Δp_m (mm Hg)	0.125	0.023	99.9
		1 + t (hrs)	0.055	0.023	97.0
		H	0	-	-
		c_{p_i} (mg %)	0	-	-
Uric Acid	0.03706	v_b	0	-	-
		Δp_m	0.105	0.024	99.9
		1 + t	0.046	0.024	92.4
		H	-1.46	0.31	99.9
		c_{p_i}	0	-	-
Inorganic Phosphate	0.1254	v_b	0	-	-
		Δp_m	0.059	0.030	93.0
		1 + t	0	-	$\sim$ 75
		H	-0.73	0.40	90.9
		c_{p_i}	0	-	-

TABLE XVI. RELATIVE PERMEABILITIES

Substance	Average Value of P_r	Standard Error of P_r (%)	Standard Error of $P_r - P_{r_{eqn}}$ Differences (%)	Reference P_r Value
Creatinine	1.064	9.9	6.8	0.990
Uric Acid	0.432	11.2	7.6	0.407
Phosphate	0.426	10.2	9.2	0.420

TABLE XVII. RESISTANCES TO TRANSFER

Substance	Variable Parameter	Membrane Resistance $(\frac{\text{min.}}{\text{cm.}})$	Blood Layer Resistance $(\frac{\text{min.}}{\text{cm.}})$	Reference Membrane Resistance $(\frac{\text{min.}}{\text{cm.}})$	Reference Blood Layer Resistance $(\frac{\text{min.}}{\text{cm.}})$
Creatinine	$v_b \frac{\text{cm.}}{\text{min.}}$	21	$219/_{v}^{0.33}$	21	52
	(1+t) (hrs)	$16.25/_{(1+t)}^{1.0}$	62	11	62
Urea	v_b	19	$170/_{v}^{0.30}$	19	46
	Δ_{p_m} (mm.Hg.)	11.4	$205\Delta_{p_m}^{0.20}$	21	44
Uric Acid	v_b	30	$325/_{v}^{0.20}$	30	135
	Δ_{p_m}	56	$730\Delta_{p_m}^{0.10}$	56	109
	1+t	$26.6/_{(1+t)}^{1.0}$	147	18	147
Inorganic Phosphate	v_b	24.5	$1175/_{v}^{0.50}$	24.5	135
	1+t	$55/_{(1+t)}^{1.0}$	123	37	123

Appendix A

The subroutine used for the regression analysis is reproduced below. The language used is Fortran IV. A flowchart for the program can be found in the literature (1).

```
$IBETC REG      DECK,LIST,REF

      SUBROUTINE REGRES(N, M, X, F1, F2, IP, ANAME)

     DIMENSION       R(25,25),S(25,25),SWTX(25),XBAR(25),SIGMA(25),
    1    BETA(25),A(25,25),B(25,25),SB(25),C(25,25),V(25)
     DIMENSION X(M,N)
     COMMON / REGOO1 / BETAZ,BETA
     COMMON / REGOO2 / SB
     COMMON / REGOO3 / SY, PHI, V
     COMMON / REGOO4 / XBAR, SIGMA
     LOGICAL PSW
     EQUIVALENCE (R,A,B,C,S),          (SWTX,SB)
     PSW = .TRUE.
     IF (IP .GE  5) PSW = .FALSE.
     IF(PSW) WRITE (6,  70) ANAME
  70 FORMAT (1H1, //, 40X, jjH***** MULTIPLE REGRESSION ANALYSIS ON DAT
    1A ', A6, 7H' *****, ///)
     IF (N .LF. 25)GO TO 120
     IF(PSW) WRITE (6, 100)
 100 FORMAT (10X, 34H*** ERROR... N GREATER THAN 25 ***)
     GO TO 2190
 120 NM  = N - 1
     DO 170 I=1,N
     DO 150 J=1,N
 150 R(I,J)=0.0
     BETA(I)=0.0
 170 SWTX(I)=0.0
     IF(PSW) WRITE (6, 190) N,M
 190 FORMAT (50H NUMBER OF INDEPENDENT AND DEPENDENT VARIABLES IS ,
    1     12, //, 26H NUMBER OF OBSERVATIONS IS , I6, //)
     IF(PSW) WRITE (6, 210) F1, F2
 210 FORMAT (33H F-LEVEL TO ENTER A VARIABLE IS  , F6.2, //,
    1     33H F-LEVEL TO REMOVE A VARIABLE IS , F6.2, //)
     IF(PSW) WRITE (6, 230) N
 230 FORMAT(28H THE DEPENDENT VARIABLE IS X,I2,//)
C BOX 1. INPUT DATA
     DO 300 I = 1,M
     DO 300 J = 1,N
     IF (X(I,J))270,300,270
        SUMS OF VARIABLES
 270 SWTX(J) = SWTX(J) + X(I,J)
        SUMS OF SQUARES AND CROSS-PRODUCTS
     DO 290 L = 1,N
 290 S(J,L) = S(J,L) + (X(I,J) * X(I,L))
 300 CONTINUE
     SUMWT=FLOAT(M)
     IF (IP-2)330,450,450
 330 WRITE(6,340)
 340 FORMAT(////,50X,18H SUMS OF VARIABLES,//)
     WRITE(6,360)
 360 FORMAT(6X2HX111X2HX211X2HX311X2HX411X2HX511X2HX611X2HX711X2HX811X2
```

```
     1HX911X3HX102X/)
      WRITE(6,380) (SWTX(I),I=1,N)
  380 FORMAT(1HO,1P10E13.5)
  390 WRITE(6,400)
  400 FORMAT(////,40X,38HRAW SUMS OF SQUARES AND CROSS PRODUCTS,//)
      WRITE(6,360)
      DO 430 I=1,N
  430 WRITE(6,440) (S(J,I),J=1,I)
  440 FORMAT(1H0,1P10E13.5,/,1H ,10E13.5,/,1H ,10E13.5)
  450 EMSQ=SUMWT**2
      DO 480 I=1,N
C BOX 3. VARIANCE-COVARIANCE MATRIX
      DO 480 J=I,N
  480 S(I,J)= (SUMWT*S(I,J)-SWTX(I)*SWTX(J))/EMSQ
      IF (IP-2)500,570,570
  500 WRITE(6,510)
  510 FORMAT (1H1)
      WRITE(6,530)
  530 FORMAT(///,40X,26HVARIANCE-COVARIANCE MATRIX,//)
      WRITE(6,360)
      DO 560 I=1,N
  560 WRITE(6,440) (S(J,I),J=1,I)
         MEANS OF VARIABLES
  570 DO 580 I=1,N
  580 XBAR(I)=SWTX(I)/SUMWT
  590 IF(PSW) WRITE (6, 600)
  600 FORMAT(////40X,24HMEAN VALUES OF VARIABLES,//)
      IF(PSW) WRITE (6, 360)
      IF(PSW) WRITE (6, 380) (XBAR(I), I=1,N)
C BOX 4.
      DO 640 I=1,N
  640 SIGMA(I)=SQRT(S(I,I))
  650 IF(PSW) WRITE (6, 660)
  660 FORMAT(////40X, 32HSTANDARD DEVIATIONS OF VARIABLES,//)
      IF(PSW) WRITE (6, 360)
      IF(PSW) WRITE (6, 380) (SIGMA(I), I=1,N)
      DO 730 I=1,NM1
      JA=I+1
      DO 730 J=JA,N
      R(I,J)=S(I,J)/(SIGMA(I)*SIGMA(J))
  730 R(J,I)=R(I,J)
      DO 750 I=1,N
  750 R(I,I)=1.0
      IF (IP-j)770,840,840
  770 WRITE(6,780)
  780 FORMAT(1H1,///,40X,24HCORRELATION COEFFICIENTS,//)
      WRITE (6,800)
  800 FORMAT(9X2HX111X2HX211X2HX311X2HX411X2HX511X2HX611X2HX711X2HX811X2
     1HX911X3HX102X/)
      DO 820 I=1,N
  820 WRITE(6,830) (R(I,J),J=1,I)
  830 FORMAT( H0,10F13.5,/,1H ,10F13.5,/,1H ,10F13.5)
C     STEPWISE MULTIPLE REGRESSION
```

```
  840 IF(PSW) WRITE (6, 850)
  850 FORMAT (////, 34H *** BEGIN STEPWISE REGRESSION ***, //)
      TOL=0.001
      SWTCH =0.0
  880 SITCH=1.0
      PHI=SUMWT - 1.0
      ISTP=1
C BOX 5.
  910 SY=SIGMA(N)*SQRT(R(N,N)*SUMWT/PHI)
      IF ( SWTCH)960,930,960
  930 IF(PSW) WRITE (6,1370) SY
      IF(PSW) WRITE (6, 950)
  950 FORMAT(//)
  960 I=1
      VMIN=10.0E20
      VMAX=0.0
      NMIN=0
      NMAX=0
C BOX 6.
 1010 IF (A(I,I)-TOL)1020,1020,1050
 1020 IF(PSW) WRITE (6,1030) I
 1030 FORMAT(20H TOLERANCE CHECK.  X,I2)
      GO TO 1170
C BOX 7.
 1050 V(I)=(A(I,N)*A(N,I))/A(I,I)
C BOX 8.
      IF (V(I))1120,1170,1070
C BOX 9.
 1070 IF (V(I)-VMAX)1170,1170,1080
C BOX 10.
 1080 VMAX=V(I)
      NMAX=I
      BETA(I)=0.0
      GO TO 1170
C BOX 11.
 1120 BETA(I)=(B(I,N)*SIGMA(N))/SIGMA(I)
      SB(I)=SY*SQRT(C(I,I)/SUMWT)/SIGMA(I)
C BOX 12.
      IF (ABS(V(I))-ABS(VMIN))1150,1170,1170
C BOX 13.
 1150 VMIN=V(I)
      NMIN=I
C BOX 14.
 1170 IF (I-(N-1))1180,1200,1200
C BOX 15.
 1180 I=I+1
      GO TO 1010
C BOX 16.
 1200 BETAZ=0.0
      DO 1220 I=1,NM1
 1220 BETAZ=BETAZ+(BETA(I)*XBAR(I))
      BETAZ=XBAR(N)-BETAZ
```

```
C DAVES INSERTION
      IF(SWTCH)1250,1520,1250
 1250 IF (K.EQ.0) GO TO 1850
      IF(PSW) WRITE (6,1260) ISTP
 1260 FORMAT(10HOSTEP NO. ,I2)
      GO TO(1320,1280), JUMP
 1280 IF(PSW) WRITE (6,1290) K
 1290 FORMAT(/6X,22H VARIABLE REMOVED IS X,I2)
      IF(PSW) WRITE (6,1350) F
      GO TO 1360
 1320 IF(PSW) WRITE (6,1330) K
 1330 FORMAT(/6X,23H VARIABLE ENTERING IS X,I2,)
      IF(PSW) WRITE (6,1350) FINK
 1350 FORMAT(/6X,11H F LEVEL    ,F17.6)
 1360 IF(PSW) WRITE (6,1370) SY
 1370 FORMAT(/6X,16H STD. ERROR OF Y,F12.6)
      RMUL=SQRT(1.0-R(N,N))
      IF(PSW) WRITE (6,1400) RMUL
 1400 FORMAT(/6X,11H MULTIPLE R,F17.6)
      IF(PSW) WRITE (6,1420) BETAZ
 1420 FORMAT(/6X,14H CONSTANT TERM,F14.6)
      ISTP= ISTP+1
      IF(PSW) WRITE (6,1450)
 1450 FORMAT(/40X45HVARIABLE    COEFFICIENT    STD. ERR. OF COEF.,//)
      DO 1500 I=1,NM1
      IF (BETA(I))1480,1500,1480
 1480 IF(PSW) WRITE (6,1490) I, BETA9I0, SB(I)
 1490 FORMAT(42X,1HX,I2,2F17.6)
 1500 CONTINUE
      IF (SITCH)1520,1850,1520
C BOX 17.
 1520 F=ABS(VMIN)*PHI/R(N,N)
      IF (F-F2)1540,1580,1580
C BOX 18.
 1540 K=NMIN
      PHI=PHI+1.0
      JUMP=2
      GO TO 1660
C BOX 19.
 1580 PHI=PHI-1.0
      FINK=VMAX*PHI/(R(N,N)-VMAX)
      IF(FINK-F1)1610,1630,1630
 1610 PHI=PHI+1.0
      GO TO 1850
C BOX 20.
 1630 K=NMAX
      SITCH = SUMWT - PHI - FLOAT (N)
      JUMP=1
C BOX 21.
 1660 IF (K.EQ.0) GO TO 1850
      DO 1780 I=1,N
```

```
      DO 1780 J=1,N
      IF (I-K)1690,1700,1690
 1690 IF (J-K)1710,1730,1710
 1700 IF (J-K)1750,1770,1750
 1710 A(I,J)=((A(K,K)*A(I,J))-(A(I,K)*A(K,J)))/A(K,K)
      GO TO 1780
 1730 A(I,N+1)=(-1.0*A(I,K)/A(K,K))
      GO TO 1780
 1750 A(N+1,J)=A(K,J)/A(K,K)
      GO TO 1780
 1770 A(N+1,K)=1.0/A(K,K)
 1780 CONTINUE
      DO 1800 I=1,N
 1800 A(I,K)=A(I,N+1)
      DO 1820 J=1,N
 1820 A(K,J)=A(N+1,J)
C END BOX 21.
      SWTCH= 1.0
      GO TO 910
 1850 IF (IP-3)1860,1950,1950
 1860 WRITE(6,1870)
 1870 FORMAT(1H1,///,60X,12HFINAL MATRIX,//)
      WRITE (6,800)
      DO 1900 I=1,N
 1900 WRITE(6,1910) (A(I,J),J=1,N)
 1910 FORMAT(    10F13.5,/,1H ,10F13.5,/,1H ,10F13.5)
      IPHI=PHI
      WRITE(6,1940) IPHI
 1940 FORMAT (////, 21H DEGREES OF FREEDOM = , I5)
 1950 IF(PSW) WRITE (6,1960)
 1960 FORMAT (////, 9X, 14HFINAL VARIANCE, 8X, 14HFINAL F-LEVELS,//)
      DO 2040 I=1,NM1
      IF (0.0 - V(I))1990,2010,2030
 1990 FF=V(I)*PHI/R(N,N)
      GO TO 2040
 2010 FF=0.0
      GO TO 2040
 2030 FF=ABS(V(I)*(PHI-1.0)/(R(N,N)-V(I))  )
 2040 IF(PSW) WRITE (6,2050) I, V(I), FF
 2050 FORMAT(2X,1HX,I2,1X,1PE16.6,1PE22.6,/)
      IF (IP-1)2070,2190,2190
 2070 WRITE (6,2080)
 2080 FORMAT (1H1, ///, 20X, 31HACTUAL  VS.  PREDICTED  RESULTS, /,
     1     5X, 7HRUN NO., 9X, 6HACTUAL, 13X, 9HPREDICTED, 11X ,
     2     9HDEVIATION, //)
      DO 2180 I = 1,M
      Z = BETAZ
      DO 2140 J = 1,NM1
      Z = Z + BETA(J) * X(I,J)
 2140 CONTINUE
      ZZ = Z - X(I,N)
      WRITE (6,2170) I, X(I,N), Z, ZZ
```

```
2170 FORMAT (7X, I3, 3X, F17.6, 3X, F17.6, 3X, F17.6)
2180 CONTINUE
2190 FORMAT (//, 38X, 50H***** MULTIPLE REGRESSION ANALYSIS COMPLETED *
    1****, ////)
     RETURN
       END
```

BIBLIOGRAPHY

1. Ralston, Anthony and Wilf, Herbert S. Mathematical Methods for Digital Computers, John Wiley and Sons, New York, 1960.

PART II

Interfacial Structure of Concurrent Air - Water Flow in a Two-Inch Diameter Horizontal Tube

INTRODUCTION AND BACKGROUND

Systems of two phases, one gas and one liquid, have been receiving increased attention in the literature. The volume of research on transport phenomena in such heterogeneous systems when both phases are in motion has substantially increased in the past two decades. This increase has been motivated by the expanded extent to which two-phase flow has been used in industry. Two-phase flow systems have been used for some time in the production and transportation of crude petroleum and petroleum products, and presently they are being increasingly used as medium for chemical reactions and for the transfer of heat and mass between phases. As yet, however, there are not nearly enough experimental results available to allow the clear understanding of the rates of transfer of momentum, energy, and mass that is required for the logical and careful design and operation of equipment and processes.

Much of the early work on flowing two-phase, gas-liquid systems in closed conduits dealt with the prediction of pressure losses in the system and with the prediction of the flow pattern existing in the system. The prediction of flow patterns and pressure drop is possible for a limited number of systems, although many systems of industrial interest are included in this number. There are a number of excellent summaries and bibliographies of the research in this area (2a, 2b, 14, 15, 34, 39). Most of the research thus far is experimental in nature, but there have been numerous empirical and semi-empirical models presented for the

prediction of pressure drops. Investigations of either heat, or mass transfer across the liquid-gas interface in two-phase flow in horizontal, closed conduits have increased considerably in the past few years (1, 3, 6, 7, 15, 28, 33, 34, 39). Only recently has significant consideration been given to the effects of the interfacial structure on heat and mass transfer across a gas-liquid interface in closed conduits (3, 7, 28).

In general, the prediction of heat and mass transfer across an interface is difficult at the present time (2c). This situation will not be improved until significantly more data are available regarding the interfacial structure in given systems and the effects of the interfacial structure upon the transfer rates. Waves on an interface effect the transfer processes across the interface by increasing the interfacial area and by altering the transfer mechanisms in the vicinity of the interface. Therefore, part of the knowledge one must have to predict the transfer processes in the vicinity of a free interface, is the knowledge of the individual wave characteristics-- wavelengths, wave heights, and wave velocities-- and if possible one should be able to characterize surface structures at many conditions in terms of a particular model or theory. Such information would bring about increased understanding of the generation, propagation, and maintenance of interfacial waves and would aid in determining their effects on transfer processes.

Efforts towards the characterization of interfacial surface structure and its effect upon transfer processes across the

interface have been made for several decades. Many types of systems have been investigated, and the results obtained in one system are usually not applicable to other systems. Experimental systems may be either horizontal or vertical, may use concurrent or countercurrent flow in any of several flow regimes (wavy, annular, slug, etc.), may use open or closed channels of various geometrical shapes, and may use an infinite variety of fluids and operating conditions. One frequently investigated system utilizes the concurrent flow of room-temperature water and air in a horizontal, closed conduit. This particular system has been subjected to a continuing investigation over the past two decades. A research group at the University of Illinois headed by T. J. Hanratty has made extensive contributions to the study of concurrent, water-air flow in a horizontal, rectangular channel with a very high width-to-height ratio. Several investigators have investigated the same system in circular tubes. The research using rectangular channels is more extensive than the work using circular tubes, and the work of this thesis further delineates the characteristics of interfacial structure in horizontal circular tubes.

The initial significant contributions for the stratified and wavy flow regimes in horizontal, closed conduits were made at the University of Delaware by Jenkins (21), Bergelin and Gazeley (4), and Gazeley (13). They investigated the isothermal concurrent flow of air and water in 1-inch and 2.065-inch-I.D. horizontal pipes. Jenkins (21) visually mapped out the stratified, wavy, slug, and

annular flow regimes in 1-inch and 2.065-inch pipes. Bergelin and Gazeley (4) carried out their work in a 2.065-inch-I.D. horizontal copper tube. They measured the depth of the flowing water in the tube over the last 12 feet of the length of a 22-foot tube. Measurement of the pressure drop over a distance from 3 to 13 feet from the free liquid overfall enabled them to calculate the friction factors for the system over this length of the system. The length falls within the exit length. Further pressure-drop measurements were made by Hoogendoorn (19) in pipes of different diameters.

For concurrent flow of air and water inside a rectangular duct 1-inch high and 12 inches wide, the initial mapping of the flow regimes and the determination of the onset of waves was done by Hanratty and Engen (16), Helfinstein (17), and Van Rossum (37). The work of Hanratty and Engen was later found to have been influenced by entrance effects (25, 26). The gas-phase pressure drop was first studied in detail in this system by Lilleleht and Hanratty (25, 26, 27). These pressure-drop measurements were extended and made more accurate by the work of Cohen and Hanratty (9, 10). Closely related work was done by Chang and Dukler (8). These pressure-drop measurements coupled with measured velocity profiles enabled the determination of friction factors by the authors.

The work discussed to this point has all dealt with the measurement of certain bulk, macroscopic properties of each of the two phases in the system. Investigators using rectangular

channels have proceeded further and studied the details of the interfacial structure--the heights, lengths, frequencies, and velocities of the waves. No work along these lines had been done in systems using circular tubes. The first complete investigation of the interfacial structure of waves in a rectangular channel was done by Lilleleht and Hanratty (25, 26, 27). They measured the heights and the frequency distribution of the interfacial waves and fitted the results of the model of a stationary Gaussian process. The results fit the model quite well except for the conditions of high flow rates of air over a relatively thin film of water. At these conditions there were too few large waves, presumably as a result of the damping effects of the bottom of the channel upon the liquid. One inconsistency of this work at the University of Illinois was a difference of 25-40 per cent between the measured film thicknesses of Lilleleht and the measured film thicknesses of another worker, Hershman (18), at identical conditions using the same apparatus but with a different entrance section. Presumably entrance effects accounted for the difference. Cohen (9, 10), using the same apparatus, extended Lilleleht's results and also used different fluids. With these results he was able to present a better theoretical background for the observed wave heights in the system.

No one had examined the interfacial structure of wavy flow in a circular tube. This work did so using water and air as the fluids in a tube with a 2-inch diameter. This work logically

needed to be done since two-phase flow in horizontal, circular tubes occurs quite frequently in industrial practice, more frequently, indeed, than flow in thin channels. A study of the interfacial structure in such a circular tube is a worthwhile and necessary step towards the understanding of the mechanisms of heat, mass, and momentum transfers across the interface in pipe flow.

The wave characteristics in this system were measured and characterized by the model of a stationary Gaussian process. The adequacy of a stationary Gaussian process to describe the results was tested. The purpose of this work was therefore to measure the interfacial wave structure in one system of engineering interest and to determine if the study of interfacial phenomena in this system may be successfully approached by considering the interface in terms of statistical distribution functions. Experimental results for the wave parameters were compared to a few theoretical expressions from the literature, but no effort was made to carry out a comprehensive comparison of the results to all of the many theories available. Also, no effort was made to generate any new theoretical results which may be necessary to explain adequately the experimental results.

The wave structure in the two-dimensional rectangular system discussed above was analyzed in the same fashion as wave structure is analyzed on large, open bodies of water. The same analysis was used in this work. The analysis, long used by oceanographers, assumes the surface structure may be characterized by a stationary

Gaussian process. The wave structure is Gaussian if the probability function used to determine the fraction of the time that the liquid level is between two heights is a Gaussian distribution function. The wave structure is stationary if the distribution function is not dependent upon the time at which the wave structure was measured. When a wave surface meets these conditions, it may be characterized as a stationary Gaussian process, the description of which is well-known and firmly rooted in theory.

The theory behind the stationary Gaussian process was developed by Rice (32). The application of this work to oceanography followed shortly thereafter and is best described by Pierson (29), Putz (30), and Kinsman (22). Putz (30) describes in excellent fashion how to analyze a wave record by this mathematical technique and how to report the results. His methods were used for the rectangular channel work previously mentioned and in this work also.

In wave analysis. the instantaneous height, h, of the liquid is designated as the sum of an average height plus a fluctuating component. The average height, $\bar{h}$, is chosen to be a time average defined as

$$h = \lim_{t \to \infty} \frac{1}{t} \int_0^t h\,dt \qquad [1]$$

and the fluctuating height, h', is then defined by the equation

$$h = \bar{h} + h' \qquad [2]$$

The r.m.s. wave height, designated as Δh, is

$$\Delta h = \left[\lim_{t \to \infty} \frac{1}{t} \int_0^t (h')^2 \, dt \right]^{\frac{1}{2}} \qquad [3]$$

A probability function, $P(h)$, may be defined so that $P(h)dh$ is the fraction of the time that the liquid height is between the height h and the height $h + dh$. If this probability function is stationary and Gaussian, then at all times

$$P(h) = \left(\frac{1}{2\pi}\right)^{\frac{1}{2}} \frac{1}{\Delta h} \exp \frac{(h - \bar{h})^2}{2\Delta h^2} \qquad [4]$$

To determine if a surface wave structure may be represented by a stationary Gaussian process, one must affirm that the probability distribution for the surface height is indeed Gaussian and that the characteristics of the function do not depend upon the time at which the wave structure in the system was measured. The former requirement is easily determined by preparing a plot of the liquid level distribution on probability graph paper. If the resultant distribution curve is a straight line, the distribution is Gaussian. If the curve deviates from a straight line, then the distribution is non-Gaussian. The test for the latter requirement is made by obtaining surface-level measurements in a system at several different times and comparing the resultant distribution curves as plotted on probability graph paper.

Once the existence of a stationary Gaussian process is confirmed, the structure of a wave surface interface is

completely characterized by measuring the r.m.s. wave height, Δh; the time-average liquid depth $\bar{h}$; the wave frequency, f_0, at $\bar{h}$; the frequency of extrema in the liquid level profile, f_1, the frequency spectrum at $\bar{h}$; and the wave velocity distribution. If a wave structure is not stationary, further modifications are available to describe the liquid surface. If a wave structure is not Gaussian, no other suitable distribution function is available which allows the surface to be readily characterized.

The frequency distribution is not reported in this work but may be obtained if desired from the original wave records. If the frequency spectrum for the fluctuating height h' is w(f), then Rice (32) showed that the fraction of $\bar{h}$ contributed by waves with frequencies between f and f+df is w(f)df. The frequency spectrum in effect distributes the wave energy over a continuum of superimposed elementary waves. The distribution of energy is important for the study of the generation and the propagation of waves. For oceanographic work, knowledge concerning this distribution is necessary to predict the sea-surface profile at another nearby location. The frequency spectrum has been measured for flow in rectangular ducts (10, 25), but its applicability to engineering design and correlations in such systems has not yet been demonstrated. Putz (30) describes the method for determining the frequency distribution from a given wave record. Although the distribution may be obtained moderately easily by the use of proper electronic equipment it is very tedious to obtain the distribution by the analysis of

wave records.

There are a variety of ways that a distribution function may deviate from the Gaussian distribution. In this work, only five deviations need be noted and given some type of specification. Figure 1 shows a Gaussian distribution and five types of deviations--labeled types I, II, III, IV and V--drawn on probability graph plots. The type II deviation was noted in the two-dimensional wave work (11, 27), although at no conditions was the break in the curve of such a magnitude as to result in a substantial deviation from the Gaussian straight line. This deviation from the Gaussian distribution was attributed by the authors to the damping effect of the channel bottom on the wave structure at low liquid levels in the system.

It is important to note that these deviations from the Gaussian distribution may only be apparent deviations in some instances, that is a Gaussian surface structure may plot as a non-Gaussian structure because of the time variation in some parameter affecting the time-average liquid level. If the time-average liquid surface level changes during the time span in which the wave record is taken, then this alteration in the value of $\bar{h}$ results in an actual Gaussian wave structure being plotted non-linearly on probability graph paper. The particular manner of deviation from linearity would depend on the manner in which $\bar{h}$ varied during the time span of the wave record. In an open sea, such a variation in $\bar{h}$ could be caused by the effect of the tides. In a system with a flowing liquid, a change in

the liquid flow rate would under most circumstances affect the $\bar{h}$ value. If a gas were flowing over the liquid, again under most circumstances a change in the gas flow rate would result in a variation in $\bar{h}$. Thus, any time a non-Gaussian wave structure is obtained, one must check that $\bar{h}$ did not change during the time span of the wave record.

The applicability of the stationary Gaussian wave model to describe interfacial structures in situations of chemical engineering interest has rarely been tested. For the wavy regime of two-phase flow in horizontal systems, Lilleleht (27) and Cohen (11) provided the only test of the applicability of the stationary Gaussian model. Their results, obtained from the two-dimensional region of a rectangular channel, did not provide a very exacting test of the applicability of the model. Nonetheless, a limitation to the usefulness of the model was approached, although not quite reached. The work reported in this thesis provided a more rigorous test of the stationary Gaussian model by measuring the interfacial wave structure of isothermal air-water flow in a horizontal Lucite tube with a 2-inch diameter. This system has, in effect, become the standard system for horizontal, two-phase flow in pipes ever since it was used by the first investigators in the field (4, 13, 21). Air and water are used as the fluids because of obvious convenience. Large pipe diameters are desirable for research studies of interfacial phenomena in pipes inasmuch as they will probably more closely approximate any ultimate industrial systems, but

on the other hand, the use of pipes of diameter greater than about 2 inches requires pump and blower capacities and floor-space requirements that are excessive for most research laboratories. Details of the experimental apparatus are presented next.

EXPERIMENTAL APPARATUS

General

The design of any experimental apparatus is made logical by knowing the possible variables which can affect the measured quantities which are to be determined in the apparatus. The number of variables which can affect the interface in two-phase gas-liquid flow is considerable, and disagreement exists regarding how many factors must be considered as important (14). Consequently, considerable difficulty is usually encountered in designing experimental systems to obtain accurate and meaningful results. The lack of a clear understanding of the phenomena involved and the dearth of experimental data in certain critical areas forces the investigator to rely largely on experience and concepts gained from analysis of single-phase flows. A trial and error approach toward the solution of many experimental difficulties is often necessary. The experimental apparatus used in this work, in its final state, the end result of many trials (and errors), is shown schematically in Figure 2.

The two rotameters for water in parallel allowed a maximum measurable flow rate of water of 2500 lb./hr. through the Lucite tube sections. The water surface in the constant-head tank

was 8 feet above the test section. All water tubing was one-inch copper tubing with the exception of a short sacrificial galvanized segment immediately after the water pump and some flexible hose on each side of the water pump to minimize the effect of pump vibration on the system.

The collecting box after the Lucite tubing was 24 1/2" x 24 1/2" x 50" in dimensions and constructed from Lucite. Air flowed from the box through flexible tubing 5-inches in diameter to the blower. From the blower the air was forced through pipe of a 2-inch diameter pipe to a surge tank 4.6 ft^3 in volume. Auxiliary air from the laboratory air line was fed, when needed, directly into the surge tank. The air rotameter and Venturi meters were capable of measuring flow rates of air from 5 lb./hr. to 350 lb./hr. when used in conjunction with 100-cm. kerosene manometers. From the measuring devices, the air was fed into the tubing entrance section of Lucite through flexible 5-inch I.D. tubing, a long, straight, 5-inch-diameter air duct, and a short, 1-inch-diameter rubber hose. The flexible air ducting and rubber hose were used to isolate the vibrations of the blower and the building from the horizontal Lucite tubing.

Lucite Tubing

The horizontal tube in which the two-phase flow was developed and measured consisted of eight sections of Lucite tubing with 2.00-inch I.D. and 1/4-inch walls. The air and water entered through the entrance section and flowed through three successive 5-foot sections of tubing before entering the 15-inch test section.

After the test section, the fluids flowed through a 3-foot and two 5-foot sections of Lucite pipe to a 2-inch-long segment of Lucite which led to the collecting box at the end of the system. The water flowed via a free overfall into the collecting box. Each 5-foot section had two pressure taps, one at each end, 0.04 inch in diameter.

The inner diameter of the Lucite tubing varied from 1.97 inches to 2.03 inches. Because the interfacial structure was disturbed by sudden alteration in the tube diameter, such as often occur when two tube sections are joined together, a great deal of care was taken to ensure that the tube sections were joined together in such a manner that no disturbance to the flow was observed visually at the joints. The tube ends were modified to make each end identical. First, the Lucite tubes were each machined to a uniform 2.03-inch I.D. at the ends by tapering the inner wall as much as was necessary in the last inch of the tubes. The inner walls of the tubes were then smoothed by polishing. Second, the Lucite tube was machined to a uniform, 2.45-inch O.D. from the nominal 2 1/2-inch O.D. for a 2-inch distance from the tube end. Third, the ends of the tube were machined to be perpendicular to the machined portion of the outer diameter. Modified in this way, all tube ends became identical. When properly butted up to one another and clamped together with standard 2-inch sewer-line clamps that had the middle ridge cut out of the rubber gasket, no evidence of disturbance caused by the joints was found in the system.

The Lucite tubes were mounted on supports that allowed both horizontal and vertical movement of the tube. The supports were bolted to the inside of the outer wall of the building. The tubes were leveled to ±0.02 inch over the length of all the tubes before each experimental run by using a cathetometer and reference lines drawn on the wall of the building. These reference lines were all drawn at the same height ±0.005 inch over the length of the system by using a surveyor's level. Split pieces of Tygon tubing between the supports and the tubes served to insulate partially the tubes from any building oscillations.

Moderate cleanliness of the fluids and the Lucite tubing was essential to obtain reproducible results. The tap water was changed after at least every other run. For a time the air from the building air line was filtered to remove oil and impurities, but this was abandoned as unnecessary before the final data were taken. The Lucite tubing sections were thoroughly scrubbed and cleaned after at least every fourth run. When the system was not sufficiently clean, the water depth showed a hysteresis dependence upon the prior condition of the system. Also, the water depth at given conditions tended to be lower when the water or tubing was not clean than when the system had been recently cleaned.

Entrance Section

The entrance section is important in two-phase flow systems. If the two phases are brought together in a "messy" fashion, the resulting turbulence and splashing will affect the flow conditions

for an exceedingly long distance downstream. One of the entrance sections used in this work is pictured in Figure 3. This design was chosen by a trial-and-error process. The other entrance section is similar to the one pictured except that the thin divider was placed 1/2 inch up from the bottom of the tube instead of 1 inch. For best results, the level of the divider in the entrance section should approximate the level of the water flowing in the tube. For this reason, the choice of entrance section for each run was determined by the depth of the water at the conditions which would exist during the run.

The divider was a sheet of Lucite 1/16-inch thick which was cemented into a slot cut through the Lucite tube walls at the appropriate height. The length of the divider was determined by a trial-and-error procedure to determine the length of calming section necessary so that when the fluids came into contact there would be no noticeable distortion of the interface because of the turbulence in each fluid induced at the entrance to the Lucite tubing. A divider 12 inches long was satisfactory at most conditions, but at high rates of fluid flow a divider 18 inches long was required. The glass wool filter was used to remove any particulate matter from the water phase. The filter was changed after each experimental run. When it became moderately brown colored during the course of a run, the system was cleaned. The filter was held in place by the copper screen.

Settling Basin

The initial tests made with the apparatus indicated the

presence at some flow conditions of a hydraulic jump 10-15 feet from the free overfall at the end of the Lucite tubes (5). The presence of this jump made measurements impossible in the system. A hydraulic jump occurs when the water changes from rapid or "shooting" flow to tranquil flow. The energy expenditure per unit tube length necessary to maintain a given mass flow rate is less in tranquil flow than in rapid flow. For this reason, systems are designed to encourage tranquil flow, and civil engineers achieve this by installing a settling basin at the start of the channel. Because the hydraulic jump occurs when the water depth first exceeds a certain critical depth, the presence of a settling basin whose bottom is significantly lower than the channel bottom causes the jump to occur in the basin and all subsequent flow is in tranquil flow. To remove the hydraulic jump problem in this system, the settling basin shown in Figure 4 was installed in the first 5-foot section of Lucite tubing after the entrance section. The jump then always occurred in the settling basin. The flow through the remainder of the tubes was tranquil and measurements of interfacial structure could be taken in a properly positioned test section.

Test Section

The proper positioning of the test section, the section in which the parameters of interest are measured, is an important, and unresolved, question in two-phase flow. The entrance length in horizontal, two-phase flow, the length that is necessary for the interfacial structure to eliminate any effects from

peculiar entrance conditions and for the pressure drop per unit length to become constant, is not well defined. It depends, of course, upon the type of entrance section used and also upon the flow conditions. There is also in two-phase flow a significant exit length; that is, a relatively long section upstream from the liquid overfall in which the hydraulic gradient is significant to such an extent that one cannot consider the liquid depth as constant for the purposes of the experiment. A test section should be located in a region of the apparatus that is between these two lengths unless one specifically wishes to study something of interest in these lengths.

The initial rectangular channel work reported in the literature (16) was done using a 16-foot channel length with the test section consisting of the final 4 feet. This test section was almost certainly in the exit section of the channel, and later work indicated the system was not long enough to eliminate entrance effects (25, 26). Later work at the same laboratory (9, 10, 11, 25, 26, 27) used a modified entrance section and a total channel length of 21 feet. The test section was 11 feet 8 inches from the start of the channel. One of the authors (11) reported an entrance length of about 40 hydraulic diameters for this system. Because the new test section was over 9 feet from the free liquid overfall, the exit length was probably considered and its influence removed from the test section. Still, another laboratory recently reported results from a similar rectangular channel 18 feet 3 inches long in which the test section was the length of channel 27 inches

to 15 inches from the free liquid overfall (17).

The initial work using a pipe (4, 13, 21) was done in a 20-foot length of pipe in which measurements were taken in the last 14 feet of the system. These measurements indicated that the exit length for the system was 10 to 12 feet. Consideration was paid to entrance effects in these works, and presumably the 6 feet before the first measuring station was sufficient to eliminate entrance effects on the data. Further work on an identical system should not be based upon this assumption, however. The entrance section used in those works was not identical to the entrance section used in this work. Another more recent work (39) used a pipe 20 feet long. Measurements were taken in the section 5 1/2 feet to 6 inches from the pipe end. This work appears to have been somewhat hastily done, and the usefulness of the results is not clear.

Much care was taken experimentally to identify the entrance and exit lengths for this experimental system. Total Lucite tube lengths after the initial divided portion of the entrance section of 15 feet, 31 feet, and 38 feet were used in the system to determine the entrance and exit lengths. The region outside of these lengths was determined to be the tube sections in which the following held true: the water depth did not change more than 0.02 inch along 15 inches of tube length; the pressure drop per length of tube was constant; and the interfacial wave structure did not visibly change along the length of the tube. The results from both the 31-foot channel and the

38-foot channel indicated both the entrance length and the exit length were about 12 feet long in this system. At some flow conditions the entrance section may have been a couple of feet longer. At other flow conditions, the exit length is as little as 6 feet.

Based on these results, a 31-foot total length of Lucite tubing was used for this work. The 15-inch test section was placed so that the front wave gage, the gage at which the interfacial structure was studied, was 14 feet 5 inches from the free overfall at the end of the Lucite tubing and 16 feet 6 inches from the end of the divider in the entrance section.

Wave Gages

Two resistance wave gages were built into the 15-inch test section as shown in Figure 5. Each gage was located 2 inches in from the end of the tube and was centered about the tube diameter. A resistance wave gage is a very sensitive device for the measurement of liquid depths and interfacial wave characteristics. Such gages have been used experimentally for some time by civil engineers and have been used recently to examine two-phase slug flow in a 1-inch diameter tube (23). The characteristics of resistance wave gages and their proper construction and use are described in the literature (31).

Although immersion-type wave gages, such as resistance gages, are very accurate when used correctly, there are a number of situations in which their use is inappropriate because the wires disturb the liquid sufficiently to affect the structure of the

interface. For very small waves, a resistance gage cannot give an accurate description of the wave structure because of the erratic dynamic behavior of the miniscus and the existence of a viscous film on the gage as the free surfaces recedes. At these very small wave conditions when all waves are capillary waves, no reproducible results can be obtained. In the system used for this work, wave structures were found sufficiently reproducible provided the r.m.s. wave height was greater than 0.002 inch, so this restriction was not serious in this work. Disturbances around the gage also occur at high liquid velocities. The greater the liquid velocity, the greater the height of the upward-directed jet at the stagnation point of each wire and the greater the cavitation in the wake. Water-phase bulk velocities of up to 20 in./sec. were obtained in this work. At the highest water flow rates, a faint standing wave was sometimes, but not always, visible about the wires. This standing wave had the appearance of a bow wave about a sailing vessel.

To determine the magnitude of the effect of this wave upon the measured water depths and wave structures, a similar wave gage with wires of an identical diameter that was mounted on a mobile support over a rectangular channel[1] 30-feet long was moved at constant velocity through a stationary water phase. For gage velocities less than 12 in./sec. no disturbance to the output signal was recorded. At this velocity, a faint standing wave, similar to the wave observed in this system, was visible. At

[1] This apparatus is located in the Caltech civil engineering department in Keck laboratory.

20 in./sec. the effects of the liquid surface disturbance were enough to cause the recorded water depth to be 0.01 inch too high. There was still, however, no apparent wave profile imposed on the recorded output signal by the standing wave. The conclusion reached from this work was that the water depth as measured in this lucite tube system may be 0.01 inch too high at the highest water velocities, but this is not certain inasmuch as the standing wave appeared much earlier in the rectangular channel system than in this system. No correction for this potential error was made to the measured water depths because of the uncertainty of the error and the magnitudes of other errors in the water depth measurements. In addition, in no instances is the interfacial wave structure significantly disturbed by the presence of the gages.

Variations in the temperature of the liquid phase result in variations of the signal from the resistance wave gages because the resistivity of the liquid is a strong function of temperature. Temperature effects were minimized in this work since the temperature of the liquid during a run was held reasonably constant so that only minor corrections to the measured water depths were necessary to account for temperature changes in the water. A resistance wave gage may be used in certain non-isothermal situations, however. Such a gage is described in appendix A.

The two resistance wave gages were used in conjunction with a Sanborn 150 series recording unit. The excitation signal to each of the wave gages was a 4.5 volt 2400 c.p.s. signal from a Sanborn 1100 preamplifier. This preamplifier was coupled with a Sanborn

150-200B amplifier, a Sanborn 154-400 power supply, and a Sanborn 154-100B recorder. A circuit diagram for the system is shown in Figure 6. Particular details may be found in the standard Sanborn manuals for the components involved.

Resistance wave gages must be calibrated before and after each experimental run in order to relate the recorded output signal to liquid depths. For this work, the gages were calibrated by placing the test section in a calibration tank 48" x 12" x 4 1/2". The test section was held by a level indicator capable of indicating changes in depth of 0.0001 inch. The tank was filled with water from the experimental system to the desired depth and the test section moved up and down known distances. The resultant record from the recorder provided the necessary calibration curve. A calibration external to the experimental system is only valid if the characteristics of the environment external to the test section itself have no effect on the output signal from the gages. Tests showed that no objects or fluids external to the 15-inch test section ever affected the wave gages in any fashion.

RESULTS

Error Analysis

The experimental results of this work are presented in tabular form in Appendix B. The water flow rates, reported in lb./hr., were with one exception held within ±2% of the reported value at all times. The water flow rate of 250 lb./hr. could only be maintained within ±5%. The water rotameters were calibrated

several times during the course of the work, and the reported values of the flow rates of water at a particular rotameter setting should not deviate from the actual flow rates of water at that rotameter setting by more than 2%. Flow rates of air were held within ±2% of the reported value during the time when data were taken. The air rotameter and Venturi meters were calibrated only once during the work. Nonetheless, the reported flow rate of air at a particular rotameter setting or Venturi meter reading should not differ from the actual flow rate of air by more than 2%.

The median water depth, $\bar{h}$, is the channel-center water depth measured at the front wave gage. It is the time-averaged water depth as measured at steady-state over a suitably long time interval, usually 30 to 60 seconds. Except when the r.m.s. wave height exceeds 0.05 inch, the reported value of $\bar{h}$ is within 0.03 inch of the actual value. 0.01 inch of this error was caused by the irreproducibility of the calibration procedure. Another 0.01 inch was caused by the effects of a ±0.5°C uncertainty in the bulk temperature of the water on the wave gage behavior. The remaining 0.01 inch of uncertainty resulted from not being able to exactly locate the median water depth with respect to the bottom of the tube. Locating the interface with respect to the tube bottom was more difficult as Δh increased. When Δh exceeded 0.05 inch, $\bar{h}$ could only be measured within ±0.04 inch.

The root-mean-square wave height, Δh, was determined as discussed by Putz (30). The fraction of the time that the water

depth exceeded a given value was plotted against water depth on probability graph paper. When the water surface distribution was Gaussian, the points fell on a straight line and Δh was the depth exceeded by the water surface 15.9% of the time minus the depth exceeded by the water surface 50% of the time. When the surface distribution was not Gaussian, the root-mean-square wave height was defined as the Δh value of a single straight line drawn such that, both from 50% to 1% and from 50% to 99%, the area under the straight line is equivalent to the area under the actual surface distribution curve. An example of this technique is illustrated in Figure 7.

The values of Δh are reproducible to ±10% of the value reported except for values of Δh less than 0.002 inch. A number of trials indicated that 5% of this irreproducibility was due to variations in the sensitivity of the wave gage at different water depths which were not accounted for when the wave gage was calibrated at only one reference water depth. The remaining 5% of the irreproducibility was probably caused primarily by the uncontrollable small variations in water and air flow rates. It was not possible to determine the accuracy of the reported wave heights by comparison to the heights determined by another experimental technique.

The reported values for wave frequencies at the median water depth, f_o, extrema frequencies, f_1, and the correlation coefficients, c, defined as the ratio f_0/f_1, all were reproducible within ±10%. The irreproducibility in all three of these variables was

apparently caused by the variations in the water and air flow rates from one run to another and during the length of time over which the wave record is taken. Possibly, the length of time of the wave records, from 5 to 12 seconds, was not sufficient to allow reproducibility to less than ±5% even when fluid flow rates were exactly controlled.

Reynold's numbers for this system may be defined in either of two fashions. The Reynold's number for a given phase may be defined on the basis of the total cross-sectional area of the tube,

$$Re_l = \frac{4\dot{m}_l}{\pi \mu D} \qquad [5]$$

or on the basis of the cross-sectional area of the tube that the given phase occupies at the point of interest, such as

$$Re_l = \frac{4\dot{m}_l}{\mu S_l} \qquad [6]$$

The Reynold's numbers presented in Appendix B are calculated in the latter fashion according to equation [6]. Air Reynold's numbers are accurate within ±5%. Water Reynold's numbers are accurate within ±5% when the water depth exceeds 0.5 inch and within ±10% when the water depth exceeds 0.2 inch.

The laminar-turbulent transitions in each phase in this system were discussed in the work by Bergelin and Gazeley (4). The water phase became turbulent independent of air flow rate at 600 lb./hr. The air phase became turbulent independent of water flow rate at a mass flow rate of 17.2 lb./hr.

The bulk water velocities presented in Appendix B were accurate within ±10% providing the water depth was greater than 0.5 inch. At a median water depth of 0.2 inch, the bulk water velocity was only accurate to ±25%. The bulk air velocities were always accurate to within ±5% of the true value. Velocity profiles in each phase were not measured, but theoretical solutions for the profiles when each phase is in laminar stratified flow are available (38).

The wave velocities were measured along the 11.35-inch distance between the front and rear wave gages in the test section. Wave records were obtained simultaneously from both gages. Individual wave velocities were calculated by matching these records one to the other and noting the time that elapsed as each particular wave traveled the 11.35 inches between the gages. At some conditions, the surface structure changes sufficiently in the distance between the gages that the two wave records could not be confidently matched. Hence, wave velocities were not reported at these conditions. At all conditions there was a distribution of observed wave velocities. These wave velocity distributions were examined at two given flow conditions and found to be Gaussian distributions. The distributions were, however, extremely narrow-banded. The maximum spread in the range of wave velocities at any given conditions was never more than 20% of the average wave velocity, and it was usually much less. Only the arithmetic average of the observed wave velocities is reported in this work. Each individual wave velocity could be measured with

an accuracy of ±2%. The arithmetic average wave velocities reported in Appendix B were almost always reproducible to ±5%. Most of the deviation in these values was probably caused by differences and fluctuations in the air and water flow rates.

Considering the work as a whole, the most significant error was caused by the uncontrollable variations in the flow rate of air during the run. The precise magnitude of the effects of the variation in air flow rate could not be calculated. The effects were particularly significant when the interface underwent rapid alterations when the flow rate of air was increased (or decreased) by a small amount. The precise determination of these transition regions is extremely important, and the relatively small variations in the flow rate of air which were tolerated in this work accounted for most of the irreproducibility of results in transition regions. Further work in systems of this sort would benefit greatly by having an accurate and precise flow controller on the air line.

Interfacial Structure

After the completion of the construction of the apparatus, but before any detailed measurements of interfacial structure were taken, certain experimental checks were made to ascertain that the system was behaving similarly to other systems whose results have been reported in the literature. Four types of measurements were taken and compared to previously reported results: the measurement of the flow rates of water and air at the initial formation of waves in the system, the measurement of

the pressure drop along the tube when air alone was flowing through the system, the measurement of the pressure drop along the tube at flow conditions measured by Bergelin and Gazeley (4), and the measurement of interfacial height at certain flow rates of water and air at a position measured by Bergelin and Gazeley (4).

The pressure drop per unit tube length was measured for the system when air alone was flowing at Reynold's numbers in excess of 10,000. The measured friction factors agreed to within 10 per cent of the values calculated by the use of the Blasius equation for turbulent flow of Newtonian fluids in pipes. The points of initial wave formation in the system were measured and are reported in Table IV of Appendix B. These results are in satisfactory agreement with previously reported values for identical and similar systems (4, 14, 20, 33). Table I presents the measured pressure drop per unit length as measured between 3 - 13 feet from the free overfall and interfacial heights 10 feet from the free overfall for both this work and the work of Bergelin and Gazeley (4). Excellent agreement was obtained.

The various wave types, or types of water surface level distribution, noted in this work are shown in Figure 1. Appendix B notes the wave distribution that was observed at each point at which data were taken.

The experimental data obtained at a flow rate of water of 250 lb./hr. showed an undesirable amount of scatter, particularly between 30 to 70 lb./hr. flow rate of air. Most of the variations in results from one run to another were believed caused

by variations in the flow rate of water. The flow rate of water could not be controlled as accurately as desired at this low flow rate. The water was in laminar flow, and at some flow rates of air the interfacial structure seemed particularly sensitive to the flow rate of water.

The median water depth at 250 lb./hr. of water is plotted in Figure 8. The scatter of points for flow rates of air less than 70 lb./hr. was greater than can be expected from errors resulting from the experimental technique. Some other variable besides the fluid flow rates appreciably affected the water depth at these conditions. This effect was noted before in similar work (39). Some of this work indicated that the effects of salts and other impurities in the water on the viscosity and surface tension may account for these variations, but definite proof is not available.

The curve drawn through the data in Figure 8 was positioned, like all other curves in this work, by eye and not by any numerical technique such as least squares.

The r.m.s. wave height at a flow rate of 250 lb./hr. of water is plotted in Figure 9. The data indicate an apparent decrease in wave height from a flow rate of air of 55 lb./hr. to a flow rate of air of 65 lb./hr. Such a decrease would be illogical and was not noticed to occur in any experimental run. Had two or more experimental runs each shown such a decrease in wave height, then it would have been considered confirmed and the line through the data would have reflected this decrease. No

two runs did, and the line through the data were considered best drawn as shown.

The wave frequency and the extrema frequency at a flow rate of 250 lb./hr. of water are plotted in Figures 10 and 11, respectively. It was difficult to draw a line through the data for wave frequencies when the flow rate of air was under 70 lb./hr., but the line was finally drawn to be similar to the line representing the data for extrema frequency in this range. Some doubt must remain as to the validity of this line as a representation of the wave frequency at these conditions.

Figure 12 shows v_w at a flow rate of water of 250 lb./hr. as a function of flow rates of air. Between flow rates of 85 and 165 lb./hr. of air the wave velocity could not be reliably determined using the technique of matching waves on wave records from different gages. A dashed line was drawn through this area to represent the probable wave velocities.

The results for higher flow rates of water did not show the undesirable scatter that characterized the results at the flow rate of 250 lb./hr. of water. For a flow rate of 750 lb./hr. of water, the water depth is plotted versus air flow rate in Figure 13. As was the case for a water flow rate of 250 lb./hr., slug flow was not quite achieved. The r.m.s. wave heights, wave frequencies, extrema frequencies, and wave velocities at a flow rate of 750 lb./hr. of water are shown in Figures 14, 15, 16, and 17, respectively.

The line through the data for wave frequency has four changes

in slope. Each change in slope was observed for at least two runs, thereby confirming its existence. Still, the points often showed a greater deviation from the line than was expected from errors in the technique. A close examination of the data showed that this scatter resulted from the fact that the points of inflection did not occur at the same flow rate of air for each run.

The median water depth for a flow rate of 1250 lb./hr. of water is plotted in Figure 18. Slug flow was achieved at a flow rate of 100 lb./hr. of air. The characteristics of the interface--r.m.s. wave height, wave frequency, extrema frequency, and wave velocity--are plotted in Figures 19 through 22. A very drastic change in all interfacial parameters occured at a flow rate of air of about 60 lb./hr. The flow rate of air at which this interfacial transition occurred was not identical for both runs and differed by 4 lb./hr. of air.

Water depth at a flow rate of water of 1750 lb./hr. is plotted in Figure 23. The onset of slug flow was different for the two runs. Slug flow did not begin during run 16 until the flow rate of air was 69 lb./hr. During run 18, however, the flow rate of air was increased much more rapidly than in run 16 and slug flow first occurred at a flow rate of air of 60 lb./hr. When the flow rate of air was then decreased somewhat during run 18 and the system allowed to stabilize, the flow rate of air could be slowly increased to 68 lb./hr. before slug flow began. The data on the interfacial characteristics are plotted in Figures 24 through 27. The data for wave frequency show scatter near the onset of slug

flow. This scatter is related to the differences in the flow conditions which caused the differences in the onset of slug flow.

Figures 28 through 33, inclusive, summarize the results for all flow rates of water. Individual points are not shown, only the lines drawn through the data. Figure 28 shows the water depths at all the conditions investigated in this work. The r.m.s. wave heights are shown in Figure 29. All four curves in Figure 29 have a similar shape-- an initial increase in wave height with increasing air flow, then somewhat of a plateau, then a steep rise and yet another plateau, and then, except for a flow rate of 1750 lb./hr. of water, a final steep rise in wave height with increasing air flow rates.

Wave frequencies are shown in Figure 30, and extrema frequencies are shown in Figure 31. At any flow rate of water, the wave frequency curve and the extrema frequency curve had much the same shape. In addition, all of the wave frequency and extrema frequency curves showed a definite peak between flow rates of 20 and 70 lb./hr. of air.

The correlation coefficient, c, has not been plotted because it may be derived from the wave frequency and extrema frequency which are plotted. Numerical values of the correlation coefficient are, however, presented in Appendix B. The absolute magnitude of c, which is a negative number, tended to decrease with increasing water flow rate and with increasing air flow rate. Except at a flow rate of 1750 lb./hr. water, this decrease

became quite rapid as slug flow is approached.

The arithmetic average wave velocities are shown in Figure 32. The curves were not particularly similar to one another, except that the wave velocities tended to increase with increasing flow rates of water and air.

The various types of water surface distributions, or wave types, that were noticed in this work were described and labeled in Figure 1. Appendix B presents the distribution present at each data point. In Figure 33 are shown the regions in which each type of water surface distribution was noted. A Gaussian surface distribution was not present over most of the conditions investigated. The small regions at flow rates of 250 and 1250 lb./hr. of water for which no distribution is reported could not be reliably investigated with resistance wave gages. The region at a flow rate of 1750 lb./hr. of water for which no distribution is reported was investigated, but no single surface distribution could be reliably designated as present in this region.

At some flow conditions, an experienced observer could have determined from visual examination of the water surface that the surface distribution function was non-Gaussian. The visual appearance of the water surface in a similar system was by Zegel (39). His descriptions of the visually-observed wave patterns was applicable to this work also. The first waves to appear on the water surface were small, two-dimensional waves extending from wall to wall. In Appendix B, these waves are labeled visual type A. As the air flow rate increased, these

small, two-dimensional waves transformed rather suddenly to large, two-dimensional waves with capillary wave trains on the wave slopes both fore and aft of the wave crest. In Appendix B, these waves are labeled visual type B. As the air flow rate increased, these visual type B waves began to break down into three-dimensional waves. Gradually the type B waves were present less and less frequently until at some air flow rate only three-dimensional waves were present on the surface. At this point the surface was classified as having visual type C waves, three-dimensional waves only, on its surface. Table V of Appendix B delineates the boundaries of each of these visual wave types.

When the wave type was predominately the visual type B waves, the surface distribution function was non-Gaussian. Any experienced observer could have satisfied himself of this fact by visual observation of the water surface because the surface possessed too regular a wave pattern to result in a Gaussian distribution for the surface level. Such an observer could also have determined the surface distribution was non-Gaussian at flow rates of air slightly less than that necessary to achieve slug flow in the system. At these flow rates of air visual type C (three-dimensional) waves were present, but occasionally a very, very large two-dimensional or three-dimensional wave was present on the surface. (At slightly higher air flow rates, of course, one of these waves would develop into a liquid slug and the system would enter slug flow.) An experienced observer would note that these very large waves occurred far too frequently to

allow the surface distribution to be represented by a Gaussian distribution function. In fact, the surface level distribution looked much like the distribution shown and approximated by a Gaussian straight line in Figure 7.

A dimensional analysis of the flow of thin liquid films (12) has shown that the properties of film flow may be characterized by the Reynold's number of each phase, the liquid Weber number and Froude number, a dimensionless shear at the free surface, and the wave frequency, wave length, and wave height. Although the water did not flow in a thin film in this work, the same parameters should affect the flow in this system. In order to determine properly the relationship of each of these dimensionless parameters to the flow characteristics in systems similar to this one, a great number of measurements would have to be made. The data from this work were presented graphically as functions of air and water flow rates. Plots were prepared showing the interfacial characteristics as functions of fluid velocities, fluid Reynold's numbers, and liquid Froude numbers. No apparent advantage was found in presenting the data in the latter fashions, so the data were presented graphically in their most untrammeled form to facilitate the formulation of a mental comprehension of the physical characteristics of the system.

The quantitative results of this work were not adequately described by any theory on the characteristics of waves in the literature. Even a glance at Figures 28 through 33 indicates that several mechanisms of wave formation and propagation must be

present in this system to account for the results. Surveys of wave theories are available for deep water waves and for waves on shallow liquid films (12, 24, 36).

An adequate first approximation to the relationship between the experimental values for wavelengths and wave velocity at wave inception is provided by classical deep-water wave theory. This theory, valid only for water depths much greater than wavelengths, states that the relationship between maximum water depth in the tube, wavelength, and wave velocity is given by

$$v_w = \sqrt{g\,\bar{h} + \frac{2\pi\sigma_\ell}{\lambda\rho_\ell}}$$

The experimental data for selected conditions presented in Tables III and IV show that this system was in a region in which the wavelengths were the same order of magnitude as, but somewhat larger than, the maximum water depth in the tube. This was a transition region insofar as theoretical considerations are concerned, and most theories cannot be expected to apply in this region. As Table II shows, however, equation [7] quite accurately predicts wave velocity at wave inception when the water depth and wavelength are known. Wavelength need not be known very accurately since the term in which it appears is relatively small.

Equation [7] failed, however, to give reliable values for wave velocities for conditions removed from the region of wave inception. The equation did predict that for a given flow rate

of air, the wave velocity increased as the flow rate of water increased, as was generally observed in this work. The equation also predicted that for a given flow rate of water the wave velocity decreased as the air flow rate increased, which was not the observed case. The reason the classical deep-water theory becomes more erroneous, of course, is that it neglects the effects of shear on the air-water interface. These effects are small for relatively low flow rates of air, but become increasingly larger as the flow rate of air increases. At the highest flow rates of air investigated in this work for a given flow rate of water, the predicted wave velocities presented in Table II are only about half the actually measured wave velocities.

A number of theories proposed for wavy flow of thin films are available in the literature (12), and selected results from several of them were applied to the data of this work. The theory of Kapitsa, applicable for laminar, two-dimensional wavy flow down inclined slopes, predicts that the ratio v_w/v_ℓ is a constant equal to 3.0. The theory of Benjamin, also for laminar, two-dimensional flow down inclined slopes, predicts the ratio to be 2.4. The experimental results for this system at selected conditions are presented in Table II. At wave inception, except for $\dot{m}_1$ = 250 lb./hr. (laminar water flow), the ratio of the wave velocity to the bulk water velocity was about 3.0. The value of this ratio decreases as the gas flow rates increases. Thus the theory of Kapitsa seems to give more applicable results to this system, although the theory is based on assumptions

clearly at odds with the actual physical processes occuring in the system used in this work. The decrease of v_w/v_1 as Re_g increased has been noted in other works involving thin liquid films (12).

The depth of the water in the tube was compared to the predictions of laminar, two-dimensional film theory to determine what similarities, if any, existed between the results in this system and predicted results for thin films. From Kapitsa's work for inclined channels comes the relation

$$\bar{h} = \frac{1.34}{(g \sin \theta)^{1/3}} \left(\frac{\mu_\ell}{\rho_\ell}\right)^{2/3} \left(\frac{Re_\ell}{4}\right)^{1/3} \qquad [8]$$

in which θ is the angle of inclination as measured from the horizontal. Inasmuch as the work done in this thesis was with a horizontal system, the equation above was replaced with the similar expression

$$\bar{h} = \alpha \left(\frac{\mu_\ell}{\rho_\ell}\right)^{2/3} \left(\frac{Re_\ell}{4}\right)^{1/3} \qquad [9]$$

in which α is an empirical constant. Table III presents the results of determining α from experimental data at wave formation for each given flow rate of water and at the highest flow rate of air for each given flow rate of water. As can be seen, only at high flow rates of water did α become relatively constant over all observed flow rates of air. α became more constant over a given range of flow rates of air as the flow rates of water increased. Fitting equation [8] to the experimental data and allowing θ to become an empirical constant (an "effective angle of inclination") resulted in the θ values presented in

Table III. They are extremely small values and vary considerably. Clearly these results of the Kapitsa theory are not particularly applicable to this work, presumably largely because of the neglect of interfacial shear effects. α may be made more constant, but still not adequate, by correcting α using Re_g.

Another results of laminar, two-dimensional thin film wave theory which was presented by Konobeev (12) relates the wavelength to the wave velocity, liquid velocity, and the depth of the liquid phase (12). The general expression is

$$\lambda = \frac{2\pi}{v_\ell} \left[\frac{\sigma_\ell \, \bar{h}}{\rho_\ell \left(\frac{v_w}{v_\ell} - 1\right) \left(\frac{v_w}{v_\ell} - \beta\right)} \right]^{1/2} \qquad [10]$$

in which β is an empirical constant. Values of β in thin film flow have been found to range from 0.67 to 0.9 (12). Rewriting equation [10] using $\beta = 0.9$ gives

$$\lambda = \frac{2\pi}{v_\ell} \left[\frac{\sigma_\ell \, \bar{h}}{\rho_\ell \left(\frac{v_w}{v_\ell} - 1\right) \left(\frac{v_w}{v_\ell} - 0.9\right)} \right]^{1/2} \qquad [11]$$

From experimentally measured values of v_1, v_w, and $\bar{h}$, λ was calculated from equation [11] and compared to the experimentally measured results. The comparisons are shown in Table IV. The calculated wavelengths were invariably lower than the experimentally measured wavelengths, the difference becoming greater as the flow rate of water increased and as the flow rate of air increased. For a given flow rate of water, equation [11] predicted λ to decrease as the flow rate of air increased, and the opposite is the case. The results of fitting equation [10] to the experimental data by

letting β be an empirical constant are presented in Table IV also. The results are not encouraging. Thus equation [10], with any constant value of β, does not fit these experimental results particularly well.

Although no one theory was found here to fit the results of this experimental work very well, it should be emphasized that the comparisons with theories were very fragmentary and can only be considered preliminary in nature. Further work along these lines should definitely be done.

Initial Wave Formation

The regions of initial wave formation are shown in Figure 33. Table IV of appendix B lists the values of the dimensionless parameters of interest at wave inception. The Froude number was calculated according to

$$Fr = \frac{\bar{v}_1^2}{g\,\bar{h}} \qquad [12]$$

and the Weber number according to

$$We = \frac{v_1^2\,\rho_1\,\bar{h}}{g_c\,\sigma_1}$$

The visually determined onset of waves in this system was in agreement with prior work (14, 34). These initial waves were capillary disturbances.

The wavelengths and wave velocities in the zone of initial wave formation could not be measured with the resistance wave

gages. Nonetheless, if the experimentally measured wavelengths and wave velocities are extrapolated to the zone of initial wave formation, there is an approximate agreement between the experimental values of λ, v_w, and $\bar{v}_g$ at wave formation and the values predicted by Jeffrey's sheltering theory (16, 20). At wave inception, Jeffrey's analysis predicts that the air velocity is 42 in./sec., the wave length is 3.2 inches, and the wave velocity is 14 in./sec. The experimentally measured air velocities range from 39 to 84 in./sec. The extrapolated wave lengths range from 1.25 to 3.2 inches, and the extrapolated wave velocities range from 15 to 19 in./sec. Not too much credence can be placed on this agreement, however, because of the weakness of the extrapolations.

CONCLUSIONS

For concurrent flow of air and water in a horizontal tube of 2-inch I.D., investigations into phenomena in the regions of flow removed from the entrance and exit lengths were carried out using the experimental system described in this work. The resistance wave gages described in this work may be used to measure wave structure in isothermal systems in which the r.m.s. wave height is greater than 0.002 inch and the bulk liquid velocity is less than about 24 in./sec. Resistance wave gages may be used in certain non-isothermal systems provided the gages are temperature-compensated as described in Appendix A.

For isothermal, concurrent flow of air and water in a horizontal tube of 2-inch I.D., the surface characteristics in the sections of

tube removed from the entrance and exit lengths are described by Figures 28 through 33. R.M.S. wave heights increased as the flow rate of air increased. The maximum observed wave height was 0.10 inch. Wave frequencies ranged from 8 cycles/sec. to 28 cycles/sec. At most conditions the observed wave frequencies were from 8 to 14 cycles/sec. Observed extrema frequency ranged from 10 cycles/sec. to 46 cycles/sec. Generally the extrema frequency was between 11 to 25 cycles/sec. Experimentally measured wave velocities ranged from 11 to 28 inches/sec. A noteworthy feature of Figures 29 through 32 is the number of times the lines change direction.

The results suggest that several mechanisms of wave formation and propagation occurred under the conditions investigated in this work. As Figure 33 points out, the surface structure of the water was not generally adequately represented as a stationary Gaussian process in this system. Work in two-dimensional systems (11, 25, 27) has suggested that some of the deviation was caused by the relatively shallow water depth in relation to the wave heights. Most of the deviation, however, was caused by the tube geometry and the very large interfacial shear stresses at high air flow rates. The substantial influence of the tube geometry negates the application of any two-dimensional work, experimental or theoretical, to systems similar to the one used in this work. No wave theories were found which adequately explained the experimental results of this work.

RECOMMENDATIONS FOR FURTHER WORK

Further experimental work with this type of system may follow

the path of developemnt of the study of the interface and its effects in similar two-dimensional systems. Velocity profiles and pressure drops may be measured to obtain interfacial friction factors. The use of different fluids would permit the examination of the effects of the physical properties of fluids in a system of this type. Tests indicate that if resistance wave gages are to be used to determine the interfacial characteristics, the liquid must have a conductivity at least equal to that of distilled water. Liquids which were found to satisfy this criterion in some laboratory tests were water-glycerine solutions and higher-molecular-weight alcohols, such as ethylene glycol and diethylene glycol, which had a small amount of salt dissolved in them. The effect of geometry on such a system may be elucidated by varying the tube diameter and using differently shaped channels.

After the attainment of additional experimental data, a logical step would be the comparison of all experimental results to the many theories advanced in the literature to explain wave phenomena and interfacial stability. Only the barest beginnings of such work have been done here. The generation of new theories may be necessary should available theories prove inadequate.

In a recent and worthwhile survey of flow and transfer at fluid interfaces, Scriven (35) raised an objection to the study of fluid interfaces by means of statistical distribution functions to the neglect of the study of the behavior of individual fluid elements at the interface. His contention was that a true understanding of the interface may be better achieved in many situations

by the study of individual fluid elements near the interface. This work indicated that Scriven's contention is a valid one. The surface distribution of water-air interfaces studied in this work displayed a number of deviations from a Gaussian distribution, and the wave parameters--wave heights, frequencies, and velocities--behaved very strangely and unexpectly. The nature of these results suggests that while the statistical study of fluid-fluid interfaces in systems similar to that used in this work may result in some useful engineering correlations, it is not likely to result in a true understanding of the interfacial phenomena involved. Such an understnading will probably be achieved only by the experimental and theoretical study of individual fluid elements at the interface. If this approach is necessary, such an understanding is probably in the distant future.

NOMENCLATURE

c	Correlation coefficient, f_0, f_1
D	Tube diameter
f	Frequency
f_0	Wave frequency at $\bar{h}$
f_1	Extrema frequency of water surface
Fr	Froude number
h	Instantaneous liquid height
h'	Fluctuating component of liquid height
$\bar{h}$	Time-average liquid height
Δh	R.M.S. wave height
$\dot{m}$	Mass flow rate
Re	Reynold's number
S	Wetted perimeter
t	Time
v	Arithmetic average velocity
$\bar{v}$	Bulk average velocity
w	Frequency spectrum
We	Weber number
σ	Surface tension
λ	Wavelength
μ	Viscosity
ρ	Density

SUBSCRIPTS

g	Gas
l	Liquid
w	Wave

BIBLIOGRAPHY

1. Anderson, J. D., et al. A. I. Ch. E. J., 10, 640 (1964).

2. Anderson, R. J. and Russell, T. W. F. Chem. Eng.

   a. Part I. 61, 139 (December 6, 1965).

   b. Part II. 61, 99 (December 20, 1965).

   c. Part III. 62, 87 (January 3, 1966).

3. Ball, John Gordon. Ph. D. Thesis, University of Texas (1965).

4. Bergelin, O. P., and Gazeley, Carl. "Heat Transfer and Fluid Mechanics Institute," 5 (1949).

5. Bloom, William G. Undergraduate Chemical Engineering Research Report, California Institute of Technology (1968).

6. Bollinger, R. E. Master of Ch. E. Thesis, University of Delaware (1960).

7. Chan, Wing-Cheng. Ph.D. Thesis, University of Minnesota (1964).

8. Chang, F. W. and Dukler, A. E. Int. J. Heat Mass Transfer, 7, 1395 (1964).

9. Cohen, L. S. and Hanratty, T. J. A. I. Ch. E. J., 12, 290 (1966).

10. Cohen, L. S. and Hanratty, T. J. J. Fluid Mech., 31, 467 (1968).

11. Cohen, L. S. Ph.D. Thesis, University of Illinois (1964).

12. Fulford, G. D. Adv. in Chem. Eng., 5, 151 (1964).

13. Gazeley, Carl. "Heat Transfer and Fluid Mechanics Institute," 29 (1949).

14. Gouse, S. W. "An Introduction to Two-Phase Gas-Liquid Flow." Engineering Products Laboratory, M.I.T. (June 1964). Report No. DSR 8734 - 3. AD No. 603659.

15. Gouse, S. William. "An Index to the Two-Phase Gas-Liquid Flow Literature," Engineering Products Laboratory, M.I.T.
    a. Part I. (May, 1963). DSR No. 8734-1 AD No. 411512.
    b. Part II. (September, 1964). DSR No. 8734-4
    c. Part III. (January, 1966). DSR No. 8734-6.
16. Hanratty, T. J. and Engen, J. M. A. I. Ch. E. J., 3, 299 (1957).
17. Helfinstein, R. A. Ph.D. Thesis, Purdue University (1967).
18. Hershman, A. Ph.D. Thesis, University of Illinois (1958).
19. Hoogendoorn, C. J. Chem. Eng. Sci., 9, 205 (1959).
20. Jeffreys, Harold. Proc. Ray Soc. Lond. A., 107, 189 (1925).
21. Jenkins, R. M.S. Thesis, University of Delaware (1947).
22. Kinsman, Blair. "Wind Waves, Their Generation and Propagation on the Ocean Surface," Prentice-Hall, Englewood Cliffs, New Jersey (1965).
23. Kordyban, E. S. and Ranov, T. A. S. M. E. Multi-Phase Fluid Flow Symposium, (November, 1963).
24. Lamb, Horace, "Hydrodynamics," Sixth Edition, Dover, New York (1932).
25. Lilleleht, L. V. and Hanratty, T. J. J. Fluid Mech., 11, 65 (1961).
26. Lilleleht, L. V. and Hanratty, T. J. A. I. Ch. E. J., 7, 548 (1961).
27. Lilleleht, L. V. Ph.D. Thesis, University of Illinois (1961).
28. Lu, Hsiang Sung. Ph.D. Thesis, University of Oklahoma (1965).
29. Pierson, W. J. "Adv. in Geophysics," Vol. 2, Academic Press, New York (1955).
30. Putz, R. R. Proc. 4th Conf. on Coastal Eng., p. 13, Council of Wave Research, University of California, Berkeley (1954).

31. Raichlen, Fredric. "Wave-Induced Oscillations of Small Moored Vessels." Keck Laboratory, Caltech, Report No. KH-R-10 (1965).

32. Rice, S. O. Bell System Tech. Jour., 23, 282 (1944) and 24, 46 (1945).

33. Ruckenstein, E. and Berbente, C. Chem. Eng. Sci., 20, 795 (1965).

34. Scott, D. S. Adv. in Chem. Eng., 4, 199 (1963).

35. Scriven, L. E. Chem. Eng. Ed., 2, 150 (1968).

36. Ursell, F. "Surveys in Mechanics," Cambridge University Press, Cambridge (1956).

37. van Rossum, J. J. Chem. Eng. Sci., 11, 35 (1959).

38. Yu, H. S. and Sparrow, E. M. A. I. Ch. E. J., 13, 10 (1967).

39. Zegel, William Case. Sc.D. Thesis, Stevens Institute of Technology (1965).

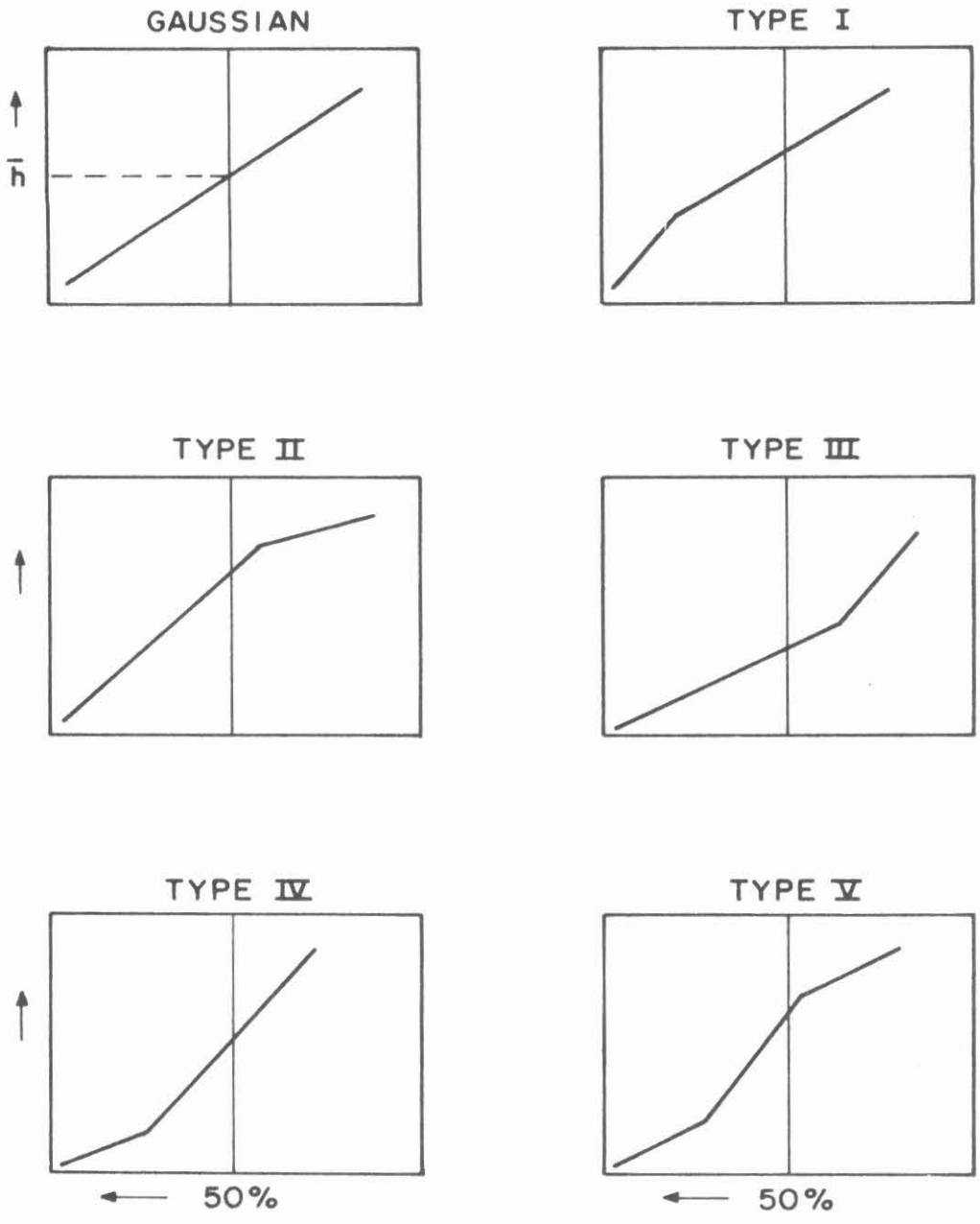

FIGURE 1. Probability Graph Plots of Liquid Surface Level Distributions

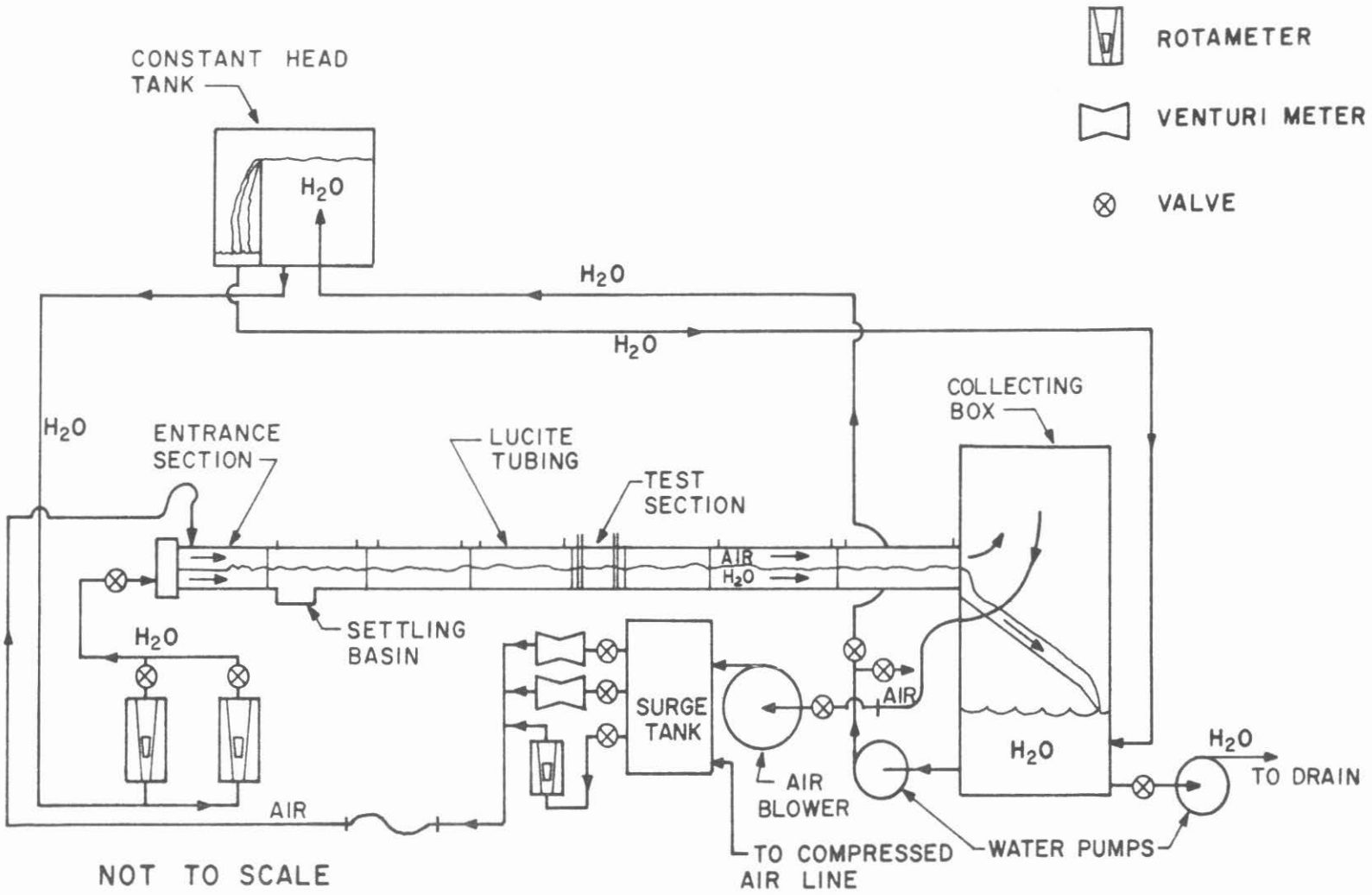

FIGURE 2. Schematic Diagram of Apparatus

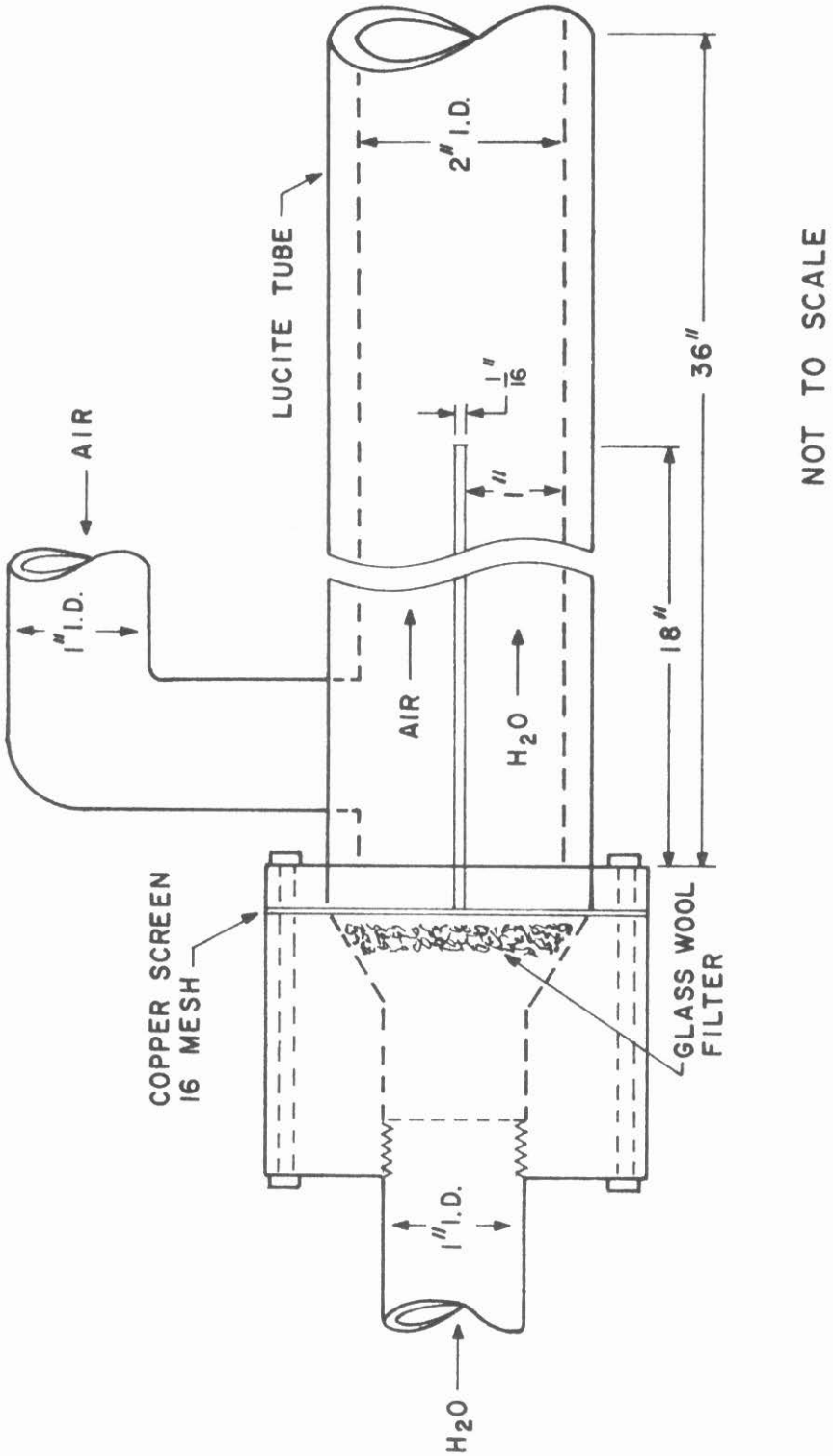

FIGURE 3. Equally Divided Entrance Section

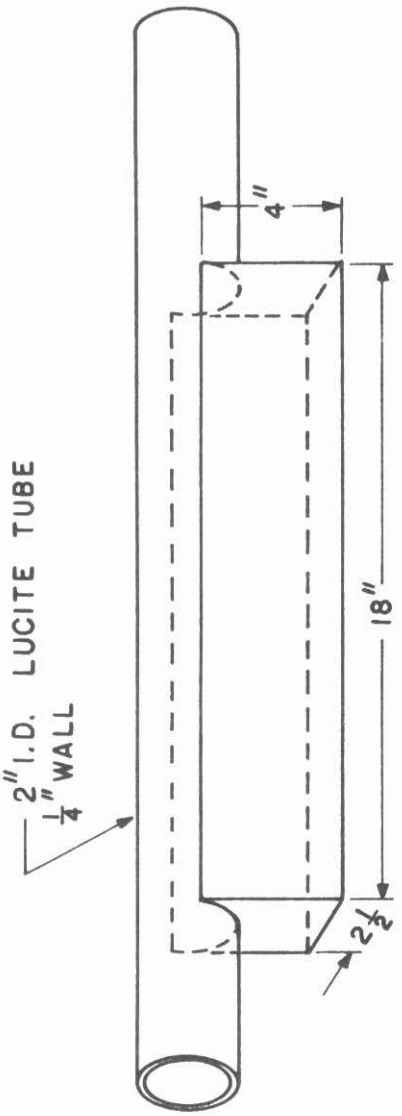

FIGURE 4. Settling Basin

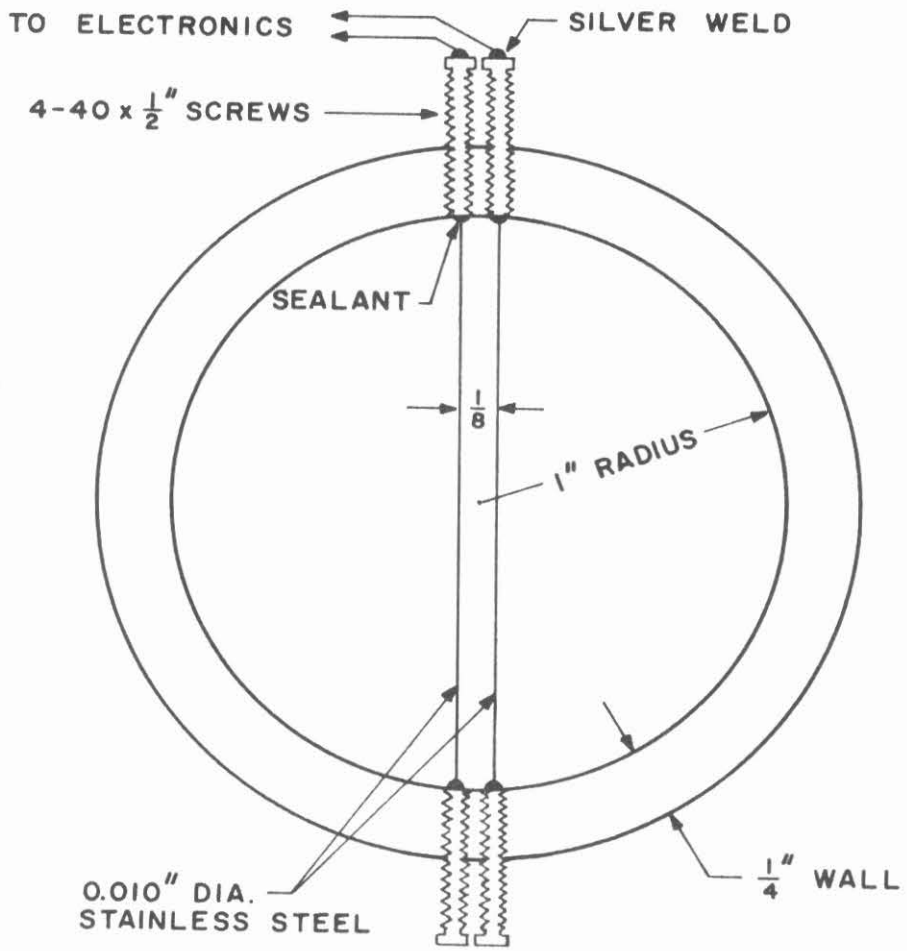

FIGURE 5. Resistance Wave Gages

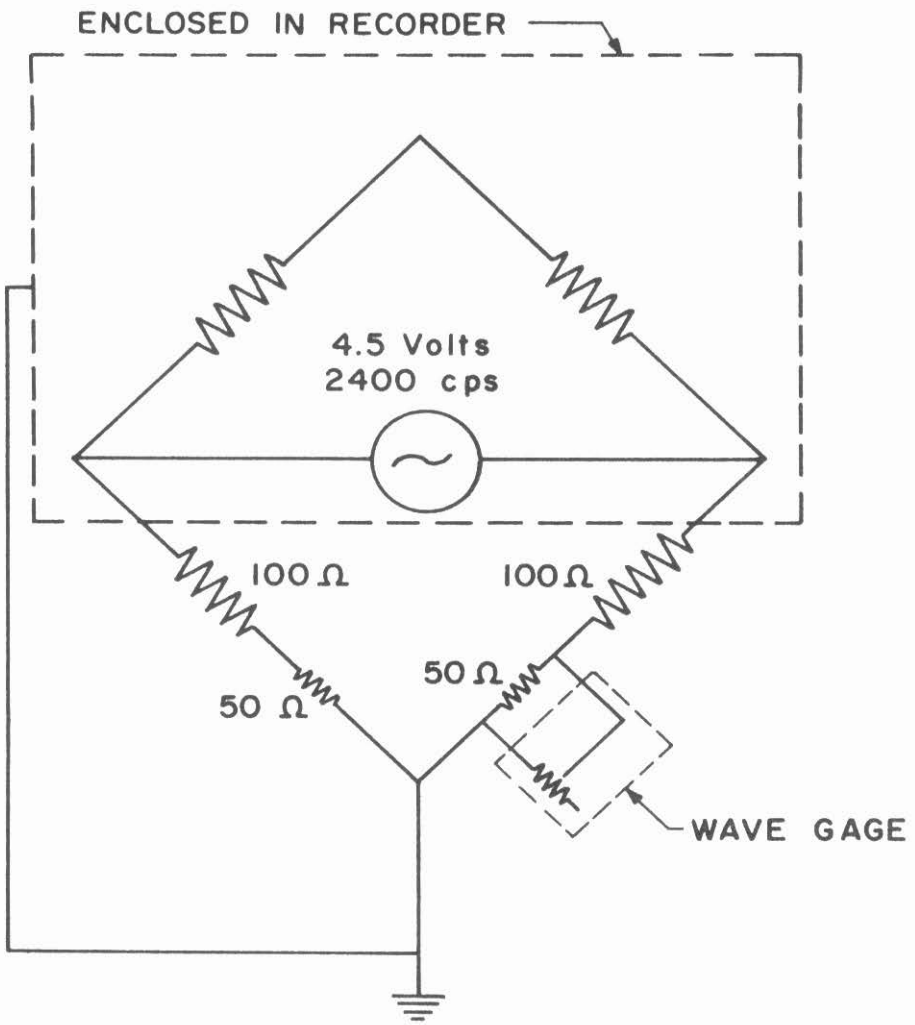

FIGURE 6. Wave Gage Circuit Diagram

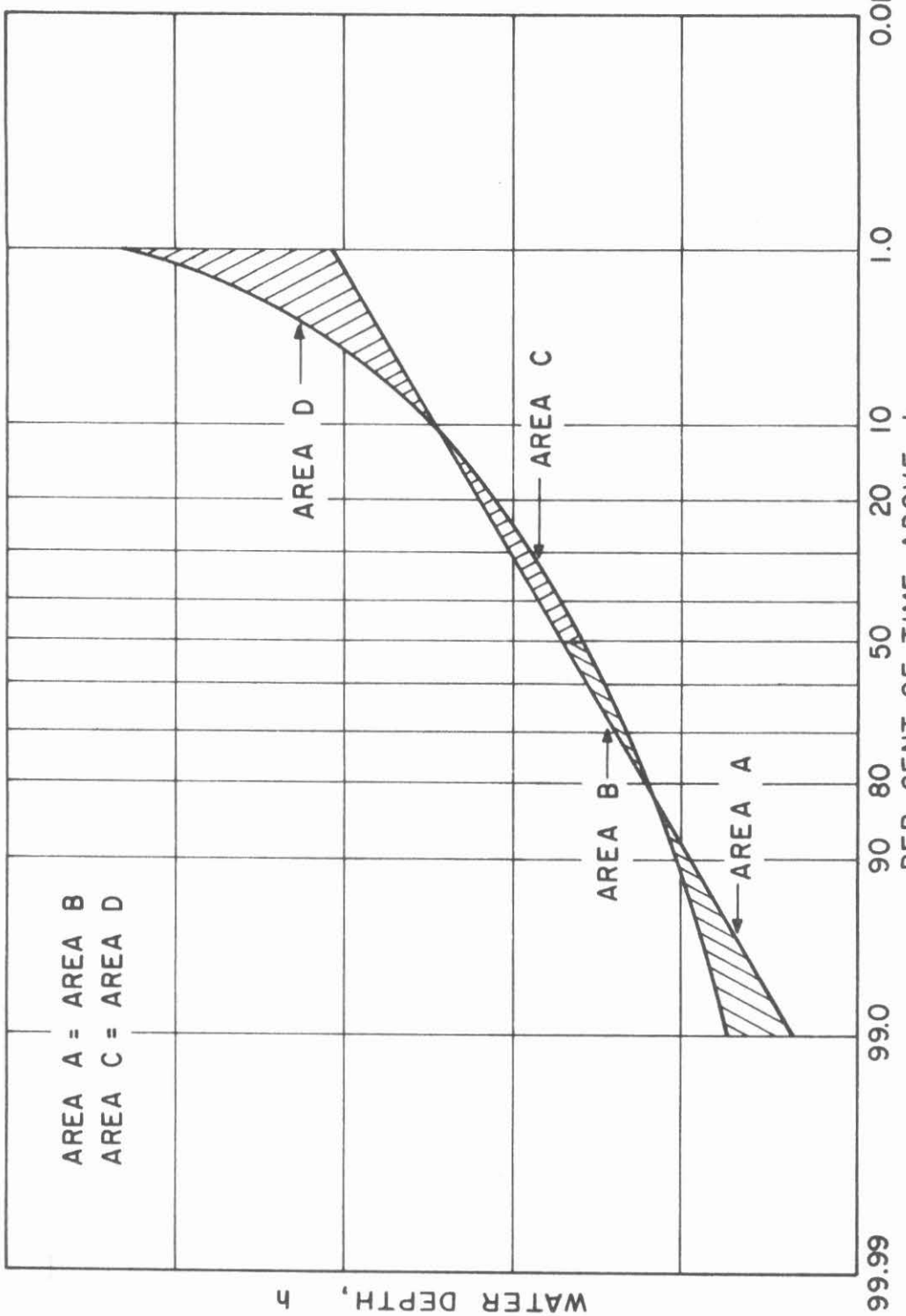

FIGURE 7. Determination of Δh for a Non-Gaussian Distribution

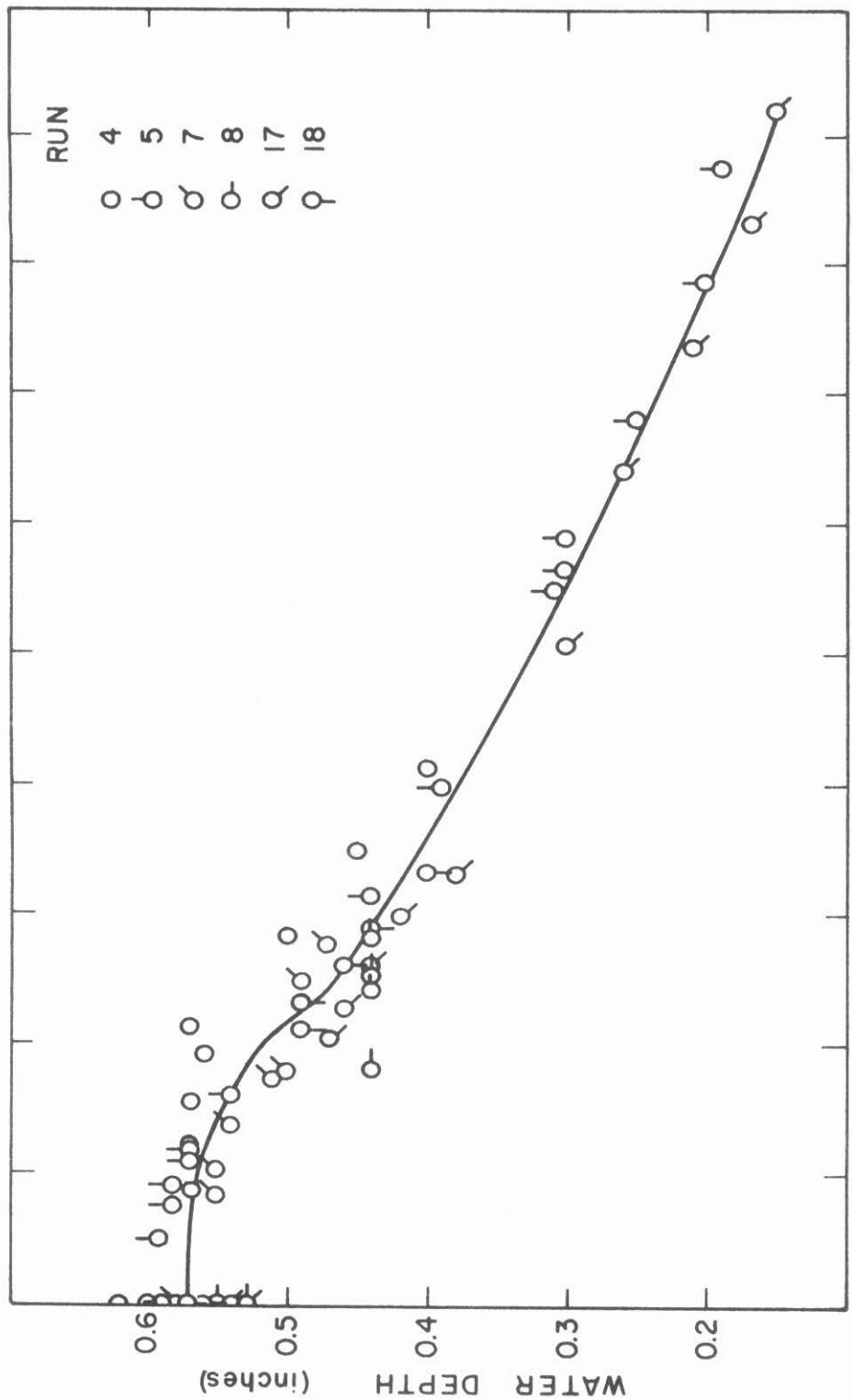

FIGURE 8. Water Depth at 250 lbs. H_2O per hour

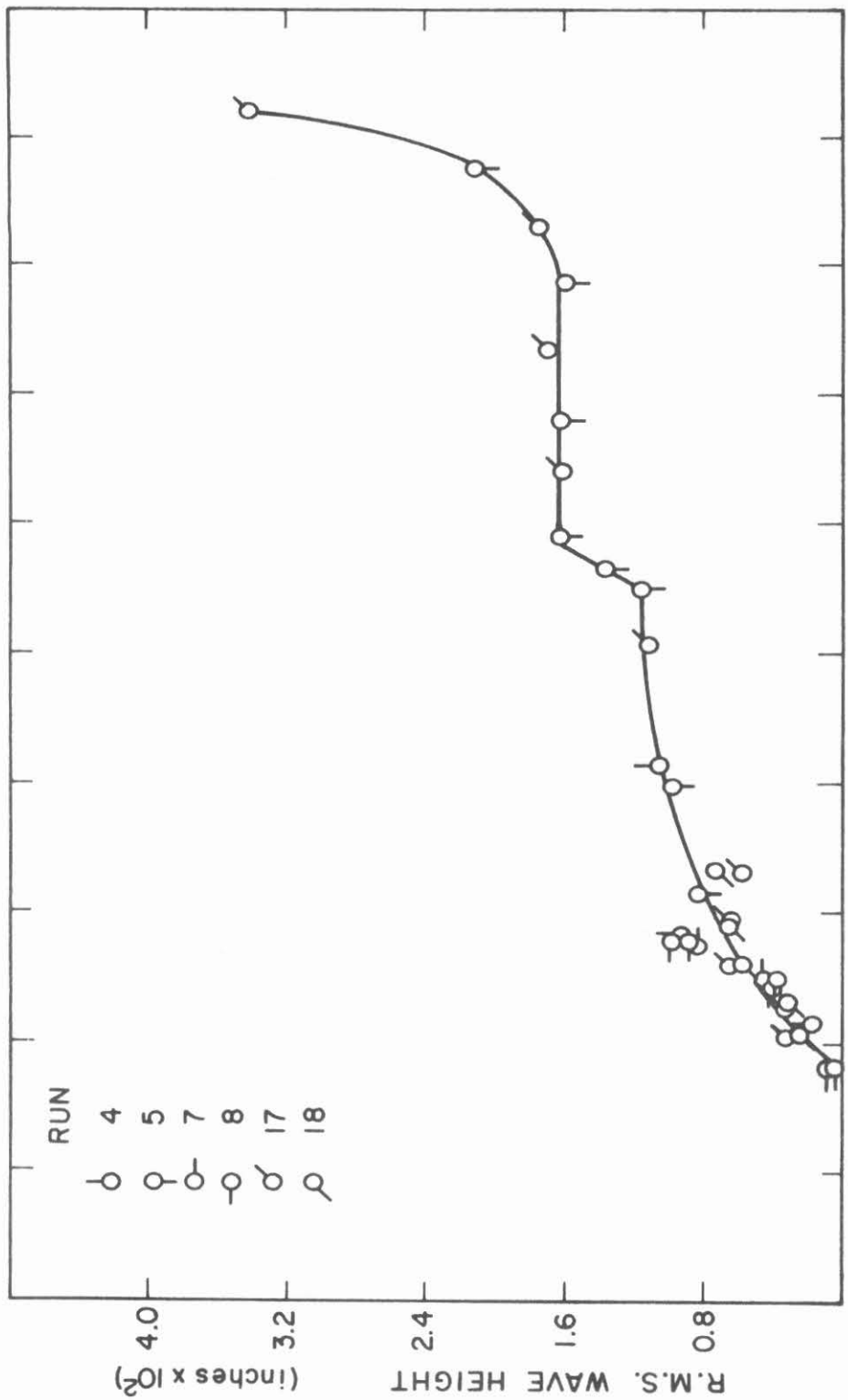

FIGURE 9. R.M.S. Wave Height at 250 lbs. H_2O per hour

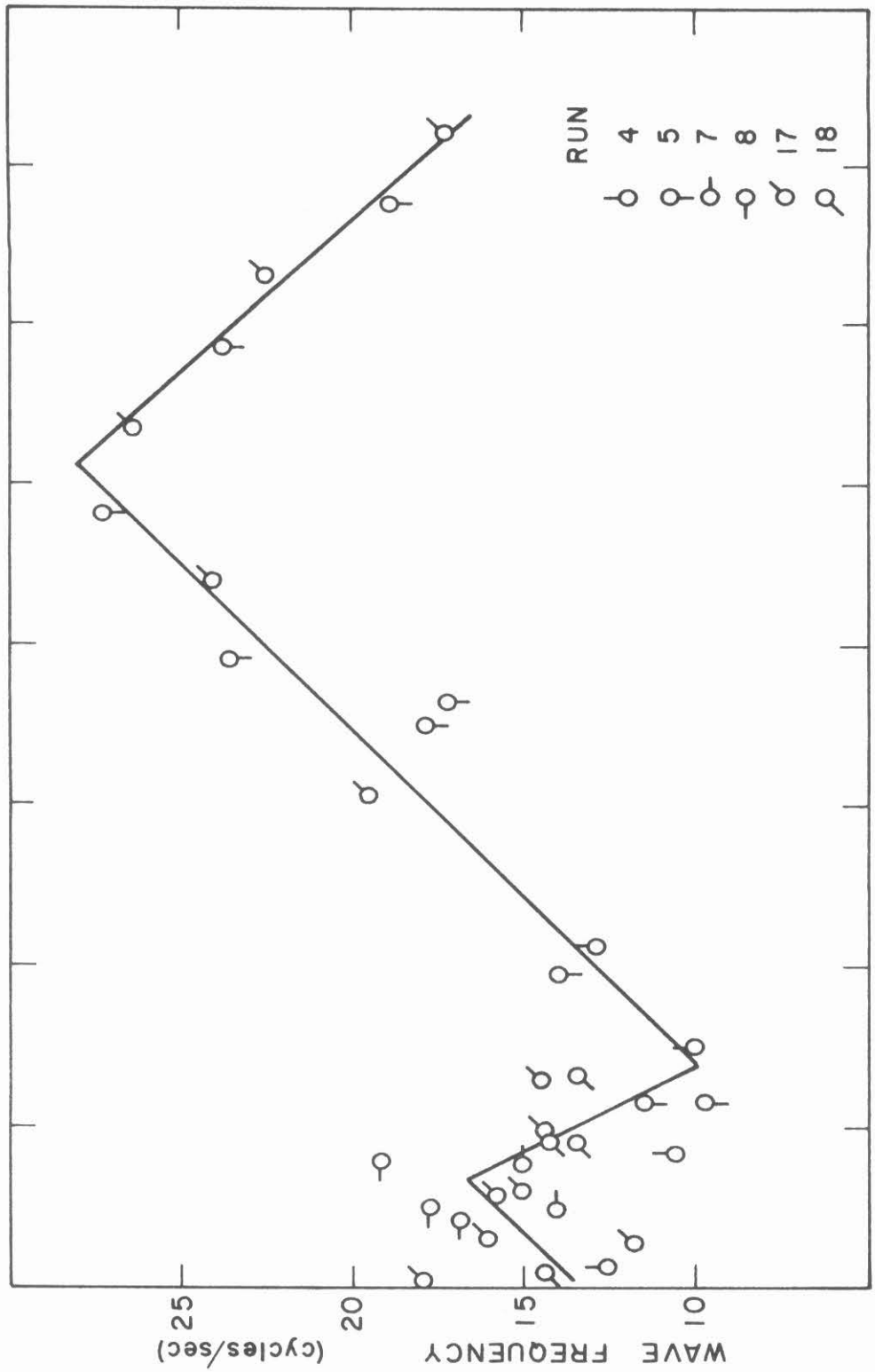

FIGURE 10. Wave Frequency at 250 lbs. H_2O per hour

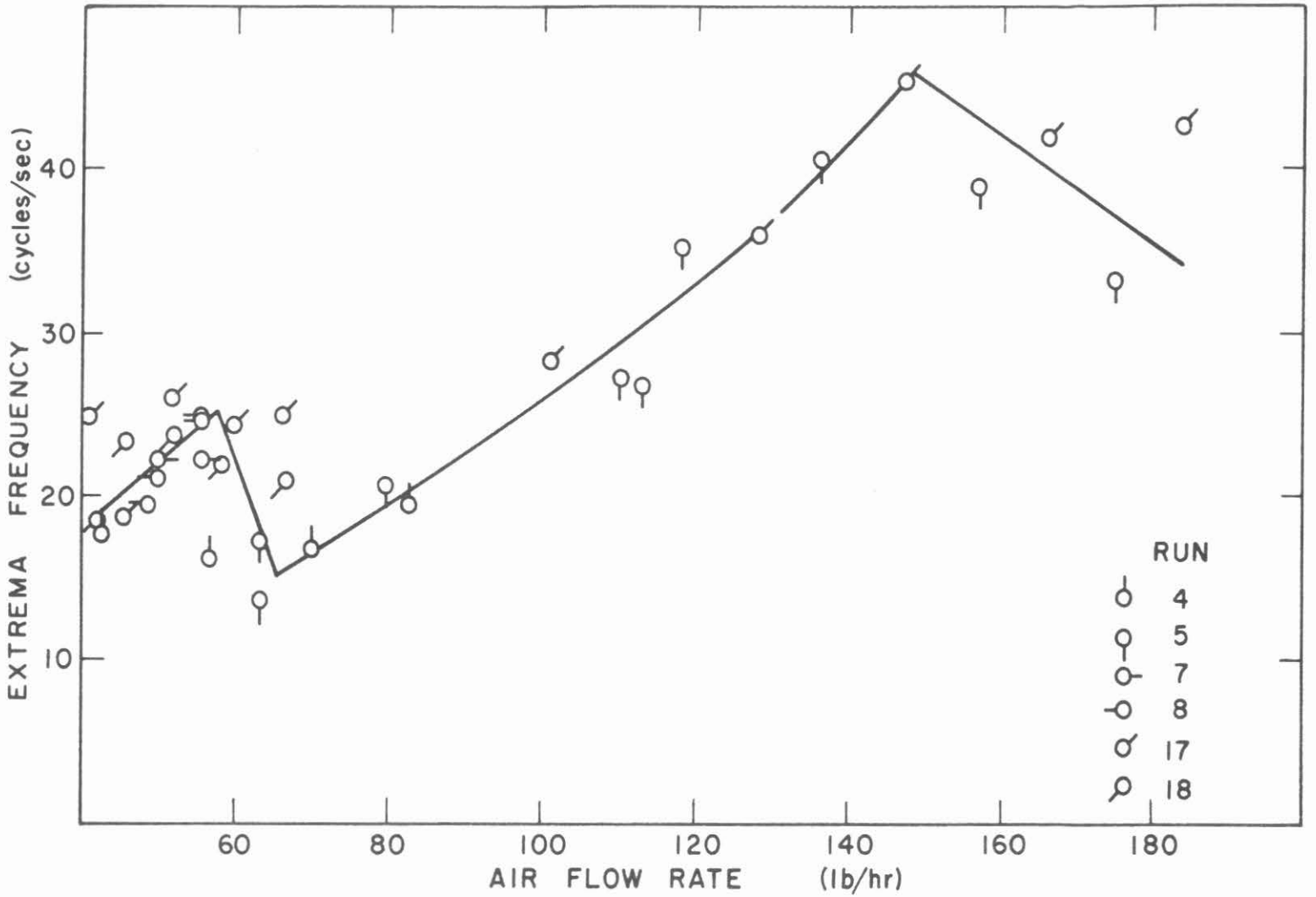

FIGURE 11. Extrema Frequency at 250 lbs. H_2O per hour

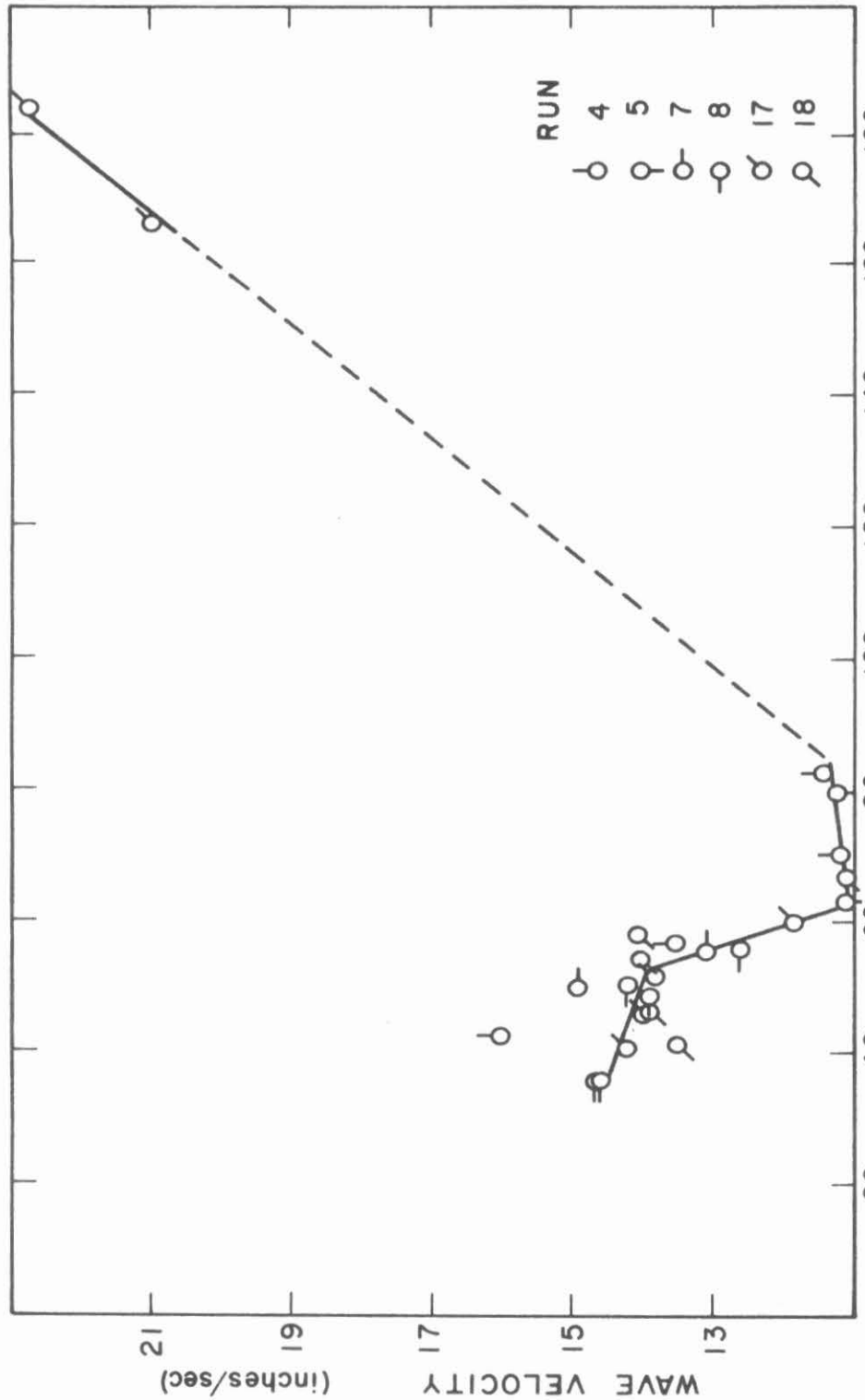

FIGURE 12. Wave Velocity at 250 lbs. H_2O per hour

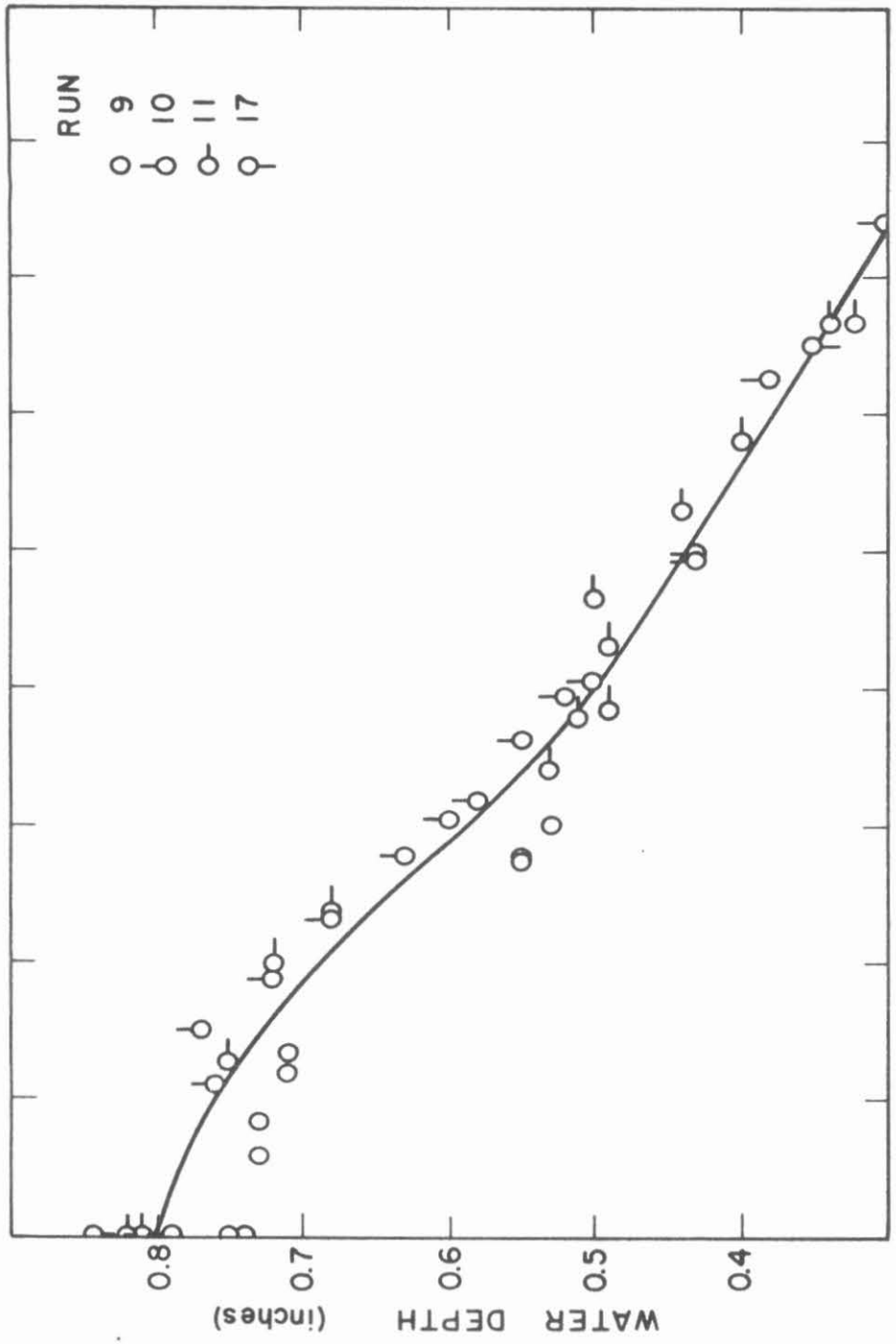

FIGURE 13. Water Depth at 750 lbs. H_2O per hour

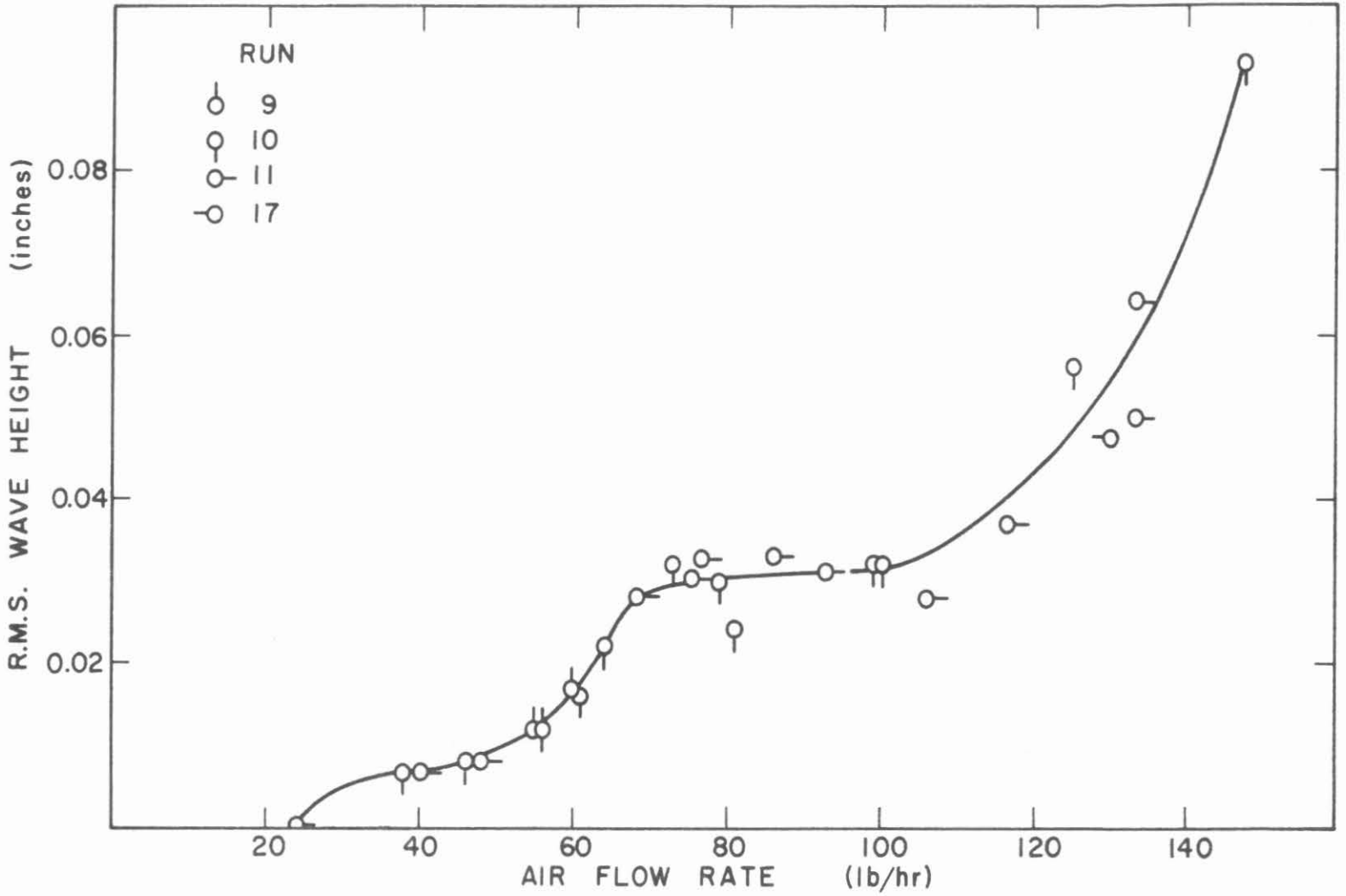

FIGURE 14. R.M.S. Wave Height at 750 lbs. H_2O per hour

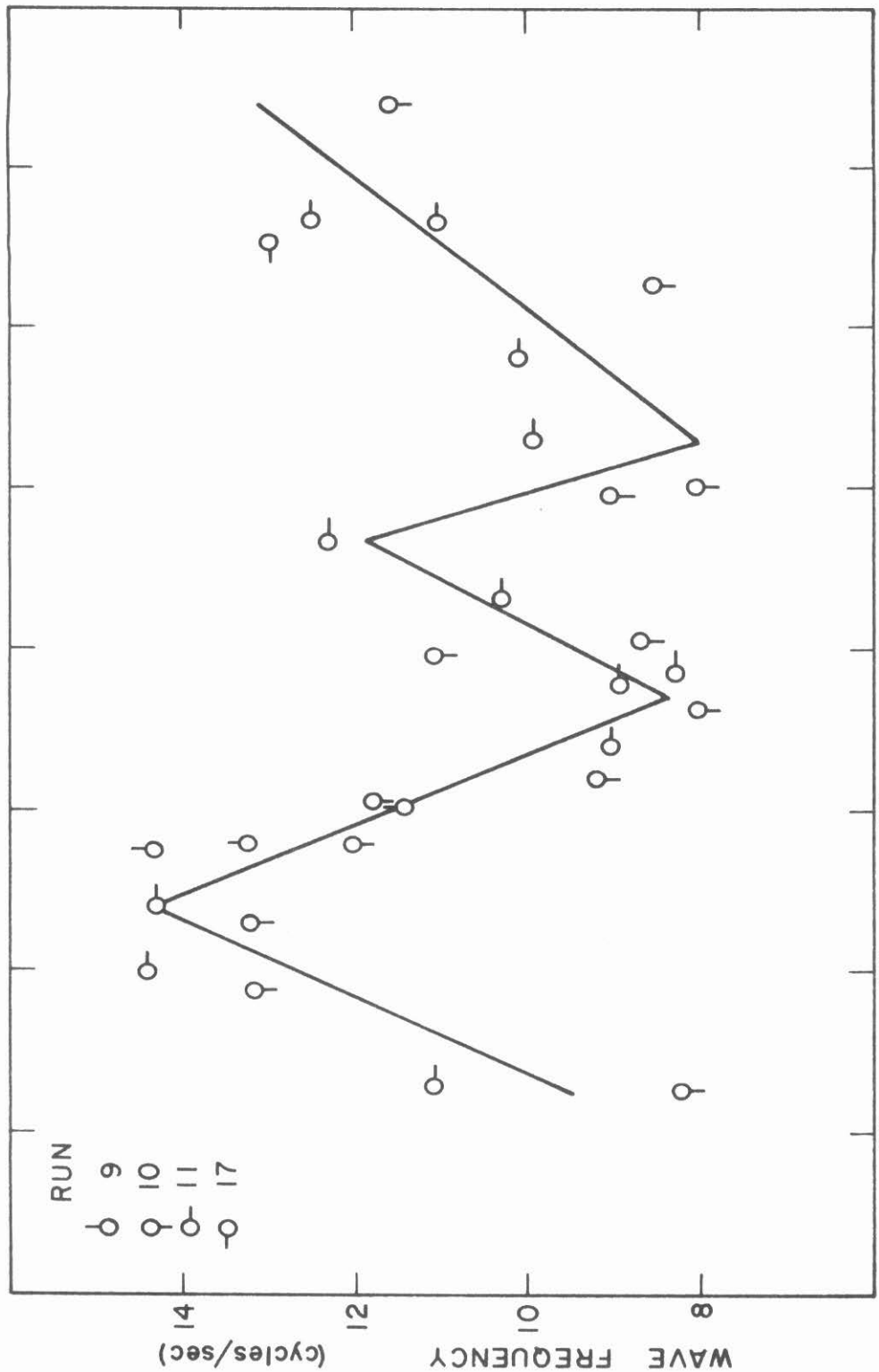

FIGURE 15. Wave Frequency at 750 lbs. H_2O per hour

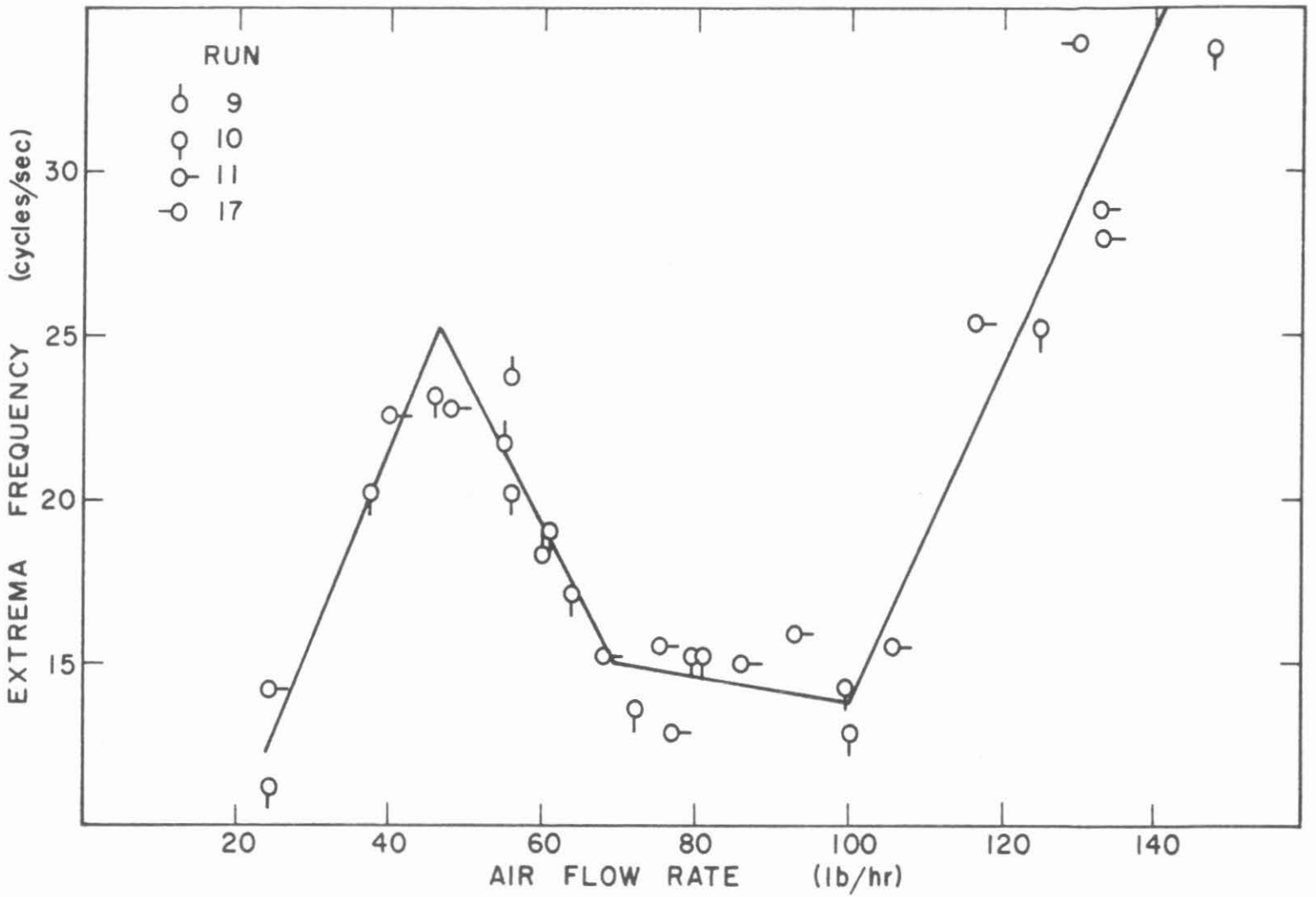

FIGURE 16. Extrema Frequency at 750 lbs. H_2O hour

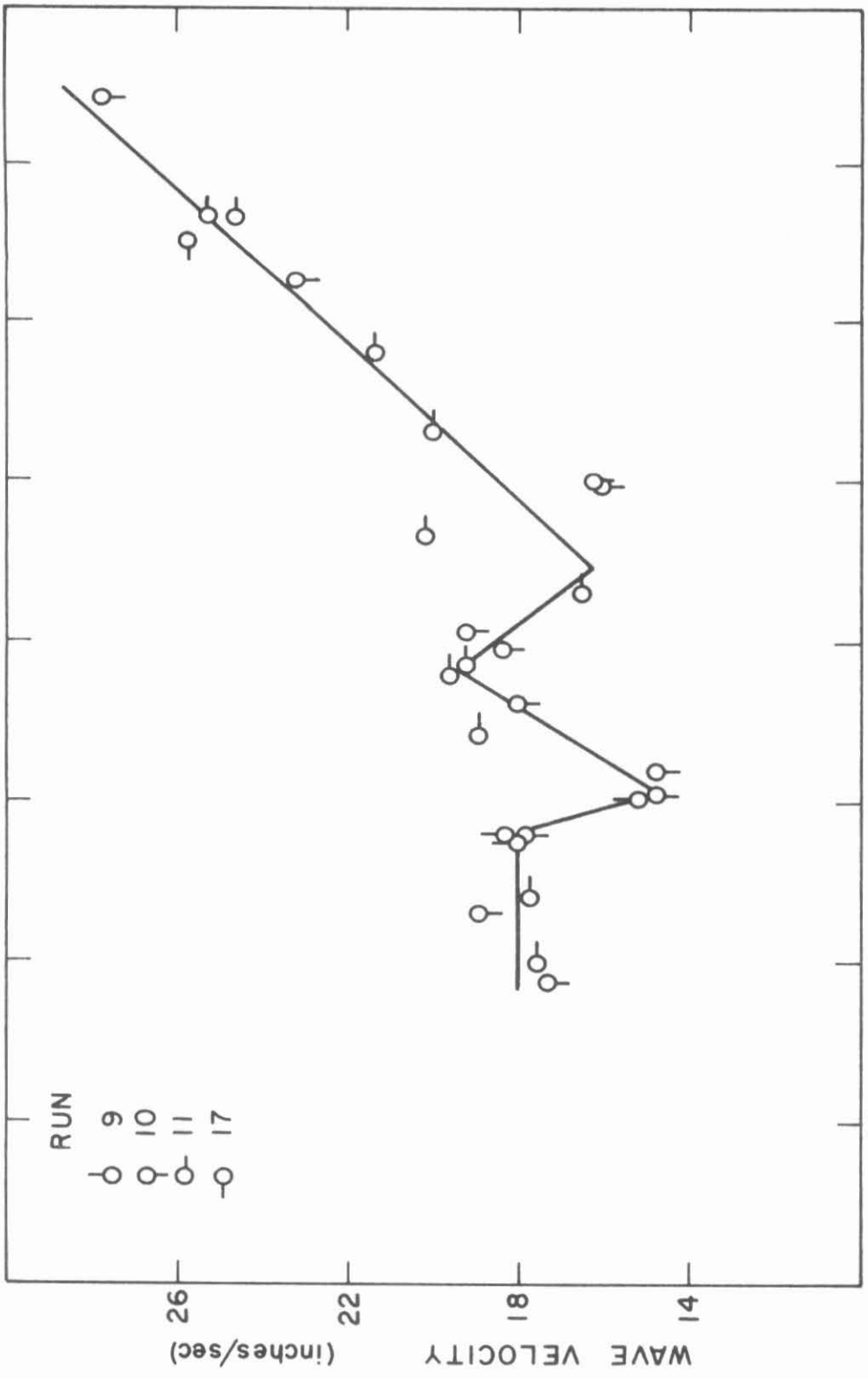

FIGURE 17. Wave Velocity at 750 lbs per hour

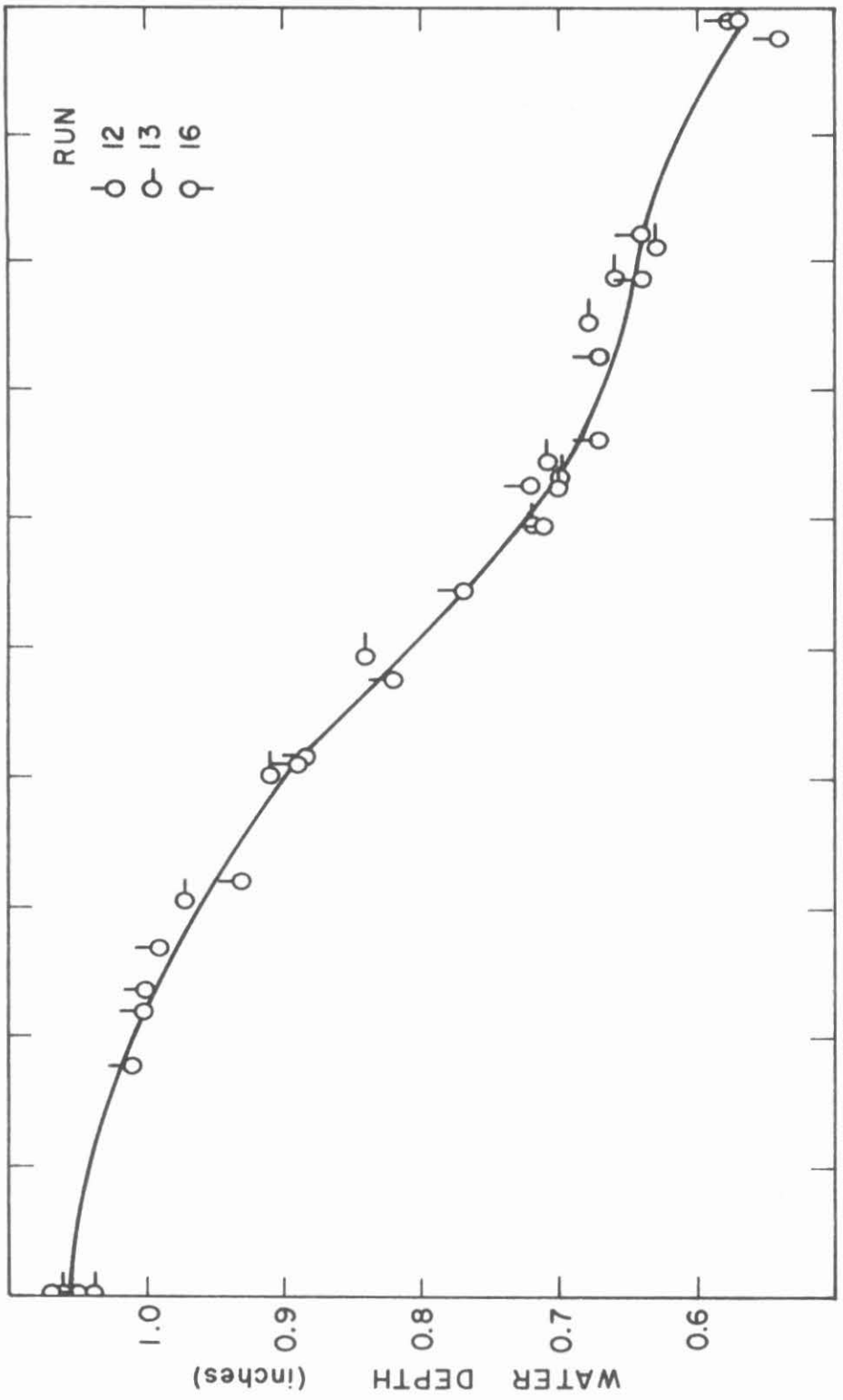

FIGURE 18. Water Depth at 1250 lbs. H_2O per hour

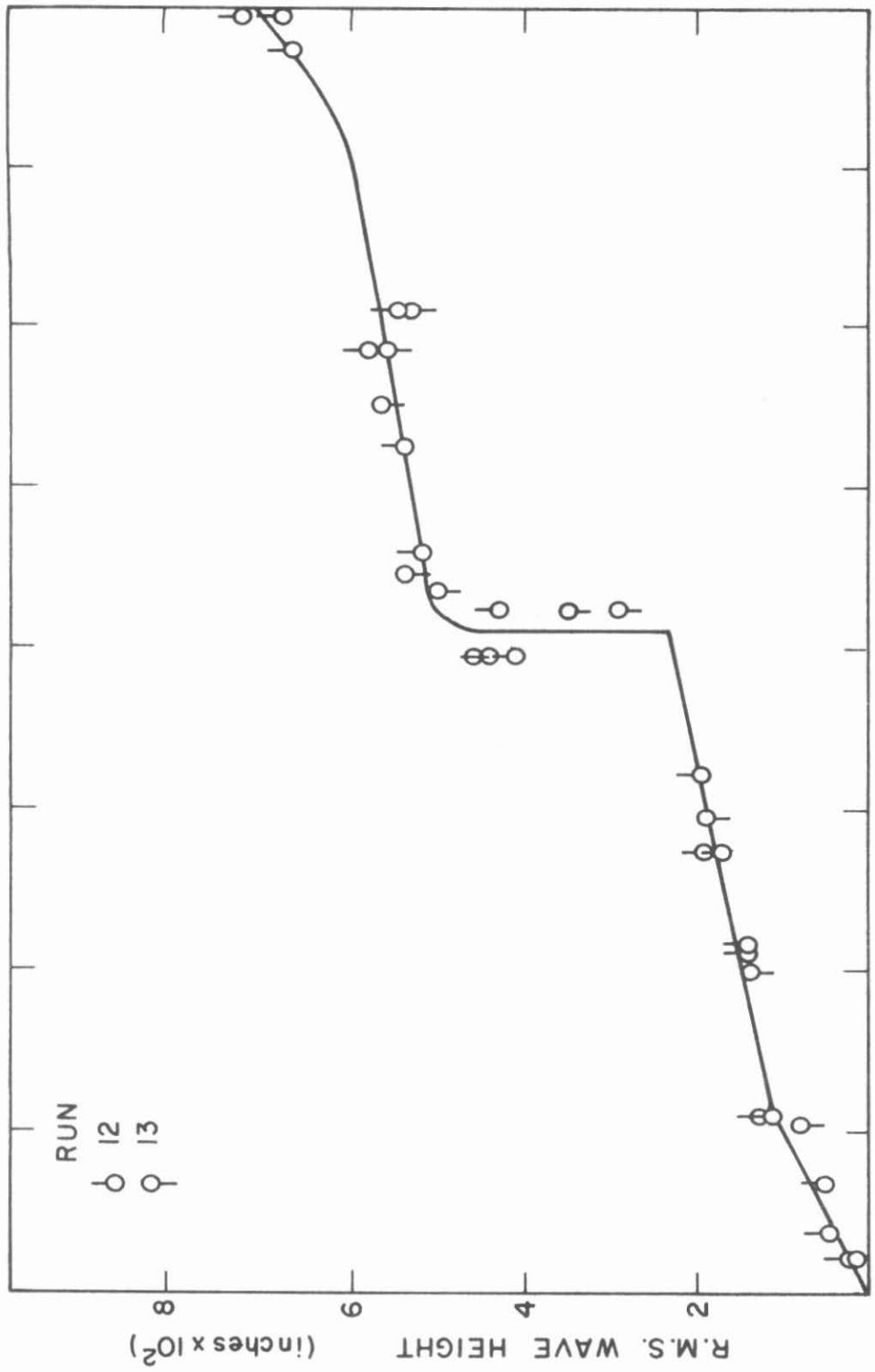

FIGURE 19. R.M.S. Wave Height at 1250 lbs. H_2O per hour

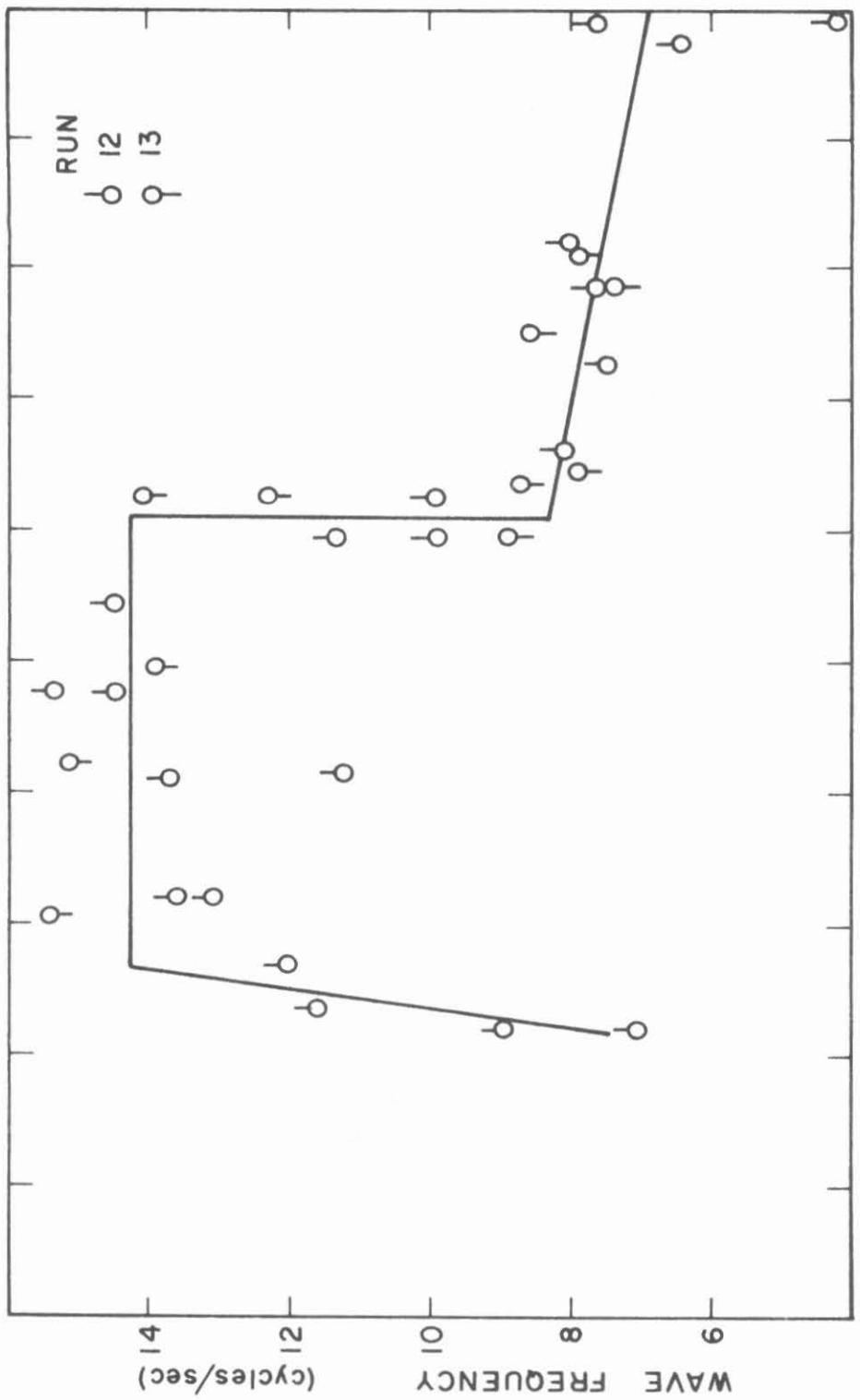

FIGURE 20. Wave Frequency at 1250 lbs H_2O per hour

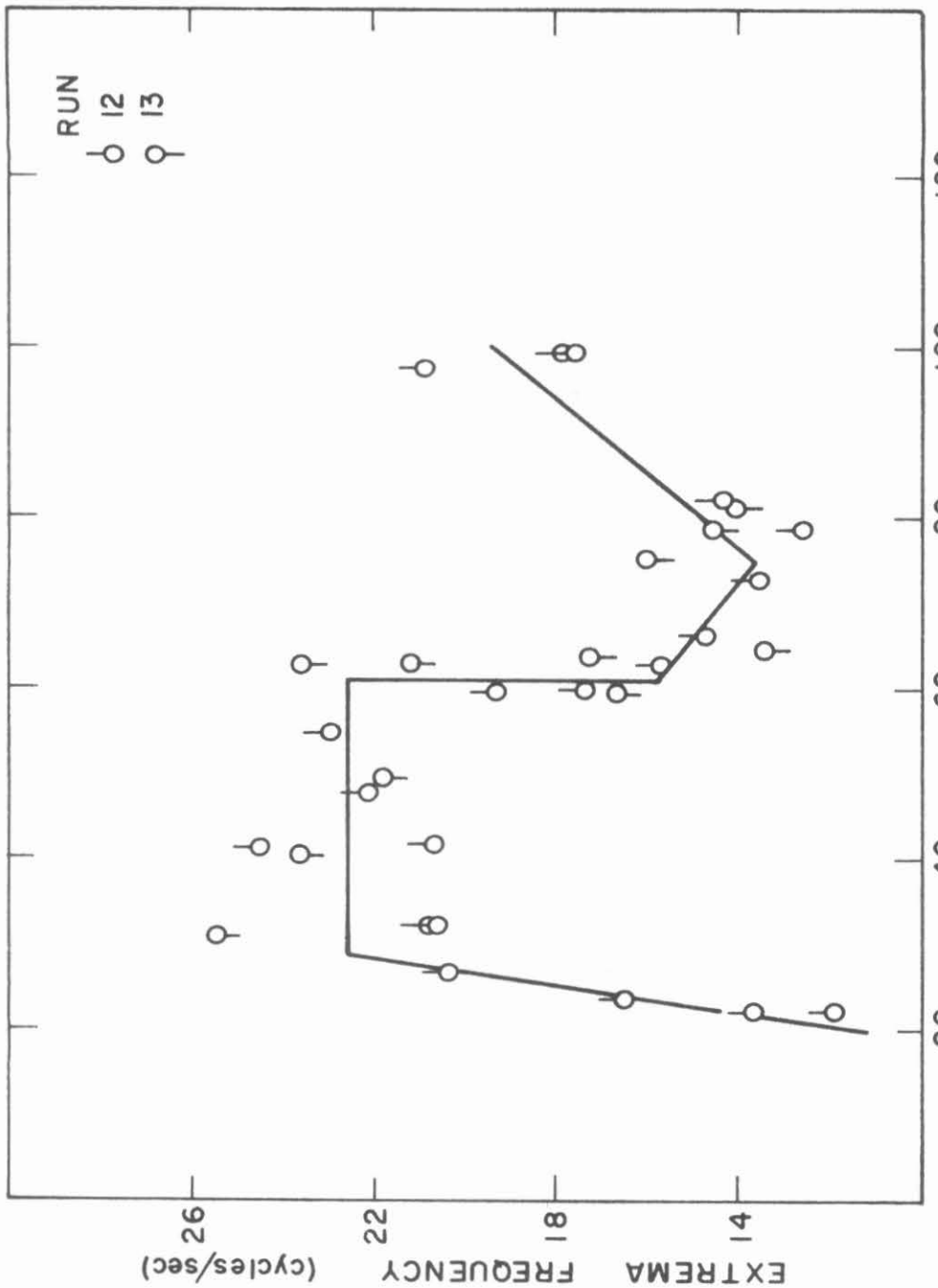

FIGURE 21. Extrema Frequency at 1250 lbs. H_2O per hour

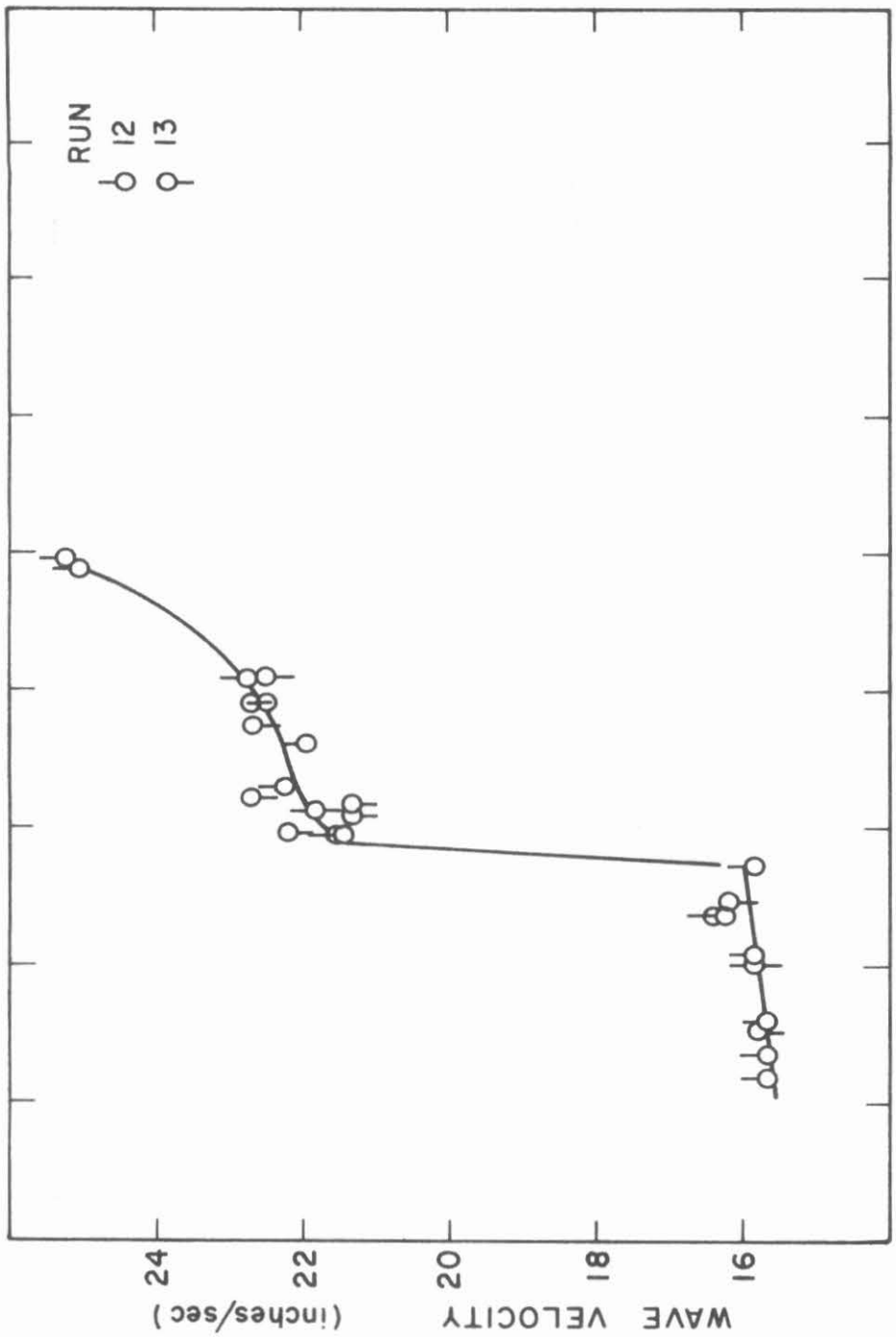

FIGURE 22. Wave Velocity at 1250 lbs. H_2O per hour

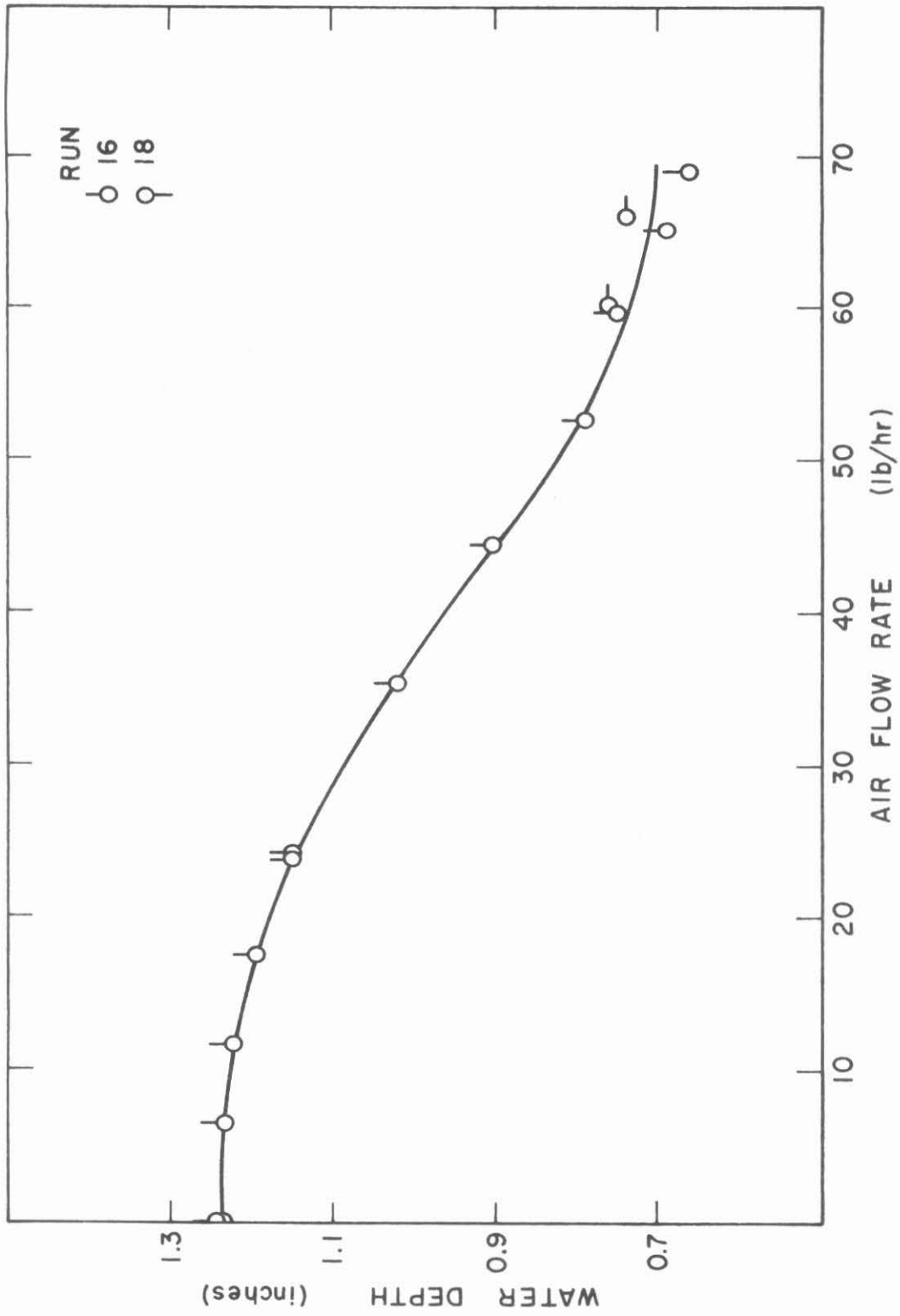

FIGURE 23. Water Depth at 1750 lbs. H_2O per hour

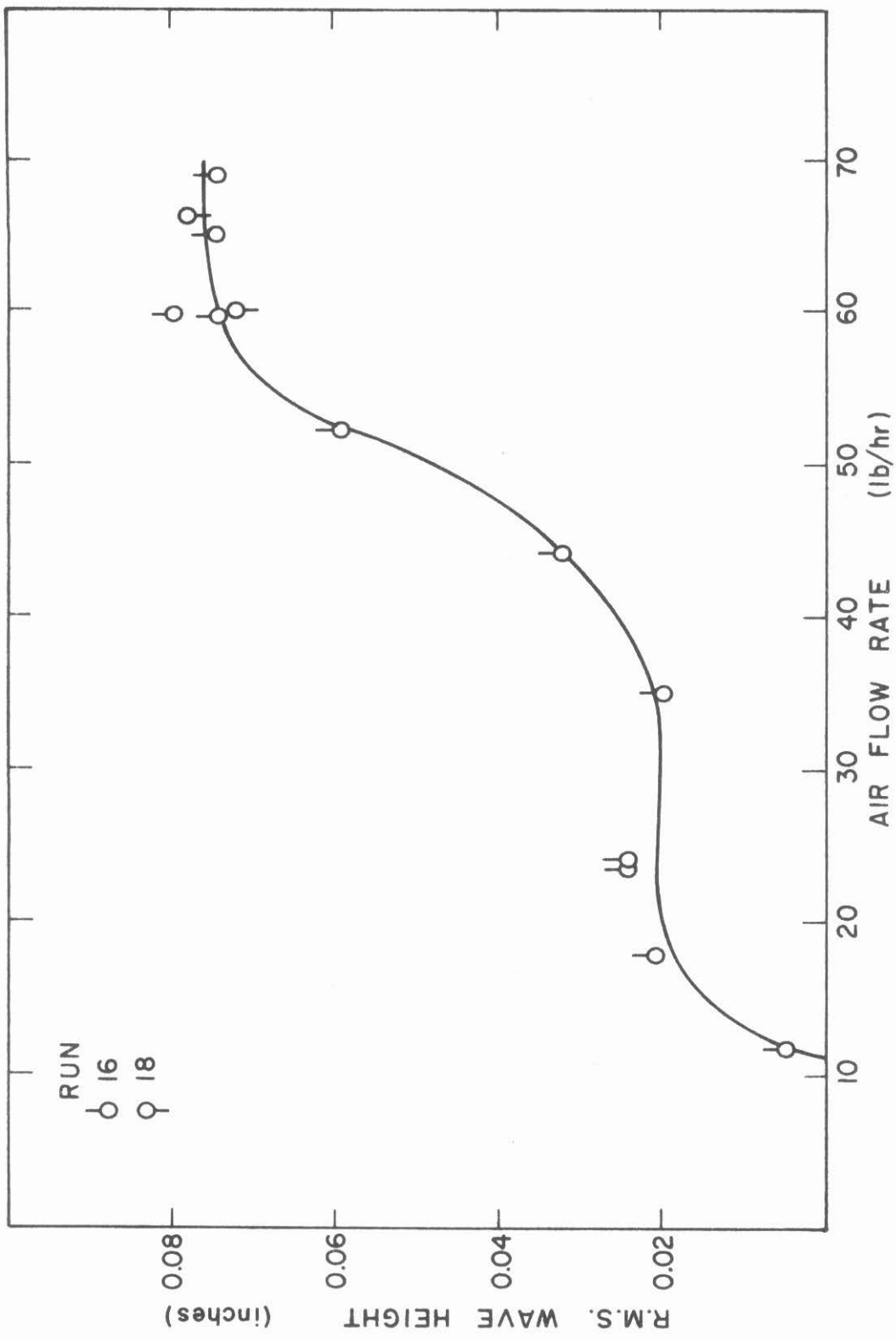

FIGURE 24. Wave Height at 1750 lbs. H_2O per hour

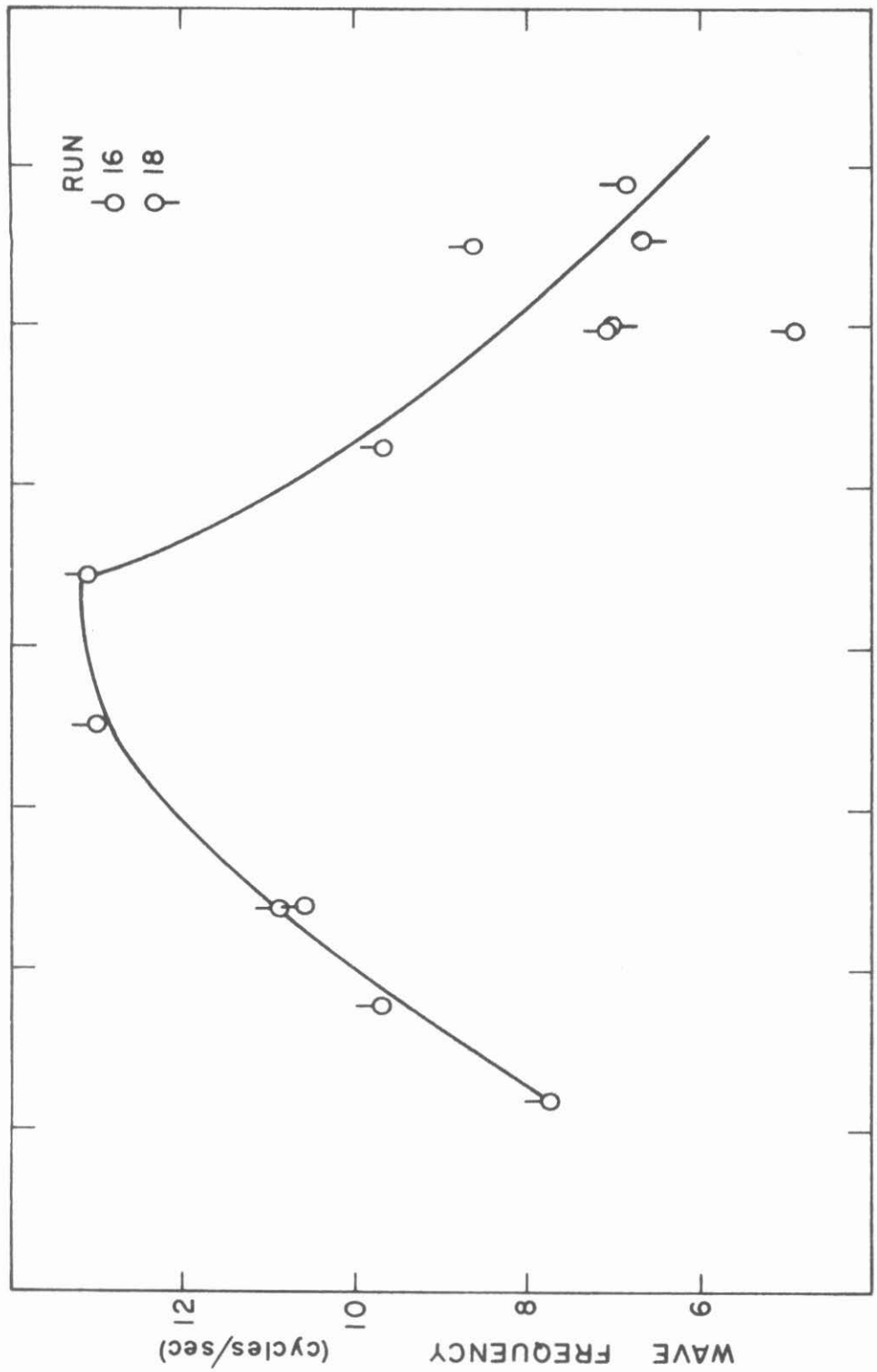

FIGURE 25. Wave Frequency at 1750 lbs. H_2O per hour

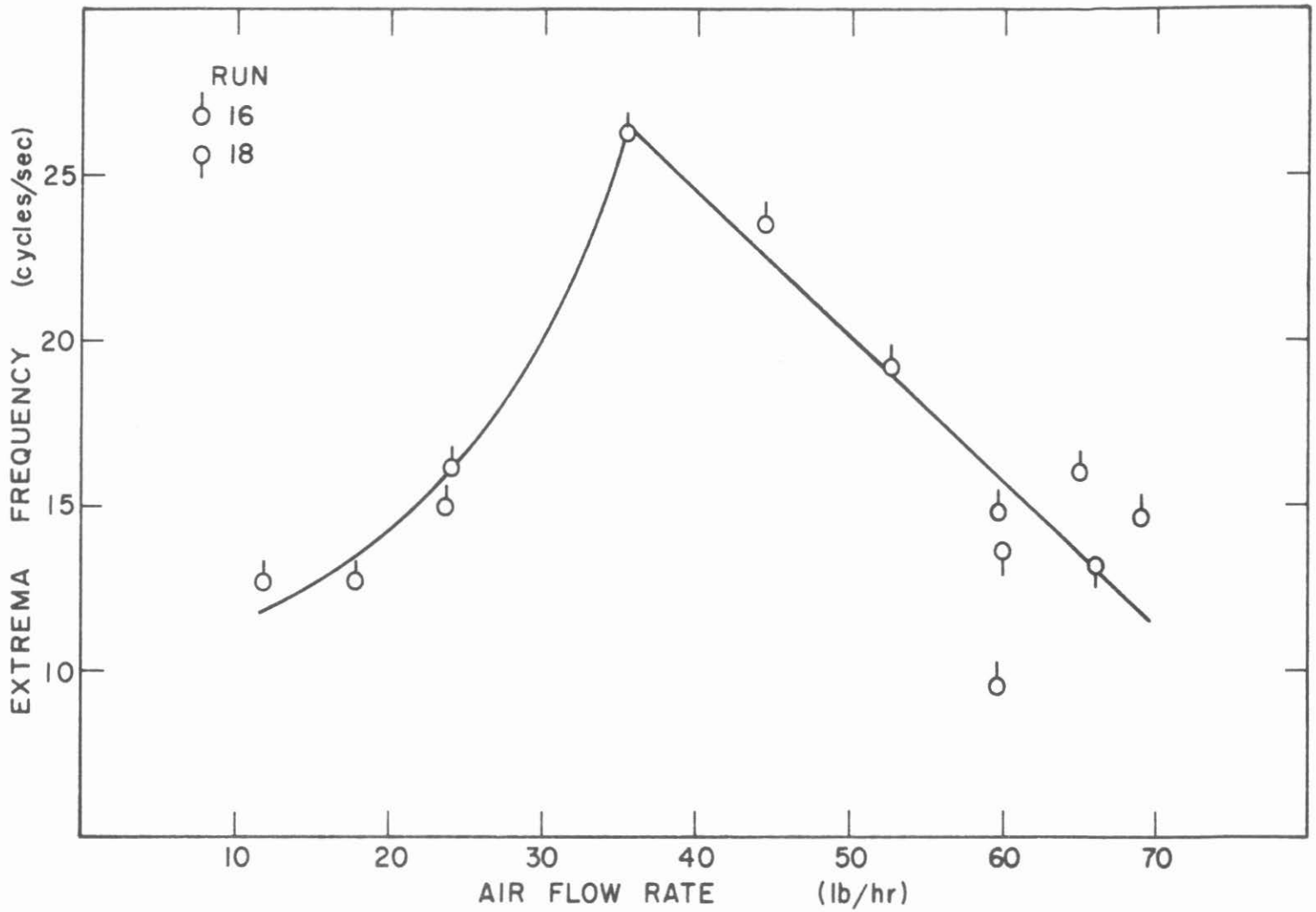

FIGURE 26. Extrema Frequency at 1750 lbs. H_2O per hour

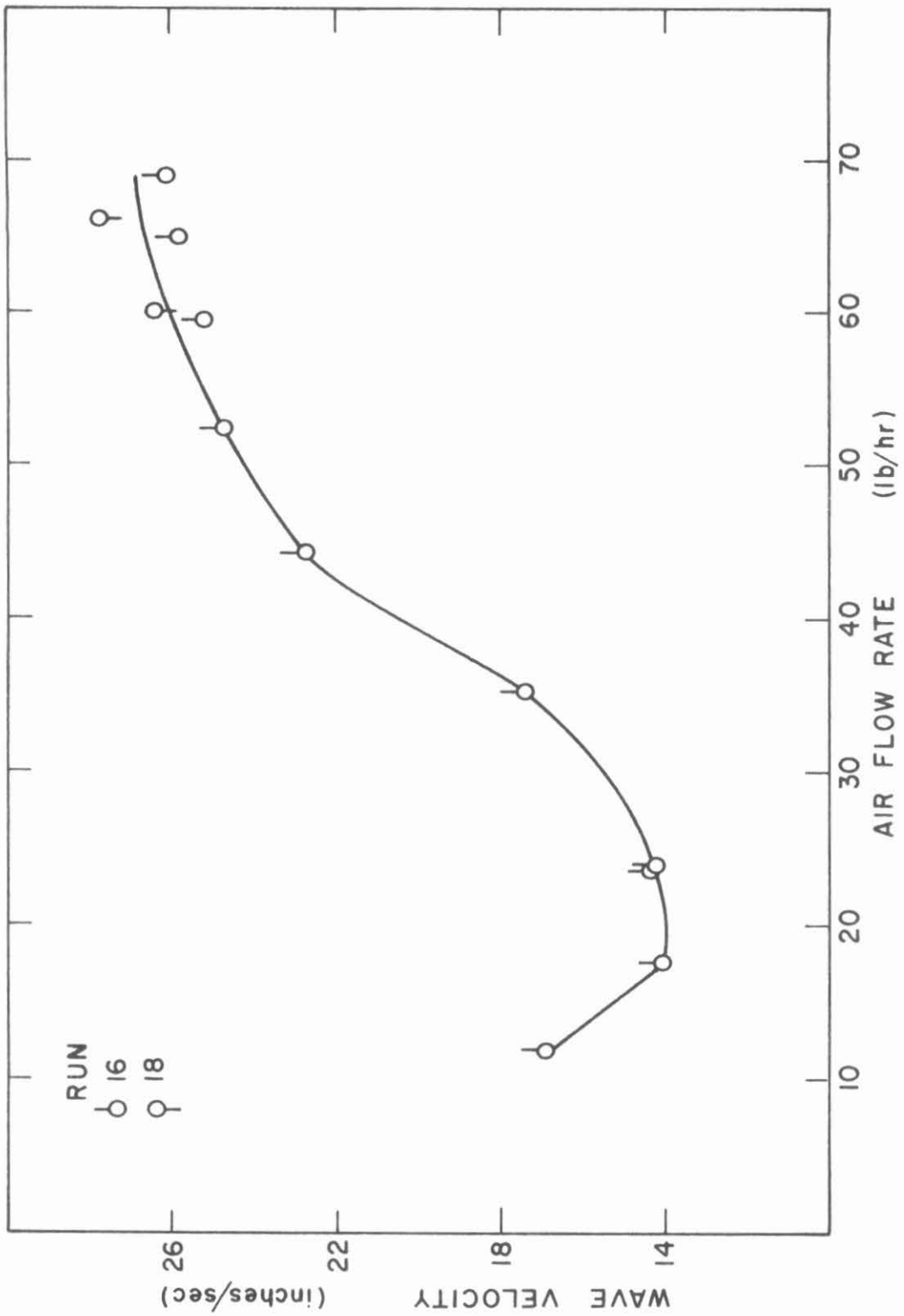

FIGURE 27. Wave Velocity at 1750 lbs. H_2O per hour

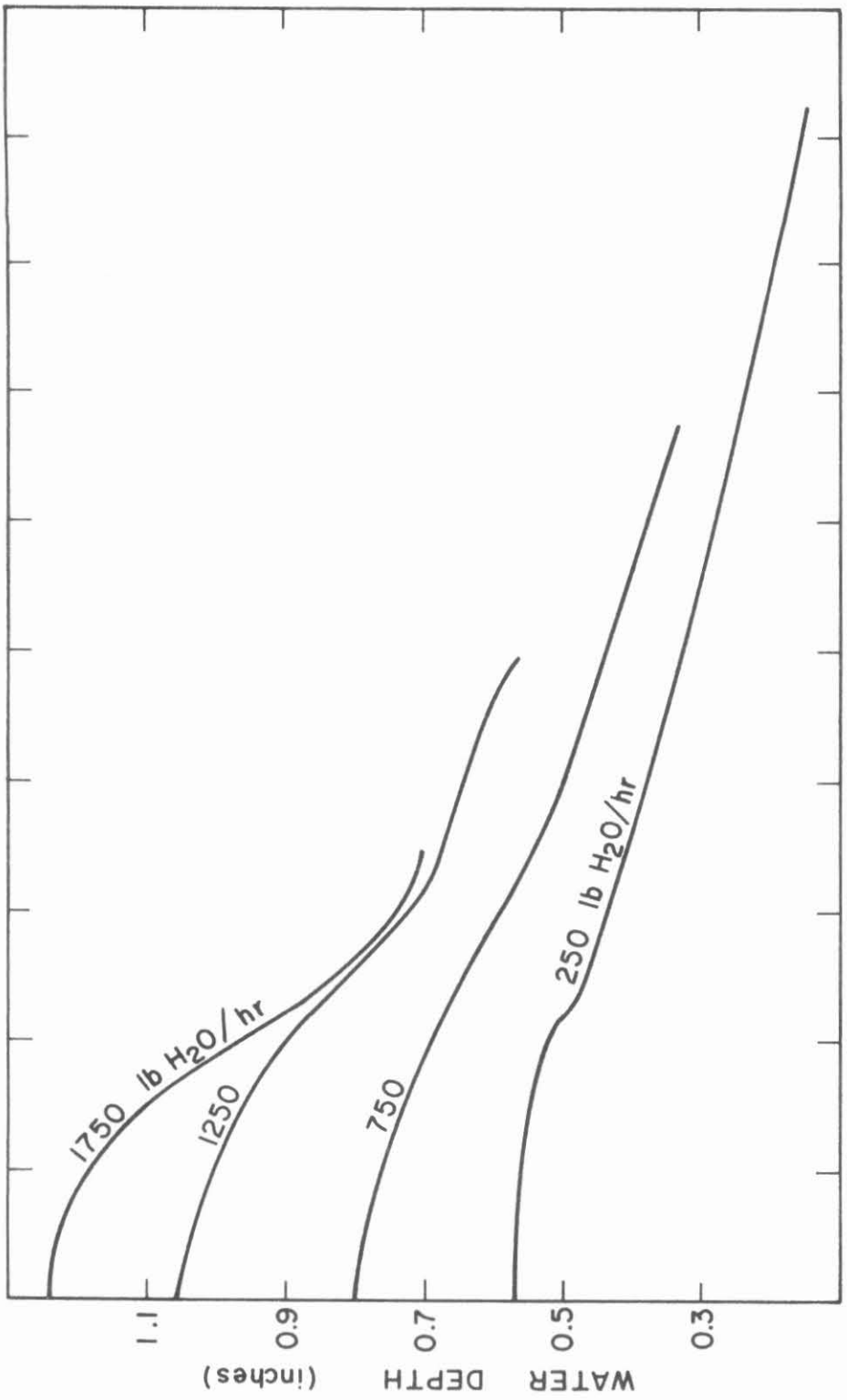

FIGURE 28. Water Depth

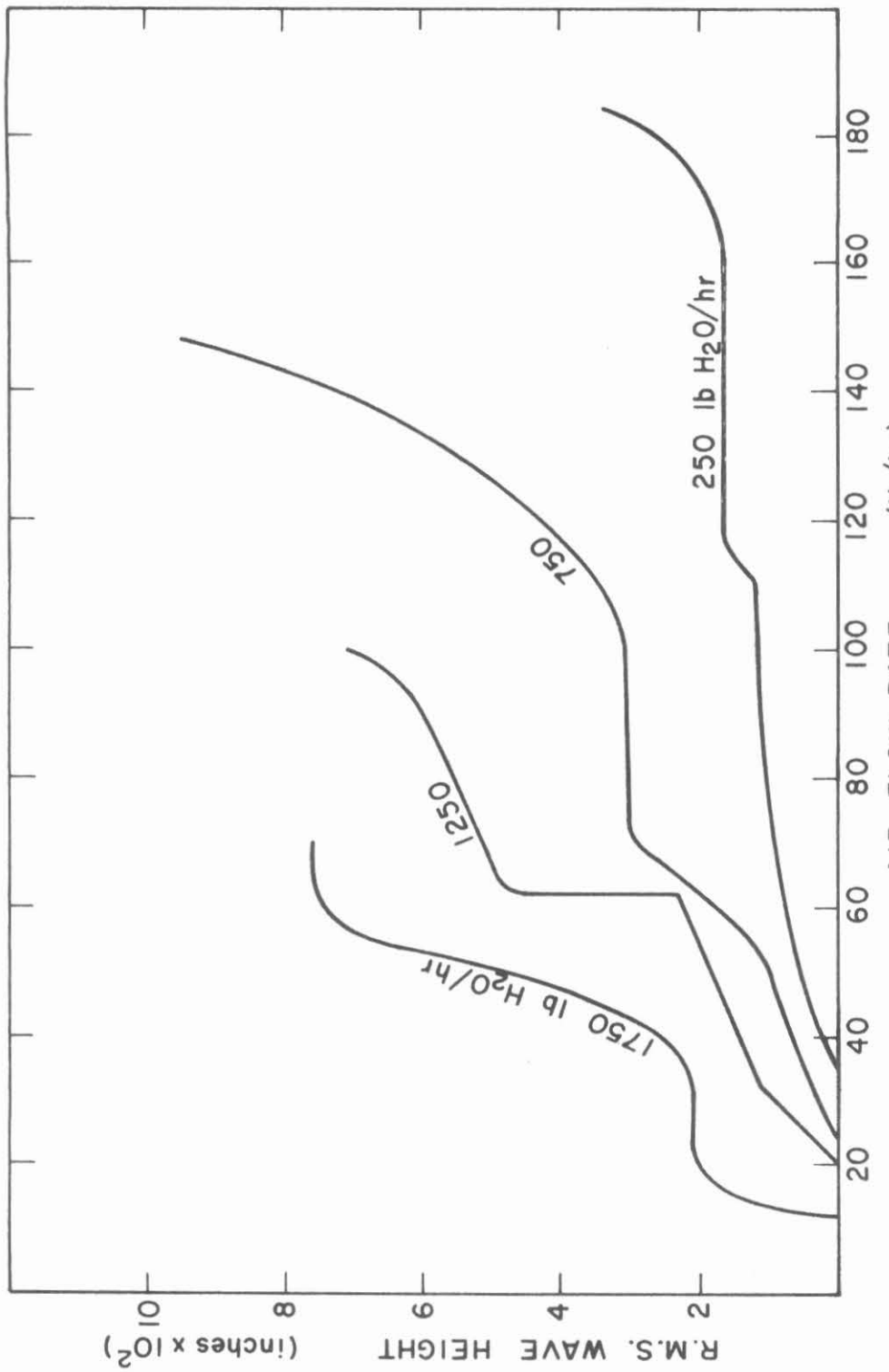

FIGURE 29. R.M.S. Wave Heights

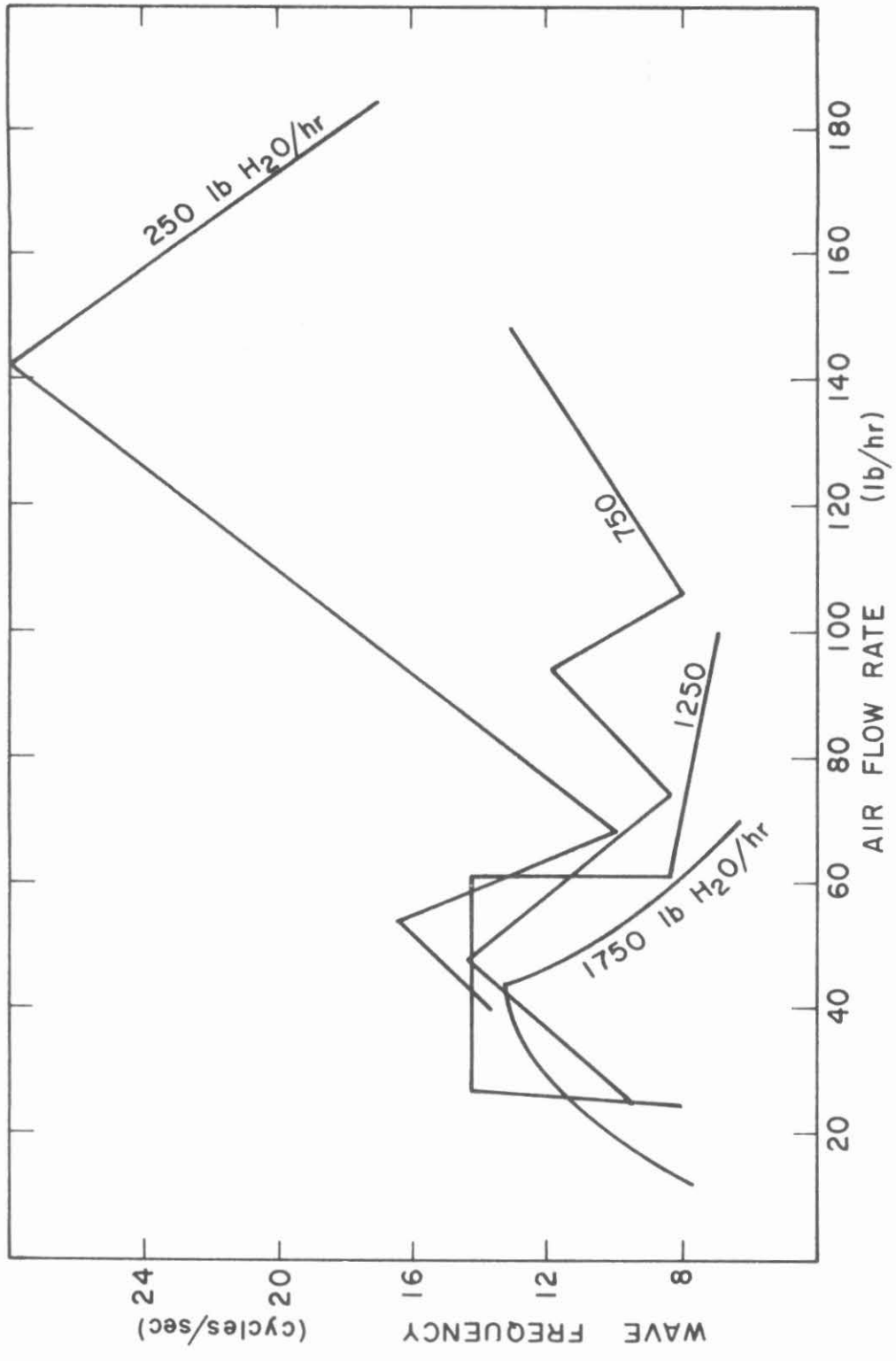

FIGURE 30. Wave Frequencies

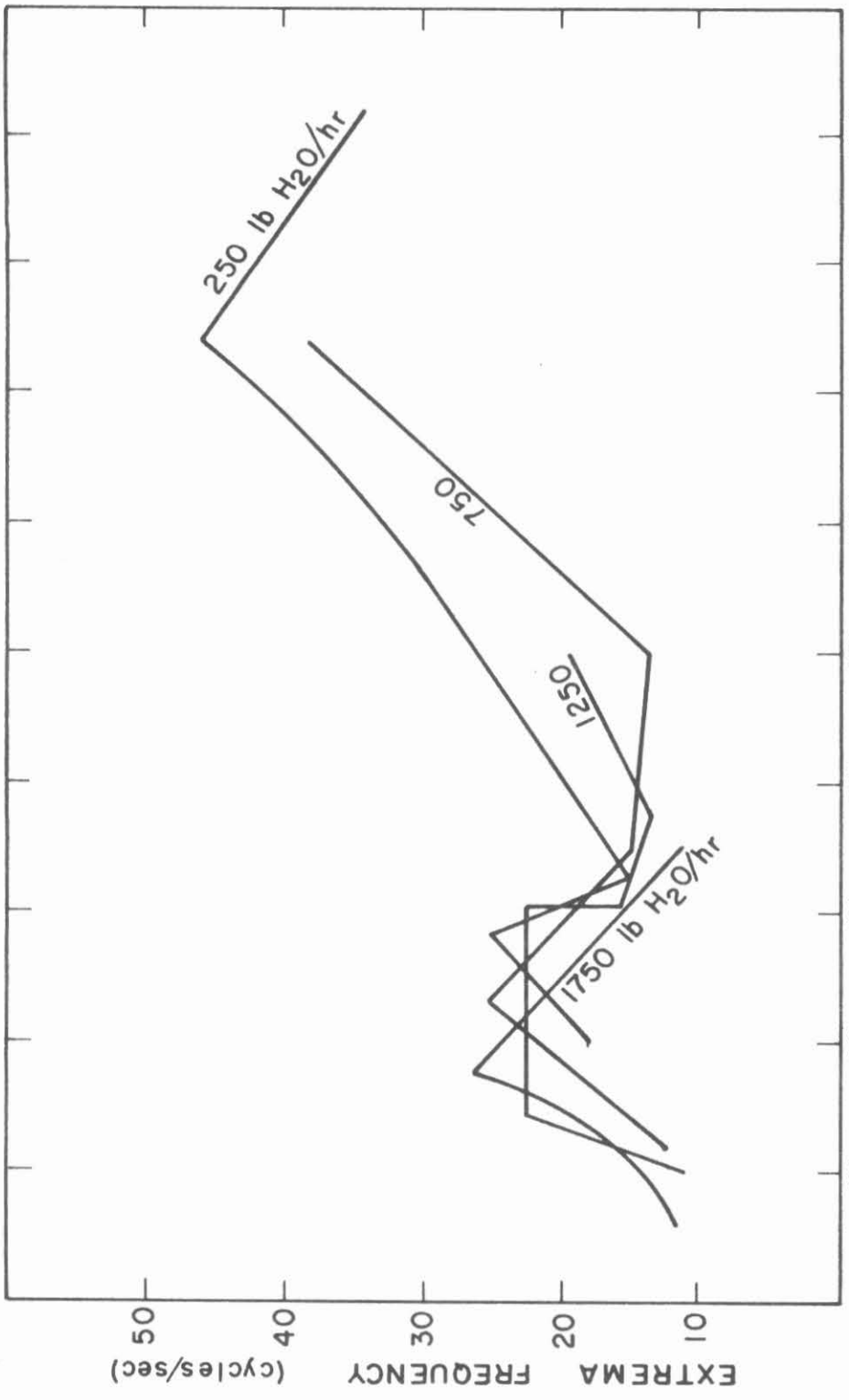

FIGURE 31. Extrema Frequencies

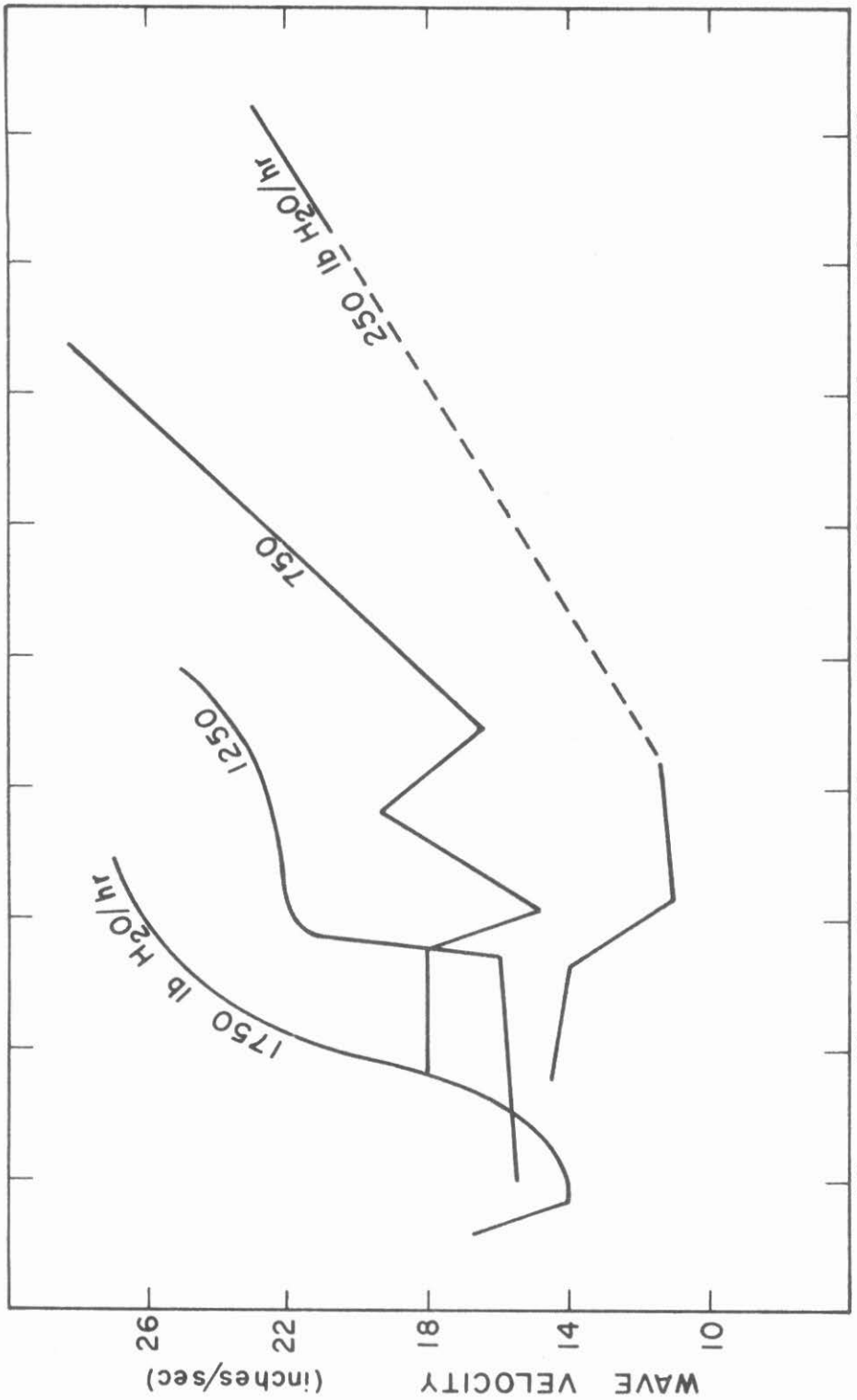

FIGURE 32. Wave Velocities

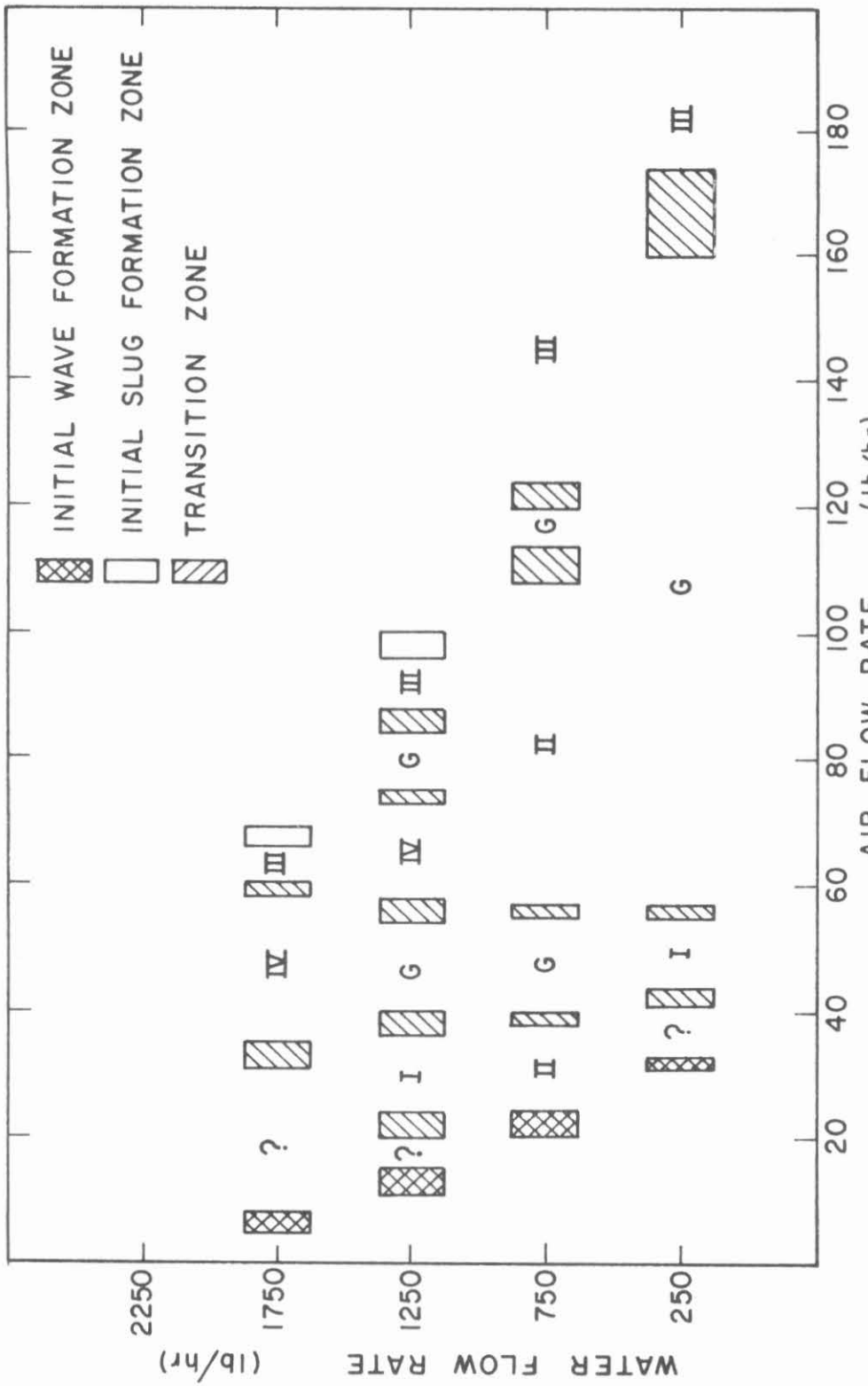

FIGURE 33. Water Surface Distributions

Table I. Comparison Data

Pressure Drop

$\dot{m}_\ell$ (lb. m/hr.)	$\dot{m}_g$ (lb. m/hr.)	$\Delta\rho$ this work $lb._f/ft.^2/ft.$	$\Delta\rho$ of reference 4 $lb._f/ft.^2/ft.$
750	29	0.011	0.0105
750	63	0.053	0.052
1500	34	0.035	0.030
1500	60	0.089	0.082
2500	35	0.072	0.065

Interfacial Height 10 feet from Free Overfall

$\dot{m}_\ell$ (lb. m/hr.)	$\dot{m}_g$ (lb. m/hr.)	$\bar{h}$ this work (inches)	$\bar{h}$ of reference 4 (inches)
250	0	0.49	0.44
250	21	0.46	0.43
250	59	0.33	0.29
250	0	0.75	0.75
750	19	0.74	0.72
750	59	0.57	0.60
1250	0	1.00	0.92
1250	23	0.94	0.88
1250	60	0.72	0.73
1750	0	1.15	1.10

Table II. Comparison with Deep Water Wave Theory

$\dot{m}_\ell$ (lb./hr.)	$\dot{m}_g$ (lb./hr.)	v_w/v_ℓ	v_w (in./sec.)	v_w from eqn. [7] (in./sec.)
250	32	5.4	15	15.5
250	180	1.5	23	10
750	22	3.5	18	18
750	150	1.5	29	11
1250	13	2.6	15	20.5
1250	100	1.9	25	15
1750	6.5	3.0	19	22
1750	70	1.9	27	16

Table III. Comparison with Predicted Film Thicknesses

$\dot{m}_\ell$ (lb./hr.)	$\dot{m}$ (lb./hr.)	$\bar{h}$ (inches)	α in eqn. [9]	θ in eqn. [8] radian/vo^5
250	32	0.54	43.8	2.87
250	180	0.14	6.06	1090
750	22	0.76	44.9	2.68
750	150	0.34	16.1	57
1250	13	1.03	53.4	1.59
1250	100	0.57	29.1	9.65
1750	6.5	1.23	58.4	1.20
1750	70	0.70	45.6	2.53

Table IV. Comparison with Predicted Wavelengths

$\dot{m}$ (lb./hr.)	$\dot{m}_g$ (lb./hr.)	λ (inches)	λ from eqn. [11] (inches)	β in eqn. [10]
250	32	1.25	0.8	3.6
250	140	0.64	0.71	1.11
250	180	1.3	0.6	0.34
750	22	2.0	0.9	3.0
750	150	2.2	0.7	1.44
1250	13	2.0	1.4	1.8
1250	100	3.5	0.6	1.87
1750	6.5	3.2	1.1	2.76
1750	70	4.5	0.8	1.87

APPENDIX A

TEMPERATURE-COMPENSATED RESISTANCE WAVE GAGE

A resistance wave gage is one of the most sensitive devices for the measurement of liquid depths and interfacial wave characteristics. One such resistance wave gage in a closed tube is shown in Figure 5 of the body of this work. The two wires are connected to a constant voltage AC power source. When a conducting liquid, such as water, is in the tube electric current will flow between the two wires through the liquid. The amount of current flowing is a function of the depth of the liquid between the wires. With the proper electronics, the relationship between current and liquid depth and/or changes in liquid depth may be determined by calibration. Then the current flowing between the wires during a test run may be recorded graphically and converted into liquid heights by use of the calibration data.

The current flowing between the wires is a function of the resistance of the liquid between the two wires. This resistance is a strong function of temperature, so resistance wave gages have been used up to now only for measurements in isothermal systems. In isothermal systems the current flowing between the wires varies only as the liquid depth varies. In nonisothermal systems, the current varies both as the liquid depth between the wires changes and as the liquid temperature in the vicinity of the wires varies. By placing two resistance wave gages into the liquid, it is possible under certain circumstances to remove the temperature dependence of the signal output of one of the wave gages.

The circuit diagram for a resistance wave gage is shown in Figure 6 of the body of this work. To remove the variations of the signal to the current recorder caused by changes in the temperature of the liquid, one inserts a modified resistance wave gage into the liquid as closely as feasible to the first. This second modified gage is shown schematically in Figure 1 of this appendix. This figure shows the circuit diagram for the temperature-compensated resistance wave gage. The use of the temperature-compensated resistance wave gage not only enables one to determine liquid depths and wave structures in a liquid with a varying temperature field, but also enables one to obtain these results when the liquid is at a temperature different from that used for the calibration of the wave gages.

The second resistance wave gage, shown schematically in Figure 1 of this appendix, must be modified somewhat from the primary gage shown in Figure 5 of the body of this work. The second gage must have the two stainless steel wires insulated throughout the gas phase to a point which is just below the liquid interface and into the liquid phase. The effect of this insulation is to prevent the resistance across the second gage from varying with the changes in liquid depth. Since this modified gage now does not notice any height changes of the liquid, its resistance varies only with the changing temperature of the liquid. The fact that the insulated portions of the two wires must extend to a point only slightly below the liquid surface limits the usefulness of this technique. When there is not a sharp temperature gradient at the

liquid surface and the total liquid depth is relatively constant, the positioning of the insulated portions of the wires relative to the interface is not critical and should be easily done. When there is a sharp temperature gradient at the interface or there is such strong wavy motion at the interface that the total depth of the liquid varies appreciably, then the positioning of the insulated portions of the wires is critical and probably will be difficult to accomplish. Because of the wide range of application of resistance wave gages, the applicability of this temperature-compensated wave gage must be determined individually for each experimental situation.

To determine the effectiveness of the temperature compensation, two resistance wave gages, each one identical to the gages discussed in the body of this work, were constructed 1/4 inch apart in a 2-inch segment of lucite tube. These gages were used with the Sanborn electronics equipment also described in the body of the work. Two tests, tests A and B, were conducted in which this test section was placed in a container of heated tap water. With only one gage connected into the circuit, the water was allowed to cool and the resultant changes in output signal from the gage recorded. By use of calibration curves, this record was analyzed to determine the apparent change in water depth caused by the change in water temperature. The results are shown in Figure 2. Next, two runs were made in an identical fashion except that now both gages were connected as is shown in Figure 1. The results of these two runs are also plotted in Figure 3. The experimental

errors are such that all but two of the points of tests A and B may be considered as lying on the line drawn through the points and all but one of the points of tests C and D may be considered as lying on the horizontal line at zero change in apparent water depth. The results show clearly that a resistance wave gage may be corrected to remove the effects of temperature change on the wave gage output signal when the liquid is at the standard calibration depth.

Although a resistance wave gage may be compensated so that changes in the temperature field of a liquid do not result in changes in the recorded signal of a wave gage (provided the height of liquid on the gage wires remains at the standard value chosen for zero indicator deffection) the wave gage calibration curve with which one converts measured currents, and hence indicator deffections, into liquid heights and height changes is a function of temperature. At any temperature, the magnitude of the change in current through a wave gage for a unit change in the depth of the liquid is directly proportional to the resistivity of the liquid at the temperature involved. Because the resistivity of a liquid is a function of temperature, the magnitude of the current change, and hence the magnitude of the deflection of the current recorder indicator, per unit height change is a function of temperature. For tap water, Figure 3 illustrates the sensitivity of a wave gage as a function of the water temperature. Because of this effect, accurate measure-

compensated resistance wave gages does necessitate knowing how the resistivity of the liquid changes with temperature and what the recorder indicator deflection is per unit height change of liquid at the temperature of the liquid.

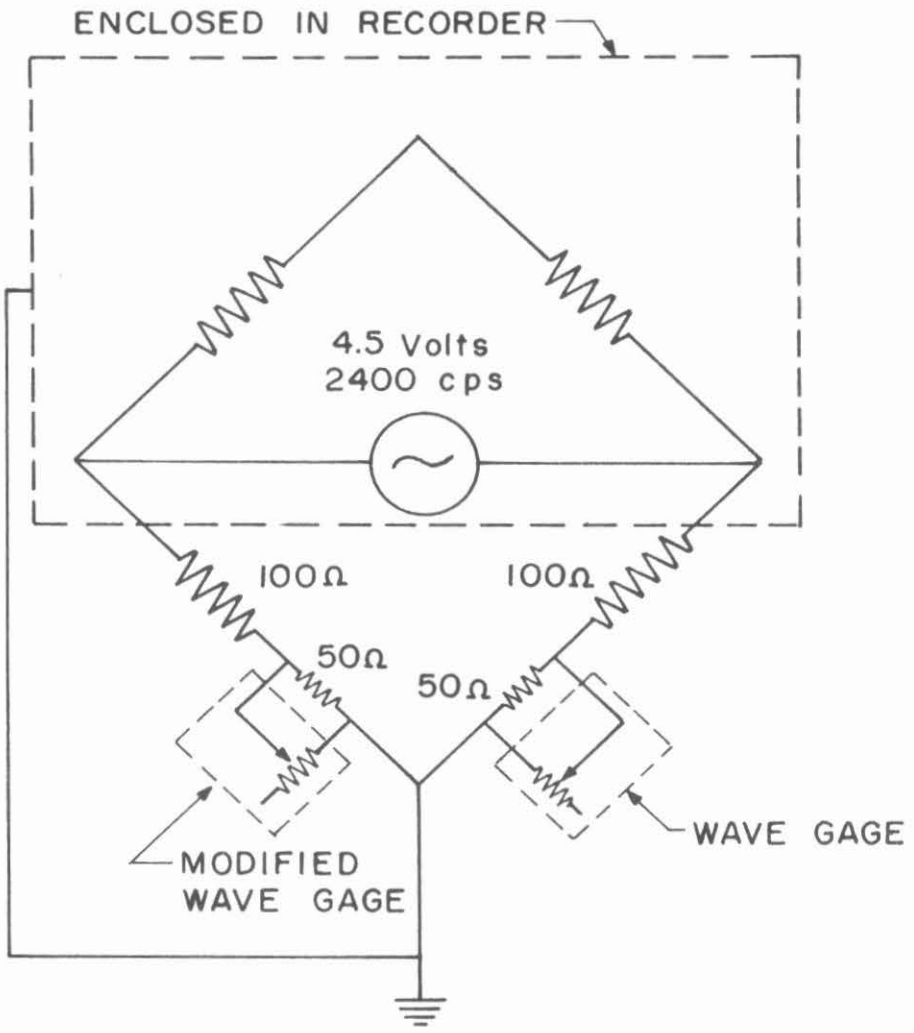

FIGURE 1. Temperature-Compensated Wave Gage Circuit Diagram

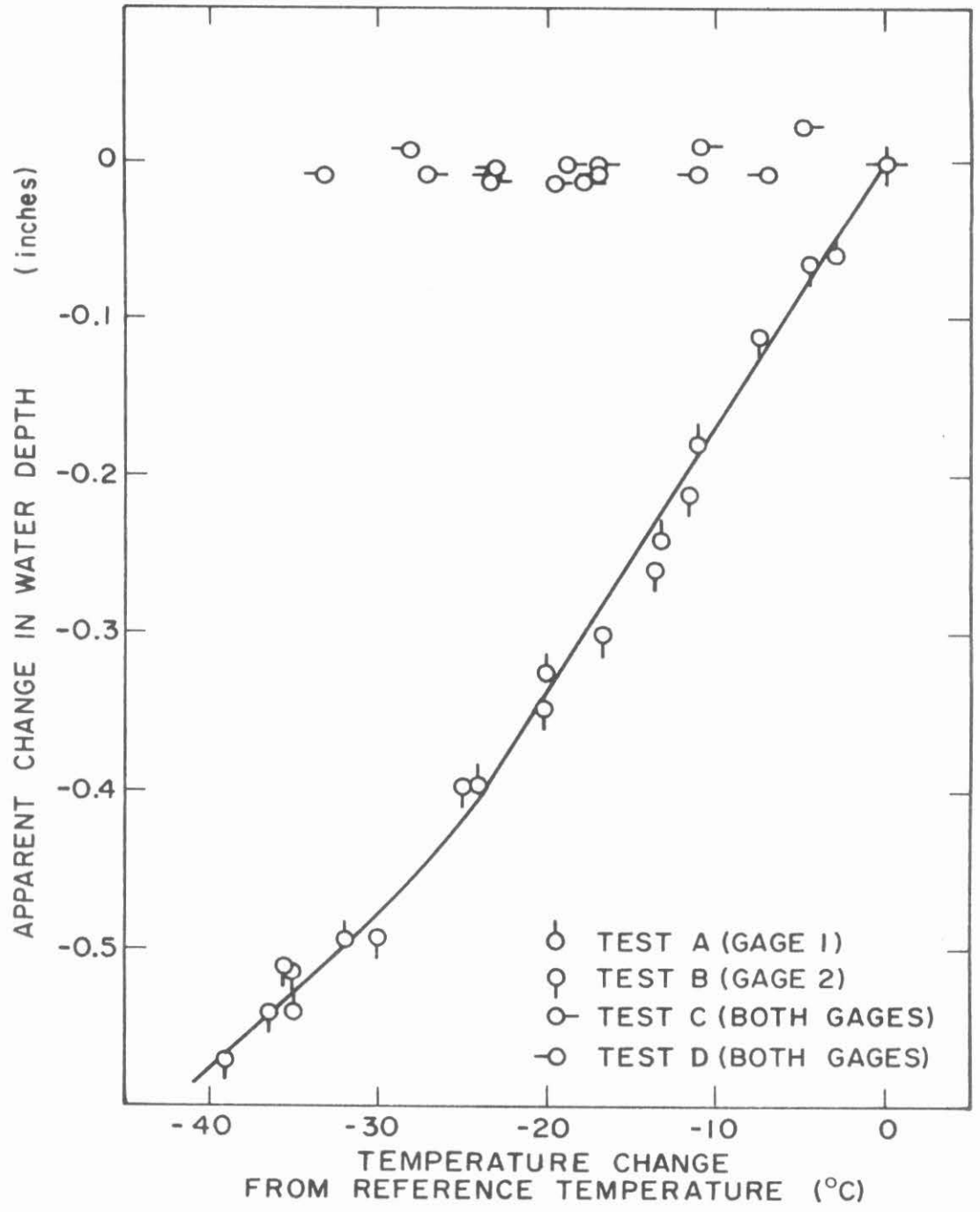

FIGURE 2. Apparent Water Depth Variation as Water Temperature Changes

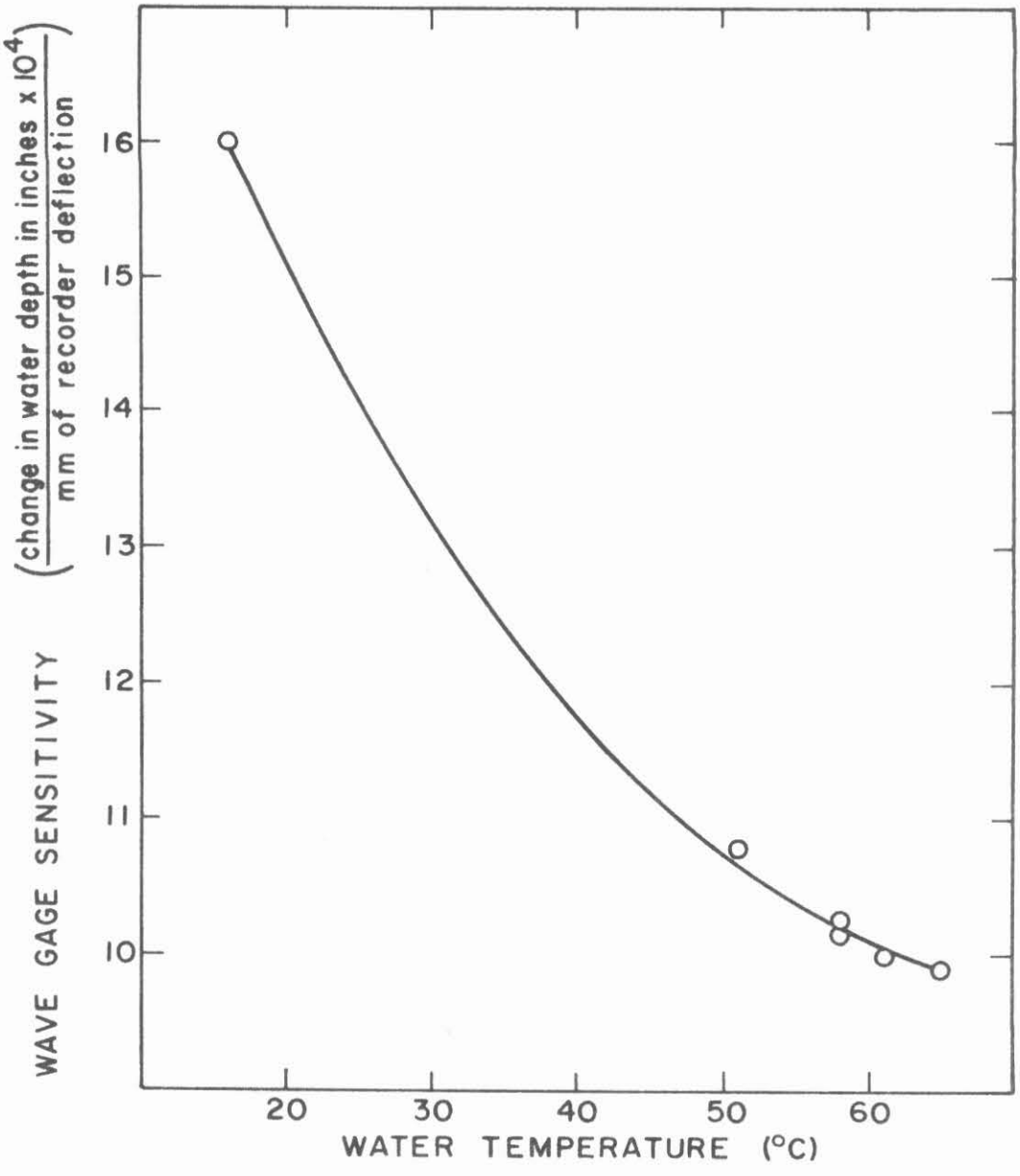

FIGURE 3. Water Temperature Effects on Wave Gage Calibration

APPENDIX B

EXPERIMENTAL DATA

The following five tables present the numerical values for all the experimental data obtained in this work.

The Reynolds numbers for water and air were calculated based upon the cross-sectional area of the phase of interest, not based upon the cross-sectional area of the lucite tubes. The results for wave type refer to the type of interfacial structure. Figure 1 of the body of this work labels the types of interfacial structure which are of interest to this work. "G" refers to the Gaussian distribution.

TABLE I. EXPERIMENTAL DATA IN WAVY FLOW

RUN #	$\dot{m}_\ell$ (lb/hr)	$\dot{m}_g$ (lb/hr)	$\bar{h}$ (inches)	Δh (inches)	$\Delta h/\bar{h}$	f_o cycles/sec	f_1 cycles/sec	c
4	250	42.7	0.57	0.00175	0.0032	12.6	17.6	-0.72
4	250	56.5	0.50	0.0091	0.0182	10.6	16.1	-0.66
4	250	70.0	0.45	-	-	10.0	16.6	-0.60
4	250	82.5	0.40	0.0105	0.0213	12.8	19.3	-0.67
5	250	63.0	0.44	0.0082	0.0186	9.7	13.6	-0.71
5	250	63.0	0.44	0.0082	0.0186	11.5	17.2	-0.67
5	250	79.5	0.39	0.0098	0.0252	14.0	20.6	-0.775
5	250	110.0	0.31	0.0116	0.0375	17.9	27.2	-0.655
5	250	113.0	0.30	0.0136	0.045	17.2	26.9	-0.64
5	250	118.0	0.30	0.0164	0.055	23.6	35.2	-0.67
5	250	136.0	0.25	0.0162	0.065	27.3	40.5	-0.70
5	250	157.0	0.20	0.0158	0.079	23.8	39.0	-0.61
5	250	175.0	0.19	0.0211	0.112	18.8	33.1	-0.57
7	250	49.5	0.49	0.0046	0.0091	14.0	22.3	-0.63
7	250	55.2	0.47	0.0084	0.0179	15.0	22.2	-0.67
8	250	36.0	0.44	0.0004	0.0009	12.7	17.1	-0.74
8	250	36.0	0.44	0.0007	0.0015	17.1	19.1	-0.895
8	250	48.5	0.44	0.0040	0.0092	16.9	19.3	-0.88
8	250	50.0	0.44	0.0037	0.0085	17.7	21.0	-0.84
8	250	55.7	0.44	0.0096	0.0218	19.2	25.2	-0.76
8	250	55.7	0.44	0.0086	0.0196	16.7	24.5	-0.68
17	250	40.6	0.47	0.0031	0.0066	17.9	24.9	-0.72
17	250	45.3	0.46	0.0034	0.0074	11.75	18.45	-0.64
17	250	51.5	0.44	0.0066	0.0150	15.8	25.8	-0.61
17	250	59.5	0.42	0.0063	0.0150	14.35	24.2	-0.595
17	250	66.0	0.38	0.0057	0.0151	14.4	24.9	-0.58
17	250	101.0	0.30	0.0110	0.0367	19.5	28.2	-0.69
17	250	128.0	0.26	0.016	0.0615	24.1	35.8	-0.68
17	250	147.0	0.21	0.0168	0.080	26.3	45.2	-0.58
17	250	166.0	0.17	0.0174	0.102	22.5	41.9	-0.54

RUN #	$\dot{m}_\ell$ (lb/hr)	$\dot{m}_g$ (lb/hr)	$\bar{h}$ (inches)	Δh (inches)	$\Delta h/\bar{h}$	f_o cycles/ sec	f_1 cycles/ sec	c
17	250	184.0	0.15	0.034	0.227	17.3	42.5	-0.41
18	250	41.0	0.49	0.0025	0.0051	14.4	18.4	-0.78
18	250	46.0	0.49	0.0051	0.0104	16.0	23.4	-0.69
18	250	52.0	0.46	0.0058	0.0126	15.0	23.7	-0.64
18	250	58.0	0.44	0.0066	0.0150	13.5	21.8	-0.62
18	250	66.5	0.40	0.0073	0.0183	13.4	20.9	-0.64
9	750	55.0	0.55	0.0118	0.0215	14.3	21.7	-0.66
9	750	55.7	0.55	0.0119	0.0217	13.2	23.6	-0.56
9	750	60.3	0.53	0.0169	0.032	11.4	18.3	-0.62
10	750	25.0	0.77	0.0005	0.0007	8.2	11.15	-0.73
10	750	37.5	0.72	0.00745	0.0104	13.15	20.2	-0.65
10	750	46.2	0.68	0.0084	0.0124	13.2	23.1	-0.57
10	750	55.7	0.63	0.0122	0.0194	12.0	20.1	-0.60
10	750	61.0	0.60	0.0160	0.0267	11.8	19.0	-0.62
10	750	64.0	0.58	0.0222	0.0383	9.23	17.1	-0.54
10	750	72.5	0.55	0.0316	0.0575	8.03	13.6	-0.59
10	750	79.0	0.52	0.0302	0.058	11.1	15.2	-0.73
10	750	81.0	0.50	0.024	0.048	8.7	15.2	-0.575
10	750	99.0	0.43	0.032	0.075	9.05	14.3	-0.63
10	750	100.0	0.43	0.032	0.075	8.05	12.9	-0.62
10	750	125.0	0.38	0.056	0.147	8.55	25.2	-0.34
10	750	148.0	0.30	0.093	0.310	11.6	33.7	-0.35
11	750	25.5	0.75	0.0015	0.0019	11.1	14.1	-0.79
11	750	39.8	0.72	0.0066	0.0092	14.4	22.6	-0.635
11	750	48.0	0.68	0.0074	0.0109	14.3	22.7	-0.63
11	750	68.0	0.53	0.0276	0.052	9.04	15.2	-0.595
11	750	75.5	0.51	0.030	0.059	8.9	15.55	-0.57
11	750	77.0	0.49	0.033	0.0675	8.3	12.75	-0.65
11	750	86.0	0.49	0.033	0.068	10.3	15.0	-0.685
11	750	93.0	0.50	0.031	0.062	12.3	15.8	-0.78
11	750	106.0	0.44	0.028	0.0636	9.94	15.5	-0.64
11	750	116.0	0.40	0.037	0.0925	10.1	25.4	-0.40

RUN #	$\dot{m}_\ell$ (lb/hr)	$\dot{m}_g$ (lb/hr)	$\overline{h}$ (inches)	Δh (inches)	$\Delta h/\overline{h}$	f_o cycles/sec	f_1 cycles/sec	c
11	750	133.0	0.32	0.050	0.156	12.5	28.7	-0.435
11	750	133.0	0.34	0.062	0.183	11.0	27.9	-0.40
17	750	130.0	0.35	0.0465	0.133	12.95	33.8	-0.38
12	1250	22.0	1.00	0.0021	0.0021	8.9	13.7	-0.65
12	1250	22.0	1.00	0.0012	0.0012	7.0	11.9	-0.59
12	1250	23.6	1.00	0.0044	0.0044	11.6	16.45	-0.70
12	1250	26.8	0.99	0.0050	0.0051	12.0	20.4	-0.59
12	1250	32.0	0.93	0.0110	0.0118	13.1	20.9	-0.63
12	1250	32.0	0.93	0.0127	0.0136	13.6	20.6	-0.66
12	1250	41.0	0.89	0.0139	0.0156	13.7	24.5	-0.57
12	1250	41.5	0.88	0.0136	0.0155	11.2	20.7	-0.54
12	1250	47.5	0.82	0.0172	0.021	14.5	22.1	-0.66
12	1250	47.5	0.82	0.0190	0.023	15.35	22.1	-0.695
12	1250	54.3	0.77	0.0190	0.025	14.5	22.9	-0.63
12	1250	59.5	0.71	0.041	0.058	11.3	19.3	-0.57
12	1250	59.5	0 71	0.044	0.062	9.85	17.3	-0.57
12	1250	62.5	0.72	0.043	0.060	9.9	15.7	-0.63
12	1250	66.0	0.67	0.052	0.078	8.05	14.65	-0.55
12	1250	72.5	0.67	0.0535	0.080	7.45	13.5	-0.55
12	1250	78.5	0.64	0.0585	0.0915	7.6	12.6	-0.61
12	1250	82.0	0.64	0.055	0.102	8.0	14.3	-0.56
12	1250	97.5	0.54	0.067	0.124	6.4	20.9	-0.30
12	1250	99.0	0.58	0.073	0.125	4.2	17.75	-0.24
12	1250	99.0	0.57	0.068	0.119	7.6	17.55	-0.43
13	1250	30.5	0.97	0.0083	0.0086	15.4	25.5	-0.605
13	1250	40.2	0.91	0.0143	0.0158	15.15	23.7	-0.64
13	1250	49.5	0.84	0.0193	0.023	13.9	21.8	-0.64
13	1250	59.5	0.72	0.046	0.0635	8.9	16.7	-0.53
13	1250	62.5	0.70	0.035	0.0505	12.3	21.2	-0.58
13	1250	62.5	0.70	0.029	0.041	14.1	23.6	-0.60
13	1250	63.5	0.70	0.050	0.071	8.7	17.3	-0.505
13	1250	64.5	0.71	0.054	0.076	7.9	13.5	-0.585

RUN #	$\dot{m}_\ell$ (lb/hr)	$\dot{m}_g$ (lb/hr)	$\bar{h}$ (inches)	Δh (inches)	$\Delta h/\bar{h}$	f_o cycles/ sec	f_1 cycles/ sec	c
13	1250	75.0	0.68	0.057	0.0835	8.6	16.1	-0.53
13	1250	78.5	0.66	0.056	0.0855	7.4	14.6	-0.51
13	1250	81.0	0.63	0.0525	0.0834	7.9	14.1	-0.56
16	1750	11.7	1.22	0.005	0.004	7.75	12.6	-0.61
16	1750	17.7	1.19	0.021	0.018	9.7	12.6	-0.77
16	1750	23.7	1.15	0.024	0.021	10.9	14.9	-0.73
16	1750	24.0	1.15	0.024	0.021	10.6	16.1	-0.66
16	1750	35.2	1.02	0.020	0.0195	13.0	26.2	-0.50
16	1750	44.3	0.90	0.029	0.032	13.1	23.4	-0.56
16	1750	52.5	0.79	0.059	0.074	9.7	19.1	-0.51
16	1750	59.5	0.75	0.074	0.099	4.9	9.4	-0.32
16	1750	59.5	0.75	0.079	0.105	7.05	14.7	-0.48
16	1750	65.0	0.69	0.074	0.107	8.6	15.9	-0.54
16	1750	69.0	0.66	0.074	0.112	6.9	14.6	-0.47
18	1750	60.0	0.76	0.072	0.095	7.0	13.6	-0.515
18	1750	66.0	0.74	0.078	0.105	6.7	13.1	-0.515

TABLE II. EXPERIMENTAL DATA IN WAVY FLOW

RUN #	$\dot{m}_\ell$ (lb/hr)	$\dot{m}_g$ (lb/hr)	Re_ℓ	Re_g	$\overline{v}_\ell$ (inches/sec)	$\overline{v}_g$ (inches/sec)	v_w (inches/sec)	Wave Type
4	250	42.7	1270	7970	2.74	113	16.0	I
4	250	56.5	1326	10440	3.14	145	13.5	G
4	250	70.0	1391	12810	3.64	173	11.2	G
4	250	82.5	1469	15000	4.31	198	11.4	G
5	250	63.0	1406	11500	3.76	155	11.1	G
5	250	63.0	1406	11500	3.76	155	-	G
5	250	79.5	1486	14400	4.46	190	11.2	I
5	250	110.0	1655	19680	6.21	251	-	G
5	250	113.0	1681	20200	6.52	257	-	-
5	250	118.0	1681	21090	6.52	268	-	G
5	250	136.0	1833	24100	8.49	301	-	G
5	250	157.0	2040	27700	11.8	341	-	G
5	250	175.0	2090	30900	12.7	378	-	III
7	250	49.5	1338	9130	3.23	126	13.9	I
7	250	55.2	1364	10140	3.42	138	13.1	G
8	250	36.0	1406	8220	3.76	111	14.7	I
8	250	36.0	1406	8220	3.76	111	14.6	I
8	250	48.5	1406	8860	3.76	119	13.9	I
8	250	50.0	1406	9130	3.76	123	14.2	I
8	250	55.7	1406	10180	3.76	137	12.6	I
8	250	55.7	1410	10180	3.76	137	-	I
17	250	40.6	1360	7460	3.42	102	14.2	I
17	250	45.3	1380	8310	3.53	113	14.0	II
17	250	51.5	1410	9410	3.76	127	13.8	I
17	250	59.5	1440	10830	4.02	145	11.8	I
17	250	66.0	1500	11940	4.63	156	-	G
17	250	101.0	1680	18050	6.52	229	-	G
17	250	128.0	1800	22750	8.02	285	-	G

RUN #	$\dot{m}_\ell$ (lb/hr)	$\dot{m}_g$ (lb/hr)	Re_ℓ	Re_g	$\overline{v}_\ell$ (inches/sec)	$\overline{v}_g$ (inches/sec)	v_w (inches/sec)	Wave Type
17	250	147.0	1990	25970	11.0	320	-	G
17	250	166.0	2210	29210	14.9	356	21.0	G
17	250	184.0	2350	32320	18.0	392	22.7	III
18	250	41.0	1340	7560	3.23	104	13.5	I
18	250	46.0	1340	8480	3.23	117	13.9	I
18	250	52.0	1340	9530	3.53	130	14.0	II
18	250	58.0	1410	10600	3.76	143	14.1	II
18	250	66.5	1470	12060	4.31	160	11.1	I
9	750	55.0	3810	10300	8.23	146	18.0	G
9	750	55.7	3810	10400	8.23	148	18.3	I
9	750	60.3	3880	11200	8.67	158	15.1	G
10	750	25.0	3290	4925	5.18	80	-	II
10	750	37.5	3390	7290	5.68	114	17.3	II
10	750	46.2	3470	8880	6.14	136	18.9	G
10	750	55.7	3590	10580	6.81	157	17.8	G
10	750	61.0	3670	11510	7.29	168	14.7	II
10	750	64.0	3720	12020	7.64	174	14.7	II
10	750	72.5	3810	13530	8.23	192	18.0	II
10	750	79.0	3910	14650	8.90	205	18.3	II
10	750	81.0	3980	15000	9.41	207	19.2	II
10	750	99.0	4260	18100	11.7	242	16.0	II
10	750	100.0	4260	18200	11.7	244	16.2	G
10	750	125.0	4510	22600	13.9	296	23.2	II
10	750	148.0	5040	26500	19.6	336	27.7	II
11	750	25.5	3330	5000	5.37	79.8	-	G
11	750	39.8	3390	7730	5.68	121	17.5	G
11	750	48.0	3470	9230	6.14	141	17.7	G
11	750	68.0	3880	12640	8.67	178	18.9	II
11	750	75.5	3940	13970	9.15	195	19.6	G
11	750	77.0	4020	14200	9.7	196	19.2	G
11	750	86.0	4020	15860	9.7	219	16.5	G

RUN #	$\dot{m}_\ell$ (lb/hr)	$\dot{m}_g$ (lb/hr)	Re_ℓ	Re_g	$\overline{v}_\ell$ (inches/sec)	$\overline{v}_g$ (inches/sec)	v_w (inches/sec)	Wave Type
11	750	93.0	3980	17180	9.4	238	20.2	II
11	750	106.0	4220	19360	11.3	261	20.0	II
11	750	116.0	4410	21140	12.9	280	21.4	G
11	750	133.0	4890	23990	17.8	306	24.6	III
11	750	133.0	4750	23990	16.3	310	25.2	III
17	750	130.0	4690	23400	15.7	303	25.8	III
12	1250	22.0	4940	4680	6.14	91.5	-	G
12	1250	22.0	4940	4680	6.14	91.5	-	G
12	1250	23.6	4940	5020	6.14	98.1	15.6	I
12	1250	26.8	4950	5680	6.21	109	15.6	I
12	1250	32.0	5080	6630	6.73	121	15.6	I
12	1250	32.0	5080	6630	6.73	121	15.6	I
12	1250	41.0	5170	8380	7.13	148	15.8	G
12	1250	41.5	5190	8460	7.24	148	15.8	G
12	1250	47.5	5340	9500	7.94	159	16.2	G
12	1250	47.5	5340	9500	7.94	159	16.4	G
12	1250	54.3	5490	10700	8.64	173	15.8	G
12	1250	59.5	5680	11530	9.64	180	21.5	IV
12	1250	59.5	5680	11530	9.64	180	21.4	IV
12	1250	62.5	5650	12140	9.46	190	21.8	IV
12	1250	66.0	5820	12660	10.4	192	22.2	IV
12	1250	72.5	5820	13910	10.4	211	21.9	IV
12	1250	78.5	5940	14950	11.1	233	22.5	G
12	1250	82.0	5940	15620	11.1	233	22.7	G
12	1250	97.5	6400	18160	14.1	257	25.0	III
12	1250	99.0	6200	18600	12.7	268	25.2	III
12	1250	99.0	6250	18600	13.0	266	25.2	III
13	1250	30.5	4990	6420	6.38	121	15.8	I
13	1250	40.2	5120	8280	6.93	149	15.8	G
13	1250	49.5	5290	9960	7.69	169	16.2	G

RUN #	$\dot{m}_\ell$ (lb/hr)	$\dot{m}_g$ (lb/hr)	Re_ℓ	Re_g	$\bar{v}_\ell$ (inches/sec)	$\bar{v}_g$ (inches/sec)	v_w (inches/sec)	Wave Type
13	1250	59.5	5650	11560	9.46	181	22.2	IV
13	1250	62.5	5710	12080	9.83	187	21.8	III
13	1250	62.5	5710	12080	9.83	187	21.3	III
13	1250	63.5	5710	12270	9.83	190	21.3	IV
13	1250	64.5	5680	12500	9.64	195	22.7	IV
13	1250	75.0	5790	14400	10.2	221	22.7	G
13	1250	78.5	5860	15020	10.7	227	22.7	III
13	1250	81.0	5980	15390	11.4	228	22.5	G
16	1750	11.7	6420	2750	6.72	67	16.9	III
16	1750	17.7	6470	4100	6.92	96	14.0	G
16	1750	23.7	6550	5380	7.21	121	14.4	V
16	1750	24.0	6550	5450	7.21	122	14.2	V
16	1750	35.2	6860	7550	8.37	149	17.4	IV
16	1750	44.3	7200	9090	9.84	162	22.7	IV
16	1750	52.5	7600	10400	11.7	170	24.7	IV
16	1750	59.5	7770	11660	12.5	186	25.2	IV
16	1750	59.5	7770	11660	12.5	186	25.2	IV
16	1750	65.0	8050	12530	14.0	193	25.8	III
16	1750	69.0	8210	13200	14.9	199	26.1	III
18	1750	60.0	7720	11790	12.3	190	26.4	III
18	1750	66.0	7810	12890	12.8	205	27.8	III

TABLE III. EXPERIMENTAL DATA FOR LOW AIR FLOW RATES

RUN #	$\dot{m}_\ell$ (lb/hr)	$\dot{m}_g$ (lb/hr)	$\overline{h}$ (inches)	Re_ℓ	Re_g	$\overline{v}_\ell$ (in./sec)	$\overline{v}_g$ (in./sec)	Waves Present?
4	250	0	0.59	1230	0	2.49	0	No
4	250	0	0.59	1230	0	2.49	0	No
4	250	0	0.60	1220	0	2.43	0	No
4	250	0	0.62	1210	0	2.32	0	No
4	250	17.3	0.57	1250	3240	2.61	46.5	No
4	250	21.7	0.57	1250	4070	2.61	58.4	Yes
4	250	23.6	0.57	1250	4420	2.61	63.5	Yes
4	250	31.0	0.57	1250	5810	2.61	83.4	Yes
4	250	38.4	0.56	1260	7180	2.68	102.5	Yes
5	250	0	0.59	1230	0	2.49	0	No
5	250	0	0.59	1230	0	2.49	0	No
5	250	0	0.59	1230	0	2.49	0	No
5	250	9.7	0.59	1230	1830	2.49	26.5	No
5	250	14.8	0.58	1240	2780	2.55	40.1	No
5	250	18.0	0.58	1240	3380	2.55	48.8	Yes
5	250	21.4	0.57	1250	4010	2.61	57.6	Yes
5	250	23.0	0.57	1250	4310	2.61	61.9	Yes
5	250	31.6	0.54	1280	5890	2.81	83.1	Yes
7	250	0	0.58	1240	0	2.55	0	No
7	250	0	0.58	1240	0	2.55	0	No
7	250	0	0.58	1240	0	2.55	0	No
7	250	0	0.58	1240	0	2.55	0	No
7	250	16.3	0.55	1270	3040	2.74	43.2	No
7	250	20.2	0.55	1270	3770	2.74	53.5	Yes
7	250	27.0	0.54	1280	5030	2.81	71.0	Yes
7	250	34.2	0.51	1310	6330	3.05	88.1	Yes
7	250	35.6	0.50	1330	6580	3.14	91.1	Yes

RUN #	$\dot{m}_\ell$ (lb/hr)	$\dot{m}_g$ (lb/hr)	$\bar{h}$ (inches)	Re_ℓ	Re_g	$\bar{v}_\ell$ (in./sec)	$\bar{v}_g$ (in./sec)	Waves?
8	250	0	0.53	1290	0	2.89	0	No
8	250	0	0.55	1270	0	2.74	0	No
17	250	0	0.54	1280	0	2.81	0	No
17	250	0	0.53	1290	0	2.89	0	No
18	250	0	0.57	1250	0	2.61	0	No
18	250	0	0.56	1260	0	2.68	0	No
18	250	0	0.56	1260	0	2.68	0	No
9	750	0	0.75	3330	0	5.37	0	No
9	750	0	0.74	3350	0	5.47	0	No
9	750	11.6	0.73	3370	2260	5.57	35.7	No
9	750	17.0	0.73	3370	3310	5.57	52.2	No
9	750	24.0	0.71	3410	4650	5.79	72.4	Yes
9	750	26.9	0.71	3410	5210	5.79	81.2	Yes
10	750	0	0.79	3250	0	5.01	0	No
10	750	0	0.79	3260	0	5.01	0	No
10	750	0	0.81	3220	0	4.84	0	No
10	750	22.0	0.76	3310	4320	5.28	69.5	Yes
11	750	0	0.81	3220	0	4.84	0	No
11	750	0	0.81	3220	0	4.84	0	No
11	750	0	0.82	3210	0	4.77	0	No
17	750	0	0.84	3180	0	4.62	0	No
12	1250	0	1.05	4840	0	5.77	0	No
12	1250	0	1.05	4840	0	5.77	0	No
12	1250	17.7	1.01	4920	3780	6.06	73.8	Yes
13	1250	0	1.04	4860	0	5.84	0	No
13	1250	0	1.06	4830	0	5.70	0	No
16	1250	0	1.07	4810	0	5.63	0	No
16	1750	0	1.24	6380	0	6.59	0	No
16	1750	0	1.23	6400	0	6.66	0	No
16	1750	6.5	1.23	6400	1540	6.66	37.7	-

TABLE IV. EXPERIMENTAL DATA FOR WAVE FORMATION

$\dot{m}_\ell$ (lb/hr)	$\dot{m}_g$ (lb/hr)	$\bar{h}$ (inches)	Re_ℓ	Re_g	Fr_ℓ	We_ℓ	$\bar{v}_\ell$ (inches/sec)	$\bar{v}_g$ (inches/sec)
250	32	0.54	1250	5980	0.0371	1.80	2.78	84
750	22	0.76	3230	4320	0.0951	2.87	5.28	70
1250	13.5	1.03	4760	2900	0.0890	2.79	5.95	58
1750	6.5	1.23	6220	1540	0.0915	2.83	6.60	39

TABLE V. AIR FLOW RATES AT WHICH VISUAL WAVE TYPES OCCUR

$\dot{m}_{\ell}$ (lb/hr)	Visual Type A (lb.air/hour)	Visual Type B (lb.air/hour)	Visual Type C (lb.air/hour)
250	32 - 42	42 - 70	70 - 184
750	22 - 56	56 - 110	110 - 148
1250	$13\frac{1}{2}$ - 58	58 - 86	86 - 99
1750	None	$6\frac{1}{2}$ - 70	None

PART III

THE ARTIFICIAL KIDNEY FOR TEACHING ENGINEERING PRINCIPLES

THE ARTIFICIAL KIDNEY
for Teaching Engineering Principles

MALCOLM C. MORRISON and **WILLIAM H. CORCORAN**, Division of Chemistry and Chemical Engineering, California Institute of Technology, and **MILTON E. RUBINI**, Wadsworth Veterans Hospital and the University of California at Los Angeles

IN THE SECOND QUARTER of their sophomore year at Caltech, chemical engineering students take their first introductory course in engineering, a course open to all other scientists and engineers. This one-term course of ten weeks traditionally has introduced concepts such as mass and energy balances, chemical equilibrium, and chemical kinetics through problems in new technological development, such as fuel cells, saline-water conversion, and fluidized catalytic cracking. In 1966-67, the course was based entirely on hemodialysis and artificial kidneys. This new framework not only significantly improved the continuity of the course but allowed a logical presentation of the concepts previously treated, as well as the presentation of many other worthwhile principles.

Organization of the Course

Because the course was introductory, all aspects of hemodialysis—engineering, medical, biological, and economic—were presented. Less time, therefore, was devoted to the teaching of engineering concepts, but the value of the course as a whole was enhanced. Somewhat more than one-third of the three class hours per week was devoted to instruction by a chemical engineering faculty member on basic principles of thermodynamics, chemical equilibrium, and transport phenomena. These principles, including their use in mathematical models, were applied to the problem of the treatment of kidney failure. Another one-third of the class hours was devoted to lectures by medical and professional people working in the field. Topics included renal function and failure; the design and function of necessary equipment for dialysis; sociologic, medical, and economic problems of home and institutional dialysis; and treatments for renal failure which involve primarily medical problems. The remainder of the class time was spent on field trips to hospitals and to a manufacturing company to acquaint the students with current development of treatments for kidney failure and to illustrate application of the information presented.

Homework for the first two weeks consisted of reading in three texts (Refs. 1, 2, 4), to acquaint the students with kidney function and with medical terminology. Reading thereafter was from a syllabus drawn primarily from a report by one of the authors (Ref. 3) to the California Legislature. This syllabus provided perspective on the material to be covered. Home problems which dealt with hemodialysis and illustrated the engineering principles discussed in class were due from the students each week. During the final three weeks, however, no home problems were due, and there was little reading. In that period the students worked individually or in pairs researching a topic of their choice in the field of hemodialysis. The projects were directed toward enabling the students to think in depth. Relatively free choice of topic was allowed to maximize the student interest in the project. A list of topics suggested is given below:

Suggested Projects on Study of Artificial Kidney:

1. Linear programming of a model of dialysis for minimum cost.
2. Analysis of membrane transport.
3. The mechanism of clotting and studies of materials in the bonding of heparin to polymer surfaces.
4. Analysis of operational data for overall transport coefficients for urea.
5. Analysis of data for coefficients in ultrafiltration.
6. Systems study of hospital dialysis for minimum cost and maximum dialysis efficiencies.
7. Systems analysis of home dialysis unit for minimum cost and maximum dialysis efficiencies.
8. Analysis of material and momentum transport in the blood stream in the Kiil dialyzer.
9. Analysis of optimal relative flows of blood and dialysant in the Kiil dialyzer .
10. Critical paper on models of blood flow in arteries.
11. Improved mathematical model of dialysis system.
12. Clearance, tubular reabsorption, and tubular secretion put on more logical basis by analysis of material balances.
13. Analysis of experimental data for osmotic and dissipative effects in transfers across dialysis membranes.
14. Critical study of blood flow in capillaries.
15. Optimization study of peritoneal dialysis.

Disadvantages in Course Structuring

In structuring the course to insure that most aspects of the problems of kidney failure and hemodialysis were mentioned, there were some disadvantages. To acquaint the students with minimum knowledge relative to the human body, the kidneys and their function, and necessary medical terminology, the first two weeks were devoted to biological and medical considerations. To avoid losing student interest, it is best not to assign too much or too difficult reading at this point. Pitts' book (Ref. 2) was found somewhat advanced for sophomore-level students who had no continuing interest in physiology.

Although a number of different lecturers permitted the students to get many different viewpoints, there was some duplication, but it was held to a minimum by

NOTE: Funds for the experiment described in this article were provided by E. I. du Pont de Nemours & Company, Inc.

circulation of advance lesson plans. These plans were especially helpful in coordinating field trips and classroom efforts, so that trips were made with certain objectives in mind and were not just guided tours.

Course Content and Source Material

Of particular importance to the course at Caltech was the availability of the report by Rubini (Ref. 3), which brought together the most information about the treatment of renal failure. From an educational standpoint, it is unfortunate that as yet no suitable unified text deals with the treatment of renal failure.

The artificial kidney is clearly the best internal organ to study because it utilizes in a simple and straightforward fashion so many of the principles common to virtually all engineering problems. Figure 1 is a schematic diagram of a typical institutional hemodialysis system. Blood is removed from the patient through a shunt in the arm or leg and is driven either by the patient's own blood pressure or by the blood pressure with a boost from a roller pump. The blood moves in laminar flow through connecting tubing to the dialyzer, enters the blood side of the dialyzer, and usually flows under laminar conditions through the dialyzer and out to a drip chamber. Here bubbles are removed from the flowing blood, and then the blood returns to the patient.

The concentrations of salts in the dialysate solution are essentially those of normal blood and are carefully controlled to meet certain specifications. Correct ionic concentrations may be obtained either by mixing a dry prepared powder with tap water or by mixing a concentrated solution with tap water by means of a proportioning pump. Once the dialysate solution is prepared, it passes through a heat exchanger in which the dialysate temperature is brought up to that of the human body. After this, the dialysate continues to flow, driven either by a pump or by gravity, to the dialyzer. It moves through the dialyzer in either laminar or turbulent flow, depending upon the type of dialyzer used, and carries the constituents removed from the blood to a drain.

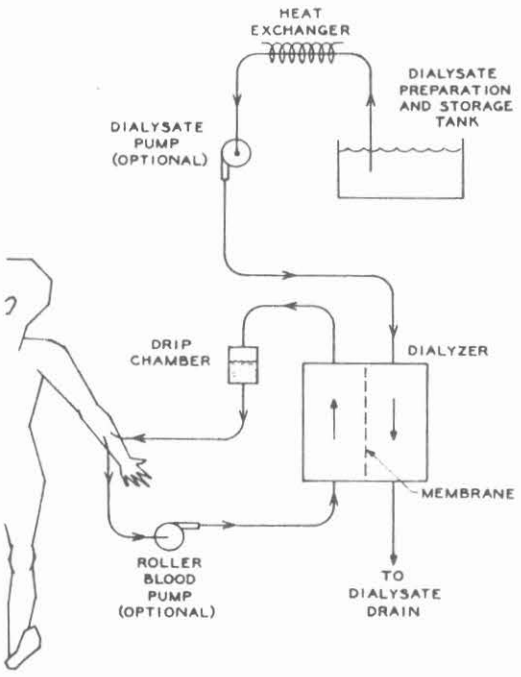

Figure 1. Schematic flow diagram for hemodialysis.

Transfer of the metabolic poisons and certain ionic constitutents of the blood across the membrane to the dialysate is primarily by molecular diffusion, since laminar flow exists at least on the blood side of the membrane. The overall driving force may be represented by the concentration gradient between the blood and dialysate sides of the dialyzer. Water may also be removed from the blood. The ultrafiltration may be brought about either by an osmotic pressure gradient induced by the presence of non-diffusible organic compounds in the dialysate or by a hydrostatic pressure gradient due to suction on the dialysate side controlled by the height of the dialysate drain.

Readily apparent, then, in Figure 1 are the roles of energy, mass, and momentum transport. These transport phenomena may be treated on a microscopic basis but preferably on a macroscopic basis by the use of the macroscopic equations of change and overall transfer coefficients. Stoichiometry plays a prevalent role in determining the proper composition of the dialysate fluid. As determination of the proper composition of the dialysate also requires an understanding of osmotic pressure, thermodynamics, with emphasis on chemical equilibrium, may be used to justify the equations commonly used to determine the osmotic pressures of solutions. Chemical kinetics is controlling in tubular secretion of certain substances in the kidney but was not reviewed in any detail in this introductory course. Because the artifical kidney basically involves a simple setup of equipment, the sophomore students rapidly develop a clear picture of relations between engineering principles and design.

Concepts and Approaches

The course was designed to present all aspects of the problems of treatment for kidney failure, thus permitting students to be introduced dramatically to the concept of the systems approach to a problem in which representatives of many disciplines (such as medicine, physiology, engineering, chemistry, and psychology) work together to solve a problem. The students readily appreciated the difficulties and advantages of the systems approach, which promises to become increasingly useful in the future. The closeness of the working relationships sensitized the students to be careful about vocabulary and definitions of terms. They not only had to learn common engineering terms but they also had to become quite familiar with medical terminology. Appreciation was developed for the problems which so often arise when communication barriers exist between professions, and the students understood the necessity of developing a clear and concise vocabulary.

The class at Caltech was composed of a variety of pure science and engineering majors. Exposure of

these students to representatives of various professions not only insured that their own interests would be discussed but also enabled them to see the obvious differences of approach and outlook among the investigators in the field. Hopefully, that experience increased their respect for other professions. Each student broadened his outlook, not only by discussions with students in other majors but also by discussions with instructors and guest lecturers with divergent interests and opinions. Conflicting opinions were evident in the evaluation of potential usefulness of various approaches to the treatment of renal failure. The students considered proposals of medical doctors to use miscellaneous internal membranes for dialysis or to treat kidney failure with transplantation. They also evaluated new dialyzer designs based upon techniques such as electrodialysis, ion-exchange, and charcoal adsorption.

Much of the progress in hemodialysis has been based primarily upon intuitive reasoning, rather than upon quantitative consideration of basic engineering principles. The students were able to see the results, some good and some not so good, of the intuitive approaches in the earlier work. After they had studied the basic engineering principles pertinent to the problem, they were then introduced to mathematical models of systems for hemodialysis and peritoneal dialysis. Those models clearly demonstrated to the students the advantages of the more quantitative approaches based upon fundamental engineering principles.

Ethics and Humanitarian Service

Because of the involvement of artificial internal organs with people, the students were exposed in a real way to the application of ethics. The immediate result of a successful hemodialysis program is to save human lives, but a failure in the program may result in loss of human lives. The too hasty introduction of a new technique or device could result in needless death of patients due to factors that could have been eliminated or mitigated by further research and development. Also, a primary factor limiting widespread use of hemodialysis is cost; so how should engineers minimize the cost and yet maintain an adequate safety factor to protect human life? Although no absolute answers could be given to the perplexing questions which always arise in such work, the questions acquainted the students with pertinent problems in ethics and with the major role of ethics in all professions.

The course at Caltech was enthusiastically received by the students, both engineers and non-engineers. They were pleased to see how engineering, science, and other disciplines could work together to fit into the real world outside of the university. They saw in a very direct manner how the principles of engineering can be used to help humanity. In a time when many students are thinking more and more in terms of humanitarian service to society, engineering educators could well focus upon more case problems involving human needs. There is no loss in communication of engineering principles. The presentation of such work early in the undergraduate curriculum could do much to encourage more of today's idealistic youth to follow careers in engineering.

References

1. Bernstein, L. M., "Renal Function and Renal Failure," Williams and Wilkins, Baltimore, 1965.

2. Pitts, R. F., "Physiology of the Kidney and the Body Fluids," Year Book Medical Publishers, Chicago, 1963.

3. Rubini, Milton E., "The Feasibility of Chronic Hemodialysis in California," Vol. I, 1966, and Vol. II, 1967, State of California Department of Public Health, Berkeley, California.

4. Wolf, A. V., and Crowder N. A., "An Introduction to Body Fluid Metabolism," Williams and Wilkins, Baltimore, 1964. △

PROPOSITIONS

PROPOSITION I

ABSTRACT

Proposition I proposes that the effects of fluid acceleration should be carefully considered when determining the pressure drop through a gas-phase, flow reactor. A plot of the fraction of the total pressure drop caused by acceleration versus the reactor length shows a minimum early in the reactor. This proposition explained the physical basis for this minimum in terms of the fluid behavior in the reactor.

PROPOSITION I

PRESSURE DROP IN PROPANE PYROLYSIS REACTORS

The proper use of the mechanical energy balance to calculate pressure changes throughout a flowing system is well known. Often, however, incomplete analyses of pressure drops are made. These analyses, though often valid approximations, have led to appreciable errors in calculated results, especially in systems where there is chemical reaction. One incomplete analysis often used neglects the effects of changes of kinetic energy and height on the pressure of a system but does include frictional effects. The neglect of changes of the kinetic energy in the mechanical energy balance can result in appreciable error in the calculated pressure profile, especially when the change in density of the flowing fluid is greater than 30% of the inlet density.

Two published analyses [1, 2] were examined to determine the effects of neglecting kinetic energy terms. Both systems involved the design of a tubular reactor for the pyrolysis of propane. The reactor designed by Myers and Watson [1] consisted of 43 sections of 30-ft. lengths of tubing having an inside diameter of 4 1/2 in. These sections were connected with 180° return bends. Pure propane at 500°F. and 70 psia. was fed to the reactor at a rate of 7455 lb./hr., and a final conversion of 85% was obtained. The reactor described by Hougen and Watson [2] consisted of 34 sections of 30-ft. tubing with an inside diameter of 5 in. Again connections were made with 180° return bends. For this reactor propane initially at 600°F. and 49.6 psia. was fed at the rate of 7000 lb./hr., and the final

conversion of propane was 82%. Both reactors were heated to a maximum temperature of 1400°F.

For each system, the analysis to determine pressure, temperature, and concentration profiles involved the simultaneous solution of twelve non-linear equations. An IBM 7094 computer was used to obtain solutions by an iterative procedure.

Hougen and Watson [2] specified that the reactor be analyzed to determine the proper inlet pressure to the reactor if the outlet pressure was to be 20 psia. An analysis which neglects the change in kinetic energy in the mechanical energy balance indicates the proper inlet pressure is 48.6 psia. An analysis including that change, however, indicates that for this inlet pressure the outlet pressure from the reactor would be 16.9 psia. and that an inlet pressure of 49.6 psia. is necessary to maintain the 20 psia. outlet pressure. Myers and Watson [1] specified that the inlet pressure to their reactor be 70 psia. Their analysis, neglecting kinetic energy effects, indicated the reactor outlet pressure would be 23 psia; but if the analysis is altered to include effects of kinetic energy, the indicated outlet pressure is 16 psia.

It is interesting to plot for each system the difference throughout the entire reactor between the pressure drop calculated by an analysis neglecting kinetic energy effects and the pressure drop obtained by an analysis including them. Figure 1 shows the effects of the neglect of the changes in kinetic energy in the mechanical energy balance on the pressure profile of each system.

The per cent error is defined as follows:

$$\% \text{ Error} = 100 \left[\frac{\Delta P_T - \Delta P_F}{\Delta P_F} \right] \qquad [1]$$

ΔP_F was chosen for the denominator of the right side of [1] instead of ΔP_T because this choice simplifies the calculation of ΔP_T using Figure 1 and known ΔP_F values.

Two features of the curves are of interest. First, there is an apparent discontinuity at $\Delta P_T/P_{IN} = 0$ since the per cent error is naturally zero when $\Delta P_T = 0$ in each system. This discontinuity occurs as a result of the definitions used for the ordinate and abscissa values, and not as a consequence of any discontinuity in the pressure profile of each system. The discontinuity simply reflects the fact that in the regions just beyond the inlet plane of the reactor the pressure drop necessitated by changes in kinetic energy is about 5% of the pressure drop due to friction no matter how small the magnitude of the total pressure drop may be.

Second, one notes the change in slope of each curve from negative to positive as the fluid proceeds through the reactor. This change of slope can be explained by combining the perfect gas law with the pressure drop expressions for a finite reactor section. For the initial reactor sections, in which the pressure is relatively constant and no chemical reaction occurs, one may derive the following approximate expression for a reactor section:

$$\text{\% Error in section N} \alpha \frac{\Delta T_N}{\langle T \rangle_N} \qquad [2]$$

This ratio decreases in the initial sections of the reactors for two reasons. First, $\langle T \rangle_N$ increases in successive reactor sections; and second, ΔT_N decreases in successive sections because the heat capacity of the fluid increases as the temperature increases. In the final sections of each reactor the per cent error is strongly affected by the relatively large decreases in pressure and average molecular weight of the fluid mixture. One can derive for these final reactor sections the approximate relation

$$\text{\% Error in section N} \alpha \frac{\Delta M_N}{\langle M \rangle_N} + \frac{\Delta P_N}{\langle P \rangle_N} \qquad [3]$$

Equation [3] explains why the per cent error increases in the final reactor sections. Not only do $\langle M \rangle_N$ and $\langle P \rangle_N$ decrease, but ΔM_N and ΔP_N increase in each successive reactor section.

The omission of kinetic energy terms in the mechanical energy balance had a negligible effect on the temperature profiles in the reactors. The calculated final conversions of propane were lowered by 1% when kinetic energy changes were considered. This difference was due to the dependence of the reaction rates upon pressure and was well within the probable errors resulting from the use of the empirically developed rate expressions. Thus the pressure was the only variable to be significantly affected by the neglect of the

kinetic energy terms in the mechanical energy balance.

Even though velocities around 700 - 900 ft./sec. were ultimately achieved in the reactors, the inclusion of kinetic energy terms in the total energy balance resulted in no substantial differences from the results obtained when neglecting changes in kinetic energy in this balance. These changes were about 1% of the total heat supplied to the reactor. In the systems investigated, the neglect of the kinetic energy terms in the total energy balance was far more acceptable than the neglect of the same terms in the mechanical energy balance.

BIBLIOGRAPHY

1. Myers, P. S. and Watson, K. M., Nat. Pet. News, 38, R-439 (1946).
2. Hougen, O. A. and Watson, K. M., "Kinetics and Catalysis," 899 - 900, John Wiley and Sons, Inc., New York, 1947.

NOMENCLATURE

$\langle M \rangle_N$	average molecular weight of the fluid in the Nth section of the reactor
ΔM_N	the decrease in the molecular weight of the fluid in the Nth section of the reactor
P_{IN}	input pressure to the reactor
$\langle P \rangle_N$	average pressure in section N of the reactor
ΔP_F	frictional pressure drop
ΔP_N	the decrease in pressure in section N of the reactor
ΔP_T	total pressure drop
$\langle T \rangle_N$	average temperature in the Nth section of the reactor
ΔT_N	increase in temperature in the Nth section of the reactor

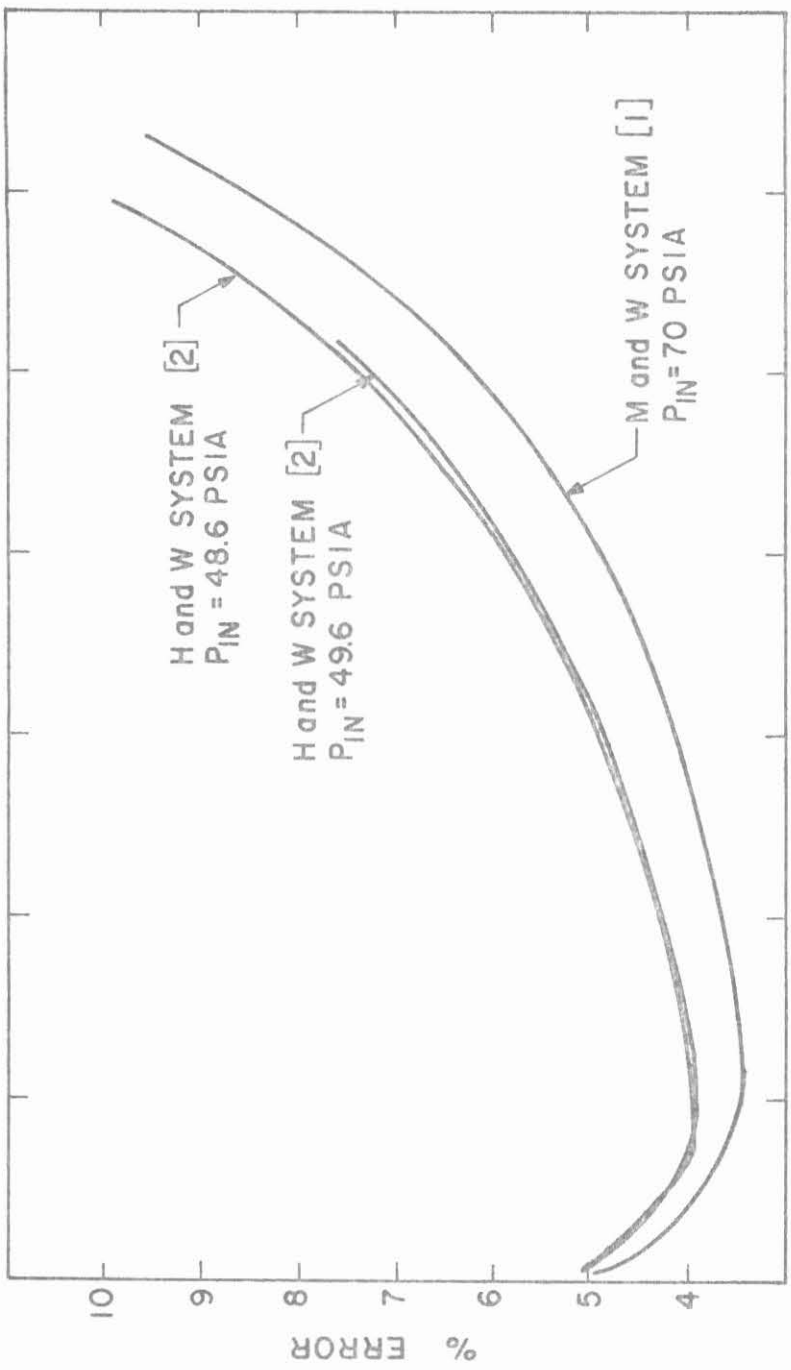

FIGURE 1. Pressure Profile Errors

PROPOSITION II

ABSTRACT

Proposition II proposes that advantages may be gained by operating a batch or plug-flow reactor at a constant heat flux rather than at isothermal conditions for the system reacting according to $A \rightarrow B \rightarrow C$. Calculations for a hypothetical system are presented showing how the yield of desirable product B may be increased by the use of a constant heat flux, how the concentration of A at a given yield of B may be increased, and how the time necessary to achieve a given yield of B may be decreased.

PROPOSITION II

NON-ISOTHERMAL REACTOR OPERATION

The series first-order reactions

$$A \xrightarrow{k_1} B \xrightarrow{k_2} D \qquad [1]$$

is exemplified by radioactive series, some hydrolyses, the chlorination of benzene, and other systems. For isothermal reaction the differential equations relating concentrations and time are readily solvable (3). In a non-isothermal, constant-volume batch reactor the differential equations are the following:

$$dA/dt = -k_1 A \qquad [2]$$

$$dB/dt = k_1 A - k_2 B \qquad [3]$$

$$dD/dt = k_2 B \qquad [4]$$

$$V\rho_T C\, dT/dt = Q - V H_1 k_1 A - V H_2 k_2 B. \qquad [5]$$

The equations for a constant-density plug flow reactor at steady state are identical. The equations above may be rearranged to give

$$d\alpha/dt = -k_1 \alpha \qquad [6]$$

$$d\beta/dt = k_1\alpha - k_2 \beta \qquad [7]$$

$$d\gamma/dt = k_2 \beta \qquad [8]$$

$$dT/dt = \frac{A_0 H_1}{\rho_T C} \left[Q/VA_0 H_1 + \left(1 + \frac{H_2}{H_1}\right) \frac{d\alpha}{dt} + \frac{H_2}{H_1} \frac{d\beta}{dt} \right]$$

These final equations may easily be solved using the Seidal numerical iterative technique (2).

The operation of the reactor at other than isothermal conditions can lead to improvements in certain characteristics of the reactor system when B, the intermediate, is the desired product. Several authors (1, 5, 6) have determined the optimum concentration of B by the calculation of the optimum temperature profile. The attainment of the optimum temperature profile requires, however, the use of a varying heat flux to the reactor which may not be easily achieved industrially. This work considers the improvements possible in one such system if the heat flux to the reactor remains constant during the course of reaction, a situation usually not difficult to achieve in practice. In addition, this work considers not only the optimization of the yield of B, but also the minimization of the amount of A reacted to achieve a given yield of B and the minimization of the time necessary to achieve a given yield of B.

Consider such a system in which the reactor feed contains no B or D and is supplied at 300°K. Both reactions are endothermic, and the rate constants satisfy an Arrhenius expression with $E_2 > E_1$. Arbitrarily specify for the system the rate constants to have either the forms

$$k_1 = 10^{15} e^{-11052.5/T} \qquad k_2 = 10^{15} e^{-11260.4/T}$$

or the forms

$$k_1 = 10^{14}\, e^{-10361.7/T} \qquad k_2 = 10^{16}\, e^{-11951.2/T}$$

For isothermal operation at the feed temperature of 300°K, the rate of heat addition must be varied. If one maintains a constant rate of heat addition to the system, considerable advantages may be obtained over isothermal reaction even though the temperature varies less than ±10°C from the initial feed temperature. For the system described above, an analysis using the IBM 7094 computer was performed to determine reactor characteristics for operation with a constant heat-input rate. The following three objectives were sought:

(1) maximization of the yield of B obtainable in the time t_M,

(2) minimization of the amount of A reacted when $\beta=\beta_M$ and $t\leq t_M$,

(3) minimization of the time necessary to achieve β_M.

The results of the numerical analysis are presented in the tables. Arbitrary values were specified for the parameters H_2/H_1 and $A_0H_1/\rho_T C$. The parameter Q/VA_0H_1 was varied to meet the desired objectives, and the values which satisfied each objective are presented in the tables.

Table I indicates little increase in the yield of B from the isothermal operation at 300°K. This is expected in view of the relative similarity of the rate constants and of the results for the optimization of B yield (1). Table II indicates that the reaction time necessary to achieve a yield of 50% can be reduced

from the isothermal time by as much as 14%. This would be a substantial saving if the time involved were of the order of magnitude of hours, as is the case for chlorination of benzene. Table III indicates that the use of this simple heat flux is sufficient to result in a substantial (up to 25%) decrease in the amount of A reacted to yield β_M in t_M. If reactant A were more valuable than product D, this knowledge would be useful.

Although only certain values of H_2/H_1 and $A_0H_1/\rho_T C$ have been considered and only two forms for the rate constants have been considered, trends may be noted which indicate whether operation with a constant heat flux would be advantageous compared to isothermal operation of a batch or constant-density plug flow reactor. If both reactions are endothermic and $E_2>E_1$, the constant heat flux reactor becomes more advantageous from the three standpoints considered here as H_2/H_1 becomes larger, as $A_0H_1/\rho_T C$ becomes larger, and as the two rate constants become less similar. It is possible however, that these generalizations may not be true in regions far removed from those analyzed here.

BIBLIOGRAPHY

1. Aris, R. Chem. Eng. Sci., 13, 18 (1960).
2. Bilous, O. and Amundson, N. R. Chem. Eng. Sci., 5, 81 - 92 and 115 - 126 (1956).
3. Faddeeva, V. N. "Computational Methods of Linear Algebra," 131 - 143, New York (1959).
4. Frost, A. A. and Pearson, R. G. "Kinetics and Mechanism," 166, John Wiley and Sons, Inc., New York (1961).

5. Horn, F. Chem. Eng. Sci.,14, 77 (1961).

6. Horn, F. Chem. Eng. Sci., 15, 176 (1962).

NOMENCLATURE

When units are not specified, any consistent units may be utilized.

A	concentration of component A
A_0	initial concentration of A in the feed
B	concentration of component B
C	heat capacity of reactive mixture, temperature units must be ^0K
D	concentration of component D
E_1	Arrhenius activation energy for first rate constant
E_2	Arrhenius activation energy for second rate constant
H_1	heat of reaction for first reaction
H_2	heat of reaction for second reaction
k_1	rate constant for first reaction
k_2	rate constant for second reaction
Q	heat input per unit time
T	temperature, ^0K
t	time
t_M	time necessary for β to reach β_M when reaction takes place isothermally, 13.8
V	volume of the reactor
α	A/A_0, dimensionless concentration of A
α_M	value of α when β reaches β_M for isothermal reaction, 0.2516
β	B/A_0, dimensionless concentration of B
β_M	maximum value of β when reaction occurs isothermally at the feed temperature, 0.5000
γ	D/A_0, dimensionless concentration of D
ρ_T	density of reacting mixture

TABLE I

MAXIMIZATION OF β FOR $t \leq t_M$

(a)

Maximum β	α At Maximum β	t At Maximum β	$\frac{H_2}{H_1}$	$\frac{A_0H_1}{\rho_T C}$	$\frac{Q}{VA_0H_1}$
0.5000	0.2535	13.8	3	100	0.108
0.5000	0.2527	13.8	3	500	0.108
0.5000	0.2526	13.8	3	1000	0.108
0.5002	0.2545	13.8	10	20	0.226
0.5003	0.2504	13.8	10	100	0.234
0.5003	0.2510	13.8	10	200	0.234
0.5003	0.2507	13.8	100	2	1.76
0.5004	0.2506	13.8	100	10	1.84
0.5005	0.2518	13.8	100	20	1.84

$k_1 = 10^{15} e^{-11057.5/T}$ $\qquad$ $k_2 = 10^{15} e^{-11260.4/T}$

$\beta_M = 0.500$ $\qquad$ $\alpha_M = 0.2516$ $\qquad$ $t_M = 13.8$

TABLE I

MAXIMIZATION OF β FOR $t \leq t_M$

(b)

Maximum β	α At Maximum β	t At Maximum β	$\frac{H_2}{H_1}$	$\frac{A_0 H_1}{\rho_T C}$	$\frac{Q}{VA_0H_1}$
0.5008	0.2721	13.8	3	100	0.102
0.5007	0.2725	13.8	3	500	0.102
0.5006	0.2653	13.8	3	1000	0.104
0.5025	0.2658	13.8	10	20	0.214
0.5029	0.2676	13.8	10	100	0.218
0.5030	0.2684	13.8	10	200	0.218
0.5030	0.2731	13.8	100	2	1.55
0.5039	0.2685	13.8	100	10	1.68
0.5041	0.2699	13.8	100	20	1.68

$k_1 = 10^{14} e^{-10361.7/T}$ $\qquad$ $k_2 = 10^{16} e^{-11951.2/T}$

$\beta_M = 0.5000$ $\qquad$ $\alpha_M = 0.2516$ $\qquad$ $t_M = 13.8$

TABLE II

MINIMIZATION OF t FOR $\beta = \beta_M$

(a)

Minimum t	α At Minimum t	$\frac{H_2}{H_1}$	$\frac{A_0 H_1}{\rho_T C}$	$\frac{Q}{VA_0H_1}$
13.8	0.2535	3	100	0.108
13.8	0.2527	3	500	0.108
13.8	0.2526	3	1000	0.108
13.2	0.2482	10	20	0.244
12.8	0.2493	10	100	0.250
12.75	0.2553	10	200	0.250
12.8	0.2508	100	2	1.92
12.4	0.2481	100	10	2.08
12.2	0.2529	100	20	2.08

$k_1 = 10^{15} e^{-11057.5/T}$ $\qquad$ $k_1 = 10^{15} e^{-11260.4/T}$

$t_M = 13.8$ $\qquad$ $\alpha_M = 0.2516$ $\qquad$ $\beta_M = 0.5000$

TABLE II

MINIMIZATION OF t FOR $\beta = \beta_M$

(b)

Minimum t	α At Minimum t	$\frac{H_2}{H_1}$	$\frac{A_0H_1}{\rho_T C}$	$\frac{Q}{VA_0H_1}$
13.4	0.2245	3	100	0.104
13.5	0.2251	3	500	0.104
13.5	0.2251	3	1000	0.104
12.7	0.2265	10	20	0.230
12.45	0.2250	10	100	0.238
12.3	0.2318	10	200	0.246
12.5	0.2752	100	2	1.76
12.0	0.2741	100	10	1.92
11.9	0.2725	100	20	1.96

$k_1 = 10^{14} e^{-10361.7/T}$ $\qquad$ $k_2 = 10^{16} e^{-11951.2/T}$

$t_M = 13.8$ $\qquad$ $\alpha_M = 0.2516$ $\qquad$ $\beta_M = 0.5000$

TABLE III

MAXIMIZATION OF α FOR $\beta = \beta_M$ AND $t \leq t_M$

(a)

Maximum α	t At Maximum α	$\frac{H_2}{H_1}$	$\frac{A_0 H_1}{\rho_T C}$	$\frac{Q}{VA_0H_1}$
0.2535	13.8	3	100	0.108
0.2527	13.8	3	500	0.108
0.2526	13.8	3	1000	0.108
0.2634	13.8	10	20	0.218
0.2653	13.8	10	100	0.222
0.266	13.8	10	200	0.227
0.2650	13.8	100	2	1.64
0.2669	13.8	100	10	1.72
0.2684	13.8	100	20	1.72

$k_1 = 10^{15} e^{-11057.5/T}$ $\qquad$ $k_2 = 10^{15} e^{-11260.4/T}$

$\alpha_M = 0.2516$ $\qquad$ $t_M = 13.8$ $\qquad$ $\beta_M = 0.5000$

TABLE III

MAXIMIZATION OF α FOR $\beta = \beta_M$ AND $t \leq t_M$

(b)

Maximum α	t At Maximum α	$\frac{H_2}{H_1}$	$\frac{A_0 H_1}{\rho_T C}$	$\frac{Q}{VA_0H_1}$
0.2919	13.8	3	100	0.096
0.2889	13.8	3	500	0.097
0.2885	13.8	3	1000	0.097
0.3050	13.8	10	20	0.180
0.3069	13.8	10	100	0.188
0.3072	13.8	10	200	0.189
0.3087	13.8	100	2	1.29
0.3123	13.8	100	10	1.38
0.3148	13.8	100	20	1.38

$k_1 = 10^{14} e^{-10361.7/T}$ $\qquad$ $k_2 = 10^{16} e^{-11951.2/T}$

$\alpha_M = 0.2516$ $\qquad$ $t_M = 13.8$ $\qquad$ $\beta_M = 0.5000$

PROPOSITION III

ABSTRACT

Proposition III proposes that the recent commercialization of a computer-input device which reads handwritten material makes computer grading of coursework feasible without requiring any significant changes in currently used teaching methods. Reactions of teachers and pupils to computer grading on the junior-high level indicate a favorable response to the proposed method of grading.

PROPOSITION III

Computer-assisted education has taken great strides in the last decade, and it is now possible to structure certain courses, particularly on the junior college level, such that all grading for the course is done by a computer rather than by the teacher (2). The development of computer-assisted education has been guided by the limitation of the available equipment, particularly the limitations of the available input devices. Although there are a number of experimental classes in which the coursework is almost entirely decided by and graded by computers, only a small minority of courses, most of them on the lower-division college level, are even graded, partially or completely, by computers. Virtually all elementary and secondary education is to date entirely unaffected by the vast capabilities of computer-assisted education.

There are a variety of reasons why computer-assisted education has not yet had full impact upon American education (1). In some subject areas, such as English composition, the necessary techniques are still being developed. Most importantly, however, the application of computer-assisted education is simply too expensive to warrant widespread use at the present time. The single most prohibitive cost of computer-assisted education has been the cost of transcribing the voluminous necessary information into a form readable by a computer. Key-punching and using specially marked coded papers are not adequate techniques for the input of a large amount of widely-varied data.

In 1968, however, IBM announced the commercial availability

of several input devices capable of reading both typed and hand-printed letters and numbers. The future generations of these devices should prove a boon to computer-assisted education. These new input devices, the 1288 series, are entirely adequate for the widespread introduction of limited grading by computer throughout the educational system.

Under this system of limited grading by computer, the teachers would still grade each piece of work submitted by the student and would, as usual, record these grades in a gradebook. The gradebook would be almost identical to the gradebook in current use but would be slightly altered to enable the computer input device to read the hand-printed letters and numbers in the gradebook. Whenever grades for the students are required (every five weeks in the Los Angeles public schools) or desired, the teacher need only place her gradebook in the intra-system mail. The mail delivers the gradebook to the central computer for the system where, overnight, the sheets from the gradebook are fed to the computer and all class grades computed. In the morning, the gradebook and computer results are returned to the teacher.

Such a limited grading system would offer many advantages to at least moderately-sized school districts. Teachers would like the system since it would relieve them of the necessity of determining grades for students several times during the school year; and, very importantly, it would do this with no noticable perturbation upon the individual teachers' established routine. Both teachers and students would appreciate having the results

of a detailed analysis of each student's continuing educational progress that only a computer could provide. Inasmuch as computer-assisted education will become more widespread in the future, students, and particularly teachers, will gain by the largely subconscious mental adjustment they will make to this foot-in-the-door form of computer-assisted education. Hopefully, further introduction of computer-assisted educational techniques would meet less resistance from teachers reluctant to alter the status-quo or to work with complex machines they don't understand and therefore fear. Since the computer and input device would be used for grading only intermittently, the school district could use the equipment the majority of the time to handle routine administrative paper work. The rental cost of the 1288 input device (about $6000/month) quite possibly could be justified by other uses entirely, and the costs of other adjustments necessary to introduce limited computer grading would be minimal.

During the second semester of the 1967-68 academic year and the first semester of the 1968-69 academic year, computer-assisted grading as discussed above was used in the seventh-and eighth-grade history and English classes of Mrs. Julia Morrison at Chester W. Nimitz Junior High in Huntington Park, California. The school is in the Los Angeles public school system. Responses from both teachers and students were obtained to evaluate the grading process.

All teachers were interested in computer grading, but most would not voluntarily use it unless they could maintain their already-established grading procedures and could avoid any

direct contact with the computer and its input devices. Virtually no teachers would use a key-punch device, as was done during these trials, to prepare input for the computer. A survey of teacher grading methods indicated that any program which would be usable by all teachers would have to satisfy at least the following conditions:

(1) Allowable class size should be variable up to a maximum of 50 students. The program should be able to account for students entering and leaving during the school year.

(2) The program should allow a variable number of grades for each student. Excused absences and extra work result in these variations. Up to one grade per school day should be allowable.

(3) The program should be able to work with either letter grades or number grades. Rarely, however, will a teacher use a combination of both. Each grade, of course, must be able to be assigned a different weighting factor.

(4) The grades for each student should be able to be placed into groups. These groups should be able to be labeled (such as tests, maps, homework, etc.), and the student's performance in each group analyzed.

(5) The program should be able to rank the students in the class and to assign, if the teacher desires, letter grades to each student on the basis of boundaries determined by the teacher. Also, the program should be able to assign to any particular student any particular grade regardless of the work that the

student has done. In a word, the computer must be able to cheat. Teachers use this option most frequently to give well-behaved, hardworking students with failing grades a passing D.

(6) Teachers should be able to choose whether to receive a simple, one-page summary of the class grades or a more detailed output that provides information for both the teacher and the student. The detailed output should provide for each student to receive a sheet detailing his grades, his relative weaknesses and strengths, his progress to date, and appropriate congratulatory or admonitory comments. A duplicate sheet should be provided for the teacher. The teacher should be allowed to suppress the comments if desired. Admonitory comments are usually suppressed for students doing their best but still failing.

A program meeting all of the above requirements, although not in the most efficient manner, was used to grade the students at Nimitz Junior High. Five classes, totaling about 170 students, were graded in the spring semester of 1967-68 and five classes, totaling about 150 students, were graded in the fall semester of 1968-69. Detailed output was provided to the students every five weeks. At the end of each semester the students were asked what they liked best and least about computer grading. One-third of the students either made no response or made no pertinent response. 111 students responded in a general sense, saying they either liked or disliked being graded by computer. 77 students said they liked being graded by computer and getting the sheet of information, and 34 students said they disliked being graded by

the computer. Of the 77 favorable responses, 59 were from good students, students making a grade of B or better, and 18 were from poor students, students making a grade of C or worse. Of the 34 unfavorable responses, 27 were from poor students and 7 were from good students. Undoubtedly, an indeterminate number of students had their opinions on computer grading shaped by the grade they received.

About 100 students responded specifically to the questions asked and noted what aspects of computer grading they liked most and least. A summary of these responses, both favorable and unfavorable, appears in Tables I and II. 46 students, most of them good students, liked receiving the sheet which described in detail areas in which they were doing well and areas in which they were doing poorly. Apparently some of the good students used this information to their advantage. The good students also liked having the computer determine the class ranking of each student. Not surprisingly, only one poor student enjoyed seeing where he ranked the class. Only three students, however, really disliked being ranked.

Sixteen students displayed their faith in the infallibility of machines by saying they liked best the fact that the machine was so accurate. This attitude was widespread throughout the students. They felt that the machine could not cheat them because of personal prejudice, and complaints about grades were significantly lowered. The students were not aware of the fact that indeed the machine could discriminate against them. One

fellow still felt cheated, however, although in his case it was not true.

As mentioned, students were given responses, congratulatory or admonitory, regarding their performance. During the first semester of computer grading, the responses the computer printed out on the sheets were not changed during the entire semester. At the end of this semester, twenty students, most of them good, complained about the comments. Their primary complaint was that the comments were the same all semester long, and they got tired of seeing the same words over and over again. The next semester, the comments were varied slightly from one grading period to the next, and this eliminated the student complaints on this point. Only three students complained about the comments after the next term, and two of these were poor students who said they disliked being told how poorly they were doing. Conversations between students and the teacher indicated, however, that many students disliked the fact that all students that did well received the same comments and all students that did poorly received the same comments. They felt that each individual student was different, and the comments should therefore be different for each student.

The seventh- and eighth-grade students did not understand some of the concepts presented to them by computer grading. Virtually none of the students initially understood the meaning of percentages and class rankings. These concepts had to be explained to them. Also, some of the words used in the comments were not understood by all the students. Care should be taken

to ensure that all students understand the information presented to them. Four students complained about this subject at the ends of the semesters.

Both teacher response and student response towards limited computer grading were favorable. Two semesters of experience with a grading program have elucidated many of the factors to be considered in computer-assisted grading. Undoubtedly, each school district would have its own peculiarities to be considered, but many factors would be common to all districts. The implementation of limited computer grading would not be expensive nor troublesome for any school district since it uses procedures and computer facilities which are already in use or which can be shared with administrative departments. Computer grading, however, is in one respect much like computer ballot-counting in elections: the computer is only called upon intermittently, but when it is called, it is expected to work correctly right away.

Acknowledgment. My thanks to Dr. Frank Yett, Chairman of the Pasadena City College Center for Computer-Assisted Learning, and to Mr. Mike Marienthal, Principal of Ninitz Junior High.

BIBLIOGRAPHY

1. Page, Ellis B. "Grading Essays by Computer" Phi Delta Kappan, January, 1966.
2. Personal Communication, Dr. Frank Yett, Center for Computer Assisted Learning, Pasadena City College, Pasadena, California, 1968.

Table I. Favorable Responses

Subject	Favorable Responses from		Total Favorable Responses
	Good Students	Poor Students	
Class Ranking	20	1	21
Fairness	12	4	16
Detailed Analysis	31	15	46
Computer Comments[1]	7	2	9
Computer Comments[2]	3	4	7

Table II. Unfavorable Responses

Subject	Unfavorable Responses from		Total Unfavorable Responses
	Good Students	Poor Students	
Class Ranking	1	2	3
Fairness	1	0	1
Detailed Analysis	4	4	8
Computer Comments[1]	13	7	20
Computer Comments[2]	1	2	3
Comprehensibility	3	1	4

[1]Second semester, 1967-1968, only

[2]First semester, 1968-1969, only